

Development of a Novel Biosensor for Rapid and Specific Detection of Viable *Legionella* Bacteria for on-site Applications

Amir Mohammad Foudeh, M.Sc.

Doctor of Philosophy

Department of Biomedical Engineering

McGill University

Montreal, Canada

Submitted December 2014



A thesis submitted to McGill University in partial fulfillment of the
requirements of the degree of Doctor of Philosophy

Copyright © Amir Foudeh, 2014.

To my parents...

Abstract

Legionellosis is a devastating disease worldwide, due to unpredictable outbreaks in man-made water systems. *Legionella*, the causative agent of this disease, was responsible for more than 30% of water-borne disease outbreaks in the USA between 2001 and 2006. The literature indicates that modern water systems, such as air-conditioning units, showers, hot tubes and industrial refrigeration towers provide optimal growth conditions for *Legionella pneumophila* (*L. pneumophila*) and propagate its transmission through aerosol. Transmission to the human host thus occurs through the inhalation of contaminated water droplets. Developing a highly specific, sensitive and rapid biosensor that detects only metabolically active bacteria is a main priority for water quality assessment. In this thesis, we proposed a detection system based on highly specific DNA capture and detector probes targeting the 16s rRNA from pathogenic *L. pneumophila* using Surface Plasmon Resonance imaging (SPRi). To achieve specific and sensitive detection, probe design and optimal hybridization conditions were implemented.

We investigated the performance of the developed biosensor for detection of *L. pneumophila* in complex environmental samples, particularly those containing protozoa. We demonstrated that the expression level of rRNA is extremely dependent on the environmental conditions. The presence of amoebae with *L. pneumophila*, especially in nutrition-deprived samples, increased the amount of *L. pneumophila* 15-fold after one week. Using the developed SPRi detection method, we were also able to successfully detect *L. pneumophila* within three hours, both in the presence and absence of amoebae in the complex environmental samples obtained from a cooling water tower.

Despite advances in miniaturization and automation of biosensors for on-site applications, progress in cutting-edge technologies, especially for monitoring environmental water samples to predict potential outbreaks are still at an early stage of development. Among different fluidic handling systems, digital microfluidics (DMF) has gained much interest. In DMF, as opposed to continuous flow microfluidics, individual droplets are manipulated independently by applying electric potential to an array of electrodes. In this setup, there is no need for external pump or tubing which makes it a

great candidate for on-site applications. In order to integrate the developed detection system with a DMF chip, some modifications, such as using fluorescent microscopy and magnetic beads were required. The conception, design and functionality of the advanced DMF device were demonstrated and the simultaneous manipulation of multiple droplets on-chip was confirmed. The various steps of the assays, including magnetic capture, hybridization duration, washing steps, and assay temperature were optimized. We were able to not only to reduce reagent volumes significantly and magnetic beads consumption, but also drop the limit of detection to 1.8 attomoles. Finally, we showed that the multiplex detection for a pathogenic and a non-pathogenic species of *Legionella* can be achieved by using capture and detector DNA probes for each 16s rRNA target. Taken all together, our results suggest that the developed DMF device combined with the proposed detection system has great potential for rapid, high-throughput, multiplex, and inexpensive on-site detection of pathogens.

Abrégé

Dans le monde entier, la légionellose est une maladie aux conséquences néfastes, tout particulièrement en raison de l'augmentation des épidémies incontrôlées au niveau des systèmes de traitement des eaux. La Légionnelle est l'agent infectieux responsable de cette maladie, et qui est également impliquée dans plus de 30% des maladies hydriques aux Etats-Unis entre 2001 et 2006. Les données de la littérature montrent que les systèmes modernes de traitement des eaux, tels que la climatisation, les systèmes de douches, et les tours de refroidissement offrent des conditions optimales de croissance et de propagation de la *Legionella pneumophila* (*L. pneumophila*) à travers la formation d'aérosols. De ce fait, la transmission de la légionellose aux humains se produit à travers l'inhalation de gouttelettes d'eau contaminée. L'un de principaux défis de l'évaluation de la qualité de l'eau serait de mettre au point des biocapteurs hautement spécifiques, sensibles et rapides. Dans cette thèse, nous avons mis au point un système SPRi de détection basé sur la capture hautement spécifique de l'ADN et sur le ciblage par sonde de détection spécifique de l'ARNr 16s provenant des *L. pneumophila* pathogéniques. Afin d'améliorer la spécificité et la sensibilité de détection des pathogènes, nous avons conceptualisé une sonde spécifique et mis en œuvre des conditions optimales d'hybridation.

Nous avons donc testé la performance de notre plateforme de détection des *L. pneumophila* sur des échantillons représentatifs d'un environnement complexe, notamment de part la présence de protozoaires. Ainsi, nous avons démontré que le taux d'expression des ARNr est fortement lié aux conditions environnementales. En mesurant l'expression des ARNr 16s, la présence concomitante d'amibe et de *L. pneumophila*, tout particulièrement dans les échantillons en carence de substance nutritive, augmente de manière significative la quantité de *L. pneumophila* après une semaine. Nous avons également détecté, par l'utilisation de notre méthode SPRi, les *L. pneumophila* en moins de 3 heures, en présence ou en absence d'amibe dans les échantillons des tours de refroidissement.

Malgré, les avancées en miniaturisation et en automatisation des biosenseurs pour l'utilisation *in situ*, il reste encore plusieurs défis à relever notamment dans l'analyse des

échantillons d'eau d'origine environnementale afin de prédire au mieux les risques potentiels d'épidémies. Les dispositifs à microfluides digitaux (DMF) sont des candidats très prometteurs en comparaison au reste des systèmes de manipulation fluidiques. De plus, à l'opposé des dispositifs microfluidiques à flux continu, le dispositif DMF permet de manipuler de manière indépendante des gouttelettes individuelles par l'application de potentiel électrique à un réseau d'électrode. Notre appareillage ne requiert aucune pompe externe ou tubes, ce qui le rend utile pour des applications sur place. Aussi, afin d'intégrer ce système de détection à la puce DMF, des modifications ont été apportées telles que l'utilisation de billes magnétiques fluorescentes. Les différentes étapes de l'analyse, incluant la capture magnétique, la durée d'hybridation, les étapes de lavage et la température optimale ont été optimisées. Le volume des réactifs et la quantité de billes magnétiques ont été réduit considérablement. De plus, le seuil de détection a été baissé à 1.8 attomoles. Finalement, nous avons démontré que notre système détecte spécifiquement l'ARN 16s. Nous avançons que ce système détient un énorme potentiel de détection multiplexe, rapide, à haut débit et peu coûteux pour divers pathogènes, et ce à partir de très petites quantités d'échantillons et de réactifs.

Acknowledgments

First and foremost, I would like to thank my supervisor, Dr. Maryam Tabrizian for her enduring support, encouragement and guidance throughout my graduate studies. I extend my gratitude for her professionalism, availability and leadership. Her support and encouragement was a great asset during difficult times. She provided an outstanding research environment, and a challenging but highly motivating project. She always challenged me to be creative and persevere. I am also very grateful for the opportunities that she gave me to participate in various international conferences and present the results of my work.

I would also like to thank Dr. Teodor Veres for his supervisory role, advice and guidance. Despite his demanding position at NRC, he always made the time for me. His help and enthusiasm for the EWOD project was instrumental for this thesis. I would also like to express my gratitude for access to the NRC facilities.

I extend my thanks to Dr. Sébastien Faucher for his immense help and advice, as well as providing access to his laboratory. His valuable insight in *Legionella* microbiology and his enthusiasm was a great driving force during my project. He taught me everything that I needed to know about *Legionella*. He also generously let me to work in his lab for all the *in vitro* transcription of RNA, microbiology experiments and amoeba culture studies.

Among other members at NRC, I would like to thank particularly Dr. Daniel Brossard for his availability, help and encouragement. I especially thank Dr. Xuefeng Zhang for his assistance in the NRC facilities. I would also like to extend my appreciation to Dr. Jamal Daoud, Karel Côté, Dr. Lidija Malic and Dr. Xuyen Hoa for their support.

I would like to thank Dr. Hana Trigui, Nilmini Mendis and Amy Li from Dr. Faucher's laboratories at the Macdonald campus, for being always helpful and available. Your company made the trips to Ste-Anne de Bellevue in the winter bearable. Thank you!

I would like to thank the members of my advisory committee: Dr. Robert Funnell, Dr. Andrew Kirk, and Dr. Jay Nadeau for all their valuable advice and guidance during our meetings. I also want to thank Jun Li for his assistance for gold coating of glass substrates in McGill microfabrication facility. Thanks to Dr Jean-Jacques Drieux and Dr Pierre Hiernaux from Magnus Inc. for their technical support, advices and background information for *Legionella*. Special thanks to Pina Sorrini and Nancy Abate in Biomedical Engineering Department for always being available and resourceful.

I would like to thank my former and present lab members. Thanks in particular goes to Dr. Tohid Didar for his collaboration on our micro-contact printing and microfluidic review paper. His friendship, enthusiasm and motivation were a great inspiration for me. I would also like to thank Sandrine Filion-Côté for her advice and input regarding SPRi and Dr. Jamal Daoud for his help with the SPR experiments and also his endless support and generous advice for both in research and professional life. Thanks especially to Mina, Kaushar, Ryan and Laila for their energy, inputs and comments for this thesis. I also thank Ana Maria Almonacid for her work and help with SPR experiments during the summer of 2013 in our lab. To all the other members of the Biomat'X lab past and present, Kristen, Steve, Samira, Lamees, Rafael, Rosey, Khalil, Hubert, Arghavan, Cathy, Christina, Leslie, Meltem, Andrew and Tim. Thanks for all of the great moments that we had together. Working with you all was a great honor.

To Molly that was caring, supportive and understanding. To my parents, Hossein and Fariba, from whom I had unconditional support and love during all these years. To my sisters, my family and my amazing friends for their endless support and inspiration. Your companionship and encouragement was the main source of energy that let me keep going during the hardest time of my research.

No matter how deep my gratitude is, the only thing I can say is: Love you all. Finally, I would like to acknowledge the funding sources that made this work possible: Natural Sciences and Engineering Research Council of Canada NSERC-CREATE Integrated Sensor Systems (ISS) program and McGill's Biomedical Engineering Department.

Table of Contents

Abstract.....	i
Abrégé.....	iii
Acknowledgments.....	v
List of Figures.....	xiii
List of Tables.....	xviii
Glossary.....	xix
Contribution of Authors:.....	xxi
Thesis Outline:.....	xxiii
Chapter 1 Introduction.....	1
Chapter 2 Rationale.....	4
2.1 16s rRNA as reliable genetic material.....	4
2.2 SPRi as detection method.....	5
2.3 Amoeba and <i>L. pneumophila</i> cohabitation.....	5
2.4 Integration of DMF with fluorescence microscopy.....	6
Chapter 3 Hypothesis and Thesis Objectives.....	8
3.1 Hypothesis.....	8
3.2 Thesis Objectives.....	8
Preface to chapter 4 to 8: Background Information and literature review.....	10
Chapter 4 Biosensors.....	11
Chapter 5 SPR Principle.....	14
Chapter 6 Digital microfluidic Principles.....	20
Chapter 7 <i>Legionella</i>	23
7.1 Legionellosis.....	23
7.2 The interaction of <i>Legionella</i> with other organisms and its significance.....	25
7.3 Standards level of <i>Legionella</i> in environmental settings.....	26
7.4 Eradication/Disinfection.....	26
7.5 Current Detection Methods for <i>Legionella</i> :.....	27
7.6 Commercially available detection kits.....	33
Chapter 8 Microfluidic designs and techniques using lab-on-a-chip devices for pathogen detection for point-of-care diagnostics.....	35

8.1	Abstract	36
8.2	Introduction	37
8.3	Biomarkers	38
8.3.1	Antibodies	39
8.3.1.1	Protein and toxin detection using antibodies	39
8.3.1.2	Whole cell detection	39
8.3.1.3	Alternatives to the antibody.....	40
8.3.2	DNA/PNA:	44
8.4	Amplification Methods	46
8.4.1	PCR and its design.....	46
8.4.2	Isothermal	48
8.5	Sample preparation.....	52
8.5.1	DEP	53
8.5.2	Particles and beads	54
8.5.2.1	Micro/nano particles	54
8.5.2.2	Magnetic beads	55
8.5.3	Filter	58
8.6	Design strategies for pathogen detection	59
8.6.1	Strategies to develop high-throughput multiplex devices	60
8.6.2	Strategies to develop POC devices	62
8.6.2.1	Droplet-based and Digital microfluidics	63
8.6.2.2	Lab on a disk devices	66
8.6.2.3	Paper-based devices.....	66
8.6.2.4	Integration towards sample-to-result POC devices	69
8.7	Outlook and future trends.....	74
	Preface to Chapter 9: Sensitive detection of 16s rRNA from <i>Legionella pneumophila</i> using surface plasmon resonance imaging.....	78
	Chapter 9 Sub-femtomole Detection of 16s rRNA from <i>Legionella Pneumophila</i> Using Surface Plasmon Resonance Imaging	79
9.1	Abstract	80
9.2	Introduction	81
9.3	Materials and methods	84
9.3.1	Chemical and reagents.....	84

9.3.2	DNA probe design.....	84
9.3.3	RNA preparation	85
9.3.4	Surface chemistry on SPRi chip	86
9.3.5	RNA pre-treatment	86
9.3.6	SPRi measurements	87
9.3.7	Statistics.....	88
9.4	Results and discussion.....	88
9.4.1	Effect of buffer composition and detector probe spacer on hybridization efficiency	89
9.4.2	L. Pneumophila 16s rRNA Pre-treatment.....	91
9.4.3	Determination of the SPRi limit of detection for 16s rRNA from L. Pneumophila ..	93
9.5	Conclusions	96
9.6	Acknowledgements	98
9.7	Supplementary Information:	98
Preface to Chapter 10: Sensitive and Specific SPRi Detection of <i>L. pneumophila</i> in Complex Environmental Water Samples.....		100
Chapter 10 Sensitive and Specific SPRi Detection of <i>L. pneumophila</i> in Complex Environmental Water Samples		101
10.1	Abstract:	102
10.2	Introduction	103
10.3	Experimental:	106
10.4	Results and Discussion:.....	107
10.4.1	Assessment of specificity and sensitivity of the SPRi biosensor	107
10.4.2	16s rRNA expression level	107
10.4.3	SPRi detection of L. pneumophila co-cultured with amoeba	109
10.4.4	Validation of sensing technique for the cooling tower water sample:.....	110
10.5	Conclusions	112
10.6	Acknowledgments	113
10.7	Electronic Supplementary Material.....	113
10.7.1	Materials and methods.....	113
10.7.1.1	Chemical and reagents.....	113
10.7.1.2	DNA probe design.....	114

10.7.1.3	Surface chemistry on SPRi biochip	114
10.7.1.4	SPRi measurements	114
10.7.1.5	Co-culture of <i>L. pneumophila</i> and <i>Amoeba</i>	115
10.7.1.6	RNA extraction.....	116
10.7.1.7	Total RNA fragmentation.....	116
10.7.1.8	Reverse transcriptase PCR and Real-time PCR.....	116
10.7.1.9	Cooling tower water sample	117
10.7.1.10	Statistics.....	117
Preface to Chapter 11: Rapid and Multiplex Detection of <i>Legionella</i> 's RNA using Digital Microfluidics.....		119
Chapter 11 Rapid and Multiplex Detection of <i>Legionella</i> 's RNA using Digital Microfluidics.....		120
Abstract		121
11.1 Introduction		122
11.2 Results and discussion.....		127
11.2.1	Design of the DMF devices	127
11.2.2	Assay design and optimization	129
11.2.3	On-chip serial dilution and hybridization	131
11.2.4	Limit of detection for <i>L. pneumophila</i> 's RNA.....	136
11.2.5	Multiplex detection of pathogenic and non-pathogenic <i>Legionella</i>	137
11.3 Conclusion.....		139
11.4 Materials and methods		140
11.4.1	Chemical and reagents.....	140
11.4.2	DMF device fabrication.....	141
11.4.3	Microfluidic platform and DMF device operation	141
11.4.4	DNA probe design and hybridization condition.....	143
11.4.5	Microparticle preparation and signal measurement.....	144
11.5 Acknowledgments		145
11.6 Electronic Supplementary Information (ESI)		147
11.6.1	Evaluation of the error caused by droplet volume variability during an exponential dilution series in digital microfluidics	147
Chapter 12 General Discussion, Conclusion		151
12.1 Summary of Achievements		151

12.2	Original claims	153
12.3	Limitations and Future Perspectives	155
12.3.1	16s rRNA expression.....	155
12.3.2	Toward development of true on-site biosensor	156
12.3.2.1	Integration of sample preparation with the DMF chip	156
12.3.2.2	Improving the limit of detection	156
12.3.2.3	Mass production	158
12.3.2.4	Transducer integration.....	159
12.3.2.5	Molecular beacons for one-step detection	159
	References.....	161
	Appendix A: Copyright Waivers and Article Reprints.....	176
	Appendix B: Curriculum Vitae	217

List of Figures

- Figure 5-1 Metal-dielectric interface. Reprinted from Willets 2007 [44] with permission from Annual Review of Physical Chemistry..... 14
- Figure 6-1 EWOD actuation configurations: (a) closed and (b) open EWOD system. Reproduced from [60] with permission from The Royal Society of Chemistry..... 20
- Figure 8-1 Schematics of isothermal amplification methodologies: (i) HDA: dsDNA is unwind by Helicase enzyme then single-strand binding protein stabilizes the strands. Finally a double-stranded copy is produced using Primers and polymerase. (Reproduced from Ref. [185] with permission from Royal Society of Chemistry.) (ii) RPA: Primers bind to template DNA and a copy of the amplicon is produced by extension of the primers using a DNA polymerase. (Reproduced from Ref. [186] with permission from Public Library of Science.) (iii) LAMP: Template synthesis initiated by the primer sets resulting in stem-loop DNAs with several inverted repeats of the target sequence. In this schematic, only the process using forward primer set is shown. (Reproduced from Ref. [185] with permission from Royal Society of Chemistry.) (iv) NASBA: (A) The initial phase to synthesize complementary RNA to the target RNA and (B) In the cyclic phase, each newly synthesized RNA can be copied, leading to exponential amplification. (Reproduced from Ref. [185] with permission from Royal Society of Chemistry.) (v) RCA: (a) Linear template and single primer (b) Circular template and single primer. Blue and green lines represent target DNA and oligonucleotide primers respectively. (Reproduced from Ref. [187] with permission from Elsevier..... 47
- Figure 8-2 (a) Schematic of the DEP integrated in a microfluidic device for continuous cell separation and concentration. (b) Fluorescence microscopy image of separation channel inflow (c) fluorescent image of separation channel outflow. (Reproduced from Ref. [206] with permission from Royal Society of Chemistry.)..... 52
- Figure 8-3 (i) Schematic diagram of integrated microfluidic LAMP system for RNA purification and NNV detection. (Reproduced from Ref. [169] with permission from Elsevier.) (ii) Schematic illustrations of an integrated PMMS-CE microdevice for multiplex pathogen detection. The microdevice consists of a passive mixer, a magnetic separation and a capillary electrophoretic microchannel to identify target pathogens. (Reproduced from Ref. [158] with permission from Royal Society of Chemistry.) 54
- Figure 8-4 (i) Schematic of microfluidic emulsion generator (MEGA) array device. (A) Design of a glass-PDMS-glass hybrid four-channel MEGA device and (B) Layout of a 32-channel MEGA device. (C) Layout of 96-channel MEGA device.(D) Illustration of complete four layer 96-channel MEGA device and the plexiglass assembly module. (Reproduced from Ref. [149] with permission from American Chemical Society.) (ii): Exploded view of the microfluidic chip containing shuttle flow channels, micropumps and microvalves. (Reproduced from Ref. [215] with permission from Royal Society of Chemistry.) (iii): (A) Schematic representation of an immunoreaction chip used for detection of algal toxins. red and blue color represent the regular valves and sieve valves respectively. (B)

and (C) Pictures of the microfluidic chip and central area of the chip. (Reproduced from Ref. [216] with permission from Royal Society of Chemistry.)	58
Figure 8-5 Activation mechanism of the Electro-hydraulic Pump. Bubbles are formed by electrolysis of the pumping fluid applying electrical current. The produced pressure is transferred through a flexible membrane to a hydraulic fluid chamber, which then pushes fluid out of the reagent chamber. (Reproduced from Ref. [225] with permission from Royal Society of Chemistry.	61
Figure 8-6 (i) Droplet based microfluidic chip implementing magnetic actuation. Demonstration of the droplet manipulation in (c) air and (d) oil mediums. (Reproduced from Ref. [198] with permission from Royal Society of Chemistry.) (ii) (a) Top view of an EWOD-based digital microfluidic device, (b) a reservoir, (c) analysis spots, and (d) region for mixing, storing and splitting droplets. (Reproduced from Ref. [226] with permission from IEEE.)	63
Figure 8-7 Schematic diagram of the microfluidic microarray. Procedure for (A) probe printing and (B) Hybridization. (Reproduced from Ref. [156] with permission from Elsevier.) ..	65
Figure 8-8 Three-dimensional paper-based microfluidic. (i) Demonstration of the fabrication, design and patterning of a three-dimensional paper-based microfluidic. (Reproduced from Ref. [245] with permission from Proceedings of the National Academy of Sciences.) (ii) Schematic of operating procedures of ELISA in a three-dimensional paper-based microfluidic. (Reproduced from Ref. [246] with permission from IEEE.) (iii) A three-dimensional paper-based microfluidic using origami principle. (Reproduced from Ref. [248] with permission from American Chemical Society.).....	68
Figure 8-9 (i) Schematic illustration of the microfluidic chip for Sample-to-answer genetic analysis of H1N1 virus. (Reproduced from Ref. [164] with permission from American Chemical Society.) (ii) Schematic diagram of the chip consisting of a lysis chamber and nanostructured microelectrodes integrated to the sensing system for detection of bacterial pathogens. (Reproduced from Ref. [152] with permission from American Chemical Society.) (iii) Picture of a foil based Lab on a disc with liquid reagent containers and its operating procedure. (Reproduced from Ref. [157] with permission from Royal Society of Chemistry.).....	71
Figure 8-10 (i) Schematic presentation and images of self-heating cartridge based device for isothermal amplification (a) exploded view, (b) green fluorescence emission from a test amplification chamber. (Reproduced from Ref. [200] with permission from Royal Society of Chemistry.) (ii) Schematic diagram of the DxBox integrated immunoassay cards for detection of the malaria antigen and S. Typhi-IgM from blood sample. (Reproduced from Ref. [250] with permission from Royal Society of Chemistry.) (iii) Schematic diagram and pictures of a POC microfluidic device based on ELISA-like assay. (a) Picture of the microfluidic chip. (b) Scanning electron microscope image of a cross-section of microchannels. (c) Transmitted light micrograph of channel meanders. (d) Illustration of the passive delivery mechanism for multiple reagents. (e) Diagram of biochemical reactions in detection zones at different steps of immunoassay. (f) Absorbance traces of a	

complete HIV-syphilis duplex test as reagent plugs pass through detection zones. (Reproduced from Ref. [251] with permission from Nature publishing group.).....	73
Figure 9-1 Schematic illustration of the RNA hybridization using capture and detector probes, before and after addition of SA-QDs. a) Mixture of target RNA and biotinylated detector probe pass through the detection surface. b) Addition of streptavidin-QDs after hybridization of target RNA to Capture probe and detector probe.	88
Figure 9-2 Effect of buffer composition on hybridization efficiency. Hybridization of 10 nM synthetic RNA for 18 min on the biochip expressed as $\Delta\%R$ as a function of buffer composition (1X-6X SSPE). The inset represents the hybridization efficiency of the Leg1 CP which control probe signals were subtracted from the Leg1 CP signals. All data is expressed as mean \pm standard deviation (n=5).....	90
Figure 9-3 Effect of fragmentation and denaturation pre-treatment methods on of 16s rRNA on hybridization efficiency. a) Hybridization of 10 nM 16s rRNA after 18 min incubation with EU, Leg1 and Leg2 capture probes. b) Effect of 16s rRNA pre-treatment on QDs post amplification. 100 nM Leg1 DP 0bp with 10nM 16s RNA were used and hybridization efficiency with Leg1 CP followed by addition of the 1nM SA-QDs was investigated. All data is expressed as mean + standard deviation (n=5, *P<0.05 versus intact, denatured and Frag1).....	92
Figure 9-4 Effect of different detector probes on hybridization efficiency. x-axis represents capture probes a,b) secondary structure diagrams for <i>L. pneumophila</i> based on <i>L. pneumophila</i> model (accession number (accession number M34113) [252] for area complementary to Leg1 CP and Leg2 CP respectively. Lines next to the diagrams indicate of the position of capture and detector probes. c,d) Change in reflectivity was measured after 18 min for three different capture probes (EU, Leg1 and Leg2 CPs) for 10 nM fragmented 16s rRNA corresponding to a and b respectively. e,f) Addition of 1 nM SA-QDs for 10 min corresponding to c and d respectively. All data is expressed as mean + standard deviation (n=5, *P<0.05 versus other capture probes).....	94
Figure 9-5 Fragmented 16s rRNA hybridization with Leg1 CP with series of ultralow RNA concentrations: 10 nM, 1nM, 100 pM, 10 pM, 1 pM a) Normalized real-time SPRi kinetic curve for detection of ultralow concentration of 16s rRNA b) The reflectivity change were plotted versus concentration after 150 min. The inset figure shows the differential reflectivity change ($\Delta\%R$) for 1 pM, 10 pM and 10 pM. All data expressed as mean \pm standard deviation (n=5, *P<0.05 versus control probe).....	96
Figure 9-6 Effect of hybridization time of 10 nM fragmented 16S rRNA with Leg1 Cp on hybridization efficiency. All data is expressed as mean \pm standard deviation (n = 5).	99
Figure 10-1 Schematic illustration of the infection cycle of <i>L. pneumophila</i> in amoebae in cooling tower water and detection of <i>L. pneumophila</i> using SPRi: a) cooling tower water containing amoebae and <i>L. pneumophila</i> , b) an amoeba infected by <i>L. pneumophila</i> , c) multiplication of <i>L. pneumophila</i> inside an amoeba, d) lyses of amoeba and release of <i>L. pneumophila</i> , e) collection and lyses of <i>L. pneumophila</i> , f) extraction and fragmentation of RNA from <i>L. pneumophila</i> , g) hybridization of extracted RNA on the SPRi chip, h)	

schematic of the RNA hybridization using capture and detector probes and use of QDs post amplification.	106
Figure 10-2 The effect of incubation time of <i>L. pneumophila</i> in AC buffer on 16s rRNA expression was examined. Ct values obtained from real-time PCR experiments and plotted against four different incubation time points. All data are expressed as mean \pm standard deviation.	108
Figure 10-3 Incubation of <i>L. pneumophila</i> in AC buffer in presence and absence of amoeba after 1, 2 and 7 days. a) Concentration of <i>L. pneumophila</i> versus incubation time b) SPRi measurements of the hybridization of extracted RNA from 1 mL of each sample with QDs post amplification. An initial concentration of 10^6 CFU of <i>L. pneumophila</i> in presence and absence of 10^6 amoebae in a 6-well plate was used. All data expressed as mean \pm standard deviation (* $P < 0.05$).	110
Figure 10-4 Incubation of a dilution series of <i>L. pneumophila</i> in a cooling water sample in the presence and absence of 1.5×10^6 amoeba for 2 days. a) CFU plate counting for each sample. b) SPRi signal measurements of the hybridization of extracted RNA from 1 mL of each sample with QDs post amplification. All data expressed as mean \pm standard deviation.	111
Figure 10-5 Specificity of the detection system was evaluated. The reflectivity change of QD post amplification after hybridization of total RNA extracted from <i>L. pneumophila</i> was compared against 2 strains of <i>E. coli</i> and one strain of <i>Pseudomonas</i> . RNA was extracted from 1 mL of 10^6 CFU/mL of each bacterium. All data expressed as mean \pm standard deviation.	118
Figure 10-6 Hybridization of fragmented total RNA extracted from <i>L. pneumophila</i> with Leg1 CP. The reflectivity change of QD post amplification after hybridization of total RNA was plotted versus the series of <i>L. pneumophila</i> concentrations. All data expressed as mean \pm standard deviation.	118
Figure 11-3 Schematics protocol showing the serial dilution and hybridization of 16s rRNA on the DMF devices. a) Creation of the exponential dilution of the RNA sample into six concentrations. b) Mixing of the diluted RNA droplets with the magnetic beads. c) Incubation of the magnetic beads with six concentrations of 16s rRNA. d) Capture of magnetic beads and separation of supernatant e) Six times washing of magnetic beads. f) Fluorescent measurement.	130
Figure 11-4 Top view image sequence showing the digital microfluidic protocol used for the RNA serial dilution and hybridization assay. a) Creation of the exponential dilution profile of the RNA sample into 6 droplets (1. to 3.). b) Mixing of the diluted RNA droplets with the magnetic beads and incubation (4. to 6.). c) Magnetic capture and washing of the incubated droplets (7. to 9.).	133
Figure 11-5 Measured relative fluorescent intensity versus <i>L. pneumophila</i> 's RNA concentration using superparamagnetic beads and Cy3 fluorescent tagged detector probe. (see ESI for the calculation of the error on the concentration). Inset: A bright-field and fluorescent images of a droplet containing captured RNA onto the magnetic beads.	135

Figure 11-6 Multiplex detection of *Legionella* 16s rRNAs including pathogenic, *L. pneumophila* (*L.p*) and non-pathogenic *L. israelensis* (*L.i*). Detector probe specific to *L.p* RNA sample was tagged with Cy3 dye while the detector probe specific to *L.i* RNA sample was tagged with Cy5 dye. Three RNA samples including *L.p*, *L.i* and mixture of *L.p* and *L.i* were incubated with two types of magnetic beads functionalized with either *L.i* or *L.p* capture probes. The fluorescent measurements were carried out with Cy3 and Cy5 filters for each droplet..... 139

List of Tables

Table 7-1 <i>Legionella</i> species and their association with human diseases.	24
Table 7-2 CFU of <i>Legionella</i> per liter based on USA Occupational Safety & Health Administration technical manual: https://www.osha.gov/dts/osta/otm/otm_iii/otm_iii_7.html	26
Table 7-4 List of the commercially available Legionella detection kit.	34
Table 8-1 Detection of pathogens implemented in microfluidic devices	42
Table 9-1 Oligonucleotide sequences employed as capture and detector probes.....	98
Table 10-1 Oligonucleotide sequences employed in the experiments.....	114
Table 10-2 Forward and reverse primers for RT-PCR	117
Table 11-1 Oligonucleotide sequences employed in the experiments.....	144

Glossary

3D	Three Dimensional
BCYE	Buffered Charcoal-Yeast Extract
CCD	Charge-Coupled Device
CFU	Colony Forming Unit
DEP	Dielectrophoresis
DMF	Digital Microfluidic
DNA	Deoxyribonucleic acid
ECL	Electrochemiluminescence
ECODSVs	Electrokinetically Controlled Oil-Droplet Sequence Valves
EDTA	Ethylenediaminetetraacetic acid
EHP	Electro-Hydraulic Pump
ELISA	Enzyme-Linked Immunosorbent Assays
EMA	Ethidium Monoazide
EWOD	Electrowetting on Dielectric
FET	Field Effect Transistors
FFD	Fluidic Force Discrimination
FRH	Flameless Ration Heater
GNP	Gold Nanoparticles
HDA	Helicase-Dependent Amplification
HIV	Human Immunodeficiency Virus
LAMP	loop-mediated isothermal amplification
LED	Light-Emitting Diode
LOC	Lab on a Chip
LOD	Limit of Detection
MALDI-MS	Matrix-assisted laser desorption/ionization mass spectrometry
MB	Magnetic Bead

MEGA	Microfluidic Emulsion Generator Array
MUA	11-Mercaptoundecanoic acid
NASBA	Nucleic Acid Sequence-Based Amplification
NNV	Nervous Necrosis Virus
PCR	Polymerase Chain Reaction
PDMS	Polydimethylsiloxane
PET	Polyethylene Terephthalate
PMA	Propidium Monoazide
PNA	Peptide Nucleic Acid
POC	Point of Care
QD	Quantum Dot
qPCR	Quantitative Polymerase Chain Reaction
RCA	Rolling Circle Amplification
RNA	Ribonucleic acid
RPA	Recombinase Polymerase Amplification
rRNA	ribosomal Ribonucleic acid
RT-PCR	Reverse Transcriptase Polymerase Chain Reaction
SARS	Severe Acute Respiratory Syndrome
SEB	Staphylococcal Enterotoxin B
SERS	Surface-Enhanced Raman Spectroscopy
SPRi	Surface Plasmon Resonance imaging
TCID50	50% Tissue Culture Infective Dose
UV	Ultraviolet
VBNC	Viable But Non-Culturable
WHO	World Health Organization

Contribution of Authors:

This thesis is presented as a collection of manuscripts written by the candidate with the assistance, collaboration and supervision of co-authors. The candidate envisioned and developed the biosensor and detection method presented in this thesis work and carried out all the characterization and experiments. All data collection and analysis was done by the candidate.

Dr. Sebastien Faucher appears as co-author in two of the manuscripts in reflection of his role as a collaborator and his valuable contribution to the microbiology aspect of the project.

Dr. Tohid Didar contributed with his ideas and comments during the preparation of the review paper in Chapter 8, which is acknowledged by the co-authorship.

Dr. Jamal Daoud appears as a co-author in the second paper (Chapter 9) to acknowledge his help with analyzing the data and his comments on the manuscripts.

Dr. Hana Tengui appears as a co-author in the third paper (Chapter 10) to acknowledge her help for QPCR and providing reagents and knowledge regarding *Legionella* bacteria.

Nilmini Mendis appears as a co-author in the third paper (Chapter 10) to acknowledge her help for the CFU counting and providing amoeba and reagents.

Dr. Daniel Brassard appears as co-author in the fourth paper (Chapter 11) to acknowledge his role in designing and providing the digital microfluidic chips; also designing the temperature control unit and his valuable comments during the preparation of the manuscript.

Dr. Teodor Veres appears as co-author on all papers to reflect his role as co-

supervisor and contributor to the digital microfluidic aspects of this thesis.

Dr. Maryam Tabrizian appears as co-author on all papers as a reflection of her primary supervisory role throughout the execution of this work, as well as her involvement in the preparation of manuscripts.

Thesis Outline:

In Chapter 1, after a general introduction to the problem statement based on a brief description of Legionellosis disease and the need for development of an on-site biosensor; the motivation of the thesis work and the accomplishments are presented. Chapter 2 discusses the rationality behind the targeting 16s rRNA, the use of SPRi and investigation of amoeba-*Legionella* interaction and utilizing of DMF. The research hypothesis and objectives are stated in Chapter 3.

Chapters 4, 5, 6, 7, 8 present background information and comprehensive literature review of the topics covered by this thesis. Chapter 4 describes the principles and requirements of a biosensor technology. An overview of the SPR biosensors and DMF devices is presented in chapter 5 and 6 respectively. An extensive literature review related to *Legionella* is reported in Chapter 7. The biology of *Legionella*, the interaction of the *Legionella* with other microorganisms, the detection requirements for the environmental setting and different ways for water disinfection are discussed. This chapter also covers the state of the art detection techniques along with commercially available detection kits for *Legionella*. Chapter 8 consists of a review article published in *Lab on a Chip*, where the state-of-the-art in using microfluidic based biosensors for pathogen detection is described. This overview provides the reader with a context for evaluating the novelty and the contribution of this work to the larger research field. Chapter 9 presents the development of a detection method targeting the *L. pneumophila* 16s rRNA using SPRi. The purpose here was to develop a detection system that potentially only detects viable bacteria while at the same time offers high specificity and sensitivity. Therefore, the different parameters for DNA/RNA hybridization and signal

amplification was investigated and optimized.

Chapter 10 reports on the successful implementation of the developed system described in Chapter 9, for the detection of the *L. pneumophila* in complex environmental samples particularly in presence of amoeba.

Chapter 11 is devoted to the integration of the developed detection system in Chapter 9 with DMF setup for multiplex and automated detection of *Legionella*. The various steps of the assays, including magnetic capture, hybridization duration, washing steps, and assay temperature were optimized. The rapid, multiplex and automated detection of pathogenic and non-pathogenic *Legionella* was demonstrated.

Finally, Chapter 12 provides a general discussion of the results and outlines the future work towards the development of biosensors for on-site detection of *Legionella* in environmental water setting. The new directions that could be implemented to maximize the diagnostic potential of this work, are also provided.

Chapter 1 Introduction

The World Health Organization (WHO) recently reported that infectious diseases are the second leading cause of mortality throughout the world after cardiovascular disease. Overall, pathogens guide the research and development in many fields, including diagnostics, pathology, drug discovery, clinics, biological warfare, food safety and disease outbreaks. Among these pathogens, *Legionella* the causative agent of Legionellosis (an acute form of pneumonia and Pontiac fever [1]) is a major concern due mainly to unpredictable outbreaks such as recent incidents reported in Canada, USA, Norway, and Germany [2-4]. *Legionella* was responsible for more than 30% of water borne disease outbreaks in USA between 2001-2006 [5]. The fatality rate of Legionellosis ranges between 10% and 40% and approaches 50% within hospital and industrial outbreak settings, particularly affecting individuals with compromised health status [1]. Presently, more than 50 *Legionella* species have been identified with approximately half of these species being associated with human disease. To have an accurate and reliable evaluation of the water risk assessment it is thus crucial to design detection systems that can distinguish between pathogenic and non-pathogenic *Legionella* [6, 7].

L. pneumophila is responsible for more than 90% of Legionellosis. *L. pneumophila* is found in most natural and engineered water systems, where it contaminates and multiplies inside amoeba [8]. Modern water systems, such as air-conditioning units, showers and industrial refrigeration towers provide optimal growth conditions for *L. pneumophila* and propagate its transmission through aerosol [9]. Transmission to the human occurs through the inhalation of contaminated water droplets.

Once in the lungs, *L. pneumophila* infects and replicates inside alveolar macrophages and causes widespread tissue damage [1].

In order to monitor the water systems routinely to predict any potential outbreaks, development of an on-site biosensor is of great importance. A biosensor for detection of *Legionella* should be specific and sensitive with capability of multiplex detection of different bacteria species. Furthermore, the biosensor for on-site applications should be portable, automated, cost-effective and rapid.

The current gold standard for detection of *Legionella* is a laboratory culture method, which is very time consuming (a matter of days) and is also unable to detect viable but non-culturable (VBNC) *Legionella* even though they are potentially pathogenic. Polymerase Chain reaction (PCR) is another popular detection method due to its sensitive and rapid analysis. Although PCR can analyze the samples within few hours, it is especially unreliable for environmental water samples due to presence of PCR inhibitors. One of the biggest drawbacks of PCR and other alternative methods such as DNA microarray and immunology-based assays [10-12], is the inability to distinguish between live and dead bacteria. Targeting ribosomal RNA is a feasible alternative that overcomes the aforementioned shortcomings. Since RNA expression level is directly correlated to the microbial activity, it provides a more reliable and accurate information for detection of *Legionella* [13]. Therefore, in this thesis, we proposed a detection system targeting the 16s rRNA from *L. pneumophila* by designing a set of DNA probes. The design of DNA probes, the surface chemistry and the optimization of the hybridization conditions were carried out in order to achieve high specificity and sensitivity of detection of *in vitro* transcribed 16s rRNA using Surface Plasmon Resonance imaging

(SPRi) and quantum dot signal enhancement. We then evaluated the performance of the proposed detection system for RNA extracted from pathogenic bacteria in complex environmental water samples containing other microorganisms such as amoeba. Finally, we focused on integrating the proposed detection system with a DMF device for rapid, automated and multiplex detection of 16s rRNA from pathogenic and non-pathogenic *Legionella* species. The detection of *Legionella* species targeting the 16s RNA within the miniaturized DMF device was found to be a promising detection system for on-site applications.

Chapter 2 Rationale

2.1 16s rRNA as reliable genetic material

The specific identification of biological species is essential for pathogen detection. Pathogens are generally recognized based on two main properties: via specific epitopes on the pathogen membrane or genetic contents. The former could be detected using antibodies or antibody alternatives such as aptamers while the latter implies the use of nucleic acid-based probes as biorecognition moieties. Since, it is very difficult to develop a library of aptamers for targeting epitopes on *Legionella*, antibodies presents the only option for their detection. However, although antibodies-based immunoassays provide rapid detection with minimal manipulation, they often suffer from a low specificity due to the cross-reaction with other species. The epitopes present on the cell's surface are normally found throughout the species. Therefore, generally a genus-level detection can be achieved [14]. Another drawback of using this method is the inability to distinguish between live and dead bacteria. Similarly to aforementioned methods, those based on targeting the DNA content [10-12], are also failed to distinguish between live and dead bacteria.

Targeting ribosomal RNA (rRNA) is a potential alternative that overcomes the aforementioned limitations, since it provides a detection system that is more reliable, accurate, and sensitive. The presence of RNA in bacteria is directly correlated with microbial activity, since following bacterial death, the associated RNA degrades relatively rapidly [15], further enhancing the accuracy and reliability of bacterial detection. Among RNA types, 16S rRNA is highly conserved between different species of bacteria and has been utilized for microbial identification [16, 17]. The presence of

high copy numbers of 16S rRNA in each bacterium is another incentive for identifying bacteria through the direct detection of 16S rRNA. However, risk of degradation and the presence of its secondary structure remain the significant shortcoming of using rRNA.

2.2 SPRi as detection method

Focusing on the detection of 16S rRNA, various sensing techniques, including electrochemical sensors [18, 19], impedance [20], fluorescent microscopy [21-23], surface-enhanced Raman spectroscopy (SERS) [24], and SPR [25, 26] were used for bacterial species-specific detection. Among these methods, SPR imaging (SPRi) has proven to be a versatile tool for the real-time study of genomic and proteomic interactions and kinetics. In contrast to classical wavelength or scanning angle SPR systems, SPRi provides visualization of the multiple interactions simultaneously in real time thanks to the integration of a charge-coupled device (CCD) camera with the associated sensogram. When compared to other end-point measurement systems, the use of SPRi allows real time monitoring and detailed kinetic analysis to further elucidate analyte's binding behavior as well as to better differentiate between specific and non-specific adsorptions.

2.3 Amoeba and *L. pneumophila* cohabitation

The interaction of protozoa, especially amoebae, with *L. pneumophila* in water systems is of great importance. *L. pneumophila* can normally survive in nutrition-deprived environments for long periods of time but cannot multiply. *L. pneumophila* has been observed to multiply in these environments only when amoebae were present. The ingestion of *L. pneumophila* by amoebae provides an intra-cellular environment for its amplification in water systems. In addition, amoebae can also act as a shelter against

harsh conditions such as low temperatures, nutrition-deprived environments and the presence of biocides [27-30]. In the case of a biocide treatment, this protection can result in treatment failure, after which *L. pneumophila* might be able to recolonize the water system rapidly. Another important impact of the amoeba-*Legionella* interaction is the enhancement of the virulence of *L. pneumophila* [31]. It has been reported that this interaction contributes to *L. pneumophila*'s virulence by priming the bacteria to infect human cells. Among amoebae, *Acanthamoeba* spp. is commonly isolated from *Legionella* contaminated water systems, a process which has been reported to support the intracellular life of *L. pneumophila* [27, 32, 33].

2.4 Integration of DMF with fluorescence microscopy

Recently, investigators have been more interested in the use of DMF in chemical and biological applications. In DMF, as opposed to continuous flow microfluidics, individual droplets (pL- μ L) are manipulated independently by applying electric fields to a series of electrodes array. Multiple droplets involving different reagents can be manipulated simultaneously and the operation scheme can be reprogrammed without the need to change the device design. Therefore, DMF is a promising candidate for applications involving complex and multistep assays [34]. Different bioassays have been performed using DMF devices such as immunoassays [35], cell culture [36], DNA hybridization [37] and PCR [38]. In the present work, in order to integrate the developed detection system into the DMF platform, some modifications including the use of magnetic beads and fluorescent microscopy were necessary. Magnetic beads provide a high surface-to-volume ratio and fast diffusion time. They can also be manipulated easily by external magnetic force which can be used for separation of the captured target from the solution.

Although the integration of the SPRi with DMF platform has been demonstrated previously [39], it has been mainly for simple and straightforward protocols. It must also be noted that in these reports, the movement of the droplets were carried out without the use of any oil shell.

For more complex droplet manipulations, the use of a thin oil shell is necessary in order to perform consistent long and automated protocols on the chip. However, the high refractive index of oil can interfere with the SPRi signal measurement and its residue on the detection spot can yield unreliable data. For these reasons, the fluorescent microscopy was used as detection mean instead of SPRi with DMF platform to fulfill the third objective of this PhD thesis.

Chapter 3 Hypothesis and Thesis Objectives

3.1 Hypothesis

It is hypothesized that designing specific DNA probes targeting the 16s rRNA of the *Legionella* integrated in DMF setup can provide a portable and cost-effective biosensor for automated and multiplex detection of viable *Legionella* bacteria.

3.2 Thesis Objectives

Based on the above hypothesis, the main objective of this thesis was to design and develop a portable biosensor system for rapid and multiplex detection of viable *L. pneumophila* in complex environmental samples with high sensitivity and specificity. This was achieved by defining three sub-objectives:

- **Develop a simple detection system that ensures the detection of viable *Legionella* with high specificity and sensitivity**

To achieve this aim a sensing platform compatible with SPRi was designed to detect viable *Legionella* bacteria through the appropriate selection of the target analyte and bioreceptor. Experimental conditions were optimized to ensure both high specificity and sensitivity.

- **Implementation of the detection platform developed in objective one for the detection of *L. pneumophila* in complex environmental water samples**

To validate the high specificity of the biosensing system, the detection of *Legionella*'s 16s rRNA was achieved in complex environmental water samples containing protozoa. The effect of residing *Legionella* in nutrition-deprived water

environment and its interaction with amoeba on the sensor output signal was investigated. Finally, the sensitivity of the detection system using environmental water samples in presence and absence of the amoeba was determined.

- **Integration of the developed detection system with a DMF chip toward on-site applications**

This goal was fulfilled by developing protocols for hybridization and droplet manipulation in the DMF chip in order to obtain the highest signal to noise ratio while minimizing the detection time and reagent consumption.

This dissertation is, therefore, a collection of published papers, or manuscripts under consideration, aimed to validate the hypothesis by fulfilling the above-mentioned objectives.

Preface to chapter 4 to 8: Background Information and literature

review

The following four chapters provide the contextual knowledge and comprehensive literature review required for the completion of this thesis project. Chapter 4 describes the principles and requirements of any biosensor technology. An overview of the SPR biosensor and DMF devices is presented in chapter 5 and 6 respectively. An extensive literature review related to *Legionella* is reported in Chapter 7. The biology of *Legionella*, the interaction of the *Legionella* with other microorganisms, the detection requirements for the environmental setting and different methods of disinfection are discussed. This chapter also covers the state of the art detection techniques along with commercially available detection kits for *Legionella*. Chapter 8 consists of a review article published in *Lab on a Chip* where the state-of-the-art in using microfluidic based biosensors for pathogen detection is presented. This review covers different topics including: biomarkers, amplification methods, sample preparation techniques and the design strategies for multiplex and point of care biosensors.

Chapter 4 Biosensors

A biosensor can be defined as an analytical device that uses biological reactions with a physiochemical detector for detecting target analytes. These devices mainly consist of two components: a bioreceptor and a transducer. A bioreceptor including antibodies, nucleic acids, enzymes, cell and viruses can recognize specifically the analyte while the transducer (optical, electrochemical, thermal and mass) generates an output signal [40] as a result of the biorecognition event. In addition to these two components, electronic parts (for processing the output signal), sample handling units and data processing algorithms constitute also the components of a biosensor. Sample handling units can include miniaturized filters for enrichment of the sample and removal of undesired compounds. Data processing algorithms allow for maximum information from the noisy measurements.

Electrochemical biosensors are great candidates for diagnostics applications. This is mainly due to their high sensitivity and compatibility with microfabrication technology towards their miniaturization. Electrochemical biosensors measure the electrical value (potential, current or impedance) from oxidation or reduction reactions [41]. The application of these biosensors are however limited to charge transfer phenomena and enzymatic reactions.

There are also biosensors based on mass measurement which detect very small changes caused by the binding of the target to the piezoelectric crystals [41]. The adsorption of the target analyte on the crystal results in a change in frequency of oscillation. This change can then be used to determine the mass of the analyte bond to the surface of the crystal. This method is simple and easy to use, however, in general it does

not provide high sensitivity in contrast to electrochemical or optical methods.

Biosensors based on optical transducers, are among the most popular ones since they allow for the measurement of different properties, such as polarization, amplitude, phase and energy. These methods include: fluorescence, adsorption, Raman, surface enhanced Raman and surface plasmon resonance.

Depending on the transduction technique and the nature of the target, receptors can be immobilized onto different substrates. These substrates can be made of a wide variety of substrates such as: polymer, glass and metal. In this context, optical methods such as fluorescence have an advantage over other techniques, as virtually any type of substrate can be employed for the detection of target species. In genomic applications, the detection of specific DNA or RNA sequences requires the design of complementary DNA/RNA to serve as the probe. In protein detection, antibody-based detection is one of the main analytical techniques for targeting specific antigens. Aptamer-based detection is an alternative for antibodies which is designed through a complex and time-consuming setup. Although very challenging, once the aptamer is designed, it offers high specificity to the target. For the detection of ions, mass spectrometry (using the mass to charge ratio) or electrochemical assays (an ion-specific chemical reaction in enzymatic conditions) are typically used. Three-dimensional templates have also been used for biorecognition elements. In this approach, generally referred to as molecular imprinting, a template of the chemical structure of the target is creating by polymerizing or crosslinking the monomers around the target.

There are many features that are required or desirable in a biosensor based on its specific application. Sensitivity, specificity and detection time are however the main

characteristics of any biosensor. In addition, for applications such as point-of-care or on-site detection, other critical features include portability, low cost, ease of use, automation, being self-contained (minimal use of accessories). Potential for mass production should also be considered. Although an ideal biosensor possesses most of these features, in practice, its capabilities may be tuned or prioritized according to the requirements of the detection platform.

Chapter 5 SPR Principle

In the early 20th century, Wood first observed that the plasmon phenomenon originates from unique electromagnetic properties of a metal-dielectric interface [42]. On the surface of the transition metal, free electrons that propagate along the surface can perform coherent fluctuations, called surface plasma oscillations [43]. These charge density oscillations along the metal-dielectric interface are accompanied by an electromagnetic field (Figure 5.1), which is described by Maxwell's Equations. In the simplest model, Maxwell's Equations are solved for semi-infinite metal in contact with semi-infinite dielectric media with complex permittivities $\epsilon_m = \epsilon'_m + i\epsilon''_m$ and $\epsilon_d = \epsilon'_d + i\epsilon''_d$, where ϵ'_j and ϵ''_j are real and imaginary parts of ϵ_j (where j is m or d).

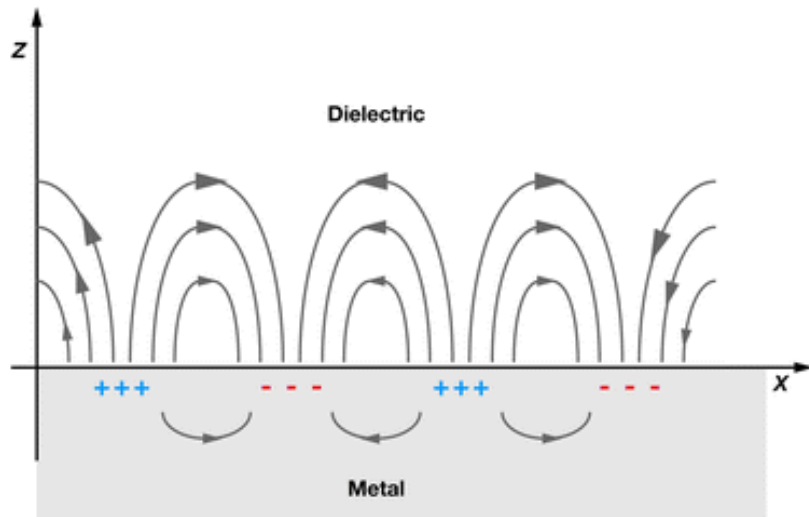


Figure 5-1 Metal-dielectric interface. Reprinted from Willets 2007 [44] with permission from Annual Review of Physical Chemistry.

The analysis of Maxwell's Equations with appropriate boundary conditions shows that only a single guided mode of electromagnetic field with electric field component along the surface (a surface plasmon) can be supported by this structure [45]. Since, surface plasmon is a transverse magnetic mode, its vector of intensity of magnetic field is in

plane with the metal-dielectric interface which is perpendicular to the direction of propagation (Figure 5-1). The electric field intensity of surface plasmon waves decays exponentially in both media with maximum intensity at the interface. The wave vector of the surface plasmon in the propagating x-axis is described by the following equation:

$$K_{sp} = \frac{\omega}{c} \sqrt{\frac{\epsilon_m \cdot \epsilon_d}{\epsilon_m + \epsilon_d}} \quad (\text{Eq. 5.1})$$

where c is the speed of light and ω is the frequency of oscillation. For a propagating wave in the presence of a dielectric medium (real ϵ_d), the second medium requires a negative dielectric function (ϵ_m) and its absolute value is bigger than ϵ_d . This can be achieved by most metals, particularly by gold and silver. For instance, for a water-gold interface, a field penetration depth at a wavelength of 850 nm is 400 nm into solution and 25 nm into the gold, can be fulfilled in a metallic medium [46].

The surface plasmon cannot be excited in free space directly by incident photons, since the latter does not have sufficient energy or momentum to couple to the surface plasmon at the metal-dielectric interface. The photon momentum should be increased to reach the required threshold to excite the surface electrons into oscillation and generate the plasmon wave. Since the electrons are resonating, this phenomenon is called SPR. As energy is absorbed in this resonance, the resonant coupling is observed as a minimum, or attenuated, reflected light intensity. There are two approaches to increase the photon momentum: attenuated total reflection and diffraction. The improvement and coupling between light and a surface plasmon is performed using a coupler. The three most commonly used couplers are prisms, waveguides, and grating couplers. The prism coupler is the most common method for excitation of the surface plasmons. In this

method the optical wave is passing through a high refractive index prism and is totally reflected at the interface between a thin metal layer and the prism, evanescently penetrating through the metal layer. This excitation causes a drop in the intensity of the reflected light that in turn results in a dip in the angular or wavelength of the reflected light.

In the grating coupler setup, corrugation is introduced to the metallic surface and the light is split into a series of beams directed away from metal surface. The interface is illuminated from the dielectric side and the reflected light is measured to track the resonance condition. This could cause noise to the measurement since the illumination traverses the sample solution. In the optical waveguide setup, the light entering via the optical waveguide, evanescently penetrates the metal film and excites a surface plasmon. A change in refractive index of the sample results in a change in the propagation constant of the surface plasmon. This subsequently leads to alteration of the characteristics of the light wave coupled with surface plasmon, such as the coupling angle and the wavelength. Based on the characteristics measured, SPR sensors are classified by the angle, intensity, wavelength or phase modulation [45].

In the angular interrogation mode, the strength of the incident light and the surface plasmon is observed by scanning the incident angle at a constant wavelength. This allows for a dip in angular spectrum of reflected light to represent the excitation of the surface plasmon. Conversely, in the wavelength interrogation mode, the surface plasmon excitation is achieved by using multiple wavelengths, such as polychromatic light at a constant incident angle. Since the resonance angle and wavelength are dependent on the refractive index, the shift in these parameters is correlated to the change

in the binding of molecules to the biosensor interface. In addition to these interrogations, intensity modulation is an alternative for monitoring the resonance condition. This is based on measuring the reflected intensity due to changes in refractive index of the analyte at a fixed angle and wavelength.

SPRi is based on the integration of a CCD camera with the sensogram which provides visualization of the multiple interactions in real time as opposed to classical SPR systems. This was first explored by Rothenhäuslar and Knoll in 1988 [47]. In this approach a monochromatic polarized light from a laser diode with a specific wavelength shines on the surface. The SPRi can spatially scan or capture changes in resonance condition over a surface area and create a contrast image. Therefore, any error of spotting or surface defects can be identified and removed from measurements. In addition, the potential for high-throughput screening of the bimolecular interaction makes this method very attractive. Among different laser wavelengths, it has been shown that the near infrared excitation wavelength (800-1152 nm), improves the performance of the SPRi [48].

One of the major shortcomings of SPR detection system is the lack of sufficient sensitivity for very dilute concentration analytes. Therefore, there have been many efforts to enhance the sensitivity of SPR detection systems mainly using nanomaterials either as substrate or as an amplification tag. Noble metallic, magnetic and liposomes based nanoparticles and carbon based materials, as well as two-dimensional nanostructures on the SPR substrates are amongst the most common ones [49]. There are different characteristics of the nanoparticles that can be used to tune the signal enhancement in the SPR systems including: nanoparticle's size, shape and dielectric constant of nanoparticles

and its surrounding medium [50].

Noble metallic nanoparticles, in particular gold nanoparticles are amongst the most popular materials for enhancing the SPR sensitivity. This is mainly due to the ease of preparation and functionalization with different chemical moieties [51]. The dominant phenomenon for the signal enhancement for gold nanoparticles is the interaction and coupling localized surface plasmon from nanoparticles and surface plasmon.

Among the different nanoparticles, quantum dots have been recently utilized for SPRi signal enhancement. For instance it has been demonstrated that the near infrared quantum dots had a more pronounced signal enhancement for SPRi in detecting DNA and proteins [37, 52]. The mechanism for this phenomenon is not well understood yet. however it has been suggested that the near infrared fluorophores couple the scattered light more strongly onto gold nanostructures [52, 53]. In addition, it has been shown that the nanometer thick gold have a stronger absorption in the near infrared compared to the visible range [54]

The use of magnetic nanoparticles [55], carbon nanotubes [56] and liposomes [57] for signal enhancements are mainly due to their large surface mass loading. Magnetic nanoparticles are particularly interesting due to their ability to be manipulated using an external magnetic force and their ease of functionalization [55]. Graphene is another interesting material for signal enhancing in SPR setup. It has been demonstrated that the graphene layer on gold surface can result in better sensitivity, which is mainly due to increasing the surface area for analytes adsorption and charge transfer from graphene to gold surface [58].

With recent advances in nanofabrication technology, two-dimensional

nanostructures have also been explored lately and integrated into the SPR detection systems [59]. The rapid and reproducible fabrication of these structures can lead to label-free SPR signal amplification.

Chapter 6 Digital microfluidic Principles

In digital microfluidic, discrete droplets are manipulated electrostatically on an array of electrodes coated with a hydrophobic dielectric insulator. There are two different formats of DMF: closed and open (Figure 6-1). In the close format, the droplet is sandwiched between two substrates patterned with electrodes. The top plate which is transparent, normally has the continuous ground electrode and the bottom plate possesses an array of actuation electrodes. In the open format, the droplet is placed on top of the electrodes array coated with a dielectric layer. In this setup, actuation and ground electrodes are in the same substrate. In both formats, a dielectric layer is deposited on top of the actuation electrodes and is followed by coating with a thin hydrophobic layer. One of the major advantages of the closed system compared to open system is reducing the evaporation of the droplet, which allows the implementation of the fluidic functions such as droplet dispensing and splitting.

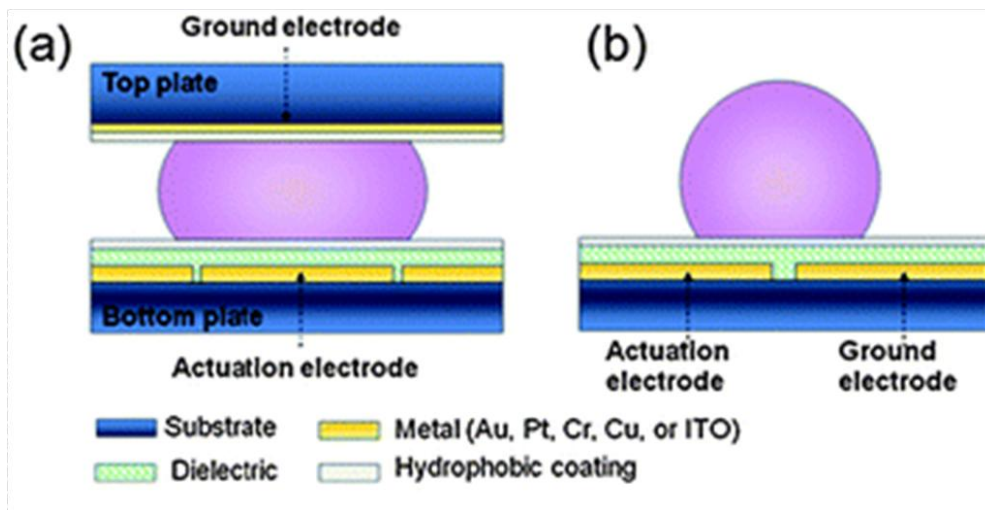


Figure 6-1 EWOD actuation configurations: (a) closed and (b) open EWOD system. Reproduced from [60] with permission from The Royal Society of Chemistry.

DMF devices were investigated and popularized in the 2000s mainly by the Fair group [61]. This technique is also called “electrowetting-on-dielectric” (EWOD).

Electrowetting on bare electrodes results in a small contact angle change which tends to be irreversible. In order to alleviate this issue, a layer of dielectric is employed to improve the contact angle change and reversibility of the electrowetting. In these devices, by applying a voltage, the free energy of the dielectric layer is changed and it reduces the solid-liquid interfacial tension, which results in a change in wettability on the surface. Therefore the contact angle of the droplet on the surface is dramatically reduced when a potential is applied.

The basic characterization of the movement of the droplet in EWOD is based on a thermodynamic approach using the Young-Lippman equation [62]:

$$\cos \theta = \cos \theta_0 + \frac{\epsilon_0 \epsilon_1 V^2}{2\gamma d} \quad (\text{Eq. 6.1})$$

In this equation, θ_0 and θ are the contact angle before and after the use of the potential, respectively. ϵ_0 and ϵ_1 represent the relative permittivity of the dielectric layer and free space, respectively. γ is the surface tension of the liquid-filler media, and d is the dielectric thickness. In the thermodynamic approach, droplet movement is described as being the result of changes in interfacial energy as a result of the accumulation of charge at the surface.

The issue with the thermodynamic approach is that it only addresses the static problem, and does not explain the change in the contact angle in mechanical terms. This can be achieved by considering the electric forces acting on the droplet. Therefore, the electromechanical approach is a better method to determine the electrical forces exerted by the electric field at the interface [63-65].

These forces can be estimated by integrating the Maxwell–Stress tensor, T_{ij} (Eq. 6.2) over any surface surrounding the droplet [66]: where δ_{ij} is the Kronecker delta, \mathcal{E} is the

permittivity of the medium surrounding the droplet, E is the electric field surrounding the droplet, and i and j refer to pairs of x , y , and z axes.

$$T_{ij} = \varepsilon \left(E_i E_j - \frac{1}{2} \delta_{ij} E^2 \right) \quad (\text{Eq. 6.2})$$

This formulation can account for the motion of dielectric liquids [67] and liquids with low tension surface that do not experience a change in contact angle [68].

Chapter 7 *Legionella*

7.1 Legionellosis

Legionellae are Gram-negative, non-spore-forming, rod-shaped bacteria. They contain branched-chain fatty acids and require L-cysteine and iron for growth. *L. pneumophila* multiplies at temperatures between 25°C to 42°C, with an optimal growth temperature of 35°C [69] and a generation time of 99 minutes under optimal conditions [70]. Its diameter and length vary between 0.3-0.9 µm and 2-20 µm, respectively [71].

Legionellae were first detected in 1976 in Philadelphia after a notable outbreak of pneumonia in a hotel on the occasion of a United States Army Veterans' meeting [72]. Legionellosis is a modern era disease, because of human alteration in the environment especially increasing the temperature in the water systems. *Legionella* in the natural water environment would be a rare cause of human disease.

The fatality rate of Legionellosis ranges between 10% and 40%, however, it approaches 50% within hospital and industrial outbreak settings, particularly affecting individuals with compromised health status [1]. Presently, more than 50 *Legionella* species have been identified with approximately half of these species being associated with humans. *L. pneumophila* is responsible for more than 90% of Legionellosis. A list of *Legionella* species and their associations with human disease is presented in Table 7-1. To have an accurate and reliable evaluation of the water risk assessment, it is thus crucial to design detection systems that can distinguish between pathogenic and non-pathogenic *Legionella* [6, 7].

L. pneumophila is found in most natural and engineered water systems, where it contaminates and multiplies inside amoeba [8]. The literature indicates that modern water

systems, such as air-conditioning units, showers and industrial refrigeration towers, provide optimal growth conditions for *L. pneumophila* and propagate its transmission through aerosol [9]. Transmission to the human host occurs through the inhalation of contaminated water droplets. Once in the lungs, *L. pneumophila* infects and replicates inside alveolar macrophages and causes widespread tissue damage [1]. Legionnaires' disease has no unique clinical or radiographic features [73, 74] which may lead to inappropriate therapy and a poor prognosis.

Table 7-1 *Legionella* species and their association with human diseases.

Species associated with disease	Species not associated with any disease
<i>L. pneumophila</i>	<i>L. spiritensis</i>
<i>L. bozemanii</i>	<i>L. jamestowniensis</i>
<i>L. dumoffii</i>	<i>L. santicrucis</i>
<i>L. micdadei</i>	<i>L. cherrii</i>
<i>L. longbeachae</i>	<i>L. steigerwaltii</i>
<i>L. jordanis</i>	<i>L. rubrilucens</i>
<i>L. wadsworthii</i>	<i>L. israelensis</i>
<i>L. hackeliae</i>	<i>L. quinlivanii</i>
<i>L. feeleeii</i>	<i>L. brunensis</i>
<i>L. maceachernii</i>	<i>L. moravica</i>
<i>L. birminghamensis</i>	<i>L. gratiana</i>
<i>L. cincinnatiensis</i>	<i>L. adelaidensis</i>
<i>L. gormanii</i>	<i>L. fairfieldensis</i>
<i>L. sainthelensi</i>	<i>L. shakespearei</i>
<i>L. tucsonensis</i>	<i>L. waltersii</i>
<i>L. anisa</i>	<i>L. genomospecies</i>
<i>L. lansingensis</i>	<i>L. quateirensis</i>
<i>L. erythra</i>	<i>L. worsleiensis</i>
<i>L. parisiensis</i>	<i>L. geestiana</i>
<i>L. oakridgensis</i>	<i>L. natarum</i>
	<i>L. londoniensis</i>
	<i>L. taurinensis</i>
	<i>L. lytica</i>
	<i>L. drozanskii</i>
	<i>L. rowbothamii</i>
	<i>L. fallonii</i>
	<i>L. gresilensis</i>
	<i>L. beliardensis</i>

7.2 The interaction of *Legionella* with other organisms and its significance

One of the critical factors that allows bacteria to amplify, is the presence of the nutritional factors inside the milieu. *Legionella* requires a unique combination of nutrients in order to grow in the laboratory setting. The nutrient levels for *Legionella* growth are rarely found in water systems. However, *L. pneumophila* can normally survive in nutrition-deprived environments for long periods of time but cannot multiply. Their multiplication occurs in these environments mainly when amoebae also present. This is due to the fact that the ingestion of *L. pneumophila* by amoebae provides an intra-cellular environment for its amplification in water systems [27, 32, 33]. In addition, amoebae can act as a shelter for *L. pneumophila* against harsh conditions, such as low temperatures, nutrition-deprived environments and the presence of biocides [27-30]. This protection may result, for instance, in the failure of the treatment, after which *L. pneumophila* can be able to rapidly recolonize the water system. Another important impact of amoeba-*Legionella* interaction is enhancing the virulence of *L. pneumophila* [31]. It has been reported that this interaction contributes to its virulence by priming the bacteria to infect human cells. The life cycle of *L. pneumophila* in amoeba resembles that of macrophages. In both amoeba and human phagocytes, coiling phagosomes engulf the bacteria, and once phagocytized, the phagosome does not acidify or fuse with the lysosomes. The interaction of *L. pneumophila* with both amoeba and mammalian phagocytes is very similar. This similarity can suggest that the virulence of *L. pneumophila* for macrophages is an outcome of its evolution as a parasite of amoebae [1]. Among amoebae, *Acanthamoeba* species (spp.) is commonly isolated from *Legionella* contaminated water systems.

7.3 Standards level of *Legionella* in environmental settings

There is a lack of consistent standards for acceptable levels of *Legionella* in an environmental setting. The level that requires action varies depending on the source of the contamination and its exposure. Table 7-1 summarizes the *Legionella's* level in different settings requiring action for the decontamination of the water source. For example, the acceptable *Legionella* level in cooling towers is generally three order of magnitude greater than domestic running water. In French healthcare setting, elderly patients with a history of alcoholism and smoking have a maximum allowable level of 10,000 CFU/L, whereas for the high-risk patients using immunosuppressants, the threshold is 250 CFU/L in the water system [75].

Table 7-2 CFU of *Legionella* per liter based on USA Occupational Safety & Health Administration technical manual: https://www.osha.gov/dts/osta/otm/otm_iii/otm_iii_7.html

Action	Cooling tower	Domestic water	Humidifier
Prompt cleaning	100,000	10,000	1,000
Immediate cleaning	1,000,000	100,000	10,000

7.4 Eradication/Disinfection

There are different methods for eradication/disinfection of the *Legionella* from water sources. These methods can be classified into four categories: 1) thermal disinfection 2) ultraviolet (UV) irradiation, 3) chemicals (chlorine, ozone, iodine), 4) metal ionization (copper and silver). Increasing the temperature above 60 °C is one of the most reliable methods for elimination of *Legionella* from water systems. An 8 log reduction in *L.*

pneumophila concentration has been demonstrated within 25 minutes of water treated at 60°C, 10 minutes at 70°C, and 5 minutes at 80°C [76]. UV irradiation is another method for eradication of bacteria. Although *Legionella* is more susceptible to UV compared to other gram-negative bacteria [77], the UV irradiation is insufficient by itself and needs to be complemented with additional disinfectant methods [78]. Among chemical disinfectants, chlorine has been widely used for disinfecting potable water and swimming pools. *Legionella* is much more resistant to chlorine than many other bacteria such as *E. coli*. The concentration of chlorine which is needed to continuously control *Legionella* is 2-6 times more than typical chlorine concentrations in domestic potable waters [78]. In addition, there are different issues, namely corrosiveness and chlorine toxicity associated with the use of chlorine, which makes it less desirable. Utilizing metal ions, especially copper and silver ions, has been shown to be effective in disinfecting the water systems. These ions are believed to interfere with enzymes and bind to DNA that ultimately lead to bacterial death [79]. Some reports suggest that for hot-water storage tanks, the use of metal ions is more effective than using periodical superheat (77°) [80]. Although using the metal ions is proven as a viable option, for hot water systems, there are not many reports on using these metal ions. It should be mentioned that because of the environmental implication of using these chemicals, the minimum concentrations should be utilized in order to minimized adverse effects.

7.5 Current Detection Methods for *Legionella*:

Current conventional detection methods include identification via laboratory culture and PCR [10, 11]. Laboratory culture is the current gold standard method employed to detect *L. pneumophila*. In order to improve the sensitivity of this method, the medium used for

the culture of *Legionella* is constantly revisited. The currently used medium is composed of buffered charcoal-yeast extract (BCYE) agar enriched with ketoglutarate [81]. Although the specificity of this method is near 100%, the sensitivity for complex samples does not exceed 60% [82, 83]. In addition, if the samples under study contain other microorganisms, they could inhibit *Legionella's* growth. Another drawback of bacteria cell culture methods is its inability to detect VBNC *Legionella*, even though they might potentially be pathogenic.

While laboratory culture entails long procedures requiring several days, PCR is a faster detection methodology and highly specific. Compared to culture method, the PCR analysis has a tremendous advantage, since it provides high negative predictive value (80– 100%) [84, 85]. A negative PCR result can be a good predictor of a negative culture. Thus, for *L. Pneumophila*, negative PCR results are quite useful as a risk indicator [84, 85]. There are some reports suggesting a correlation between data obtained by culture method and via PCR for hot water samples. However, only two publications could be found that discuss this correlation in the case of cooling tower water samples [84, 85]. This could be due to negative culture reading and high positive PCR results since in general, the later provides greater accuracy than culture reading [86, 87].

Although very reliable, one should also deal with many disadvantages of PCR technique, notably laborious post-amplification procedures, time consuming, limited assay optimization and validation, false positive results and issues with distinguishing between live and dead cells [88]. There is on-going research to address these problems. For example, Chang *et al.* [89] used ethidium monoazide (EMA) and propidium monoazide (PMA) to prevent dead cells from participating in the PCR reaction. The authors showed

that although both materials were useful for this assay, the required amount of EMA was one quarter of that of PMA. Yang *et al.* used real time PCR with 23-5S rRNA as target. In this study, *L. Pneumophila* and *Legionella* spp were detected with a LOD of 7.5 CFU/mL [88].

In addition, real-time PCR results depend strongly on the nature of the testing site and its treatment that very often make the interpretation of the results and its comparison with data obtained through bacterial culture very challenging. In a thorough study that compared the culture method to real-time PCR of samples in cooling water systems obtained from different sites in Europe, a significant difference between the results of real-time PCR and culture methods was observed. Real-time PCR reading of bacteria number always exceeded the CFU count of the culture methods [90].

Other methods, namely antibody-based detection, have also been utilized extensively [91]. The Choi group [92] used antibody-based SPR for detection of *L. pneumophila*. The authors used a self-assembled protein G layer on a gold surface along with monoclonal antibody to specifically target *L. pneumophila* and achieved a LOD of 10^5 bacteria/mL. Protein G is a cell wall protein found in most species of Streptococci [92] and has been used for improving the orientation of antibodies. It exhibits a specific interaction with the Fc portion of IgG [91]. Another group used side-polished optical fibers with a 850 nm LED and halogen light source in a surface plasmon resonance setup. A specific chemistry was used to immobilize antibodies against *L. pnemophila* and a LOD of 10 CFU/mL was achieved [93]. Similarly, *legionella* and *E. coli* were detected in 3 hours with a LOD of 10^6 cells/mL using antibodies by surface acoustic waves [94].

In order to lower the LOD and reduce the data collection time, new trends

concentrate on improving the transducers capabilities. A compact SPR sensor targeting the *L. pneumophila* using specific antibodies was developed that was able to detect 10^3 CFU/mL in approximately one hour [95]. The use of a electrochemical impedance spectroscopy with a disposable immunochip was expanded for *Legionella*'s detection in spiked water samples with a sensitivity of 2×10^2 cell/mL in around one hour [96]. Besides, an optical sensing method so-called 'Optical Waveguide Light mode Spectroscopy' was introduced for detection of *Legionella*. Glutaraldehyde was used to bind antibodies to the sensor surface. This detection system was able to detect 10^4 CFU/mL in 25 min [97].

Flow cytometry alone or in combination with other methods, is also used for the detection of *Legionella*. For instance, in a recent demonstration, 5×10^5 cell/mL was detected in less than 3 hours [98]. Further, filtration and immunomagnetic separation were combined with flow cytometry, resulting in detection of 50 *Legionella* cells per liter in two hours. Although this technique offered a good sensitivity, no correlation to plate counting was observed, making the interpretation of the data difficult [99].

The antibody detection method is fairly rapid, but cross-reactivity between species is a critical shortcoming that limits the specificity of the technique. DNA/ Peptide nucleic acid (PNA) microarray-based detection targeting DNA in bacteria is another alternative that provides the desired specificity by targeting species-specific sequences in DNA [100].

The main drawback of all the aforementioned methods is their inability to differentiate between live and dead bacterial cells. This feature is critical for achieving accurate and reliable read out. To overcome the limitations of using DNA and antigen targeting-based

techniques, detection of the bacterial RNA is a viable alternative approach. A summary of different detection setups, including the advantages and limitations of each detection method is presented in Table 7-2. The presence of RNA in bacteria can be correlated with microbial activity, since following bacterial death, the associated RNA degrades relatively rapidly [15]. Among RNA types, 16s rRNA is highly conserved between different species of bacteria and has been utilized for microbial identification [16, 17, 101]. The presence of high copy numbers of 16s rRNA in each bacterium is another motivation to identify bacteria through the direct detection of 16s rRNA. However, instability and the presence of a secondary structure are significant drawbacks of using ribosomal RNA. The secondary structure renders access to the target sequence difficult. This is why methods such as using multiple adjunct probes, heat denaturation, and fragmentation are often used to circumvent this issue [22, 26]. Focusing on the detection of 16S rRNA, various sensing techniques, including electrochemical sensors [18, 19], impedance [20], fluorescent microscopy [21-23, 102], surface-enhanced Raman spectroscopy (SERS) [24], and SPR [25, 26] were used for bacterial species-specific detection. Among these methods, SPRi has proven to be a versatile tool for the real-time study of genomic and proteomic interactions and kinetics. In contrast to classical wavelength or scanning angle SPR systems, SPRi provides visualization of the multiple interactions simultaneously in real time thanks to the integration of a CCD camera with the associated sensogram.

Table 7-3 Comparison of different detection techniques for pathogenic bacteria

Method	Advantages	Limitations
PCR	<ul style="list-style-type: none"> • high sample throughput • high sensitivity • quantitative (Real-time PCR) 	<ul style="list-style-type: none"> • no live/dead cell differentiation • susceptible to polymerase inhibitors
Antibody-based methods	<ul style="list-style-type: none"> • differentiation of subspecies • quantitative and qualitative 	<ul style="list-style-type: none"> • low sensitivity • low specificity • high cross-reactivity • slow and expensive assay
Conventional culture based methods	<ul style="list-style-type: none"> • inexpensive • simple • specific • gold standard method 	<ul style="list-style-type: none"> • laborious and time-consuming • inability to detect VBNC • low sample throughput
Ribosomal RNA based methods	<ul style="list-style-type: none"> • detects only living cells • minimal interference by sample matrix • high specificity • quantitative and qualitative • detects VBNC 	<ul style="list-style-type: none"> • limited probe design

In contrast to other end-point measurement systems, the use of SPRi allows detailed kinetic analysis that is monitored in real time, to further elucidate analyte binding behavior as well as to differentiate better between specific and non-specific adsorptions. To date, few reports on detecting 16S rRNA within an SPR setup are available in the literature. Nelson *et al.* [103] detected 16S rRNA from *E. coli* with a limit of detection (LOD) of 2 nM through the use of DNA probes. Joung *et al.* [25] used PNA probes and electrostatic interaction between positively charged gold nanoparticles and negatively charged RNA as a signal post-amplification method, achieving a LOD of around 100 pM,

which is far from the desired sensitivity in the context of the detection of pathogenic *L. pneumophila* in a water sample.

7.6 Commercially available detection kits

A list of commercially available detection kits targeting *Legionella* is summarized in Table 7-3. Among these detection kits, several of them are based on immunochromatographic tests, including FastPath, Legipid, VIRapid and *Legionella* Testing Kits. In these kits, specific antibodies are functionalized onto the strips on the detection pad and the change in color of strips is used to evaluate the presence of target bacteria. Therefore, they provide only a positive or negative readout of target pathogens within our hour, when the bacteria concentration is over 100 CFU/mL; no further information is available regarding the number and state of the bacteria.

In an approach developed by a Vermicon Inc, a German company, the culture method and direct immunofluorescence are combined. In this technique, bacteria are first pre-cultivated for 2-3 days and then stained using two different fluorescent dyes for detection of both *Legionella* spp. and *L. pneumophila*.

There are also detection kits based on real-time PCR. These kits are not normally self-sustaining and require a thermo cycler and fluorescence reader. Although these kits only facilitate the process, they are not suitable for on-site experiments. For instance, Qiagen and Pall provide *Legionella* detection kits based on real-time PCR in less than one hour.

Sigma-Aldrich recently released a new detection system called HybriScan for various pathogenic bacteria including *L. pneumophila*. The detection technique is based on targeting the 16s rRNA within the bacteria using capture and detector probes. It

possesses also a labeled detection probe that allows for an enzyme-linked optical signal readout. This detection technique is composed of a filtration and enrichment step, cell lysis, RNA recovery, hybridization with DNA probes, immobilization onto binding plates, enzyme coupling, detection reaction and finally, signal measurements and readouts. This detection method detects only viable bacteria with high specificity but it is very laborious and has to be performed by specialized technicians.

Table 7-4 List of the commercially available Legionella detection kit.

Name	Company	LOD	Time	Pre-treatment	Comments	Reference
FastPath	NALCO	100 cells/mL	25 min	--	Sensitivity=80% yes or no result immunochromatographic test	http://www.nalco.com/services/fastpath.htm
Legipid	Biotica	LOD=100 CFU	1 hour	yes	magnetic bead	http://www.biotica.es/en/Videos
Legionella Testing Kits	hydrosense	100 CFU/mL	25 min	No	Yes or no result immunochromatographic test	http://www.hydrosense.biz/kits.php
VIRapid® LEGIONELLA CULTURE	Vircell	--	15 min	--	immunochromatographic test Yes or no result	http://en.vircell.com/products/rapid_tests/?tx_gtkvircell_pi1%5Buid%5D=830&cHash=c5c52bbd68b9fb0fa61998b730e51805
mericon Quant Legionella spp Kit	Qiagen	10 GU per reaction	>1 hour	yes	qPCR required sample prep, Thermal cycler and fluorescent reader	http://www.qiagen.com/products/catalog/assay-technologies/complete-assay-kits/food-safety-testing/mericon-quant-legionella-spp-kit#technicalspecification
GeneDisc Rapid Microbiology System	PALL	5 GU/PCR well	3 hours	yes	qPCR the primers and probes are dried out within the plate	http://www.pall.com/main/biopharmaceuticals/product.page?id=52011
HybriScan	Sigma-Aldrich	--	2.5 hours	yes	Detection of rRNA	http://www.sigmaaldrich.com/technical-documents/articles/microbiology-focus/legionella-detection.html

Chapter 8 Microfluidic designs and techniques using lab-on-a-chip devices for pathogen detection for point-of-care diagnostics

Amir M. Foudeh,^a Tohid Fatanat Didar,^a Teodor Veres^{a,b} and Maryam Tabrizian^{a*}

^a Biomedical Engineering Department, McGill University, Montreal, QC,

H3A 2B4, Canada. E-mail: Maryam.Tabrizian@mcgill.ca; Fax: +1-514-298-7461; Tel: +1-514-398-8129

^b National Research Council of Canada, 75 Boul. de Mortagne, Boucherville, Québec, Canada, J4B 6Y4

8.1 Abstract

Effective pathogen detection is an essential prerequisite for the prevention and treatment of infectious diseases. Despite recent advances in biosensors, infectious diseases remain a major cause of illnesses and mortality throughout the world. For instance in developing countries, infectious diseases account for over half of the mortality rate. Pathogen detection platforms provide a fundamental tool in different fields including clinical diagnostics, pathology, drug discovery, clinical research, disease outbreaks, and food safety. Microfluidic lab-on-a-chip (LOC) devices offer many advantages for pathogen detection such as miniaturization, small sample volume, portability, rapid detection time and point-of-care diagnosis. This review paper outlines recent microfluidic based devices and LOC design strategies for pathogen detection with the main focus on the integration of different techniques that led to the development of sample-to-result devices. Several examples of recently developed devices are presented along with respective advantages and limitations of each design. Progresses made in biomarkers, sample preparation, amplification and fluid handling techniques using microfluidic platforms are also covered and strategies for multiplexing and high-throughput analysis, as well as point-of-care diagnosis, are discussed.

8.2 Introduction

The World Health Organization (WHO) recently reported that infectious diseases is the second leading cause of mortality throughout the world after cardiovascular disease [104]. This problem is particularly severe in developing countries and deprived areas of developed countries, that suffer from poor hygiene and limited access to centralized labs for diagnostics and treatments. Half of the mortality in poor countries is due to infectious disease [105]. As in developed countries, despite great progress in enhancing health conditions, there are still several issues that remain to be resolved in regards to food industries, pathogen outbreaks, and sexually transmitted diseases [106]. It is worth mentioning that in the USA alone, food-borne pathogens were the main cause of more than 50 million illnesses reported in 2011 [107]. Overall, pathogens are of great importance in many different fields, including diagnostics, pathology, drug discovery, clinical research, biological warfare, disease outbreaks, and food safety.

Conventional and standard methods of pathogen detection include cell culture, PCR, and enzyme immunoassay, which are often laborious and take from several hours to days to perform. Pathogen detection methods should be cost-effective, fast, sensitive, and accurate. For point of care (POC) applications, the detection platform should also be simple to use and interpret, stable under a wide range of operating conditions (such as temperature, humidity), preferably portable and disposable [108]. Furthermore, they should provide the required sensitivity and specificity [109]. The ability to perform multiplex tests is another important prerequisite for pathogen detection devices, especially in the case of diseases with several pathogen sources, such as lower respiratory infections [108]. One of most successful non-microfluidic POC devices is so far the

immuno-chromatographic strip (ICS), which is currently used in developing countries [110-112]. Despite some issues with the test's sensitivity and specificity, ICS has been considered an ideal model for the development of microfluidic-based devices for the pathogen detection by taking advantages of low cost, sensitivity, specificity, portability, and simplicity of microfluidic option. Microfluidics provides a higher surface to volume ratio, a faster rate of mass and heat transfer, and the ability to precisely handle very small volumes of reagents, ranging from nano to picoliters, in microchannels. Because of these characteristics, microfluidic devices provide better performance than conventional systems for providing a rapid detection time. The use of microfluidics in the context of Lab-on-a-Chip (LOC) devices has begun to play an important role in the analytical investigations of biological and chemical samples in a single miniaturized device. These devices inherently possess the characteristics that make them suitable for POC applications.

Here, we review the present status of microfluidic-based devices for pathogen diagnostics, emphasizing innovative designs, strategies, and trends during the past three years.

8.3 Biomarkers

The specific identification of biological species or their strains is essential for pathogen detection. Pathogens are generally recognized based on two main properties: by genetic contents, using nucleic acid-based probes, or by specific epitopes on the pathogen membrane or their produced toxins, using antibodies or antibody alternatives. Usually, the latter approach provides a lower specificity compared to nucleic acid-based approach, because the epitopes present on the cell's surface are normally found throughout the

species. Then, generally, genus-level detection is achieved [14], but this can provide results in a shorter time with less manipulation. List of different biomarkers used to detect pathogens summarized in Table 8-1.

8.3.1 Antibodies

Antibody-based detection is one of the main analytical techniques used for the detection of pathogens. Although labour-intensive, Antibody-based detection has proven to be a crucial and important factor in the specific and high-affinity detection of pathogens. Engineering antibody fragments, recombinant antibody-fragments (rAbs), single chain variable fragments (scFv) and monovalent antibody fragments (Fabs) are recent approaches that have originated from the antibody-based detection. These use of these fragments is more cost-effective while providing the same specificity limit as conventional antibody methods [113]. The detection of specific proteins and of the whole cell are the two most common applications of antibody-based probes.

8.3.1.1 Protein and toxin detection using antibodies

Recently, antibody-based probes were used for the detection of several toxins, including Ricin A Chain (RCA), Staphylococcal Enterotoxin B (SEB) toxin surrogate [114], ovalbumin [115], and cholera toxin subunit B (CTB) [116]. Microarray immunoassays have also been used extensively for the multiplex detection of proteins and toxins [117, 118].

8.3.1.2 Whole cell detection

Antibody cell-based pathogen detection in microfluidic systems has been demonstrated using different biosensing tools, including Surface Plasmon Resonance (SPR) [119],

fluorescence [120], impedance [121], chemiluminescence [93], and conducting polymers [122], and impedance [123].

Applying a whole-cell detection approach, pathogens such as influenza [124], *E. coli* [125, 126], *L. pneumophila* [127], hepatitis B, hepatitis C and HIV [128] could be detected.

8.3.1.3 Alternatives to the antibody

Although antibodies are widely accessible and easy to use, they have several drawbacks, such as expensive cost, poor chemical and physical stability, large size, use of animals for antibody production, limited antibody availability for all potential analytes, and quality-assured preparations. There are several emerging alternatives to antibodies, including enzyme-substrate reactions [129], molecular imprinted polymers [130], protein-based [131], small molecule probes [132] aptamers [133-137], and antimicrobial peptides (AMPs) [138].

The main advantage of enzyme-substrate reactions in comparison to Ab-Ag is that they can be regenerated several times without loss of affinity or specificity. For instance, there are enzyme inhibition-based sensors for toxin detection, e.g., the detection of Sarin (a highly toxic material) in blood by using immobilized cholinesterase on a microfluidic chip [129]. Enzymes can also be used to target proteins. For instance, Le Nel *et al.* [139] developed a microfluidic chip for the detection of pathological prion protein (PrP) by proteinase K (PK)-mediated protein digestion.

Molecular imprinted polymers (MIPs), which can be produced at a low cost in relatively high stability and reproducibility, are another alternative to antibodies [140, 141]. A microfluidic chip coupled to the MIP method was developed for the detection of

the Tobacco Mosaic Virus (TMV) and the Human Rhinovirus serotype 2 (HRV2) using impedance measurement [130].

Protein-based pathogen detection is another approach in which the crucial point is preserving the native state and orientation of the protein in order to provide high specificity and sensitivity [142]. For instance, heat shock protein 60 (Hsp60), which is a receptor for listeria adhesion protein (LAP) during *L. monocytogenes* infection, was utilized for the detection of the LAP. By using Hsp60, higher sensitivity and capture efficiency was achieved in comparison to the use of a monoclonal antibody. Another feature of this protein is that it can be produced in *E. coli* by the recombination of cDNA, making it a cost-effective choice [131].

Small molecule probes have also emerged as alternatives to antibody-based detection. For instance, Kell *et al.*[132] developed a vancomycin-modified nanoparticle for the isolation of gram-positive and -negative bacteria. Although its selectivity is less than those of monoclonal antibodies, it is a useful tool for capturing a wide range of bacteria with single vancomycin-functionalized nanoparticles. It was shown that the architecture and orientation of the molecule are crucial to an efficient target capture. Overall, by using small molecule probes, the long-term stability, reaction conditions, and temperature for surface modification are more flexible compared to those of an antibody-based approach.

Aptamers are fairly recent options to replace antibodies [135]. Aptamers are nucleic acid molecules developed by an *in vitro* process, which can bind to their molecular targets, such as small molecules, proteins, or cells [136], with high affinity and specificity [143]. Aptamers have several distinct advantages over antibodies, including

Table 8-1 Detection of pathogens implemented in microfluidic devices

Pathogen	Probe	LOD	Sample	Time of analysis	Amplification	Ref	
<i>E. coli</i> O157:H7	antibody	10 ⁶ CFU mL ⁻¹	Soil sample	–	–	[144]	
	Antibody, primer	200 CFU mL ⁻¹	Synthetic	–	PCR	[145]	
	Primer	3.58×10 ⁵ copies μL ⁻¹	Synthetic	Hotdog, banana, milk	13 min	PCR	[146]
		10 ⁸ CFU mL ⁻¹					
	AMP(Antimicrobial peptide magainin I)	1 bacteria μL ⁻¹	Synthetic	–	–	[138]	
	DNA probe	25 CFU mL ⁻¹	Synthetic	–	–	[147]	
	Antibody	32 CFU μL ⁻¹	Synthetic	20 min	–	[126]	
	Antibody/DNA probe	100 bacteria	Synthetic	–	PCR	[148]	
	Primer	1 cell in 10 ⁵	Synthetic	4 hr	PCR	[149]	
Polycloonal antibody/primer	0.6 CFU L ⁻¹	Lake water	5 hr	PCR	[150]		
<i>E. coli</i> K12 and O157:H7	antibody	10 CFU mL ⁻¹	Iceberg lettuce	6 min	–	[151]	
<i>E. coli</i> K12	Antibody	55 cells mL ⁻¹	PBS	1 hr	–	[125]	
		100 cells mL ⁻¹	Milk				
<i>E. coli</i> BL21	Primer	10 ⁶ cells mL ⁻¹	Blood samples	1 hr	PCR	[22]	
<i>E. coli</i> DH5α, <i>S.s</i> <i>aprophyticus</i>	PNA probe	1 CFU μL ⁻¹	Synthetic	30 min	–	[152]	
		100 CFU μL ⁻¹	Urine				
<i>E. coli</i> (BL21(DE3))	Antibody	10 ⁴ CFU mL ⁻¹	Synthetic	–	–	[123]	
<i>E. coli</i> XL-1	Primer	1000 Bacteria mL ⁻¹	Synthetic	30 min	NASBA	[153]	
<i>E. coli</i> DH5R	DNA probe	10 ⁸ CFU mL ⁻¹	Clinical urine sample	40 min	–	[23]	
		80 CFU mL ⁻¹	Synthetic				
<i>Botrytis cinerea</i>	Antibody	0.008 μg mL ⁻¹	Apple (Red Delicious)	40 min	–	[154]	
	DNA probe	8 fmol	Synthetic	1 hr	–	[155]	
<i>B. cinerea</i> , <i>D. bryoniae</i> , and <i>B. squamosa</i>	Primer/probe	0.2 ng μL ⁻¹	Synthetic	3 min	PCR	[156]	
<i>Staphylococcus aureus</i>	Primer	<10 copies	Synthetic	<20 min	RPA	[157]	
	Antibody	1 CFU	Synthetic	30 min	–	[158]	
<i>Salmonella</i> <i>Enterica</i>	Primer, probe	8.8 ng mL ⁻¹	Synthetic	–	RCA	[159]	
<i>Salmonella</i> <i>berta</i>	DNA probe	10 ³ CFU mL ⁻¹	Synthetic	25 min	–	[160]	
<i>Bacillus globigii</i>	Antibody	1 CFU mL ⁻¹	Synthetic	30 min	–	[122]	
Surrogate biotoxin (ovalbumin)	Antibody	50 ppb (18 ng mL ⁻¹)	Raw milk sample	–	–	[115]	
Cholera toxin subunit B (CTB)	Antibody	1.0 ng mL ⁻¹	Synthetic	1 hr	–	[116]	
Botulinum toxoid	DNA/antibody	25 pg	Synthetic	–	–	[161]	
Phage M13K07	Anti-M13	10 ⁹ pfu mL ⁻¹	Synthetic	–	–	[162]	
Rotaviruses	Primer	3.6×10 ⁴ RNA copies μL ⁻¹	Stool	1 hr	RT-PCR	[163]	
H1N1	Primer/probe	10 TCID ₅₀	Throat swab	3.5 hr	RT-PCR	[164]	
Swine influenza virus	Antibody	610 TCID ₅₀ mL ⁻¹	Synthetic	6 min	–	[124]	
Influenza A virus (AH1pdm)	Primer	5.36×10 ² copies mL ⁻¹	Synthetic	15 min	RT-PCR	[165]	
Influenza B, coronavirus OC43, influenza A, and human metapneumo virus	Primer	4.8, 6.3, 10, and 167 copies, respectively	Synthetic	2 hr	RT-PCR	[166]	
HIV-1	Primer	10 HIV particles	Spiked saliva sample	–	RT-LAMP	[167]	
Noroviruses (NVs) and Rotaviruses (RVs)	Primer	6.4×10 ⁴ copies μL ⁻¹	Synthetic	1 hr	RT-PCR	[168]	
Nervous necrosis virus (NNV)	Primer	10 fg of cDNA	Grouper larvae	1 hr	RT-LAMP	[169]	
Pseudorabies virus (PRV)	Primer	10 fg DNA μL ⁻¹	Synthetic	1 hr	LAMP	[170]	
Severe acute respiratory syndrome (SARS) virus SARS DNA	Primer	3×10 ⁷ copies μL ⁻¹	Synthetic	–	HDA	[171]	

enhanced affinity and specificity, resulting in better limit of detection (LOD) for biosensing applications. Typically, they are also smaller than antibodies, enabling them to bind to epitomes that are otherwise inaccessible to antibodies [136]. Aptamers are selected in conditions similar to those of a real matrix and can be modified during immobilization, without any adverse effect on their affinity. Finally, they can be subjected to several cycles of regeneration [172].

On the other hand, aptamers require a long selection time and several resources to target a specific epitope. Normally, the systematic evolution of ligands by exponential enrichment (SELEX) is used to isolate aptamers. Lou *et al.* [133] developed a magnetic bead-assisted SELEX technique using microfluidics to reduce processing time. This design could isolate the target aptamers after a single round, as compared to conventional SELEX methods, which usually require 8–15 rounds of selection. A particular feature of this device is ferromagnetic patterns imbedded in the microchannel, which are capable of producing highly localized magnetic field gradients that provide precise control over a small number of beads. This device also benefits from the laminar flow characteristics, which result in minimizing the molecular diffusion to obtain higher purity. As a proof of concept, aptamers were selected for Botulinum neurotoxin type A. In another effort to reduce aptamer discovery time, Ahmad *et al.*[134] developed a microfluidic SELEX platform in which they found new aptamer sequences for PDGF-BB in only three rounds. Antimicrobial peptides (AMPs) are also used to take benefit from their intrinsic stability, ease of synthesis, and long-term functionality compared to antibodies. AMPs can be found in nature, such as in the extracellular milieu of bacteria and on the skin of higher organisms [138]. Mannoor *et al.* [138] AMP for the detection of *E. coli*, using impedance

measurement as a label-free and portable biosensor platform. The semi-selective antimicrobial peptide magainin I, which occurs naturally on the skin of African clawed frogs, was immobilized on the arrays of gold electrodes for the detection of *E. coli*. The LOD of one bacterium per μL was obtained. Depending on the targeted application, AMPs provide advantages and disadvantages. If the goal is to detect a broad range of pathogens, they would be useful because AMPs are semi-selective toward their target. However for the identification of a very specific target in a pathogenic mixture, they might not be appropriate.

8.3.2 DNA/PNA:

DNA hybridization assays provide unique advantages compared to conventional antibody-based approaches due to their capabilities for sensitive, specific, and rapid detection of target nucleic acids [173]. Recently, various microfluidic DNA-based probes were coupled to different measurement techniques, including SPRi [37], conductance impedance [164, 174-176], and (FRET) fluorescence [177]. For more information please refer to a review paper [178] for DNA microfluidic based and an integrated microfluidic system for DNA analysis [179].

Wang *et al.* [155] implemented two different methods to distinguish a single mismatch using gold nanoparticles (GNP). In the first approach, a glass surface was coated with a monolayer of GNP, which increased the hybridization efficiency due to nano-scale spacing between the probes. In the second approach, a DNA amplicon bounded to GNP was introduced to the probe-functionalized surface. Riahi *et al.* [23] used a double stranded DNA probe for the detection of bacterial 16s rRNA. Double stranded DNA is composed of an actual complementary DNA probe to the target with a fluorescent dye at

the 5' end. A shorter probe is then hybridized to the first probe, with a quencher at the 3' end, in which the 5' of the first probe is in the proximity of the 3' of the second probe. After introducing the target, the quencher probe is replaced by the target, resulting in a fluorescent signal. This setup was used to detect different pathogens in a clinical urine sample, and a total experimental time of less than 40 min was achieved.

Peptide nucleic acid (PNA) is a DNA analogue with a peptide backbone instead of a sugar phosphate backbone. PNAs normally exhibit chemical and thermal stability, resistance to enzymatic degradation, faster hybridization kinetics, and the ability to hybridize at lower salt concentrations. Lower salt concentrations help to denature the secondary structures of targets, such as RNA. PNA beacons were designed for the detection of 16s rRNA from *E. coli* in a droplet-based microfluidic device, without any pre-amplification steps. In this method, DNA beacons were labeled with fluorescent dyes and quenchers at both ends. Because of the loop shape of the beacons, they are both in proximity of each other in an unhybridized state. After hybridization, this loop broke down, and the quencher became ineffective, due to its distance from the dye, resulting in the fluorescence emission [180]. In another approach, PNA molecular beacons were used for the detection of the PCR amplicons. The PNA beacon had a reporter and a quencher at each end in proximity of each other before hybridization. After hybridization with the target DNA, fluorescence emission from the reporter occurred upon excitation. This setup could discriminate a single-base mutation at a 100 nM concentration [181]. Conversely, a LOD of 1 CFU μL^{-1} in 30 minutes was obtained by Lam *et al.* [152] when a PNA probe immobilized on the nanostructured microelectrodes (NMEs) is used for the detection of *S. saprophyticus* and *E. coli*. One of the drawbacks of the PNA probes is their relatively

higher cost compared to DNA probes.

8.4 Amplification Methods

8.4.1 PCR and its design

Polymerase Chain Reaction (PCR) is a molecular technique for DNA amplification. It plays a key role in genetic analysis, biology, and biochemistry research, since it is able to replicate a specific fragment of a target nucleic acid by cycling through three temperature steps and creating several million DNA copies within a few hours. Integrating microfluidics with PCR not only could provide the previously mentioned advantages in implementing microfluidic systems, but also could yield lower thermal capacity and a higher heat transfer rate, and could significantly reduce the reaction time [182]. Pan *et al.* [183] developed a multichamber PCR microfluidic chip coupled to multichannel separation and temperature control units for parallel genetic analysis. The device did not require any additional fluidic control unit and was easy and simple to operate. PCR products were separated and detected in these channels utilizing electrophoresis. The hepatitis B virus (HBV), *Mycobacterium tuberculosis* (MTB), and the genotyping of human leucocyte antigen (HLA) were detected using this platform.

Preventing the sample evaporation is one of the main challenges to overcome with using PCR in microfluidic systems. This issue is particularly problematic in open reaction channels. To address this challenge, Wang *et al.* [184] used non-miscible mineral oil to cover the liquid and prevent its evaporation during the experiment. *Salmonella enterica*, *Escherichia coli*, and *Listeria monocytogenes* could then be simultaneously detected using an oscillatory-flow multiplex PCR. This design achieved an evaporation loss of less than 5% while decreasing the detection time to less than 24 min.

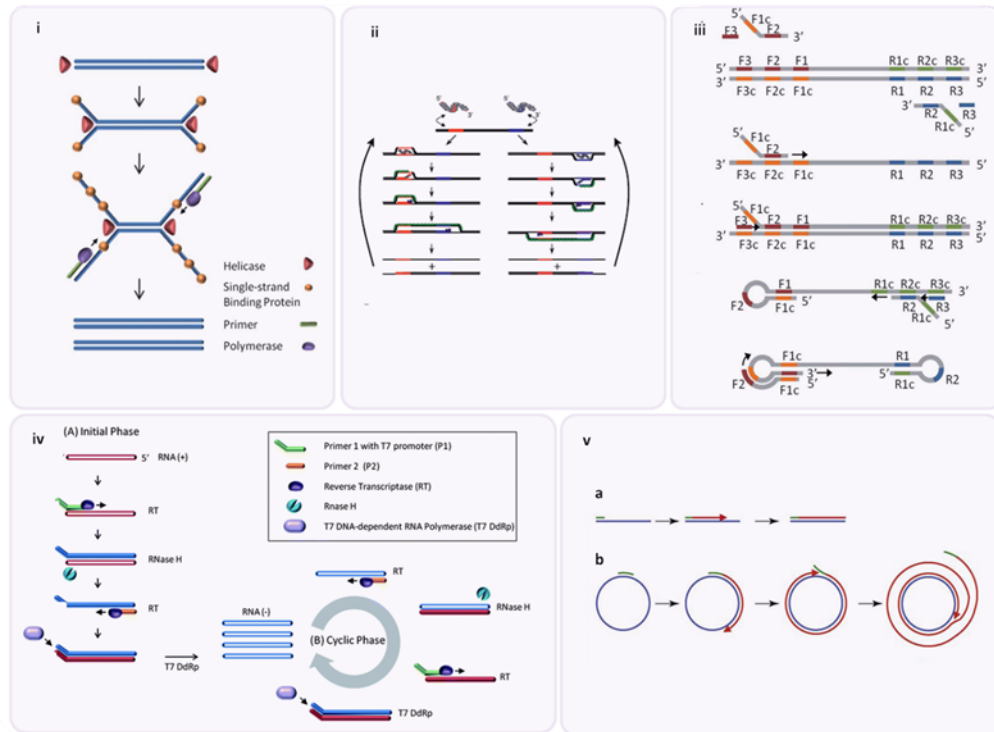


Figure 8-1 Schematics of isothermal amplification methodologies: (i) HDA: dsDNA is unwind by Helicase enzyme then single-strand binding protein stabilizes the strands. Finally a double-stranded copy is produced using Primers and polymerase. (Reproduced from Ref. [185] with permission from Royal Society of Chemistry.) (ii) RPA: Primers bind to template DNA and a copy of the amplicon is produced by extension of the primers using a DNA polymerase. (Reproduced from Ref. [186] with permission from Public Library of Science.) (iii) LAMP: Template synthesis initiated by the primer sets resulting in stem-loop DNAs with several inverted repeats of the target sequence. In this schematic, only the process using forward primer set is shown. (Reproduced from Ref. [185] with permission from Royal Society of Chemistry.) (iv) NASBA: (A) The initial phase to synthesize complementary RNA to the target RNA and (B) In the cyclic phase, each newly synthesized RNA can be copied, leading to exponential amplification. (Reproduced from Ref. [185] with permission from Royal Society of Chemistry.) (v) RCA: (a) Linear template and single primer (b) Circular template and single primer. Blue and green lines represent target DNA and oligonucleotide primers respectively. (Reproduced from Ref. [187] with permission from Elsevier.

In some cases when entire bacteria were introduced to the detection PCR platform, captured bacteria inside the microfluidic device could be lysed by thermal [188], chemical [189], physical [190, 191] and electrical means [192]. For instance, Cheong *et al.* [193] developed a one-step real-time PCR method for pathogen detection. In this design, Au nanorods were used to transform near-infrared energy into thermal energy and subsequently lyses the pathogens. Next, DNA was extracted and amplified in the PCR chamber. This one-step lysis improved the overall efficiency of the device because there

was no need to change or remove reagents.

PCR was integrated with different sample preparation and separation devices to obtain higher sensitivity and specificity. For instance, sample cleanup was used along with PCR to detect human respiratory viral pathogens. Capillary electrophoresis was implemented for the post amplification sample cleanup and separation step in conjunction with PCR, and results were obtained in less than two hours [166]. Target enrichment, capture, lysis, and real-time qPCR were used for the detection of *E. coli* in water samples in eight different samples independently and simultaneously. Before capturing the target cell, two filtration steps were performed to remove particles, followed by sample enrichment. Antibodies coated on the PMMA surface were used to capture the target cells in the next step. After washing to remove nonspecific attachment, cells were removed using a cell stripper solution and thermally lysed. Next, the genetic contents were used in real-time PCR amplification, and the LOD of 6 CFU was achieved in less than 5 hours [150].

8.4.2 Isothermal

The isothermal amplification [185, 194] of DNA/RNA have recently drawn interest since it does not require a large thermal momentum and energy for temperature cycles as compared to PCR systems. Therefore, it is a simpler and more energy efficient approach, making it an excellent choice for POC applications. Methods for isothermal amplification, include loop-mediated isothermal amplification (LAMP) [195-197], helicase-dependent amplification (HDA) [198], nucleic acid sequence-based amplification (NASBA) [153], recombinase polymerase amplification (RPA) [157, 199] and rolling circle amplification (RCA) [187].

One of the most common isothermal amplification methods is LAMP. Although this technique is primarily used for DNA amplification, by reverse transcriptase it can also be implemented for RNA samples. The obtained signal can be visualized either by fluorescent intensity measurement or by the naked eye for turbidity due to precipitation, which makes it suitable for locations with limited resources. Generally, four primers are used to recognize six distinct sequences of the target DNA with a working temperature of around 60-65 °C (Figure 8-1-iii). Fang *et al.* [170] used LAMP amplification for the detection of Pseudorabies viral

DNA. The design consisted of eight parallel microchannels, enabling simultaneous reactions for high-throughput analysis. The entire device is sealed with uncured PDMS, which prevents evaporation and bubble formation. The result can be visualized by a compact real-time absorbance device or even by the naked eye. Using this method, 10 fg of DNA per μL were detected within 1 hr, which is faster and more sensitive than PCR, and consumes less sample volume. The higher sensitivity, simplicity, and low cost of this design make it suitable for use in POC diagnostics. In another approach, the LAMP method was used in a disposable self-heating cartridge [200]. The temperature control was provided by the exothermic reaction, using a Flameless Ration Heater (FRH) activated by water. A DNA sample collected from *E. coli* in urine samples was detected via the LOD of the 10 *E. coli* DNA within 1 hr. LAMP was also integrated with a low-cost CCD-based fluorescent imaging system [201]. Various features of the imaging system, such as gain, offset, and exposure time, were optimized to achieve better sensitivity. The performance of this low-cost CCD imaging system was comparable to commercially available PCR systems. Six different waterborne pathogens were tested

with this device, and it could detect single DNA copy in 2 μ L in less than 20 min. Using RNA as a target in the LAMP method requires a reverse transcription to convert the RNA into DNA. This method was implemented to detect HIV RNA [167] and the nervous necrosis virus (NNV) in grouper larvae [169]. For NNV detection, functionalized magnetic beads (MB) conjugated with a specific probe were used to capture the RNA from the grouper tissues. To generate a uniform temperature, an array-type micro-heater was utilized. As a result, more specific and faster extraction could be achieved. A LOD of 10 fg of DNA was found which was 100-fold more sensitive than RT-PCR.

For HDA method, the helicase enzyme opens the double-stranded DNA in order to let the primers hybridize, extend, and become two copies (Figure 8-1-i). This mechanism operates at the same temperature range as LAMP, but it is simpler because it requires two enzymes and, similar to PCR, only two specific target oligos. However, compared to the LAMP method, it is longer. The HDA method was successfully used to detect the ovarian cancer biomarker Rsf-1 [198], severe acute respiratory syndrome (SARS) virus DNA [171], and *E. coli* [202].

HDA was also used in a fully integrated microfluidic system, which contained bacteria lysis, extraction, and HDA amplification of the DNA on a disposable cartridge. With this setup, 10 CFU of *E. coli* were detected in less than one hour [202].

In the transcription-based RNA amplification system or NASBA, initially developed by Compton *et al.* [203] (Figure 8-1-iv), three enzymes are involved in the reaction, namely avian myeloblastosis virus reverse transcriptase, RNase H, and T7 RNA polymerase. Generally, NASBA produces more than 10^9 copies in 90 min at a temperature around 40 °C and different types of nucleic acids, including tmRNA, rRNA, mRNA, ssDNA, and

virus nucleic acid, can be analyzed. One of the drawbacks of this method is its inability to amplify the double strand of DNA since an initial temperature of 95 °C is required, adding more complications to the design. Dimov *et al.* [153] used a NASBA method for the detection of *E. coli*. The tmRNA (10Sa RNA) was used as target because of its high stability compared to mRNA, high copy number, and presence in most bacteria. This characteristic increased the sensitivity and shortened the experimental time. Before the amplification step, silica beads were used for the purification and concentration of the RNA from the sample. Applying real-time detection, the LOD of 100 cells in less than 30 min was achieved.

RPA first introduced in 2006 [186], (Figure 8-1-ii) for DNA amplification at low temperature (37 °C). RPA couples strand-displacement DNA synthesis with isothermal recombinase-driven primer targeting of the sample, resulting in an exponential amplification. The sensitivity of the RPA is similar to that of conventional PCR. For instance, the *mecA* gene from *Staphylococcus aureus* was detected with an LOD of 10 copies in less than 20 min [157].

RCA is another alternative method to RPA, which is also performed at a low temperature (37 °C). RCA (Figure 8-1-v) is useful for circular DNAs, such as viruses, plasmids, and bacteriophage genomes. This method can be used to amplify circular probes, which are designed to circularize upon binding to a target and seal by ligation [204]. For instance, it has been shown that circular viral DNA could be amplified by RCA using bacteriophage phi29 DNA polymerase without the use of primers [187]. *V. cholerae* DNA was also detected with an LOD of 25 ng DNA in around 1 hr using an electrophoretic microchip setup [205].

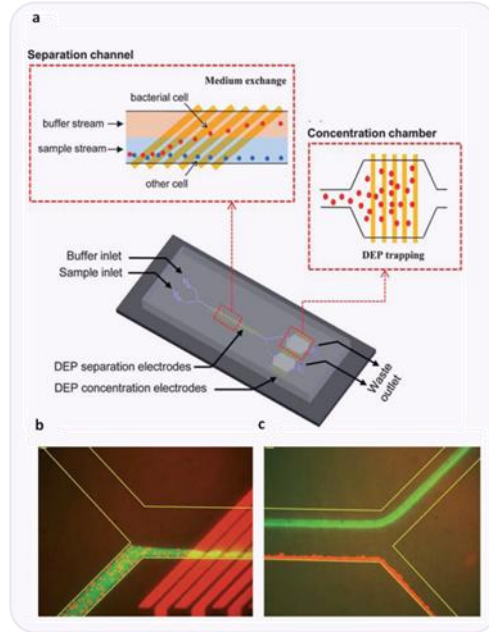


Figure 8-2 (a) Schematic of the DEP integrated in a microfluidic device for continuous cell separation and concentration. (b) Fluorescence microscopy image of separation channel inflow (c) fluorescent image of separation channel outflow. (Reproduced from Ref. [206] with permission from Royal Society of Chemistry.)

In another attempt, Sato *et al.* [159] developed a fully integrated microchip by using padlock probes and RCA in which solid phase capture in the microchannel was used to employ RCA on the bead for single molecule detection. Thirty amol genetic DNA from *Salmonella* were detected by this system.

8.5 Sample preparation

Placing the initial sample in contact with the biomarker without sample preparation would hinder sensitivity and specificity. Therefore, the sample preparation steps are of high importance in achieving high sensitivity and specificity in any detection platform. The enrichment of the target analyte and/or the removal of inhibitors are two main strategies in this regard. This is especially important in the case of complex matrices, such as blood, saliva, interstitial fluid, and environmental samples composed of many

different entities. Dielectrophoresis (DEP), micro/nano particles, and filters are three simple and straightforward approaches for sample preparation.

8.5.1 DEP

In the presence of electric fields, particles express dielectrophoretic activity. When subjected to a non-uniform electric field, polarised particles will move towards regions of high or low electric fields. A particle's polarisability in its surrounding medium induces dielectrophoretic motion towards (positive DEP) or away from (negative DEP) the electrode

surface. The strength of this force depends on several factors, including the particle's electrical properties, shape and size, and the frequency of the electric field. Therefore, to manipulate a group of desired particles, a particular frequency should be applied. However, positive DEP cannot be used to enrich bacteria in physiological media, which has a high conductivity, since it only works in the media with low conductivity.

To overcome said limitation, Park *et al.* [206] used a combination of positive and negative DEP to continuously separate and concentrate bacteria from physiological samples, such as cerebrospinal fluid and blood. This microfluidic platform was used to concentrate the bacteria up to 104-fold by taking millilitre volumes of the target samples. The separation efficiency in the buffer was 87.2% for *E. coli* in human cerebrospinal fluid and blood, as shown in Figure 8-2.

In another effort [207], a DC insulator DEP was developed in which arrays of cylindrical insulators were implemented inside a microchannel. By using negative DEP, *E. coli* and *Saccharomyces cerevisiae* were enriched and separated in less than 2 min. Applying different configuration of electrodes would be effective in terms of the decay of

the field and control over targets. For example, three-dimensional DEP was developed by positioning the electrodes on the top and bottom of a microchannel. In this research, different bacteria, such as *Staphylococcus aureus* and *Pseudomonas aeruginosa*, were continuously sorted and concentrated with a higher efficiency than that of 2D electrode configuration [208].

8.5.2 Particles and beads

Magnetic, metallic, polymeric, and liposome-based micro/nano particles have proven to be effective in obtaining higher sensitivity and selectivity for pathogen detection. Microbeads, due to their high surface-to-volume ratios and low diffusion times, can increase the chance of biorecognition [114].

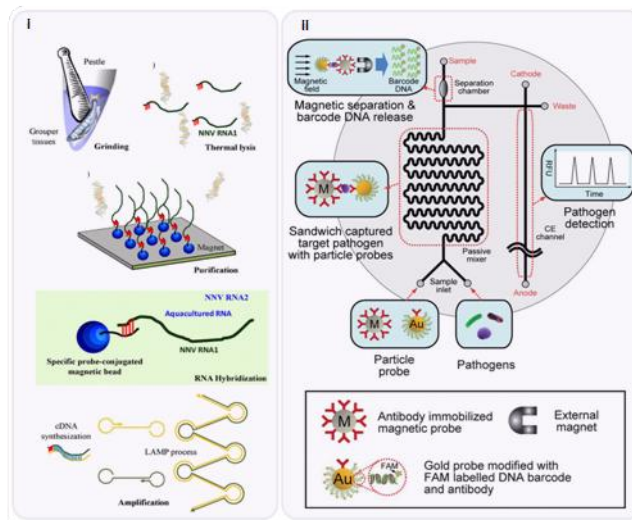


Figure 8-3 (i) Schematic diagram of integrated microfluidic LAMP system for RNA purification and NNV detection. (Reproduced from Ref. [169] with permission from Elsevier.) (ii) Schematic illustrations of an integrated PMMS-CE microdevice for multiplex pathogen detection. The microdevice consists of a passive mixer, a magnetic separation and a capillary electrophoretic microchannel to identify target pathogens. (Reproduced from Ref. [158] with permission from Royal Society of Chemistry.)

8.5.2.1 Micro/nano particles

Micro/nano particles have been extensively used for nucleic acid extraction and enrichment [149, 153, 169, 209] or for whole cell enrichment [125, 126, 145, 149, 158,

210, 211]. Silica beads were employed to extract RNA from biological samples in a microfluidic system [153, 209], reducing the chance of contamination and RNA degradation. Bhattacharyya *et al.* [209] used a solid-phase extraction system, which was formed by trapping silica particles in a porous polymer monolith. RNA of the influenza A (H1N1) virus could attach to silica particles, be isolated from the infected mammalian cells and detached later for further manipulation. In another approach, silica beads were immobilized on a bed to purify and concentrate RNA from a mammalian cell sample infected with influenza. Immobilized beads increased the capture efficacy by passing the solution back and forth on the bed to increase the RNA capture efficiency by 10^2 -to 10^3 -fold as compared to that of non-immobilized beads [153]. For whole-cell detection, antibody-immobilised glass beads were applied inside a microchannel to capture *E. coli* with up to 96% efficiency [126].

8.5.2.2 Magnetic beads

Although microparticles provide a high surface-to-volume ratio and fast diffusion time, their manipulation is uniquely dependent on the applied flow conditions. To add another degree of freedom for particle manipulation, magnetic beads can be used and controlled by magnetic fields. This would increase the selectivity through enhanced discrimination between specific and non-specific targets [212, 213].

A popular strategy for magnetic bead-based detection relies on enhancing the mixing and capturing of the probe-functionalized beads with the sample, followed by applying a magnetic field to capture the beads and surface rinsing. For instance, Wang *et al.* [169] used a specific probe conjugated to magnetic beads to capture the target RNA from the entire tissue lysate. After target hybridization, the beads are immobilized on the surface

using a permanent magnet, and the lysate is washed out in the channel. This is followed by isothermal amplification of the captured RNA (Figure 8-3-i). Applying this strategy, magnetic beads were also used to capture and enrich target cells from the sample. To obtain an even distribution of beads in the channels, the beads were situated after each split in a bifurcated channel. In this way, a bed of beads is formed by a magnetic field. The sample flowed through this bed, and after washing, off-chip PCR and CE were performed to enhance the capture efficiency of *E. coli* O157 in a background of *E. coli* k12 [145]. Using the same approach, magnetic beads could be functionalized with enzyme-labeled antibodies for the electrochemical detection of pathogens, such as *E. coli* [125]. Since non-specific binding is at least an order of magnitude weaker than specific ligand-receptor binding [214], the Fluidic Force Discrimination (FFD) method could be used to control target attachment and nonspecific detachment under flow conditions in microfluidic channels, as well as target capture selectivity [114]. Mulvaney *et al.* [114] employed FFD by applying sufficient force using the speed of laminar flow to selectively remove the nonspecific binding materials and to distinguish between specific and non-specific binding. Magnetic beads were used for the detection of the target in complex matrices, such as whole blood. After capturing the analyte by magnetic beads on the surface, the controlled flow passed over the analyte to remove the non-specific bindings due to the fact that non-specific bindings are at least an order of magnitude weaker than the specific ligand-receptor bindings [214]. The number of the beads was counted either by optical microscopy or magnetoelectronic sensor to obtain the density of the beads. As such, ricin A chain (RCA) and staphylococcal enterotoxin B (SEB) were detected with an LOD of around 300 fM.

Mujika *et al.* [210] developed a magnetoresistive immunosensor for the detection of *E. coli*. The device could detect small variations in the magnetic field caused by the conjugation of magnetic beads to previously immobilized antigens on the surface (antibody-antigen-antibody-magnetic bead). The results showed a very high specificity for *E. coli*, with the 105 CFU mL⁻¹ *E. coli* being compared to *salmonella* spp. as a negative control.

Passive mixing and detection using magnetic beads is another strategy in which mixing and target capture occur in flow conditions. Microfluidic design and flow control are important factors in this approach. Antibody-conjugated magnetic beads as capture probes and gold nanoparticles conjugated to the same antibody and fluorescently labelled DNA barcodes as complementary probes were used to detect bacteria that were sandwiched between the functionalized magnetic particle and gold nanoparticles [158]. Passive mixing was obtained through the design of the micromixer, which was used to attain the maximum cell capture efficiency. This design included an intestine-shaped serpentine around 18 cm in length, which could hold around 4 μ L (Figure 8-3-ii). Increasing the retention time in this setup caused higher mixing, and as a result, a high cell capture efficiency up to 75% capture was achieved with 20 min retention time. This was followed by separation of the MB-*E. coli*-GNP complex through applying a magnetic field and then purification of the non-conjugated particles by rinsing. DNA barcodes were then detached from the GNPs by heating (up to 90 °C) and were detected using fluorescence microscopy. A high number of the obtained DNA barcodes per GNP resulted in the single-cell detection of three different pathogens (*Staphylococcus aureus*, *E.coli O157:H7*, and *Salmonella typhimurium*) in less than 30 min.

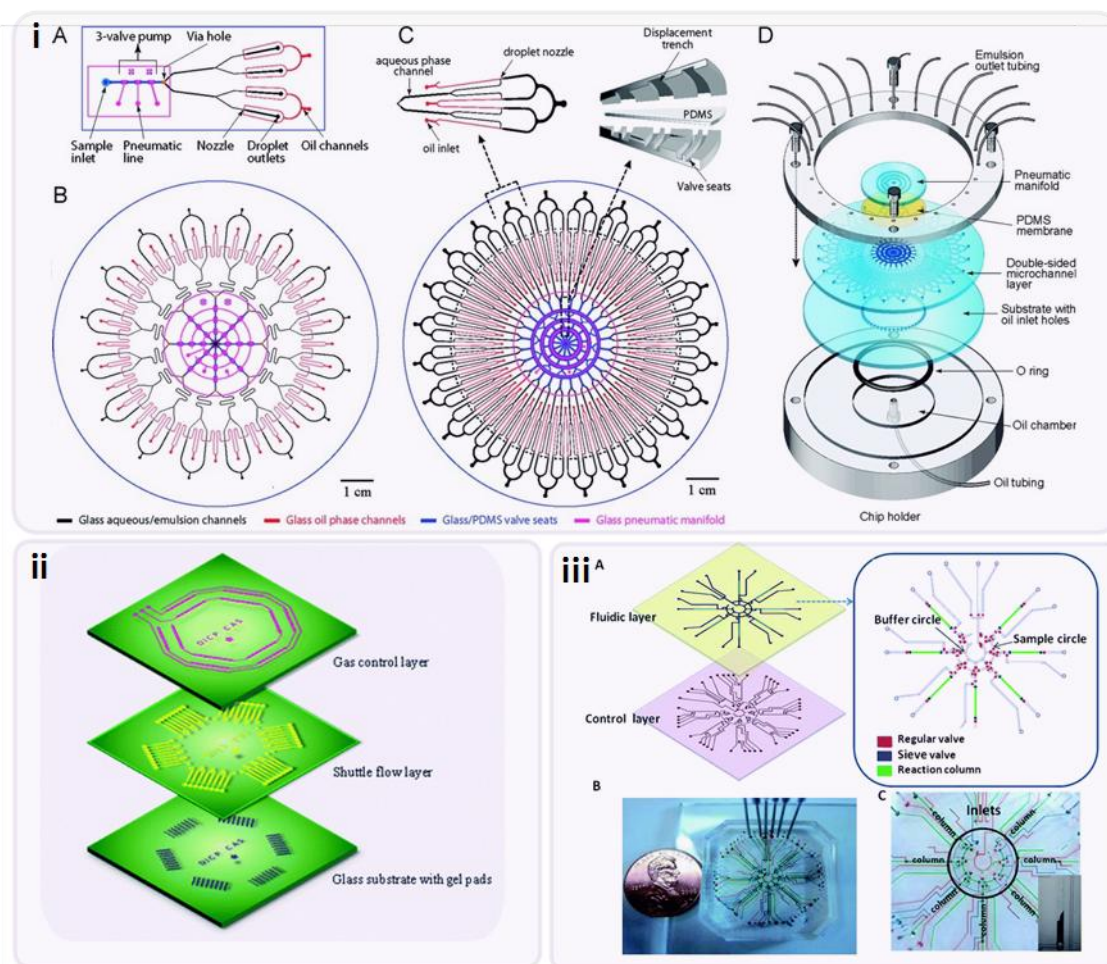


Figure 8-4 (i) Schematic of microfluidic emulsion generator (MEGA) array device. (A) Design of a glass-PDMS-glass hybrid four-channel MEGA device and (B) Layout of a 32-channel MEGA device. (C) Layout of 96-channel MEGA device. (D) Illustration of complete four layer 96-channel MEGA device and the plexiglass assembly module. (Reproduced from Ref. [149] with permission from American Chemical Society.) (ii): Exploded view of the microfluidic chip containing shuttle flow channels, micropumps and microvalves. (Reproduced from Ref. [215] with permission from Royal Society of Chemistry.) (iii): (A) Schematic representation of an immunoreaction chip used for detection of algal toxins. red and blue color represent the regular valves and sieve valves respectively. (B) and (C) Pictures of the microfluidic chip and central area of the chip. (Reproduced from Ref. [216] with permission from Royal Society of Chemistry.)

8.5.3 Filter

Filters are a cost-effective and straightforward alternative for the rapid preparation and enrichment of samples. Physical filtration systems can be made of aluminum oxide [217], polyimide [218], chitosan [219], poly carbonate [220], SU-8 [221] and silica [222]. Using multistep polycarbonate-based membranes (10 μm and 0.1 μm), *E. coli* cells could be

enriched up to 2×10^2 -fold in a microfluidic system [150]. Nano-sized membranes can also be used to separate small biological elements, such as antibodies and viruses. For example, Reichmuth *et al.* [124] used nanoporous polyacrylamide membranes (10 nm) to detect the influenza virus. The size-exclusion characteristics of the *in situ* polymerized membrane led to the simultaneous concentration of viral particles and the separation of virus-fluorescent antibody complexes, while unbound antibodies passed through the membrane. Compared to electrophoretic immunoassay solely, applying the membrane resulted in a faster detection time and higher sensitivity [124].

Filters can be chemically functionalized to be even more specific to selectively capture the target. For instance, Liu *et al.* [167] used Flinders Technology Associates (Whatman FTA) membranes as a filter for the isolation, concentration, and purification of nucleic acids. This filter specifically captures nucleic acids and also enhances the removal of inhibitors, which drastically increases the sensitivity of the detection platform.

3D microstructures in microfluidic platforms can be applied to physically filter biological elements. In this regard, microfabrication is required to produce structures such as micro-pillars. The patterned micropillars can later be chemically functionalized using microfluidics. Hwang *et al.* [22] implemented microfabricated micropillars with an affinity for bacterial cells inside a PCR chip to detect *E. coli* in blood samples. Bacteria were first captured on the micropillars, and the rest of the sample, containing PCR inhibitors, was washed away.

8.6 Design strategies for pathogen detection

Many efforts have been made towards the development of novel designs based on microfluidic principles for rapid, automated, and high-throughput analysis of pathogen

detection in order to obtain robust and detailed information from complex samples containing different pathogens.

8.6.1 Strategies to develop high-throughput multiplex devices

Rapid, multiplex and high-throughput detection of multiple pathogens requires the implementation of parallel microchannels, embedding micro-pumps, micro-valves, and/or discretizing the flow into controllable droplets. These features could be only obtained through appropriate design of automated microfluidic LOC platforms that can assure the operation of the device, especially for non-technical operators [128, 149, 215, 223, 224].

An automated shutter flow device embedded with micro-valves and a micro-pump was implemented for the high-throughput hybridization of dengue virus DNA (Figure 8-4-ii) [215]. This device was composed of 48 hybridization units, which could run assays in high-throughput mode. An LOD of 100 pM was achieved in only 90 sec using 1 μ l of sample.

Combining an embedded micro-pump with droplet-based microfluidics could enhance automation and high-throughput analysis. For instance, Zeng *et al.* [149] developed a droplet-based microfluidic system for single-cell genetic analysis (Figure 8-4-i). In this setup, multiplex PCR amplification integrated with a microfluidic emulsion generator (up to 3.4×10^6 droplets per hour) was performed for large-scale quantitative genotypic studies of biological samples. The design included glass-PDMS-glass hybrid substrates that were integrated with a three-valve diaphragm micropump, which helped transport and encapsulate cells inside the droplets. The entire process, including PCR amplification, lasted around 4 hours, and led to single-cell-level sensitivity.

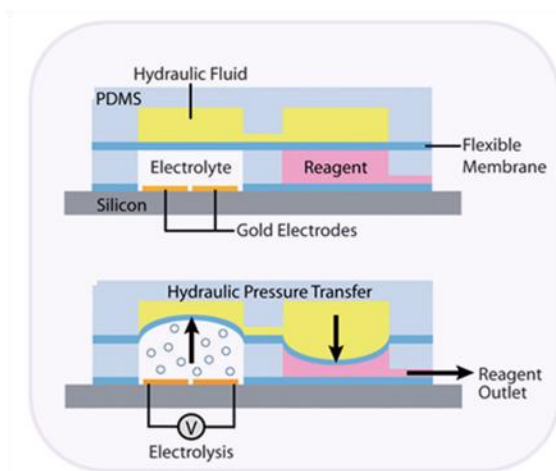


Figure 8-5 Activation mechanism of the Electro-hydraulic Pump. Bubbles are formed by electrolysis of the pumping fluid applying electrical current. The produced pressure is transferred through a flexible membrane to a hydraulic fluid chamber, which then pushes fluid out of the reagent chamber. (Reproduced from Ref. [225] with permission from Royal Society of Chemistry.

Designing parallel detection chambers is a simple approach to performing high-throughput sample analysis (Figure 8-4-iii). Zhang *et al.* [216] developed a chip composed of two layers: a patterned, fluidic layer at the top and a pneumatic control layer at the bottom. This chip consisted of seven immune-reaction columns with micromechanical valves, and concentrations of target toxins were read out by measuring the color intensity of the micro-columns. Detection of the toxins, such as microcystin, were achieved in less than 25 min with an LOD of 0.02 ng mL^{-1} .

Microfluidic quantum dot (QD)-based barcodes for multiplex high-throughput detection of the hepatitis B virus, hepatitis C virus, and HIV were developed. Three QDs with different emission wavelengths were selected and conjugated to a specific antibody for each target. Using an electrokinetically driven, microfluidic system, real-time readout of the barcodes with a picomolar LOD was achieved in less than one hour [128]. Despite efforts to develop multiplex high-throughput devices, they still cannot be used in POC or on field detection systems.

8.6.2 Strategies to develop POC devices

Recently, efforts have been made to develop detection platforms suitable for POC diagnostics. Low cost, portability, ease of use, fast detection time, and minimal side accessories are the main characteristics of microchips for POC diagnostics. Several factors should be considered in developing microchips with the aforementioned specifications. Transducers and pumping systems normally occupy larger spaces, consume more power, and are costly. Indeed, most research in this field is being directed towards eliminating or minimizing the need for external accessories and power.

For instance, a low-power and low-cost pump system so-called Electro-Hydraulic Pump (EHP) was developed by Lui *et al.* [225]. This system consists of two separate sections: an electrolyte chamber and a reagent chamber. On top of these two chambers, there is a hydraulic fluid separated by a flexible membrane. First, gold electrodes are used for electrolysis. As a result, bubbles are formed and expand the flexible membrane. This pressure forces the fluid to move out of the reagent chamber. Since this system is mainly made of PDMS and polystyrene, it is suitable for mass production. A broad range of flow rates generated by EHP (from 1.25 to 30 $\mu\text{L min}^{-1}$), and its simple fabrication method makes it a suitable option for many lab-on-a-chip applications (Figure 8-5) [225].

Since handling liquids in microfluidic devices, without pumps or valves, would be a tremendous step towards developing portable POC devices, Weng *et al.* [160] developed a microfluidic chip that does not require syringe pumps, valves, and tubing for liquid handling. The device operates by gravity-based pressure-driven flow, and electrokinetically controlled oil-droplet sequence valves (ECODSVs) were implemented inside this microfluidic chip. Electroosmotic flow was used to control the ECODSVs and

hence the sequential fluidic operation of the chip. Using this setup, an RNA-DNA hybridization assay was carried out in less than 25 min.

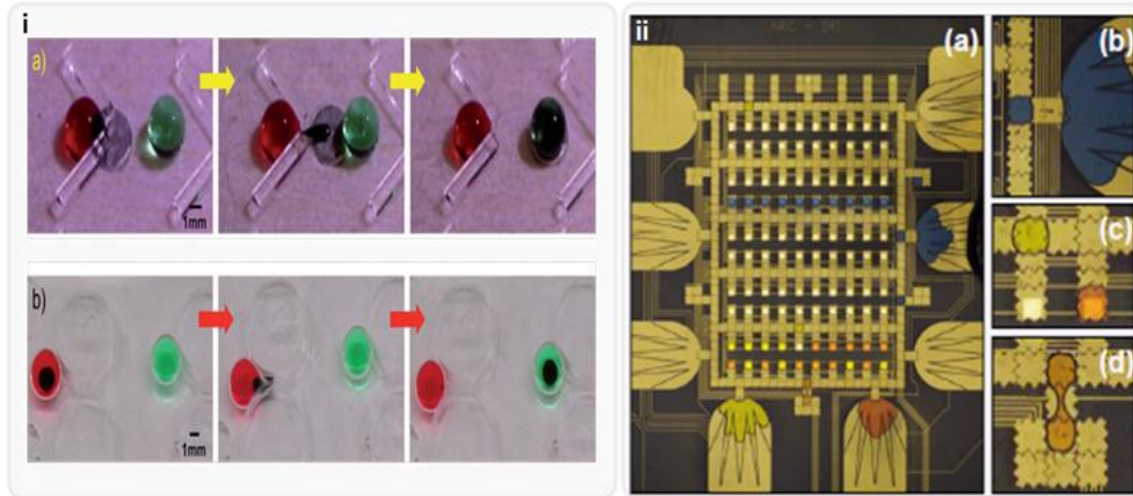


Figure 8-6 (i) Droplet based microfluidic chip implementing magnetic actuation. Demonstration of the droplet manipulation in (c) air and (d) oil mediums. (Reproduced from Ref. [198] with permission from Royal Society of Chemistry.) (ii) (a) Top view of an EWOD-based digital microfluidic device, (b) a reservoir, (c) analysis spots, and (d) region for mixing, storing and splitting droplets. (Reproduced from Ref. [226] with permission from IEEE.)

8.6.2.1 Droplet-based and Digital microfluidics

Another approach that eliminates the need for pumping and valve systems can be achieved by droplet-based microfluidics. The overall configuration and process is straightforward, which makes the setup practical for POC applications. Droplet-based microfluidics [227, 228] is based on the generation and manipulation of individual droplets. Therefore, each droplet can potentially be a bioreactor, which is an important advantage compared to continuous flow microfluidic devices. Droplets are typically generated by the flow of at least two liquids, and controlled either by volume or pressure. Unlike continuous flow microfluidics, scaling up does not increase device size or complexity, making it a good candidate for high-throughput screening and analysis. Different biological assays, such as PCR [229] and DNA hybridization [180, 230], were

carried out with droplet-based microfluidics. For instance, a droplet-based platform was used for the high-throughput detection of *E. coli* [180]. PNA probes were designed to specifically target 16s rRNA from *E. coli*. To do so, the cell sample and detection probes were mixed, and after droplet production, cell lyses and hybridization was carried out in each droplet. Finally, using confocal fluorescence spectroscopy, a detection signal was obtained.

In a new design for transporting reagents between droplets, micro-elevation was implemented to form slits that facilitate the splitting of the super paramagnetic particles from droplets (Figure 8-6-i). Material transfer between each droplet was carried out by silica superparamagnetic particles, which acted as carriers. The embedded slits were either V-shaped or pairs of micropillars. Genetic analysis, steps of cell lysis, DNA binding, washing, elution, amplification, and detection are performed within each individual droplet. This platform was also equipped with a thermal cycler for PCR amplification. Using this chip, PCR and HDA (Helicase dependent amplification) were performed for the detection of ovarian cancer biomarker Rsf-1 and *E. coli*. Although this material transfer method is a simple solution to reduce complexity, it is still dependent on magnetic forces, which makes it's applications in POC diagnostics challenging [198].

In droplet-based microfluidics, droplets are moved in series in one direction, restricted to microchannel geometries. Unlike the droplet-based microfluidic setup, digital microfluidic analysis (DMF) is able to address each droplet discreetly in an array of electrodes which can then be moved based on the electrowetting on dielectric (EWOD) principle on a 2D plane. This ability makes the DMF an excellent choice for multiplex high-throughput assays. So far, DMF has been used for many applications, including cell

culturing [36], DNA hybridization [37, 231], PCR [38], and immunoassays [35]. Different transducers have also been integrated with DMF, such as SPR imaging [39], field effect transistors (FET) [232], matrix-assisted laser desorption/ionization mass spectrometry (MALDI-MS) [233, 234], and UV/Vis spectroscopy [235].

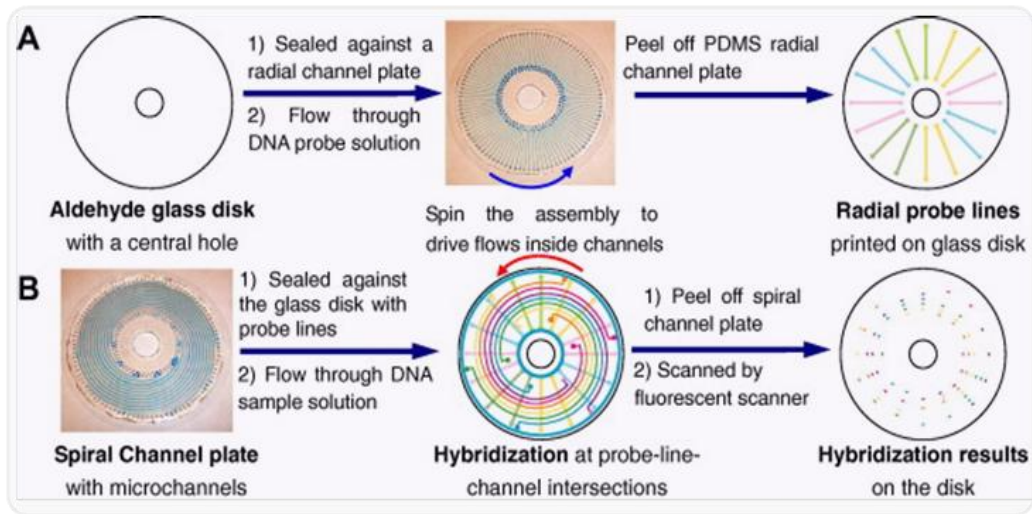


Figure 8-7 Schematic diagram of the microfluidic microarray. Procedure for (A) probe printing and (B) Hybridization. (Reproduced from Ref. [156] with permission from Elsevier.)

For instance, a DMF platform made of 500 electrodes in the bottom substrate and a disposable plastic top substrate with 100 detection spots was developed. In this setup, many detection tests could be carried out by replacing the top plastic substrate with a 5 DC USB connection (Figure 8-6-ii). Overall, having the capability of high-throughput analysis with an exchangeable disposable plastic detection layer and running on a very low power supply, makes DMF a platform suitable for locations with few resources [226]. A portable DMF cartridge was designed, which benefited from magnetic bead-based immunoassay and PCR, which was primarily targeted for POC applications because of its low cost of fabrication and versatility [236].

8.6.2.2 Lab on a disk devices

Centrifugal pumping, also called "lab-on-a-CD" is another approach to eliminate the need for tubing and external pumping systems because it only requires a simple electric motor for fluid handling [157, 237]. Compared to conventional (vacuum suction) systems, this method provides less signal variations between replicate samples. Wang *et al.* [156] developed a sophisticated microfluidic microarray in which centrifugal pumping was the driving force (Figure 8-7). This device was composed of radial and spiral microchannels for parallel DNA detection at the level of single-base-pair discrimination. The hybridization occurred in the intersection of the radial probe line and spiral channels, which deliver the target. Sensitivity was further enhanced by controlling the flow rate and channel depth. By lowering the flow rate, the residence time will increase, resulting in better hybridization. At the same time, mass transport was enhanced by decreasing the channel depth, resulting in a better signal to noise ratio because the shallower channel has better mass transport as compared to the deeper channel. Using this device, over 100 samples were analyzed in parallel in 3 min.

A variety of phenomena in nature operate based on capillary forces. Mimicking this concept and implementing it into microfluidic devices is an ideal alternative for accessory-free liquid handling. For instance, a capillary-based microfluidic platform was implemented to simultaneously detect four different waterborne pathogens using real-time PCR [238].

8.6.2.3 Paper-based devices

Compared to other capillary-based microfluidic devices developed for pathogen detection, paper-based microchips [239, 240] provide an innovative approach to produce disposable, biodegradable, cost-effective, portable and simple chips. These devices are

generally made from abundant materials such as cellulose fiber, have low volume and are easy to fabricate [241].

Various detection strategies have been implemented in paper -based microfluidic devices to recognize pathogen presence, most of which are based on the colorimetric method [242, 243]. Lateral flow immunochromatographic is one such common test method where the result can be observed by the naked eye. Abe *et al.* [244] used immunochromatography to detect IgG antibodies and a LOD of $10 \mu\text{g L}^{-1}$ was achieved within 20 min. It is noteworthy that conventional single-layer paper-based platforms are not comparable with conventional LOC devices in terms of sensitivity, accuracy, and multiplex analysis capabilities. As a result, there have been many efforts to design multiplex paper-based devices with higher sensitivities. Specifically, paper-based three-dimensional microfluidic devices have emerged to enable more complicated analysis. In addition to movement along each layer, reagents can also move up and down between the top and bottom layers. Martinez *et al.* [245] developed such a microfluidic platform (Figure 8-8-i) by stacking layers of patterned paper in which each layer can have a different pattern of biomarkers and reagents. Despite the sophisticated technology involved in the fabrication of this device, its final cost is very low, making it a promising candidate for POC diagnostics in resource-limited settings.

Enzyme-Linked Immunosorbent Assays (ELISA) [246] and Electrochemiluminescence (ECL) have also been performed using 3D paper-based microfluidics [247]. Liu *et al.* [246] reported a 3D paper-based device using ELISA in which all necessary reagents were stored within the device in dry state. Using this setup, only 2 μL of sample was required to perform the analysis (Figure 8-8-ii). The

colorimetric results can be captured by cell phone or scanner and sent to an off-site location for further analysis. Using this setup, the IgG antibody was detected in 43 min with an LOD of 330 pM [246].

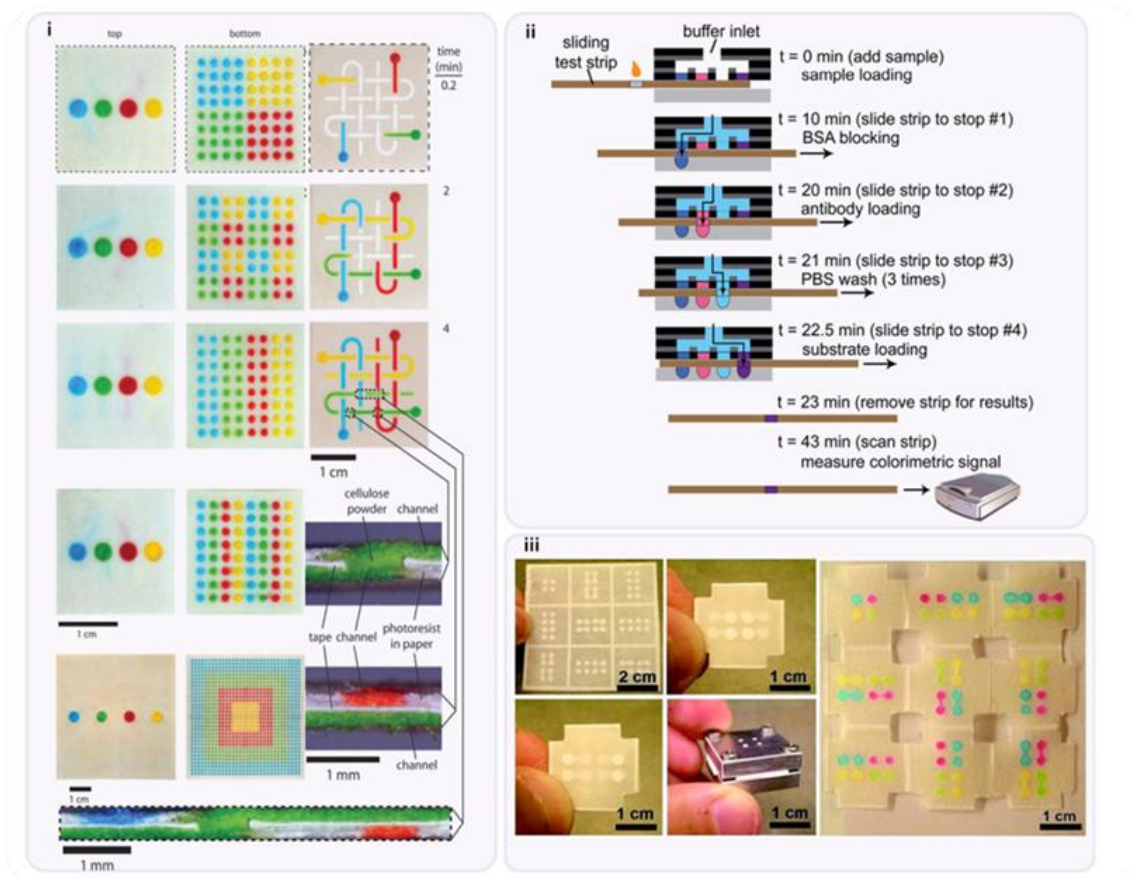


Figure 8-8 Three-dimensional paper-based microfluidic. (i) Demonstration of the fabrication, design and patterning of a three-dimensional paper-based microfluidic. (Reproduced from Ref. [245] with permission from Proceedings of the National Academy of Sciences.) (ii) Schematic of operating procedures of ELISA in a three-dimensional paper-based microfluidic. (Reproduced from Ref. [246] with permission from IEEE.) (iii) A three-dimensional paper-based microfluidic using origami principle. (Reproduced from Ref. [248] with permission from American Chemical Society.)

ECL immunoassay was also integrated on a 3D paper-based microfluidic device [247]. In this setup, eight working carbon electrodes were screen-printed on the first paper substrate and on the second paper channel substrate all patterns included both the same Ag/AgCl reference and carbon counter electrodes. In addition to the advantages provided by 3D

design, the device could also benefit from the higher sensitivity and specificity provided by the ECL method [247].

Although the emergence of such devices is an important step towards producing real diagnostic devices for POC applications, there is still a need to reduce fabrication complexity while benefiting from the advantages of 3D design. The origami concept can be used in this regard to simplify fabrication complexity. Origami is a traditional Japanese paper folding technique, which is used to construct 3D geometries from a single paper sheet. Liu *et al.* [248] fabricated an entire paper-based device from a single sheet using one-step photolithography based on origami demonstrating that complex patterns can be produced without additional fabrication overhead. Another advantage of this system is that it is performed using an automated printing technique and assembled without tools (Figure 8-8-iii) [248].

8.6.2.4 Integration towards sample-to-result POC devices

A multitude of design and detection methods were introduced in the previous sections, each providing specific advantages regarding pathogen detection. The proper integration of these techniques into a single chip would address most of the drawbacks seen when each one is used individually. This would bring the end goal of developing POC devices into reality by performing sample-to-result diagnostic tests with low LODs in a reasonable time.

A fully integrated, disposable, and portable device was developed to detect the H1N1 virus from a throat swab sample, based on microfluidics [164] where the immunomagnetic target capture, pre-concentration and purification, PCR amplification, and sequence specific electrochemical detection steps were performed on a single monolithic chip (Figure 8-9-i). A DNA probe complementary to the H1N1 virus was

immobilized on a gold electrode. The amplified ssDNA was introduced for 30 min and target hybridization induced a conformational change in the probe that led to a decrease in the electrical current. The LOD of this device for the H1N1 influenza virus was 10 TCID₅₀, four orders of magnitude below those of clinically relevant viral titers with total analysis time of 3.5 hours. This device could have a great potential in POC applications because of its high sensitivity in testing real samples. Further improvement, such as finding alternatives for the syringe pumps and heaters would make these devices an excellent option for POC applications.

Another fully integrated device was developed by Lam *et al.* [152] (Figure 8-9-ii). This platform enabled the detection of pathogenic bacteria in urine samples in less than 30 min. Generally, cells were first lysed in a chamber by applying an electrical field resulting in the release of their genetic content. Then, nanostructured microelectrodes were implemented for the electrochemical detection of the genetic content. *E. coli* and *S. saprophyticus* were successfully tested in urine samples with 100 CFU μL^{-1} (clinical relevant concentration) using this platform. The device does not require sample preparation or amplification steps while providing the necessary sensitivity in a faster time and more straightforward approach.

Lutz *et al.* [157] developed a self-sufficient lab on a foil system, based on a centrifugal lab on a CD principle for automatic nucleic acid amplification, capable of performing 30 reactions simultaneously. The structure was micromilled on a cyclic olefin copolymer, and foil formation was achieved by hot embossing. The reagents for signal amplification were stored inside a glass capsule, which increased the shelf life of the device. The liquid was then released by crushing the glass capsule container, and

centrifugal forces was applied to control the fluid flow between chambers. Isothermal amplification at a low temperature (37 °C) was performed to minimize energy consumption (Figure 8-9-iii). The total detection time was less than 20 min.

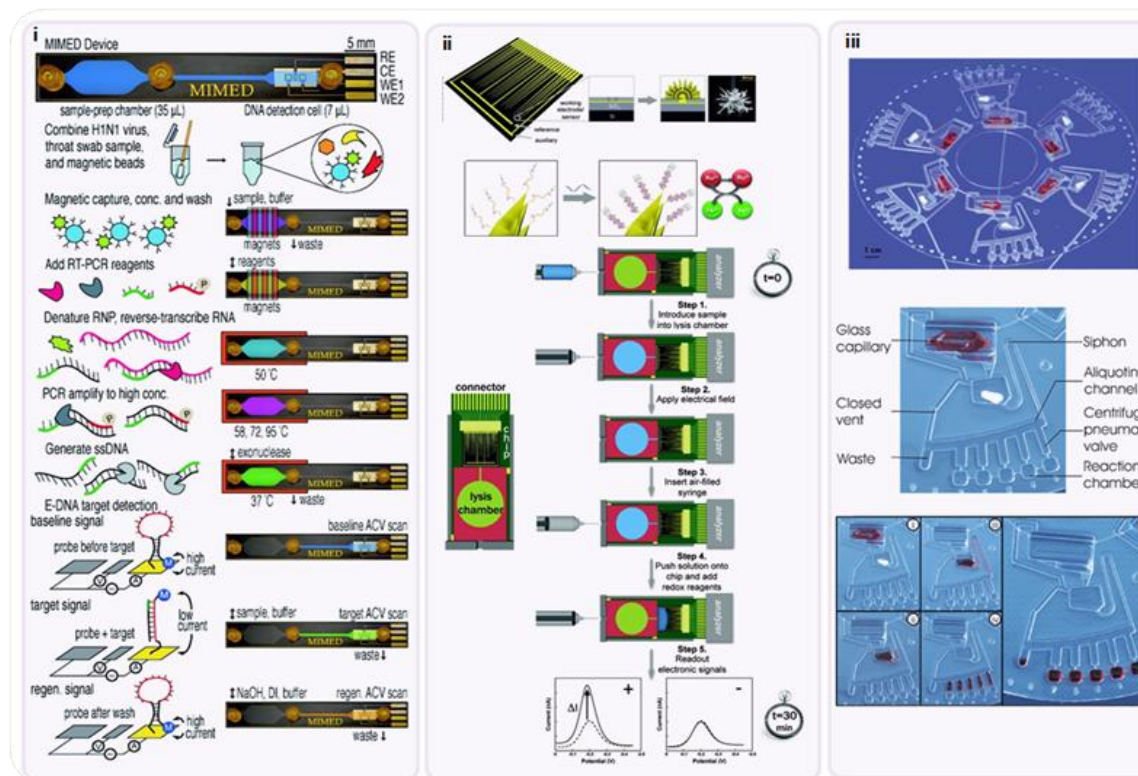


Figure 8-9 (i) Schematic illustration of the microfluidic chip for Sample-to-answer genetic analysis of H1N1 virus. (Reproduced from Ref. [164] with permission from American Chemical Society.) (ii) Schematic diagram of the chip consisting of a lysis chamber and nanostructured microelectrodes integrated to the sensing system for detection of bacterial pathogens. (Reproduced from Ref. [152] with permission from American Chemical Society.) (iii) Picture of a foil based Lab on a disc with liquid reagent containers and its operating procedure. (Reproduced from Ref. [157] with permission from Royal Society of Chemistry.)

A microfluidic device based on a nucleic acid was developed to detect different pathogens. This device was mainly made of low cost and disposable materials (polycarbonate). The operation was automatically controlled by an analyzer that provided pouch and valve actuation via electrical motors. The presence of bacterial *B. Cereus*, viral armored RNA HIV, and the HIV I virus in saliva samples was tested [249].

Lafleur *et al.* [250] developed a disposable multiplexed sample-to-result microfluidic device based on immunoassay (Figure 8-10-ii). This device was able to detect disease-specific antigens or IGM antibodies from blood. For instance, the detection of the malaria antigen and IgM to *Salmonella* Typhi LPS was carried out. This microfluidic chip was based on flow through the membrane immunoassay on porous nitrocellulose. After introducing the blood to the system, blood cells were removed by passing the sample onto the plasma extraction membrane. The separated plasma was divided into two samples, one for antigen detection and another for IgM detection. For IgM detection, the IgG antibodies present inside the sample were removed using protein-G beads. After capturing the target, signal enhancement was achieved using gold nanoparticles conjugated with detection antibodies. An LOD of 10-20 ng mL⁻¹ was achieved in 30 min, which is comparable to benchtop ELISA tests. Bubble formation caused by the pneumatic fluid handling system in this device is one of the challenges that will need to be addressed. In addition, finding an alternative to the fluidic handling system (preferably accessory free) would help to reduce the size, cost, and complexity of device operation.

An interesting example of accessory-free POC devices was developed by Liu *et al.* [200]. In this disposable self-heating cartridge-based device, after performing isothermal amplification, the outcome could be visualized by the naked eye using a low-cost LED signal (Figure 8-10-i). Heat was provided by an exothermic reaction of the Mg-Fe alloy and water, and the flow rate was controlled by utilizing a porous filter paper inside the device. Temperature control was achieved using paraffin as a phase change material. If

necessary, paraffin could absorb the extra heat during melting. Using this device, as few as 10 *E. coli* DNA copies were detected [200].

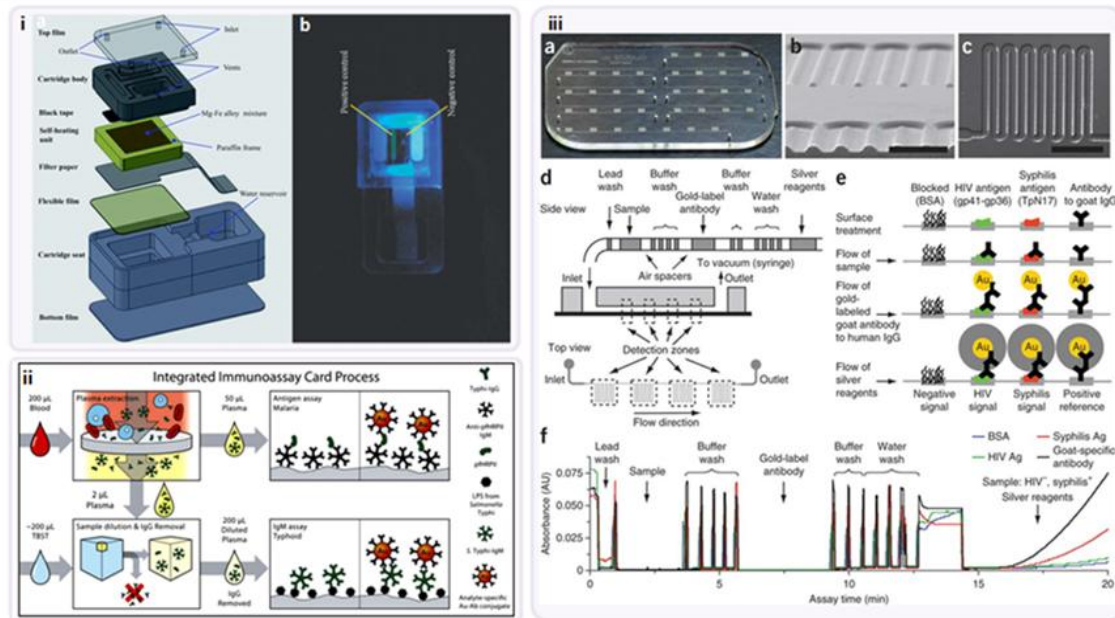


Figure 8-10 (i) Schematic presentation and images of self-heating cartridge based device for isothermal amplification (a) exploded view, (b) green fluorescence emission from a test amplification chamber. (Reproduced from Ref. [200] with permission from Royal Society of Chemistry.) (ii) Schematic diagram of the DxBio integrated immunoassay cards for detection of the malaria antigen and *S. Typhi*-IgM from blood sample. (Reproduced from Ref. [250] with permission from Royal Society of Chemistry.) (iii) Schematic diagram and pictures of a POC microfluidic device based on ELISA-like assay. (a) Picture of the microfluidic chip. (b) Scanning electron microscope image of a cross-section of microchannels. (c) Transmitted light micrograph of channel meanders. (d) Illustration of the passive delivery mechanism for multiple reagents. (e) Diagram of biochemical reactions in detection zones at different steps of immunoassay. (f) Absorbance traces of a complete HIV-syphilis duplex test as reagent plugs pass through detection zones. (Reproduced from Ref. [251] with permission from Nature publishing group.)

Recently, another promising POC microchip for the simultaneous detection of HIV and syphilis was developed, which was also tested in field studies in three developing countries (Figure 8-10-iii). This cost-effective handheld microchip uses only 1 μL of unprocessed blood sample, without a need for any moving parts, electricity, or external instrumentation. Implementing injection molding technology was the key to mass producing the device, resulting in a very low final cost. The passive reagent delivery

method was utilized to manipulate the reagents and samples in which blocks of reagents were introduced sequentially into a tube and separated by air spacers. For capturing HIV and treponemal-specific antibodies from blood, the envelope antigen and the outer membrane antigen (Tpn17) were immobilized on the chip surface, respectively. In the next step, a gold-labeled antibody to human IgG was introduced, and signal amplification was achieved through the reduction of silver ions onto gold nanoparticles. The optical density of the silver film could be measured through low-cost and robust optics, such as light-emitting diodes and photodetectors. This device could provide sensitivity and specificity comparable to bench-top ELISA and other conventional detection methods within 20 min on the site [251]. The very promising field study results obtained using the device open new avenues in the implementation of microfluidic-based devices for POC applications all over the world, especially in developing countries with poor healthcare resources.

8.7 Outlook and future trends

During the past decade, engineering tools have been implemented to study different aspects of pathogen detection platforms, including design, micro/nanofabrication, sample preparation and amplification, miniaturization, automation, multiplexing, and high-throughput analysis. Despite recent technological advances, the development of a cost effective, accessory-free single device capable of simultaneously achieving high-throughput and multiplex analysis with high specificity and sensitivity remains elusive. Biomarkers with higher specificity along with miniaturized, cost-effective designs with minimum side accessories and high sensitivity are required to achieve this goal.

Biomarker selection is a critical factor in obtaining the required specificity. Antibodies are the most common biomarkers, although they cannot deliver the desired specificity, nor are they available to diagnose all pathogens. However, in terms of the detection of epidemic and life-threatening diseases, such as HIV and tuberculosis, especially in developing countries, they can play a critical role in controlling the rate of disease propagation. Among new alternatives to antibodies, aptamers are promising candidates. However, the time and cost required to discover and design aptamers should be reduced. For cases requiring very high specificity, molecular-based diagnostics can be implemented. This could be achieved by designing DNA probes for target hybridization, followed by specific primers for the amplification of the target gene. In the applications where high stability is required, PNA probes could provide better stability and hybridization than DNA probes.

Molecular amplification of the target genes is an essential component of bench-top diagnostic techniques in order to attain higher sensitivity. Among these techniques, PCR has been widely used through its integration into microfluidic chips. However, the requirement for precise temperature control for thermo-cycling at the micro scale makes the chip design more complicated as compared to macro-scale experiments. To address this issue, isothermal amplification techniques have emerged as an alternative to PCR in microfluidic chips. Among isothermal methods, low-temperature isothermal amplification could be useful because it operates at 37 °C. However, the LAMP technique that requires a higher performance temperature (60 °C), is currently at the center of attention for POC applications as test results can be visualized with the naked eye.

Sample preparation is key to achieving high sensitivity and specificity. Among the diverse techniques for sample preparation, the use of magnetic beads is one of the most promising approaches, it is not only sensitive and cost-effective, but also provide better control over captured reagents' motions inside the chip.

In designing microchips, the desired biosensor chip should be able to deliver the same LOD as bench-top methods (around 10-1000 CFU mL⁻¹). Automation, the potential for mass production, and portability are also important specifications to be considered in the design of microchips for POC applications. LOD and assay time for detection of different pathogens summarized in Table 8-1.

In terms of automation and high-throughput analysis, digital microfluidics has proven to be one of the most interesting technologies since thousands of individual droplets can be discreetly manipulated and analyzed. Though there is still a need for modification to produce a portable and accessory-free system, selecting proper materials in the fabrication of LOC devices can play an important role in producing cost effective devices. Paper-based microfluidic devices are very promising platforms to provide a disposable, portable, biodegradable, and easy-to-fabricate detection microchip. Despite the efforts made in developing paper-based devices, such as the production of 3D-paper-based platforms and the integration of different detection methods, these devices do not provide the desired sensitivity. In this regard, the proper functionalization and immobilization of biomolecules on the paper-based substrates can enhance device sensitivity.

This review pointed out that the design and modification of various components for the development of a universal sample-to- result LOC device should be performed

with a clear vision of producing a totally integrated self-contained, accessory-free microchips that also provide the required sensitivity and specificity. The future will belong to simple LOC microfluidic devices that possess the desired the sensitivity and specificity while providing complex diagnostics in remote areas, without a need for centralized laboratories.

Acknowledgments

The authors acknowledge the financial support from Genome Quebec and NanoQuebec. A.M. Foudeh would like to thank the NSERC-CREATE integrated sensor systems program for its financial support. T.F. Didar would like to thank the faculty of medicine at McGill and Fonds de recherche du Québec - Nature et technologies (FQRNT) for their financial support .The authors would also like to thank Dr. J. Daoud and K. Bowey for their comments on the manuscript.

Preface to Chapter 9: Sensitive detection of 16s rRNA from *Legionella pneumophila* using surface plasmon resonance imaging

In order to meet the first objective of this thesis, that is to design a simple detection system for detection of viable *Legionella* with high specificity and sensitivity using the SPRi, an investigation into the design of DNA probes and optimization of the hybridization kinetics was undertaken.

The effect of the design of two probes, one to capture the RNA on the substrate and the other to increase the detection sensitivity, on specificity of the detection system was investigated. To overcome the lack of desired SPRi sensitivity for the detection of this species, near-infrared quantum dots (QDs) was employed as a post-amplification strategy. In addition, the effect of experimental parameters, including temperature, buffer composition, length of the spacer between the detector probe and the biotin, and the pre-treatment of 16s rRNA were investigated and optimized to reach a high sensitivity for detection of *L. pneumophila*.

The results of this study were presented in following manuscript entitled “Sub-femtomole detection of 16s rRNA from *Legionella pneumophila* using surface plasmon resonance imaging”, which was published in *Biosensor and Bioelectronics* in 2014.

Chapter 9 Sub-femtomole Detection of 16s rRNA from *Legionella*

Pneumophila Using Surface Plasmon Resonance Imaging

Amir M. Foudeh¹, Jamal T. Daoud¹, Sebastien P. Faucher³, Teodor Veres^{1,4} and Maryam Tabrizian^{1,2*}

¹ Department of Biomedical Engineering, Faculty of Medicine, McGill University, Montreal, Canada

² Faculty of Dentistry, McGill University, Strathcona Anatomy & Dentistry Building 3640 University Street Montreal, Quebec Canada

³ Department of Natural Resource Sciences, McGill University, Quebec, Canada,

⁴ National Research Council of Canada, Quebec, Boucherville, Canada

Amir Foudeh: 3775 University Street, Department of Biomedical Engineering, Faculty of Medicine, McGill University, Montreal (QC), H3A 2B4 Canada. Tel: +1 (514) 398-3469, Fax: +1 (514) 398-7469, E-mail: amir.foudeh@mail.mcgill.ca

Jamal Daoud: 3775 University Street, Department of Biomedical Engineering, Faculty of Medicine, McGill University, Montreal (QC), H3A 2B4 Canada. Tel: +1 (514) 398-3469, Fax: +1 (514) 398-7469, E-mail: jamal.daoud@mail.mcgill.ca

Sebastien P. Faucher, Department of Natural Resource Sciences, Macdonald Campus, 12 McGill University, 21,111 Lakeshore, Ste-Anne-de-Bellevue, Quebec, H9X 3V9. Tel: 1-514-398-13 7886; Fax: 1-514-398-7990; e-mail: sebastien.faucher2@mcgill.ca

Teodor Veres: National Research Council Canada, 75 Boul. de Mortagne, Boucherville, QC, Canada J4B 6Y4. Tel: +1(450)641-5232; Fax: +1(450)641-5105 Teodor.Veres@cnrc-nrc.gc.ca

Maryam Tabrizian: 3775 University Street, Department of Biomedical Engineering, Faculty of Medicine, McGill University, Montreal (QC), H3A 2B4 Canada. Tel: +1 (514) 398-8129, Fax: +1 (514) 398-7461, E-mail: maryam.tabrizian@mcgill.ca

*Correspondence should be addressed to Maryam Tabrizian

9.1 Abstract

Legionellosis has been and continues to be a life-threatening disease worldwide, even in developed countries. Given the severity and unpredictability of Legionellosis outbreaks, developing a rapid, highly specific, and sensitive detection method is thus of great pertinence. In this paper, we demonstrate that sub-femtomole levels of 16S rRNA from pathogenic *L. pneumophila* can be timely and effectively detected using an appropriate designed capture, detector probes, and a QD SPRi signal amplification strategy. To achieve specific and sensitive detection, optimal hybridization conditions and parameters were implemented. Among these parameters, fragmentation of the 16s rRNA and further signal amplification by QDs were found to be the main parameters contributing to signal enhancement. The appropriate design of the detector probes also increased the sensitivity of the detection system, mainly due to secondary structure of 16s rRNA. The use of 16S rRNA from *L. pneumophila* allowed for the detection of metabolically active pathogens with high sensitivity. Detection of 16S rRNA in solutions as dilute as 1 pM at 450 μ L (0.45 femtomole) was achieved in less than three hours, making our approach suitable for the direct, timely, and effective detection of *L. pneumophila* within man-made water systems.

Keywords: *Legionella pneumophila*, surface plasmon resonance imaging, pathogen detection, 16s rRNA, quantum dot, hybridization

9.2 Introduction

Legionellosis is an acute form of pneumonia and Pontiac fever, a milder form of the disease with flu-like symptoms [1] that has been and continues to be devastating worldwide, even in developed countries. This is mainly attributed to unpredictable outbreaks, such as recent incidents reported in Canada, the U.S.A., Norway, and Germany [2-4]. *L. pneumophila* is the causative agent of Legionellosis. The fatality rate of Legionellosis ranges between 10% and 40% and approaches 50% within hospital and industrial outbreak settings, particularly affecting individuals with compromised health status [1]. *L. pneumophila* is found in most natural and engineered water systems, where it contaminates and multiplies inside amoeba [8]. The literature indicates that modern water systems, such as air-conditioning units, showers, and industrial refrigeration towers provide optimal growth conditions for *L. pneumophila* and propagate its transmission through aerosol [9]. Transmission to the human host thus occurs through the inhalation of contaminated water droplets. Once in the lungs, *L. pneumophila* infects and replicates inside alveolar macrophages and causes widespread tissue damage [1].

Current conventional detection methods include identification via laboratory culture and polymerase chain reaction (PCR) [10, 11]. Laboratory culture is the gold standard method employed to detect *L. pneumophila*. However, laboratory culture suffers from low sensitivity, especially if the samples under study contain microorganisms that inhibit *Legionella*'s growth. Another drawback is its inability to detect VBNC *Legionella* even though they might potentially be pathogenic. While laboratory culture entails long procedures requiring several days, PCR is a faster detection methodology and highly specific. However, it is laborious and normally requires centralized laboratory facilities.

PCR is especially unreliable when analyzing environmental samples due to the presence of PCR inhibitors.

Other methods, namely antibody-based detection, have also been investigated [127]. This method is fairly rapid, but cross-reactivity between species is an important shortcoming that limits the specificity of the technique. DNA/PNA microarray-based detection targeting DNA in bacteria is another alternative that provides the desired specificity by targeting species-specific sequences in DNA [100].

The main drawback of all the aforementioned methods is their inability to differentiate between live and dead bacterial cells, which is critical for achieving accurate and reliable results.

To overcome the limitations of using DNA and antigen targeting-based techniques, detection of the bacterial RNA is a viable alternative approach. The presence of RNA in bacteria is directly correlated with microbial activity since, following bacterial death, the associated RNA degrades relatively rapidly [15], further enhancing the associated accuracy and reliability of bacterial detection. Among RNA types, 16S rRNA is highly conserved between different species of bacteria and has been utilized for microbial identification [16, 17]. The presence of high copy numbers of 16S rRNA in each bacterium is another motivation to identify bacteria through the direct detection of 16S rRNA. However, instability and the presence of a secondary structure are significant drawbacks of using ribosomal RNA. The secondary structure renders access to the target sequence difficult. This is why methods such as using multiple adjunct probes, heat denaturation, and fragmentation have been used to circumvent this issue [22, 26].

Focusing on the detection of 16S rRNA, various sensing techniques, including electrochemical sensors [18, 19], impedance [20], fluorescent microscopy [21-23], surface-enhanced Raman spectroscopy (SERS) [24], and surface plasmon resonance (SPR) [25, 26] were used for bacterial species-specific detection. Among these methods, SPR imaging (SPRi) has proven to be a versatile tool for the real-time study of genomic and proteomic interactions and kinetics. In contrast to classical wavelength or scanning angle SPR systems, SPRi provides visualization of the multiple interactions simultaneously in real time thanks to the integration of a charge-coupled device (CCD) camera with the associated sensogram. In contrast to other end-point measurement systems, the use of SPRi allows detailed kinetic analysis, monitored in real time, to elucidate analyte binding behavior further, as well as to differentiate better between specific and non-specific adsorptions. To date, few reports on detecting 16S rRNA within a SPR setup are available in the literature. Nelson et al. detected 16S rRNA from *E.coli* with a limit of detection (LOD) of 2 nM through the use of DNA probes [103]. Joung *et al.* used PNA probes and electrostatic interaction between positively charged gold nanoparticles and negatively charged RNA as a signal post amplification method, achieving an LOD of around 100 pM [25], which is far from the desired sensitivity in the context of the detection of pathogenic *L. pneumophila* in a water sample.

This work presents the first report on utilizing 16S rRNA for the detection of *L. pneumophila* with SPRi. To overcome the lack of desired SPRi sensitivity for the detection of this species, near-infrared quantum dots (QDs) are employed as a post-amplification strategy. We previously demonstrated that QDs with an emission of 800 nm induce the strongest SPR signal enhancement among QDs with differing wavelengths

[37]. As such, our aim was to address the main challenges associated with the detection of *L. pneumophila* through the use of 16S rRNA from *L. pneumophila*, allowing for the detection of only metabolically active pathogens with high sensitivity. With the design of two probes, one to capture the RNA on the substrate and the other to increase the detection sensitivity, for each target region, the high specificity of the detection system is further ensured (Figure 9-1). The effect of experimental parameters, including temperature, buffer composition, length of the spacer between the detector probe and the biotin, and the pre-treatment of 16s rRNA were investigated and optimized to reach a sensitivity detection of *L. pneumophila* in the femtomole range.

9.3 Materials and methods

9.3.1 Chemical and reagents

6-Mercapto-1-hexanol (MCH), potassium phosphate dibasic solution, 1 M, pH 8.9 (1 M K_2HPO_4), sodium chloride (NaCl), sodium hydroxide (NaOH), sulfuric acid (H_2SO_4), hydrogen peroxide (H_2O_2), and ethanol were purchased from Sigma-Aldrich (St. Louis, MO, U.S.A.). A fragmentation kit was obtained from Ambion. Oligonucleotides (ODN) were purchased from Integrated DNA Technologies (Coralville, IA, U.S.A.). Streptavidin-coated quantum dots, QD 800 STVD, SSPE buffer (20X buffer is 3.0 M NaCl, 0.2 M NaH_2PO_4 , and 0.02 M EDTA at pH 7.4.), Denhardt's solution [50X solution is 1% Ficoll (type 400), 1% polyvinylpyrrolidone, and 1% bovine serum albumin] were purchased from Invitrogen (Carlsbad, CA, U.S.A.).

9.3.2 DNA probe design

Two specific DNA capture probes (CP), referring to leg1 CP and leg2 CP, complementary to *L. pneumophila*'s 16s rRNA, were designed using bioinformatics

software packages from Cardiff University, England. Particular features in the sequence, such as loops and hairpin curves, were checked and avoided. The specificity of these probes was confirmed by submitting the sequence to the Check Probe program of the Ribosomal Database Project (RDP). In terms of detection probes, two different biotinylated probes with gap of 0 bp and 7 bp (Leg1 DP 0/7 bp and Leg2 DP 0/7 bp) between the capture and detection probes for each target RNA sequence were designed. Finally, a DNA probe and a universal probe (EU capture probe) were used as negative and positive controls, respectively. The length of each detector probe was determined to ensure similar melting temperatures while avoiding cross-reactivity and hybridization to any capture probes. This was verified by including a detector-only control for each hybridization experiment conducted (data not shown). The secondary structure model of *L. pneumophila* was obtained from <http://www.rna.ccbb.utexas.edu> [252].

9.3.3 RNA preparation

Synthetic 60 bp RNA from the *L. pneumophila*'s 16S rRNA, which contains complementary sequences for Leg1 capture and detector probes, was synthesized by Integrated DNA Technology (Table 9-1). Moreover, 16S rRNA of *L. pneumophila* was produced using T7 RNA polymerase-driven *in vitro* synthesis methodology. Briefly, the 16S rRNA gene of *L. pneumophila* was amplified by PCR from DNA extracted from *L. pneumophila* using specific primers (5'-AGACAAACTGTGTGGGCACTTTGG-3' and 5'-TGGGCACTTTGATTCTTCTGTGC-3'). The PCR fragment was then inserted into the pGEM-T (Promega) vector downstream of the T7 promoter. The plasmid was then transformed and propagated in JM109 high-efficiency competent cells. The PCR fragments could become inserted in the sense or antisense orientation. Plasmids carrying

fragments in the sense orientation were identified and utilized for further experiments. The identification of colonies carrying plasmids containing fragments in each orientation were identified by PCR, and the correct sequence of the fragment was validated by sequencing. The plasmids carrying the correct sequences were isolated and used as a template for T7 RNA polymerase (New England Biolabs) to produce 16S rRNA. The resulting RNA product was further purified by acid-phenol and stored in -80 °C for further use.

9.3.4 Surface chemistry on SPRI chip

Gold-coated slides (Horiba, France) were cleaned with UV/ozone for 10 min, rinsed thoroughly with MQ water, and treated with piranha solution for another 5 min. After rinsing with MQ water, the slides were dried under a stream of nitrogen. DNA immobilization was performed using 1 μ M thiol-modified oligonucleotide probes comprising a 10T spacer in 1M KH_2PO_4 for 180 min. Following the immobilization, substrates were treated with 1 mM MCH for 90 min to improve the orientation of the probes and attenuate non-specific adsorption. The slides were further passivated with 2.5X Denhardt solution for 10 min and stored at 4 °C before further use.

9.3.5 RNA pre-treatment

Denaturation of the 16s rRNA were carried out by the incubation of samples in 65 °C for 5 min. Fragmentation of the 16s rRNA were performed according to the protocol provided by the manufacturer (Ambion) except that different concentrations of the fragmentation buffer (zinc solution) were used in these experiments. Frag.1 and Frag.2 represent the use of 1 and 2 μ L of the fragmentation buffer, respectively. Then the solution was mixed with 1.28 μ g of 16s rRNA in 20 μ L of total reaction volume. The

solution was kept at 75 °C for 15 min, followed by the addition of blocking solution (EDTA). The samples were kept on ice until further use.

9.3.6 *SPRi measurements*

SPRi detection of biomolecular binding to the chip surface was performed using a scanning-angle SPRi instrument (model SPRi-Lab+, GenOptics, France). The SPRi apparatus, equipped with an 800 nm LED source, a CCD camera, and a microfluidic cell, was placed in an incubator (Memmert Peltier, Rose Scientific, Canada). The SPRi measurements for each spot were taken as described previously [37]. The entire biochip surface was imaged during the angular scan. At least five spots were selected for each experiment to monitor the binding events with both the probes and the controls, and each experiment was repeated at least three times.

RNA hybridization experiments were carried at 37°C with an injection volume of 450 µL. A baseline signal was first obtained for the hybridization buffer, followed by the hybridization signal for the targets. Detector probes were pre-mixed with the RNA samples before injection. Following the hybridization of the target RNA with the capture probe and the detection probe, streptavidin-conjugated Qdots (SA-QDs), 1 nM in concentration in hybridization buffer, were injected and allowed to bind to the biotinylated detector probes for 10 min. At each step, the substrate was washed with buffer, and the difference in the reflected intensity (% ΔR) was computed by taking the difference between the initial and final buffer signals. Successive hybridizations were followed by surface regeneration using 50 mM NaOH, without significant binding efficiency loss.

9.3.7 Statistics

The lower detection limit was defined as the smallest concentration of an analyte, calculated as the blank signal plus or minus three standard deviations. All data were expressed as the mean \pm SD. Statistical comparisons between two groups were done using Student's paired t-test, while multiple comparisons were done using one-way ANOVA, followed by the post hoc Tukey test.

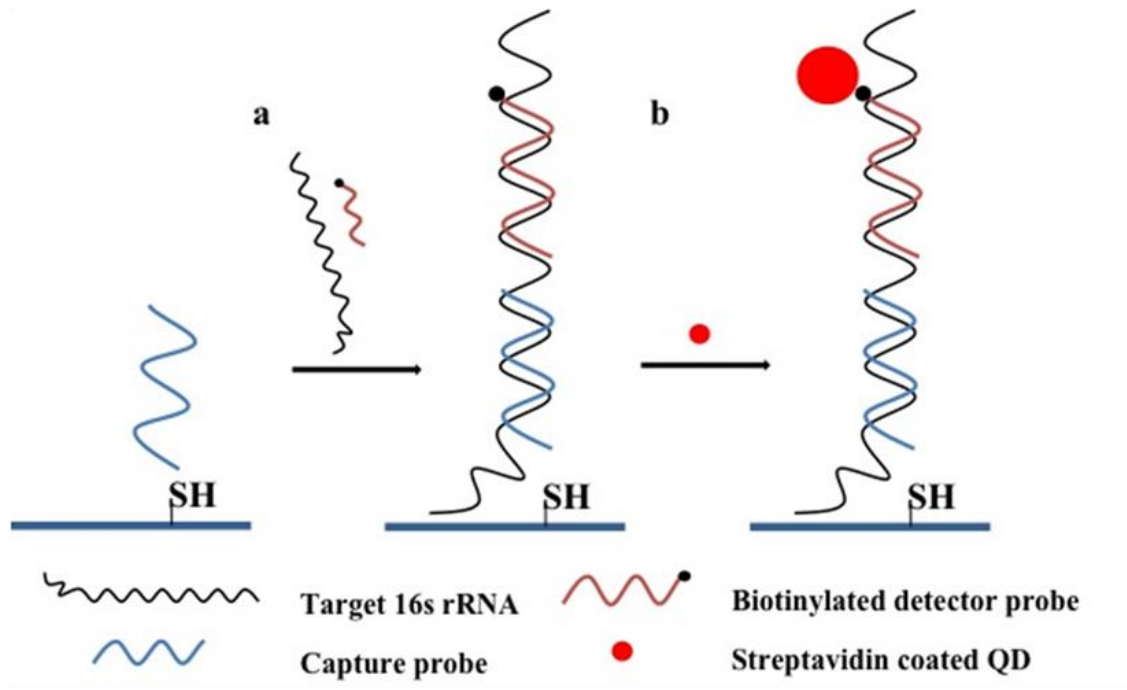


Figure 9-1 Schematic illustration of the RNA hybridization using capture and detector probes, before and after addition of SA-QDs. a) Mixture of target RNA and biotinylated detector probe pass through the detection surface. b) Addition of streptavidin-QDs after hybridization of target RNA to Capture probe and detector probe.

9.4 Results and discussion

Two different regions of the *L. pneumophila*'s 16s rRNA sequence were targeted to investigate the regional effects on hybridization efficiency and specificity, as well as the

proximity of the detector and capture probes. One specific capture probe was designed for each region. In addition to these two specific capture probes for *L. pneumophila*, one universal probe and one control probe were selected as positive and negative controls, respectively. A summary of the oligonucleotide sequences for probes is given in Table 9-1.

Since significant non-specific hybridization to the control probes was observed at room temperature (data not shown) the hybridization temperature was set at 37 °C. Then, to detect *L. pneumophila* with high specificity and in very low concentrations, the effect of experimental parameters, namely the buffer composition, the length of the spacer between detector probe and biotin, and the pre-treatment of 16s rRNA were investigated.

9.4.1 Effect of buffer composition and detector probe spacer on hybridization efficiency

In addition to the hybridization temperature, the buffer composition and the proximity between the detection probe and its respective biotin functional group also play an important role in the stringency and efficiency of the hybridization [18, 26].

A 60bp synthetic RNA sequence was selected from *L. pneumophila's* 16s rRNA sequences complimentary to the Leg1 CP. Therefore, 60bp synthetic RNA (Table 9-1) was utilized to investigate the effect of the buffer composition and the detector probe spacer.

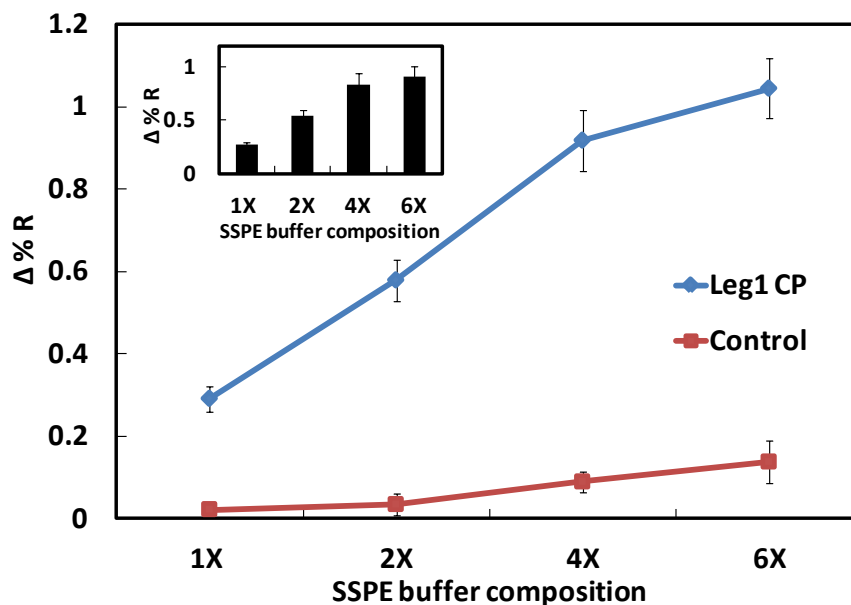


Figure 9-2 Effect of buffer composition on hybridization efficiency. Hybridization of 10 nM synthetic RNA for 18 min on the biochip expressed as $\Delta\%R$ as a function of buffer composition (1X-6X SSPE). The inset represents the hybridization efficiency of the Leg1 CP which control probe signals were subtracted from the Leg1 CP signals. All data is expressed as mean \pm standard deviation (n=5).

Synthetic RNA hybridization for an incubation time of 18 minutes is illustrated in Figure 9-2. To better compare the different buffer compositions, the signals obtained from the control probes were subtracted from the Leg1 CP hybridization signals at each buffer composition (Figure 9-2 inset). Increasing the salt concentrations by four-fold (from 150 to 600 mM) resulted in higher hybridization efficiency. A further increase of the salt concentration to 900 mM showed a slight increase in hybridization efficiency but caused an increase in non-specific adsorption to the control probe. Thus, 600 mM SSPE was set as the optimal hybridization buffer. As for the optimal biotinylated spacer, different spacers, such as dT and TEG (containing a 15 C spacer), were investigated, whereas TEG yielded the highest signal (data not shown). These optimized hybridization parameters were then set for the detection of 16s rRNA in further investigations.

9.4.2 *L. Pneumophila* 16s rRNA Pre-treatment

Conversely, to address the steric hindrance resulting from the secondary structure of 16S rRNA, the effect of different pre-treatment methods was investigated. Figure 9-3a shows the changes in SPRi differential reflectivity signals representing 18-minute hybridization for pre-treated, as well as intact, 16s rRNA to the Leg1, Leg2 and EU CPs.

In general, Leg1 CP produced stronger hybridization signals compared to the Leg2 and EU capture probes. This may be attributed to several factors, including: i) the higher melting temperature of Leg1 CP compared to the Leg2 and EU CPs, ii) the position of the Leg1 CP complementary sequence, located on the more exposed region of the 16s rRNA secondary structure, and iii) the weaker secondary structure of 16s rRNA to be disrupted by the Leg1 CP compared to the Leg2 and EU capture probes (Figures 9-4a and 9-4b). To arrive at the optimized fragmentation protocol, two methods with varying fragmentation solution concentrations were used to obtain the 16S rRNA fragments, referred to as Frag1 and Frag2. As shown in Figure 9-3a, denaturation through heating of the 16s rRNA resulted only in a significant increase of $\Delta\%R$ for hybridization to EU CP, but not Leg1 and Leg2 CPs. The same trend was also observed for Frag1. In addition, Frag2 resulted in the highest improvement in hybridization efficiency among the three capture probes relative to intact 16S rRNA. This is due to the higher concentration of cations in Frag2 compared to those in Frag1, which results in smaller fragments and, in turn, higher accessibility of the capture probes. For simplicity's sake, fragmentation will henceforth refer to Frag2.

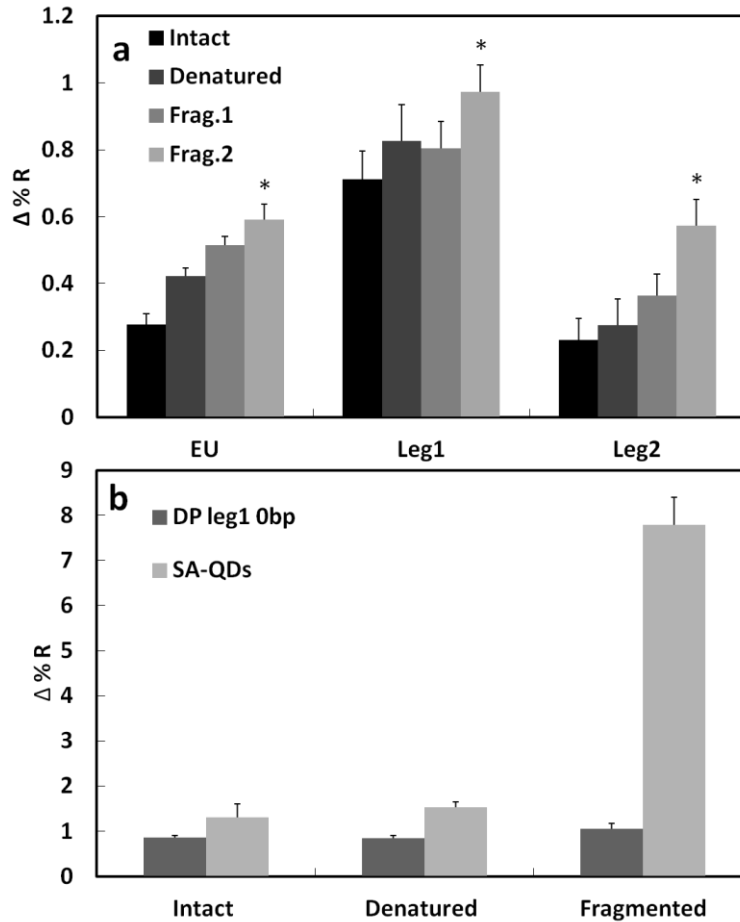


Figure 9-3 Effect of fragmentation and denaturation pre-treatment methods on of 16s rRNA on hybridization efficiency. **a**) Hybridization of 10 nM 16s rRNA after 18 min incubation with EU, Leg1 and Leg2 capture probes. **b**) Effect of 16s rRNA pre-treatment on QDs post amplification. 100 nM Leg1 DP 0bp with 10nM 16s RNA were used and hybridization efficiency with Leg1 CP followed by addition of the 1nM SA-QDs was investigated. All data is expressed as mean + standard deviation (n=5, *P<0.05 versus intact, denatured and Frag1).

To further investigate the effect of pre-treatment of the 16S rRNA, biotinylated detector probes located 0 bp away from the Leg1 CP were investigated for hybridization efficiency and subsequent signal amplification through the addition of SA-QDs. Leg1 DP 0bp was pre-mixed with fragmented, denatured, and intact 16S rRNA samples before injection into the SPRi system. Figure 9-3b shows the $\Delta\%R$ for hybridization, using Leg1 CP, of 16S rRNA pre-mixed with Leg1 DP 0bp for 18 minutes, followed by the addition of SA-QDs and a 10 min reaction time, as a function of the pre-treatment methodology.

Addition of the detector probe resulted in a slight increase in the signal, with the highest for fragmented 16S rRNA. SA-QDs addition also resulted in a drastic change in $\Delta\%R$ for fragmented 16S rRNA versus slight signal enhancement for intact and denatured RNAs. The enhanced hybridization efficiency could be explained by a higher number of hybridized detector probes for fragmented RNA due to the easy access of smaller RNA as well as the ease of access of SA-QDs to the small 16S rRNA fragments compared to the whole 16S rRNA.

9.4.3 Determination of the SPRi limit of detection for 16s rRNA from *L.*

Pneumophila

The optimal experimental parameters, the pre-treatment fragmentation, and the SA-QD post amplification strategy were used to investigate two more critical factors, the distance between the capture and the detector probe and the hybridization time, affecting the specificity and efficiency of the target sequence hybridization extracted from *L. pneumophila* and to determine the SPRi limit of detection (LOD) [26].

To investigate the effect of the detector probe's proximity to the capture probe on the specificity and sensitivity of the detection system, two detector probes for the Leg1 and Leg2 capture probes were designed to hybridize to the 16S rRNA sequence 0 and 7 bp away from the respective capture probes (Figures 9-4a and 9-4b). Figures 9-4c to 9-4f show the hybridization of four detector probes with fragmented 16s rRNA along with the use of SA-QD signal amplification for incubation times of 18 and 10 min, respectively. The results indicated that Leg2 CP possessed a higher signal when Leg2 DPs (Leg2 DPs at 0 and 7bp) were used compared to Leg1 DPs (Leg1 DPs at 0 and 7bp) (Figures 9-4c and 9-4d). This was further accentuated after the addition of SA-QDs. Both Leg2 DPs

produced significantly higher signals compared to Leg1 DPs (Figures 9-4e and 9-4f). This could be due to the position of these probes on the secondary structure of 16s rRNA. As shown in Figure 9-4b, Leg2 CP and Leg2 DP target the same stem-loop in the 16s rRNA secondary structure. The presence of Leg2 DPs, therefore, causes disruption of this stem-loop and further facilitates the reaction with Leg2 CP.

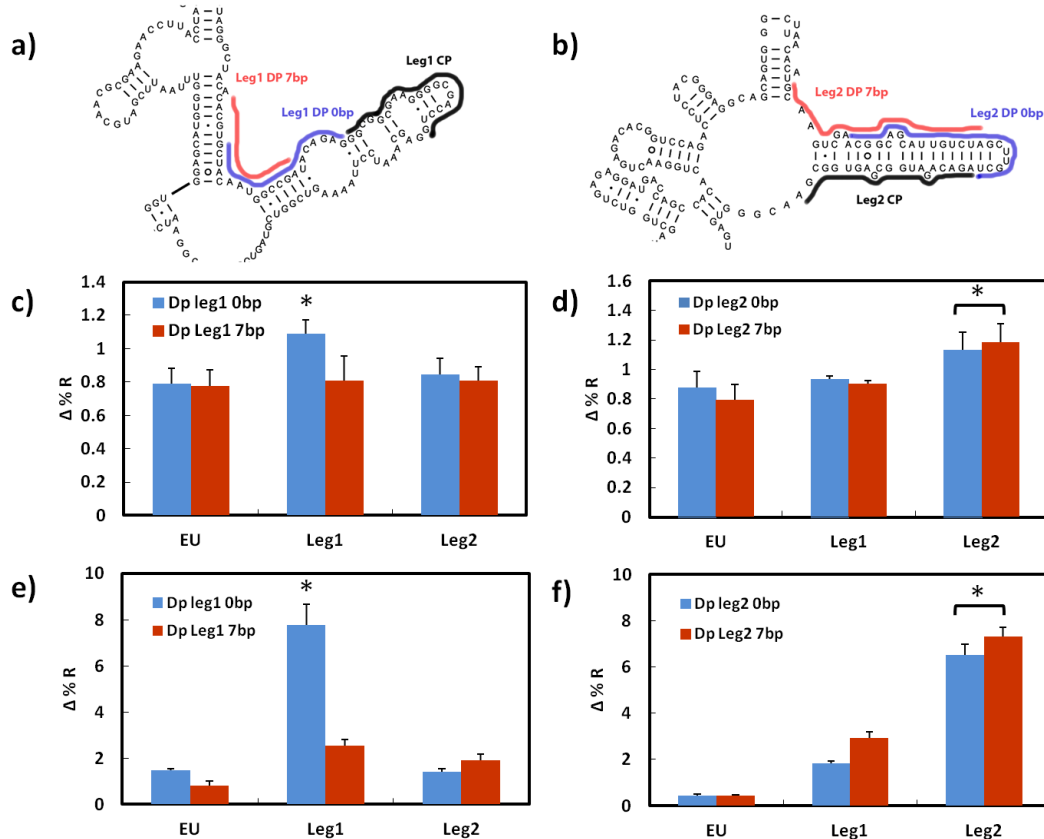


Figure 9-4 Effect of different detector probes on hybridization efficiency. x-axis represents capture probes a,b) secondary structure diagrams for *L. pneumophila* based on *L. pneumophila* model (accession number (accession number M34113) [252] for area complementary to Leg1 CP and Leg2 CP respectively. Lines next to the diagrams indicate of the position of capture and detector probes. c,d) Change in reflectivity was measured after 18 min for three different capture probes (EU, Leg1 and Leg2 CPs) for 10 nM fragmented 16s rRNA corresponding to a and b respectively. e,f) Addition of 1 nM SA-QDs for 10 min corresponding to c and d respectively. All data is expressed as mean + standard deviation (n=5, *P<0.05 versus other capture probes).

The same hybridization trend was therefore expected for Leg1 CP with both Leg1 DPs. However, only Leg1 DP 0bp showed a markedly enhanced signal either with 16s rRNA hybridization or the following SA-QD post amplification. Further examination of the secondary structure of *L. pneumophila* revealed that the position of Leg1 DP 0bp and Leg1 DP 7bp contributes significantly to this difference. As shown in Figure 9-4a, Leg1 DP 0bp contains two internal loops compared to Leg1 DP 7bp, which possesses only one internal loop. Upon further examination of the secondary structure, it was apparent that, for Leg1 DP 7bp hybridize to 16S rRNA, it needs to overcome a stronger secondary structure compared to Leg1 DP 0bp (14 bonds compared to 9). Since the Leg1 DP 0bp produced the most pronounced SPRi signal, it was selected for further experiments.

Finally, to determine the effect of hybridization time, fixed volumes of fragmented 16s rRNA were used with incubation times ranging from 4.5 to 150 min, obtained by varying the flow rate to the SPRi system. The range of incubation was purposely selected to maintain the time of analysis comparable to that of PCR. Figure 9-6 presents the effect of hybridization time on $\Delta\%R$ for Leg1 CP. As expected, increased incubation time was directly related to enhanced hybridization efficiency. An incubation time of 150 min was then chosen, along with optimal hybridization conditions, to investigate the SPRi sensitivity and its LOD for the detection of 16S rRNA from *L. pneumophila*. 16S rRNA hybridization with multiple samples containing fragmented 16s rRNA varying in concentration from 1 pM to 10 nM, with 100 nM Leg1 DP 0bp in 4X SSPE buffer were taken, and the hybridization adsorption kinetics were monitored in real time with SPRi measurements employing the SA-QD signal amplification strategy.

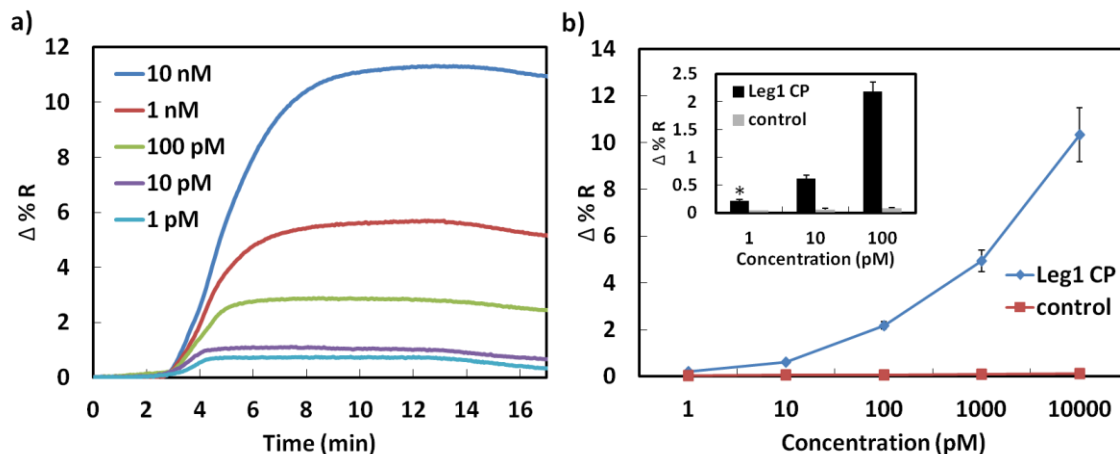


Figure 9-5 Fragmented 16s rRNA hybridization with Leg1 CP with series of ultralow RNA concentrations: 10 nM, 1nM, 100 pM, 10 pM, 1 pM a) Normalized real-time SPRi kinetic curve for detection of ultralow concentration of 16s rRNA b) The reflectivity change were plotted versus concentration after 150 min. The inset figure shows the differential reflectivity change ($\Delta\%R$) for 1 pM, 10 pM and 100 pM. All data expressed as mean \pm standard deviation (n=5, *P<0.05 versus control probe).

The normalized SPRi kinetic curves for SA-QD adsorption for various 16s rRNA concentrations ranging from 1 pM to 10 nM are given in Figure 9-5a. Figure 9-5b shows the plot of the $\Delta\%R$ for Leg1 and control capture probes for the aforementioned concentrations. The inset in Figure 9-5b shows the $\Delta\%R$ for low concentrations of 16s rRNA (1,10, and 100 pM). A significant difference in the SPR signal was observed between Leg1 CP and the control probe even at 1 pM 16S rRNA clearly established a limit of detection on the order of 1 pM *L. pneumophila* 16s rRNA. This value could be translated to the equivalent of 88.5 CFU μL^{-1} with the assumption of 6,800 ribosomes per bacteria [102]. This limit of detection is far lower than the previously reported value for RNA detection using an SPR biosensing system [25, 103].

9.5 Conclusions

Developing a detection system that distinguishes metabolic active pathogens with the desired specificity, sensitivity, and time of detection is of great importance and relevance

for the rapid detection of pathogens in environmental samples. In this paper, we conclusively demonstrated that a sub-femtomole level of 16S rRNA from pathogenic *L. pneumophila* can be specifically detected using an optimized experimental protocol, adequate design of capture and detector probes, and employing a QD signal amplification strategy with a SPRi biosensor. The proposed approach offers several distinct advantages compared to other conventional detection systems, including high specificity through the design of two probes (capture and detector) for the target, high sensitivity through using QD signal post amplification, and rapid and reliable quantification using *L. pneumophila*'s 16S rRNA, which is a good representation of metabolically active bacteria.

To achieve specific and sensitive detection, optimal hybridization conditions and parameters were implemented. We showed that the SPRi detection of 16S rRNA in solutions as dilute as 1 pM at 500 μ L (0.5 femtomole) can be achieved in less than three hours, making the SPRi detection system suitable for the direct detection of *L. pneumophila*, in man-made water systems. Through the integration of a microfluidic system with SPRi and further automation, it would be possible to reduce further the detection volume to less than 1 μ L and improve the LOD significantly.

9.6 Acknowledgements

We acknowledge National Science and Engineering Research Council of Canada- Collaborative Research program and Discovery program, Genome Canada/Genome Quebec, Nano-Quebec and Le Fonds Québécois de la Recherche sur la Nature et les Technologies-Centre for Biorecognition and Biosensors for their financial support. The authors would also like to thank Dr J-J Drieux and Dr P. Hiernaux from Magnus for their technical support and advices, S. Shapka and S. Filion-Côté for scientific discussions regarding SPRi and Dr T. Fatanat Didar for his comments on the manuscript. Work in SPF laboratory is supported by NSERC Discovery Grant 418289-2012.

9.7 Supplementary Information:

Table 9-1 Oligonucleotide sequences employed as capture and detector probes.

Name	Sequence 5'--3'
EUB342	ACTGCTGCCTCCCGTAG
Control	TCAATGAGCAAAGGTAT
<i>Legionella pneumophila</i> 1	CAGGTCGCCCCTTCGCCGCC
<i>Legionella pneumophila</i> 2	TCGCCACTCGCCATCTGTCT
Detector probe Leg1 0bp	CTCTGTATCGGCCATTGTAGC
Detector probe Leg1 7bp	TCGGCCATTGTAGCACGTGTG
Detector probe Leg2 0bp	AGCAAGCTAGACAATGCTGCCGT
Detector probe Leg2 0bp	TAGACAATGCTGCCGTTCTGACTTGC
Synthetic <i>Legionella pneumophila</i> 's RNA	UACACACGUGCUACAAUGGCCGAUACAGAGGGCGG CGAAGGGGCGACCUGGAGCAAUCC

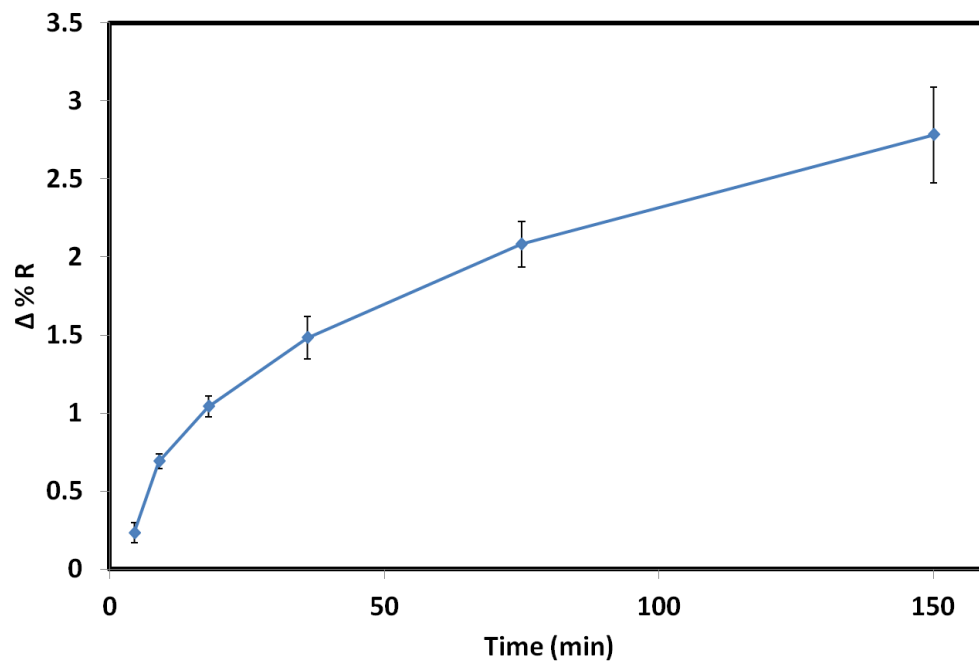


Figure 9-6 Effect of hybridization time of 10 nM fragmented 16S rRNA with Leg1 Cp on hybridization efficiency. All data is expressed as mean \pm standard deviation (n = 5).

Preface to Chapter 10: Sensitive and Specific SPRi Detection of *L.*

***pneumophila* in Complex Environmental Water Samples**

To fulfill the second objective of this thesis, the sensitivity and specificity of the system developed in the first objective were validated for the detection of *L. pneumophila* in complex environmental water samples.

The cohabitation of the amoeba with *L. pneumophila* in the nutrition deprived buffer and the environmental water samples was investigated. Furthermore, the accuracy of this detection approach in these conditions and their effects on the biosensor performance was studied.

The results of this study are reported in the following manuscript entitled "Sensitive and Specific SPRi Detection of *L. pneumophila* in Complex Environmental Water Samples" which is under consideration for publication in the journal *Analytical and Bioanalytical Chemistry* journal.

Chapter 10 Sensitive and Specific SPRi Detection of *L. pneumophila* in Complex Environmental Water Samples

Amir M. Foudeh^a, Hana Trigui^b, Nilmini Mendis^b, Sebastien P. Faucher^b, Teodor Veres^{a,c}, and Maryam Tabrizian^{a}*

^a Department of Biomedical Engineering, Faculty of Medicine, McGill University, 3775 University Street, H3A 2B4, Montreal (QC), Canada. E-mail: maryam.tabrizian@mcgill.ca

^b Department of Natural Resource Sciences, Macdonald Campus, 12 McGill University, 21,111 Lakeshore, H9X 3V9, Ste-Anne-de-Bellevue, Quebec, Canada.

^c National Research Council Canada, 75 Boul. de Mortagne, J4B 6Y4, Boucherville, QC, Canada.

10.1 Abstract:

Legionellosis is a very devastating disease worldwide mainly due to unpredictable outbreaks in man-made water systems. Developing a highly specific and sensitive rapid detection system that detects only metabolically active bacteria is a main priority for water quality assessment. We previously developed a versatile technique for sensitive and specific detection of synthetic RNA. In the present work, we further investigated the performance of the developed biosensor for detection of *L. pneumophila* in complex environmental samples, particularly those containing protozoa. The specificity and sensitivity of the detection system was verified using total RNA extracted from *L. pneumophila* in spiked water co-cultured with amoebae. We demonstrated that the expression level of rRNA is extremely dependent on the environmental conditions. The presence of amoebae with *L. pneumophila*, especially in nutrition-deprived samples, increased the amount of *L. pneumophila* 15-fold after one week. Using the developed SPRi detection method, we were also able to successfully detect *L. pneumophila* within three hours, both in the presence and absence of amoebae in the complex environmental samples obtained from a cooling water tower. These findings suggest that the developed biosensing system is a viable method for rapid, real-time and effective detection not only for *L. pneumophila* in environmental samples, but also to assess the risk associated with the use of water contaminated with other pathogens.

10.2 Introduction

Legionella species are the causative agent of Legionellosis, and among them, *Legionella pneumophila* (*L. pneumophila*) is responsible for more than 90% of Legionellosis. Legionellosis is a very devastating disease worldwide mainly due to unpredictable outbreaks. Legionellosis which is transmitted through aerosol, is manifested as a form of pneumonia or Pontiac fever, a milder form of the disease with flu-like symptoms [1]. Between 2001-2006, 30% of waterborne disease outbreaks in the USA were caused by *Legionella* [5]. The fatality rate of Legionellosis can approach 50% within industrial and hospital outbreaks, especially affecting individuals with a compromised health condition [1]. *L. pneumophila* is found in most natural and engineered water systems, such as air conditioning, showers and cooling towers where it contaminates and multiplies inside amoeba [8].

Currently, *L. pneumophila* is mainly detected by laboratory culture, polymerase chain reaction (PCR), immunology-based methods and DNA microarray methods [10-12]. However, these detection methods all have shortfalls. The culture method is very time consuming, does not have the ability to detect viable but nonculturable cells (VBNC). PCR is unreliable in many situations, due to false-positive detection of nonviable bacteria and the presence of inhibitors in environmental water [253]. DNA microarrays are also unable to distinguish between live and dead bacteria. Targeting rRNA is a viable alternative that overcomes the aforementioned limitations: it provides a detection system that is more reliable, accurate, and sensitive. This is due both to the correlation of RNA expression level in bacteria with microbial activity, and to the presence of high copy numbers of 16S rRNA in each bacterium.

We developed an effective, technique for detection of synthetic RNA [13], through the design of specific DNA capture and detector probes along with the use of Quantum dots (QDs) for signal amplification. We were able to detect sub-femtomole levels of synthetic RNA with the Surface Plasmon Resonance imaging (SPRi) biosensor in less than three hours. Although detection of synthetic RNA is the first step towards the development of a biosensor for on-site detection, the main challenge remains to validate the performance of the developed biosensor for much more complex situations such as the detection of RNA extracted from pathogenic *L. pneumophila* in environmental water samples, particularly when protozoa are present.

The interaction of protozoa, especially amoebae, with *L. pneumophila* in water systems is of great importance. Most of the conventional biosensors are unable to detect the *L. pneumophila* hidden inside amoeba and failed to provide any meaningful information regarding the interaction of *Legionella* with protozoa especially in the environmental water samples. *L. pneumophila* can normally survive in nutrition-deprived environments for long periods of time but cannot multiply. They multiply in these environments mostly when amoebae were also present [27]. The ingestion of *L. pneumophila* by amoebae provides an intra-cellular environment for its amplification in water systems. In addition, amoebae can also act as a shelter against harsh conditions such as low temperatures and the presence of biocides [27-30], In the case of biocide treatment, this protection can result in treatment failure, after which *L. pneumophila* might be able to recolonize the water system rapidly. Another important impact of amoeba-*Legionella* interaction is the enhancement of the virulence of *L. pneumophila*

[31]. It has been reported that their combined action contributes to *L. pneumophila*'s virulence by priming the bacteria to infect human cells [254].

Therefore, in our current work, we investigated the interaction of the amoeba with *L. pneumophila* in the nutrition deprived buffer and the environmental water samples. We further examined the specificity and sensitivity of our detection approach in these conditions and their effects on the biosensor performance with the ultimate goal of developing an on-site detection system (Figure. 10-1). In order to ensure specificity of the detection system, we first examined total RNA (tRNA) extracted from different bacteria and then the limit of detection of tRNA extracted from pathogenic *L. pneumophila* was determined with our SPRi-based biosensor setup. In addition, the effect of residency of *L. pneumophila* in nutrition-deprived water samples and amoeba-*Legionella* interaction in a co-culture system with defined water composition on 16s rRNA expression and on the SPRi signal at different time points were assessed. Finally, cooling tower water samples contaminated with *L. pneumophila*, in the presence and absence of amoebae, were examined to explore the viability of the developed technique for detecting *L. pneumophila* in a complex environment.

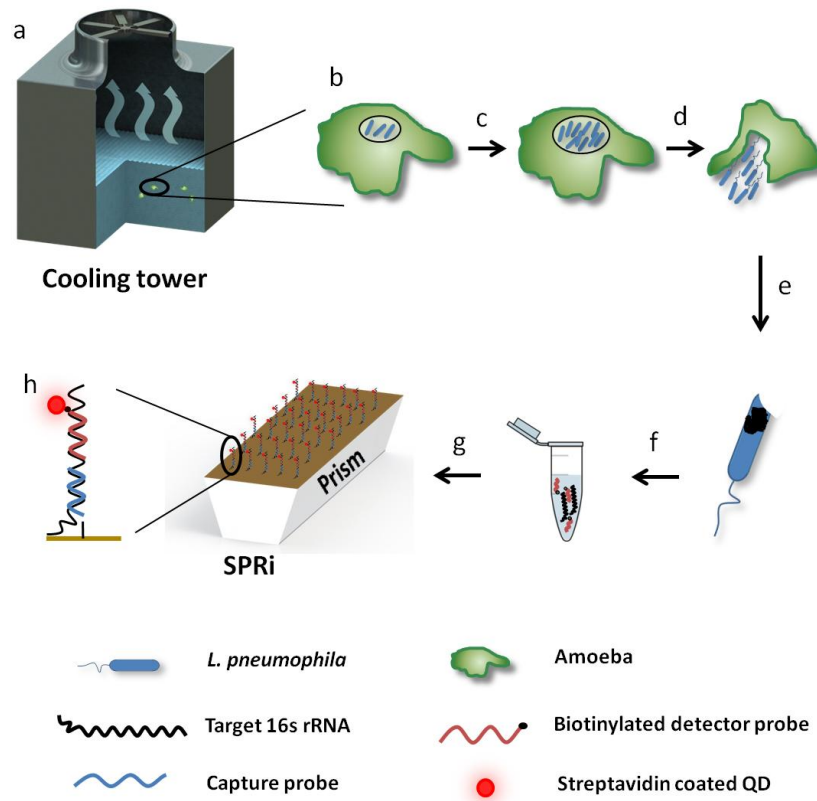


Figure 10-1 Schematic illustration of the infection cycle of *L. pneumophila* in amoebae in cooling tower water and detection of *L. pneumophila* using SPRi: a) cooling tower water containing amoebae and *L. pneumophila*, b) an amoeba infected by *L. pneumophila*, c) multiplication of *L. pneumophila* inside an amoeba, d) lyses of amoeba and release of *L. pneumophila*, e) collection and lyses of *L. pneumophila*, f) extraction and fragmentation of RNA from *L. pneumophila*, g) hybridization of extracted RNA on the SPRi chip, h) schematic of the RNA hybridization using capture and detector probes and use of QDs post amplification.

10.3 Experimental:

"Materials and Methods" can be found in the Electronic Supplementary Material.

10.4 Results and Discussion:

10.4.1 Assessment of specificity and sensitivity of the SPRi biosensor

In order to evaluate the specificity of the detection system, the change in SPRi reflectivity ($\Delta\%R$) of tRNA hybridization from 10^6 CFU/mL of *L. pneumophila*, two different strains of *E. coli* (DH5 α and K12) and *Pseudomonas aeruginosa* was measured. As shown in Figure 10-5, hybridization of tRNA extracted from all bacteria except for *L. pneumophila* did not result in a significant SPR signal. This confirmed that the designed capture and detector probes allowed for highly specific detection of *L. pneumophila*. To determine the sensitivity and limit of detection (LOD) for tRNA, a dilution series of *L. pneumophila* in AYE medium ranging from 3×10^4 to 3×10^8 CFU/mL was made, and 1 mL of each sample was used for RNA extraction. The extracted RNA was then fragmented and the hybridization kinetic was monitored in real-time with SPRi biosensor, employing the SA-QD signal amplification. The results indicated that RNA could be extracted from very low concentrations of bacteria, ranging from 3×10^4 - 3×10^8 CFU/mL. A LOD comparable to that obtained for the detection of Synthetic RNA [13] was achieved thereby confirming the high sensitivity of the developed detection system in a complex mixture of RNA (Figure 10-6).

10.4.2 16s rRNA expression level

The presence of *L. pneumophila* in non-optimal conditions, especially in nutrition-deprived environments, has been reported to affect its metabolic activity which in turn influences the expression of 16s rRNA [255]. To investigate the metabolic activity of *L. pneumophila* in nutrition-deprived environments, *L. pneumophila* was incubated in AC buffer at different time points from 0-48 hours. Reverse transcriptase PCR was first

performed to convert RNA to cDNA, and then real-time PCR was carried out to quantify the expression level of 16s rRNA. Since in real-time PCR, the cycle threshold (Ct) is defined as the number of cycles required for the signal to exceed the background level, the Ct value is inversely proportional to the amount of RNA in the sample (Figure 10-2). It has been reported that *L. pneumophila* cannot grow in AC buffer [256] and we further confirmed this by CFU counting for each sample (data not shown). Our results suggest that, even after 6 hours of exposure of *L. pneumophila* to AC buffer, the level of 16s rRNA expression dropped significantly and this trend continued up to 48 hours (Figure 10-2). This further shows that the metabolic activity of bacteria is extremely dependent on their milieu, and confirms that targeting 16s rRNA in bacteria could give meaningful insight into the metabolic state of bacteria.

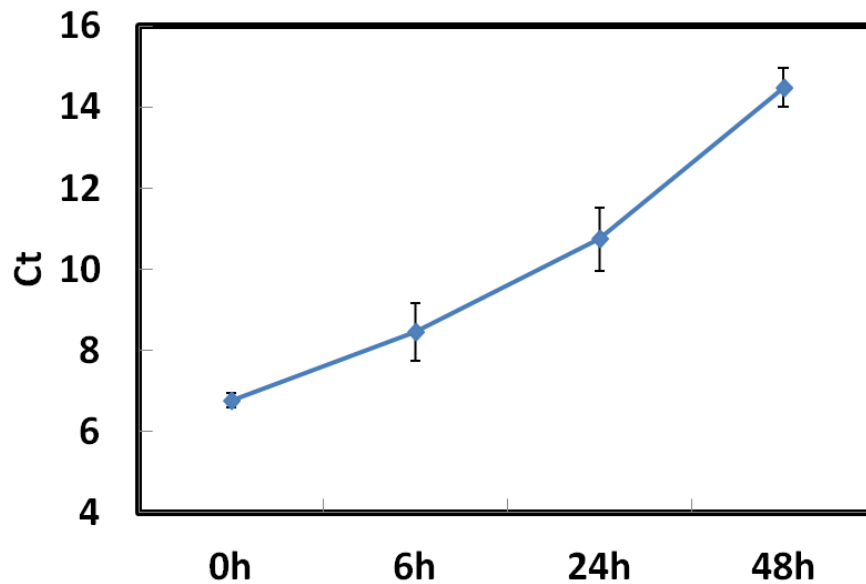


Figure 10-2 The effect of incubation time of *L. pneumophila* in AC buffer on 16s rRNA expression was examined. Ct values obtained from real-time PCR experiments and plotted against four different incubation time points. All data are expressed as mean \pm standard deviation.

10.4.3 SPRi detection of *L. pneumophila* co-cultured with amoeba

In order to investigate the effect of amoebae presence on *L. pneumophila* purulence, 1.5×10^6 amoebae were co-cultured with 1.5×10^6 CFU of *L. pneumophila* in AC buffer. Figure 10-3 shows changes in SPRi signal as a function of *L. pneumophila* concentration after 1, 2 and 7 days in the presence and absence of amoebae. Interestingly for *L. pneumophila* in AC buffer, the SPRi signal dropped to 0.18 ± 0.09 as of day one (Figure 10-3b) which is significantly lower than at the same concentration in AYE (2% change in reflectivity is expected at the same concentration in AYE, according to Figure 10-6). This lower SPRi signal is obviously due to the reduction of 16s RNA expression of *L. pneumophila* in a nutrient-poor medium as compared to the SPRi signal in an AYE medium. The drop in SPRi signal is also in agreement with our previous observation, depicted in Figure 10-2. The Ct value for day 1 was significantly lower than that for day 0. The SPRi signal for day 1 was stronger for the co-cultured samples than for the *L. pneumophila* cultured alone: (0.18 ± 0.09 versus 0.72 ± 0.13) while the CFU count remained the same for both (Figure 10-3a). This further confirmed that the of amoebae would enhance *L. pneumophila* 16s rRNA expression.

In order to examine the effect of RNA extracted from amoebae on the detection system performance, the negative control samples containing only amoebae were also tested at all time points. No signals for amoeba samples were observed (data not shown). As seen in Figure 10-3a, although the concentration of *L. pneumophila* in AC buffer remained the same from day 1 to 7, the presence of amoebae in co-culture samples resulted in a significant increase of *L. pneumophila* concentration after 2 and 7 days as compared to day 1. The same trend could be observed with SPRi results. The reflectivity

change for the co-culture sample increased with incubation time. We believe that the increase in the SPRi signal is mainly due to the increase of *L. pneumophila* concentration and partly due to the increased expression of 16s rRNA.

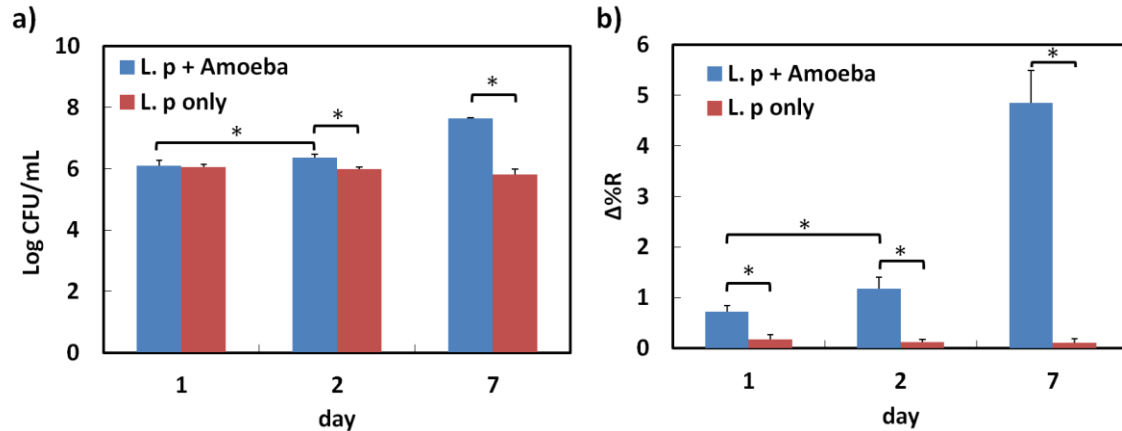


Figure 10-3 Incubation of *L. pneumophila* in AC buffer in presence and absence of amoeba after 1, 2 and 7 days. a) Concentration of *L. pneumophila* versus incubation time b) SPRi measurements of the hybridization of extracted RNA from 1 mL of each sample with QDs post amplification. An initial concentration of 10^6 CFU of *L. pneumophila* in presence and absence of 10^6 amoebae in a 6-well plate was used. All data expressed as mean \pm standard deviation (* $P < 0.05$).

10.4.4 Validation of sensing technique for the cooling tower water sample:

To demonstrate the specificity and sensitivity of the system for the detection of *L. pneumophila* in complex environmental samples, *L. pneumophila* with a concentration ranging from 2×10^4 to 2×10^8 CFU/mL was spiked in a water sample from a cooling tower. A series of the SPRi measurements were performed in the presence and absence of amoebae after two days to assess the effect of the this complex water sample on the *L. pneumophila* purulence and the 16s rRNA expression. As shown in Figure 10-4a, the concentrations of *L. pneumophila* samples did not change after two days (1:1 linear correlation between day 0 and 2) while a significant increase of *L. pneumophila* concentration was observed when *L. pneumophila* was co-cultured with amoebae for all

initial concentrations used in this study. After day 2, the increase in *L. pneumophila* concentrations in the co-cultured samples was greater for the initial concentrations of 4, 5.3 and 6.2 Log CFU/mL than for the initial concentrations of 7.1, 7.4 and 8.2 Log CFU/mL. This could be due to the difference in the infection ratio of *L. pneumophila* to amoebae. Since the initial amoebae concentration was chosen as 6.2 Log amoebae per sample, the infection ratio of less than one (samples with initial concentrations of 4, 5.3 and 6.2 Log CFU/mL) resulted in a more pronounced increase in concentration of *L. pneumophila*. This result is in agreement with literature reporting that at a higher infection ratio (when there are more bacteria per amoeba), the amoebae are lysed more rapidly [257, 258]. Therefore, there would be less amoebae for *L. pneumophila* to grow in, which would explain the reason behind our overall observation.

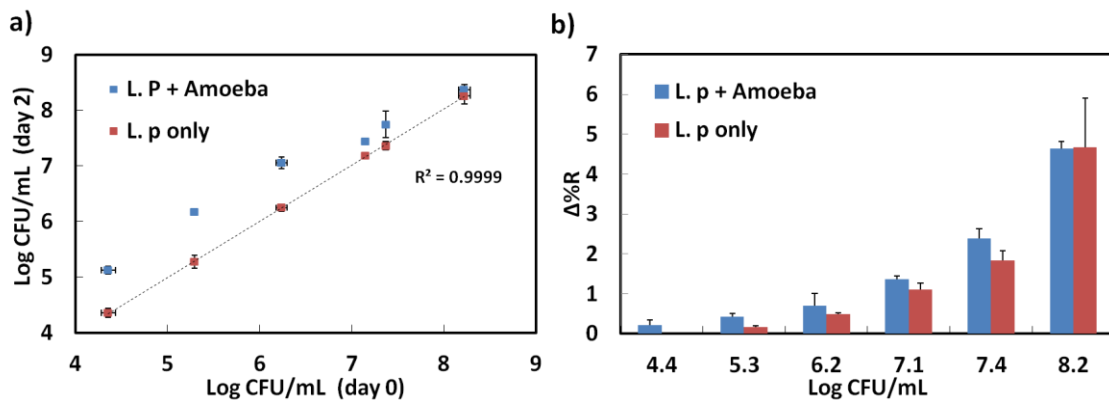


Figure 10-4 Incubation of a dilution series of *L. pneumophila* in a cooling water sample in the presence and absence of 1.5×10^6 amoeba for 2 days. a) CFU plate counting for each sample. b) SPRi signal measurements of the hybridization of extracted RNA from 1 mL of each sample with QDs post amplification. All data expressed as mean \pm standard deviation.

The presence of *L. pneumophila* in cooling tower water samples resulted in a higher SPRi signal as compared to signals from AC buffer samples shown in Figure 10-4b. For instance, the sample with a concentration of 6.2 and 5.3 Log CFU/mL resulted in $0.499 \pm$

0.02 and 0.17 ± 0.02 changes in reflectivity, respectively. These reflectivity changes were higher than the reflectivity change of 0.12 ± 0.05 obtained from 6 Log CFU/mL in AC buffer after 2 days (Figure 10-3b). This could be explained by the fact that the cooling tower water sample might contain more nutrition elements than the AC buffer. This higher concentration of nutrients can enhance the metabolic activity of the *L. pneumophila* and therefore the 16s rRNA expression level. As such, we could successfully detect *L. pneumophila* samples in the presence of amoebae with initial *L. pneumophila* concentrations as low as 4.4 Log CFU/mL (Figure 10-4b).

10.5 Conclusions

Monitoring metabolically active bacteria rapidly with high specificity and sensitivity is the main challenge in water quality assurance to prevent any potential outbreaks due to contaminated water systems. Using total RNA extracted from *L. pneumophila* along with SPRi technology, we investigated RNA as a viable genetic moiety that can provide a highly specific and sensitive detection modality for the detection of *L. pneumophila* in environmental water samples. We demonstrated that targeting 16s rRNA in *L. pneumophila* gives meaningful insight into the metabolic state of the bacteria by exposing bacteria to a nutrition-deprived environment and monitoring the change in 16s rRNA expression with time. Our results showed that after only six hours of exposure of *L. pneumophila* to a nutrition-deprived environment, the 16s rRNA expression level decreased significantly. Interestingly, the presence of amoebae with *L. pneumophila*, in nutrition-deprived AC buffer enhanced the expression of 16s rRNA after one day and resulted in a 15-fold increase in *L. pneumophila* concentration after one week. Further development of this biosensing approach for detection of *L. pneumophila* would certainly

contribute to the implantation of tools and platform for rapid, real-time and multiplex detection of bacteria, which is essential for water risk assessment of various sources.

10.6 Acknowledgments

We acknowledge National Science and Engineering Research Council of Canada-Strategic and Discovery program, Genome Canada/Genome Quebec and Nano-Quebec. The authors would also like to thank R. Tien Sing Young for helping with illustrations design, L. Li for the amoeba culture and Dr. K. Bowey for her comments on the manuscript. The Work in SPF laboratory is supported by NSERC Discovery Grant 418289-2012.

10.7 Electronic Supplementary Material

10.7.1 Materials and methods

10.7.1.1 Chemical and reagents

Oligonucleotides (ODN) were purchased from Integrated DNA Technologies (Coralville, IA, USA). Streptavidin-coated quantum dots (Qdot 800 STVD), Denhardt's solution [50× solution is 1% Ficoll (type 400), 1% polyvinylpyrrolidone, and 1% bovine serum albumin], and SSPE buffer (20× buffer is 3.0 M NaCl, 0.2 M NaH₂PO₄, and 0.02 M EDTA at pH 7.4) were purchased from Invitrogen (Carlsbad, CA, USA). Random primers and superscript II reverse transcriptase were purchased from Life Technologies, (Gaithersburg, MD, USA). ITaq Universal SYBR Green Supermix was purchased from Bio-Rad (Hercules, CA, USA). A fragmentation kit was obtained from Ambion (Carlsbad, CA, USA). All other reagents were purchased from Sigma-Aldrich (St. Louis, MO, USA) unless stated otherwise.

10.7.1.2 DNA probe design

DNA capture probe (CP), detector probe (DP) and control probe were designed and were immobilized on the biochip gold surface as described previously (Table 10-1) [13].

Table 10-1 Oligonucleotide sequences employed in the experiments.

Name	Sequence 5'--3'
Control probe	TCAATGAGCAAAGGTAT
<i>Legionella pneumophila</i> 1 (Leg1 CP)	CAGGTCGCCCCTTCGCCGCC
Detector probe (Leg1 DP)	CTCTGTATCGGCCATTGTAGC

10.7.1.3 Surface chemistry on SPRi biochip

Gold-coated slides (Horiba, France) were cleaned by UV/ozone treatment and piranha solution and rinsed thoroughly with MQ water. DNA immobilization was performed using 1 μ M thiol-modified oligonucleotide probes in 1 M KH_2PO_4 for 180 minutes [13]. Following the immobilization, substrates were treated with 1 mM MCH for 90 minutes, further passivated with 2.5 \times Denhardt solution for 10 minutes and stored at 4 $^\circ\text{C}$ before further use.

10.7.1.4 SPRi measurements

SPRi experiments were performed using a scanning-angle SPRi instrument (model SPRi-Lab+, Horiba, France). The SPRi apparatus, equipped with an 800 nm LED source, a CCD camera and a flow cell, was placed in an incubator (Mettmert Peltier, Rose

Scientific, Canada). The SPRi measurements were performed by imaging the entire biochip surface during the angular scan [37]. At least five spots were selected for both the probes and the controls in each experiment and repeated at least three times. RNA hybridization assays were carried out as described previously [13]. Briefly, 450 μ L of each sample was used for each experiment, which were all carried out at 37°C. A baseline signal was first obtained for the hybridization buffer consists of 4 \times SSPE buffer, followed by the hybridization signal for the RNA targets mixed with biotinylated detector probes. Next, 1 nM streptavidin-conjugated Qdots (SA-QDs) were injected and allowed to bind to the detector probes for 10 minutes. At each step, the chip was rinsed with buffer, and the difference in the reflected intensity ($\Delta\%R$) was computed. Successive hybridizations were followed by surface regeneration using 50 mM NaOH prior to each measurement.

10.7.1.5 Co-culture of L. pneumophila and Amoeba

Acanthamoeba castellanii (a common amoeba which support intracellular life of *L. pneumophila* [27, 32, 33]) were cultured in peptone yeast glucose (PYG) broth (20 g proteose peptone, 1 g yeast extract, 0.1 M glucose, 0.4 mM MgSO₄, 0.05 mM CaCl₂, 0.1 mM sodium citrate, 0.005 mM Fe(NH₄)₂(SO₄)₂, 0.25 mM Na₂HPO₄ and 0.25 mM KH₂PO₄, adjusted pH to 6.5 with HCl) at 30 °C. For the co-culture experiments, 1.5×10^6 cells in 1ml of PYG were seeded into each well of a 6-well plate. After 40 minutes, the media in each well was removed and washed three times with AC buffer (0.4 mM MgSO₄, 0.05 mM CaCl₂, 0.1 mM sodium citrate, 0.005 mM Fe(NH₄)₂(SO₄)₂, 0.25 mM Na₂HPO₄ and 0.25 mM KH₂PO₄, pH to 6.5). The laboratory wild type JR32, a streptomycin resistant, restriction-negative mutant of the *L. pneumophila* strain

Philadelphia-1, was used. Strains grown on BCYE agar (10 g/L Yeast extract, 10g/L ACES buffer, 15 g/L Agar, 2 g/L Activated Charcoal, 0.25 mg/ml ferric pyrophosphate and 0.4 mg/ml L-cysteine) were suspended in AYE broth (ACES-buffered yeast extract broth supplemented with 0.25 mg/ml ferric pyrophosphate and 0.4 mg/ml L-cysteine) at an OD₆₀₀ of 0.1 and then further diluted to obtain an approximate desired concentration. CFU counts at different time points were performed to track growth of the bacteria.

10.7.1.6 RNA extraction

RNA extraction was performed from 1 mL of each sample. For the co-culture experiment, pipetting was performed several times to make sure all amoebae and bacteria were in suspension before collecting a sample. The RNA extraction was then performed using a column-based PureLink RNA mini kit from Ambion, according to the manufacturer recommendations.

10.7.1.7 Total RNA fragmentation

Total RNAs extracted from bacteria were fragmented using a fragmentation kit from Ambion. The mixture was incubated at 75 °C for 15 minutes, followed by the addition of the blocking solution [13]. The samples were kept on ice until further use.

10.7.1.8 Reverse transcriptase PCR and Real-time PCR

For analysis of the 16s RNA expression by Reverse transcriptase PCR (RT-PCR) and real-time PCR (qPCR), RNA was extracted from *L. pneumophila* and exposed to AC buffer with different incubation times. Four microliters of extracted RNA was then converted to cDNA by using random primers and Superscript II reverse transcriptase, following the manufacturer's instructions (Life Technologies). For each sample, a

negative control without reverse transcriptase was carried out. Real-time PCR reactions were then performed with 1 µl of cDNA using the iTaq Universal SYBR Green Supermix following the manufacturer's instructions (Bio-Rad). A primer set used for real-time PCR analysis is as Table 10-2.

Table 10-2 Forward and reverse primers for RT-PCR

Forward	5'-AGAGATGCATTAGTGCCTTCGGGA-3'
Reverse:	5'-ACTAAGGATAAGGGTTGCGCTCGT-3'

10.7.1.9 Cooling tower water sample

The environmental water sample was provided by the “Service de l’environnement Ville de Laval” originating from a municipality cooling tower. This cooling water sample was filtered with 0.2 µm and spiked with *L. pneumophila* accordingly.

10.7.1.10 Statistics

The lower detection limit was defined as the smallest concentration of an analyte, calculated as the blank signal plus or minus three standard deviations. All data were expressed as the mean ± SD. Statistical comparisons between two groups were done using Student’s paired t-test.

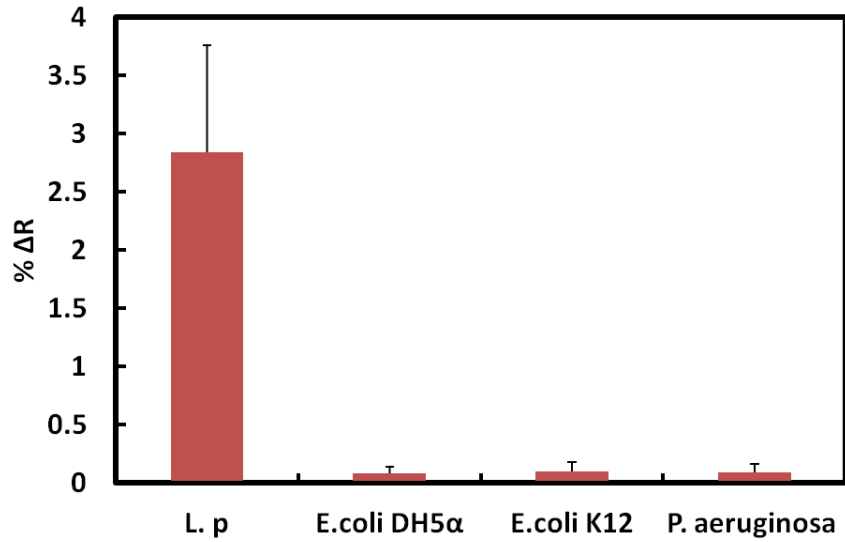


Figure 10-5 Specificity of the detection system was evaluated. The reflectivity change of QD post amplification after hybridization of total RNA extracted from *L. pneumophila* was compared against 2 strains of *E. coli* and one strain of *Pseudomonas*. RNA was extracted from 1 mL of 10^6 CFU/mL of each bacterium. All data expressed as mean \pm standard deviation.

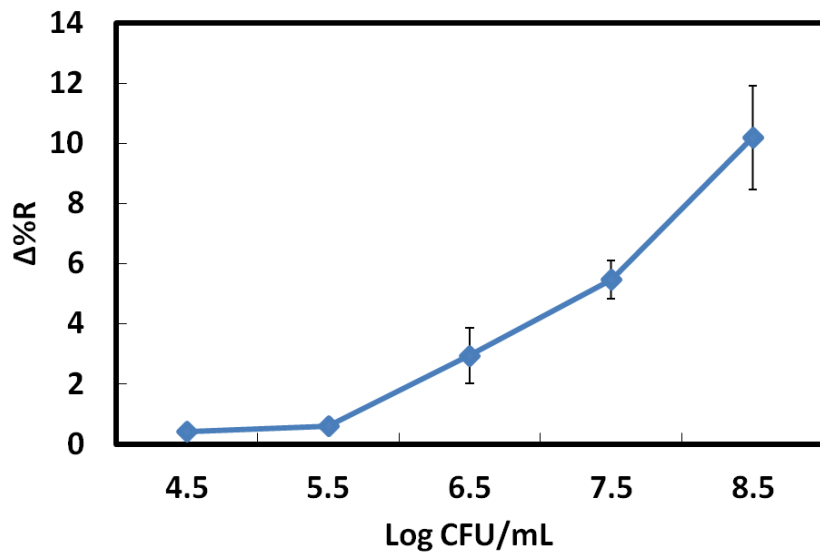


Figure 10-6 Hybridization of fragmented total RNA extracted from *L. pneumophila* with Leg1 CP. The reflectivity change of QD post amplification after hybridization of total RNA was plotted versus the series of *L. pneumophila* concentrations. All data expressed as mean \pm standard deviation.

Preface to Chapter 11: Rapid and Multiplex Detection of *Legionella*'s RNA using Digital Microfluidics

The ultimate goal of this project was to develop a low-cost rapid biosensor allowing miniaturization for on-site applications. To reach this goal, the third objective of this thesis project was set in order to adopt the developed detection platform during the first objective with a DMF chip. The modifications were included the use of magnetic beads as 16s rRNA bearing moieties within the DMF device and fluorescence microscopy as optical transducer. Such as, simultaneous manipulation of multiple droplets on-chip allowed to determine the optimal hybridization conditions including magnetic capture, hybridization duration, washing steps, and assay temperature. Further, the multiplex detection of 16s rRNA from two different species of *Legionella*: *L. pneumophila* and *L. israelensis* was demonstrated. A limit of detection of 1.8 attomoles RNA could be achieved.

These finding are resulted in a manuscript entitled "Rapid and Multiplex Detection of *Legionella*'s RNA using Digital Microfluidics" which is published in *Lab on a Chip* in 2015.

Chapter 11 Rapid and Multiplex Detection of *Legionella*'s RNA using Digital Microfluidics

*Amir M. Foudeh, ‡^a Daniel Brassard, ‡^b Maryam Tabrizian^a, and Teodor Veres^{*a, b}*

^a 3775 University Street, Department of Biomedical Engineering, Faculty of Medicine,
McGill University H3A 2B4, Montreal (QC), Canada.

^b National Research Council Canada, 75 de Mortagne Blvd., J4B 6Y4 Boucherville, QC,
Canada. Tel (450) 641-5232 Cell (514) 449 3370 Fax (450) 641-5105

*E-mail : teodor.veres@cnrc-nrc.gc.ca

‡: These two authors made equal contributions.

Abstract

Despite recent advances in the miniaturization and automation of biosensors, technologies for on-site monitoring of environmental water are still at an early stage of development. Prevention of outbreaks caused by pathogens such as *Legionella pneumophila* would be facilitated by the development of sensitive and specific bioanalytical assays that can be easily integrated in miniaturized fluidic handling systems. In this work, we report on the integration of an amplification-free assay in digital microfluidics (DMF) for the detection of *Legionella* bacteria based on targeting 16s rRNA. We first review the design of the developed DMF devices, which provide the capability to store up to one hundred nL-size droplets simultaneously, and discuss the challenges involved with on-chip integration of the RNA-based assay. By optimizing the various steps of the assay, including magnetic capture, hybridization duration, washing steps, and assay temperature, a limit of detection as low as 1.8 attomoles of synthetic 16s rRNA was obtained, which compares advantageously to other amplification-free detection systems. Finally, we demonstrate the specificity of the developed assay by performing multiplex detection of 16s rRNAs from a pathogenic and a non-pathogenic species of *Legionella*. We believe the developed DMF devices combined with the proposed detection system offers new prospects for the deployment of rapid and cost-effective technologies for on-site monitoring of pathogenic bacteria.

11.1 Introduction

Water-related diseases are responsible for more than 3.4 million deaths annually [259]. Among these diseases, Legionellosis, an acute form of pneumonia, is a major concern for outbreaks, as shown by recent incidents reported in Canada, USA, Norway, and Germany [2-4]. *Legionella*, the causative agent of this disease, was responsible for more than 30% of water borne disease outbreaks in USA between 2001-2006 [5]. Legionellosis outbreaks are associated with high mortality rates (15 to 20%)[260], which can reach up to 50% for individuals with a compromised health condition [1]. *Legionella* is found in most natural and man-made water systems [8] such as cooling towers, air conditioners and showerheads. These systems not only provide optimal growth conditions, but can also propagate *Legionella* through aerosol [261]. Presently, more than 50 *Legionella* species have been identified with approximately half of these species being associated with human disease [6] [7]. To have an accurate and reliable evaluation of the risk involved with various water systems, it is thus crucial to design detection systems that can distinguish between pathogenic and non-pathogenic *Legionella*. A biosensor for detection of *Legionella* should thus be specific and sensitive with capability of multiplex detection of different bacteria's species. Also, development of on-site systems that are portable, automated, cost-effective and rapid is required to monitor the water systems routinely and better predict any potential outbreaks. Today, detection of *Legionella* continues to rely to a large extent on the conventional culturing method, which is very time-consuming and expensive.

Molecular methods such as polymerase chain reaction (PCR), DNA microarray and immunology have also been used for the detection of *Legionella* in laboratory settings.

Automatic robotic liquid handling systems using standard well plates can be used to perform the numerous liquid handling steps required by these methods. These robotic systems can perform at rate of tens of assays per minute. However, they require sample volumes of μL or more. Below this level, evaporation and capillary forces are major issues [262]. In addition the robotic liquid handling systems are very sensitive to the viscosity and nature of the sample solutions. For instance handling solution containing nucleic acid and proteins with high concentrations would be challenging [263]. Large size, instrumentation complexity and cost are among other major drawbacks of these robotic systems that make them less practical for field applications such as on-site monitoring. Also, field applications do not necessarily require high speeds and massive parallelisation, but rather precise control over complex protocols with instrumentation that have small footprint and low-cost.

Therefore, miniaturization of pathogen detection methods and their integration in microfluidic devices has been gaining much attention as it can not only lead to the reduction of reagent consumption and analysis time but can also facilitate on-site deployment of chemical and biological assays [11]. Digital microfluidics (DMF) has recently arisen as a promising and versatile platform for chemical and biological applications. In DMF, as opposed to continuous flow microfluidics, individual droplets (of pL to μL) are manipulated independently by applying electric potential to an array of electrodes. Multiple droplets containing different reagents can be manipulated simultaneously and the operation scheme can be reprogrammed without the need to change the device design.

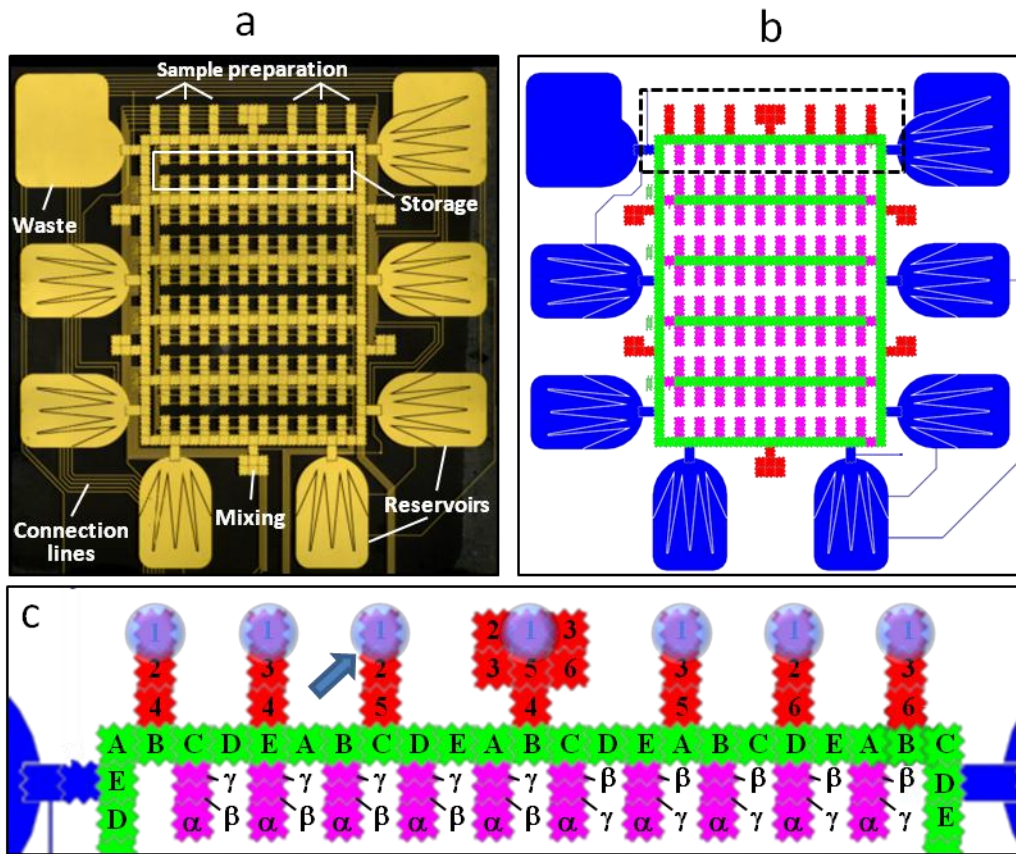


Figure 11-1 a) Top view of the developed digital microfluidic device. b) Schematic of electrical input pin to electrowetting electrode assignment. Each color represents a partition to which specific input pins are assigned. The partitions were defined according to the functions of the electrowetting electrodes: dispensing (blue), transportation (green), preparation (red), and storage (purple). c) Example of pin assignment in top section of the chip, each number/letter representing a specific electrical input.

Each droplet can thus act as microreactor from which independent tests can be performed concurrently in a confined environment, therefore making DMF a promising candidate for applications involving complex and multistep assays [34]. Also, compared to conventional continuous flow microfluidic devices using fixed channel arrangements, the very high reconfigurability of DMF can help improving assay optimization and decrease development costs. On the other hand, until recently, most DMF devices were primarily designed and utilized for simple assays requiring only a few steps and limited number of droplets. The developed devices thus typically lacked the complexity required to perform

multiplexed bioassays in which numerous tests must be performed concurrently.

While different bioassays have been performed using DMF, including immunoassays [35], cell culture [36], DNA hybridization [37], PCR [38] and isothermal amplification [264], most pathogen detection assays were based on either immunoassay or DNA hybridization and PCR amplification. Even if PCR and other amplification techniques provide rapid results with high sensitivity, they are susceptible to inhibitors, which is a key issue for samples coming from environmental water systems. Another major drawback for the DNA-based and immunoassay techniques is their inability to distinguish between live and dead bacteria. This is a major concern in environmental water settings because of the false-positive results that can occur after water treatments. In contrast, targeting ribosomal RNA (rRNA) is a viable alternative that overcomes the aforementioned shortcomings. Indeed, since RNA expression level is directly correlated to the microbial activity, it provides a more reliable and accurate target for detection of live *Legionella*. [13]

There have been only few attempts to develop detection assays in DMF based on RNA. For example, Jebrail *et al.* [265] demonstrated the feasibility of RNA extraction from blood using magnetic beads within a DMF device. In another recent work, Rival *et al.* [266] performed single cell analysis using micro RNA from human HaCaT cells followed by mRNA capture on magnetic beads, mRNA conversion to DNA and Reverse Transcriptase PCR (RT-PCR) amplification. The use of RT-PCR, even if it provides high sensitivity, can require elaborate sample preparation steps, expensive enzymes and reagents, and precise control of the temperature, making this method less desirable for on-site applications.

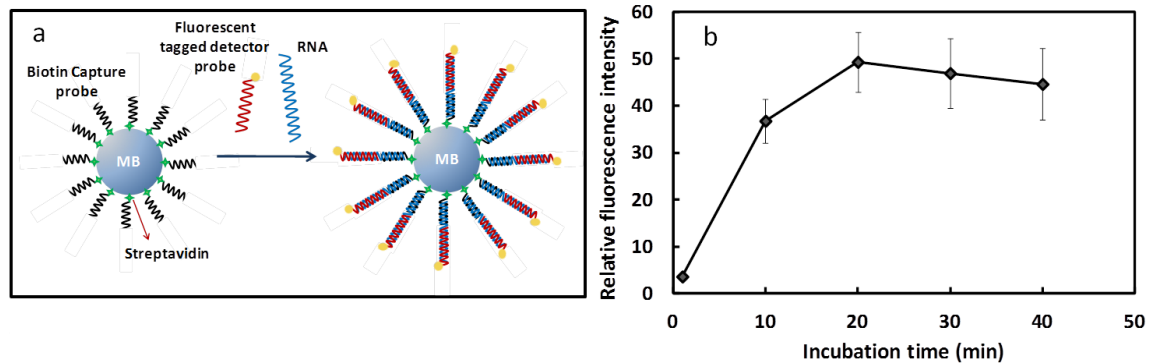


Figure 11-2 a) Schematic showing the hybridization of target RNA on the magnetic beads using designed capture and detector probes b) Effect of the incubation time on the detected fluorescence intensity for on-chip hybridization assays performed at a concentration of 100 nM target RNA.

In this work, we report the multiplex and amplification-free detection of synthetic 16s rRNA from *Legionella* bacteria using DMF devices capable of handling complex assays. We present the design and conception of the DMF devices, demonstrate simultaneous manipulation of multiple droplets on-chip and investigate the optimal hybridization conditions and limit of detection for *L. pneumophila* 16s rRNA. We additionally demonstrate that the developed assay, which is based on two sets of DNA as capture and detector probes, can achieve a high degree of selectivity by showing the multiplex detection of rRNA from two different species of *Legionella*, one pathogenic (*L. pneumophila*) and one non-pathogenic (*L. israelensis*). We believe the DMF device combined with the proposed detection system have great potential for rapid, high-throughput, multiplex, and inexpensive detection of pathogens with minimal sample and reagent volume.

11.2 Results and discussion

11.2.1 Design of the DMF devices

The integration of multiplex protocols in DMF requires the development of devices that can manipulate and store multiple droplets simultaneously to perform the dilution, mixing and analysis steps required by the assay. Unfortunately, it is challenging to design and fabricate DMF devices containing enough active electrodes to handle complex protocols while simultaneously keeping fabrication cost and process complexity low enough for typical biomedical applications. To simplify the fabrication of the devices, we have developed a process where negative SU-8 photoresists is used directly as the dielectric for the fabrication of advanced DMF requiring multiple levels of metallization (see Materials and methods section for more details) [226]. We have indeed found that SU-8 not only offers good electrical properties (dielectric breakdown ~ 4 MV/cm and relative dielectric constant of about 4), but also ease of deposition and patterning, long term resistance to humid environment and saline buffers, resistance to scratches and pinhole formation, and good temperature stability.

The design of the developed DMF devices is shown in Figure 11-1a. The device contains 560 active electrodes, 7 reservoirs and multiple regions for mixing and sample preparation. The device also includes enough storage regions to hold up to 100 individual droplets, as we have found that the maximum assay complexity that can be integrated in DMF is often limited by the maximum number of droplets that can be stored simultaneously on-chip. It is noteworthy that the DMF device shown in Figure 11-1 is capable of handling assays even more complex than those demonstrated in this paper. This was done on purpose to so as to take full advantage of the very high

reconfigurability of DMF, where only one chip can be easily designed to handle the needs of various different assays by simply changing the droplet programming sequence.

To limit the complexity of the electronic circuits and facilitate electrical connection to the device, we have limited the number of independent electrical inputs to only 24. Thus, each electrical input is connected simultaneously to multiple active electrodes by using connection lines placed on a different metallization level. The assignment of the electrical inputs to each active electrode has to be cleverly designed to avoid as much interferences as possible when multiple droplets are on the DMF devices simultaneously. To minimize unwanted interactions between the fluidic operations, the input-to-electrode assignment has been divided into partitions [267] according to the function of the electrodes (see Figure 11-1b): 8 electrical input pins were assigned for dispensing (blue), 5 pins for transportation (green), 6 pins for preparation (red), 4 pins for storage (purple), and 1 pin is connected to top plate (not shown). As shown in Figure 11-1c, the pin assignment within each partition has also been optimized to maximize interdependence of fluidic operations when multiple droplets are located in the same partition. For example, to move only the droplet marked with an arrow from the sample preparation to the transportation partition, the electrical input pins would be actuated as follow: 2 – 5 – 1 – C. The input pins are also assigned in a similar manner in the storage region, except that smaller active electrodes (labelled γ and β) are used to minimize the real estate of the device. Finally, the distribution of the 8 independent electrical pins within the reservoir partition (blue color in Figure 11-1b), ensures that a droplet can be dispensed independently from each reservoir.

11.2.2 Assay design and optimization

Due to presence of many species of *Legionella*, it is critical to design assays with a high selectivity capable of differentiating pathogenic from non-pathogenic species. As shown schematically in Figure 11-2a, we have developed an assay based on the hybridization of *Legionella*'s 16s rRNA on magnetic beads. In order to achieve high specificity, two DNA probes were designed for each target. One probe served as a capture probe and was immobilized on magnetic beads while the second probe, in addition to ensuring the high specificity, is used as a detector probe functionalized with a fluorescent dye (Figure 11-2a).

Before integrating the assay in the DMF devices, different critical parameters were evaluated to obtain the highest hybridization efficiency with minimum analyte consumption, and the shortest assay time. The following factors were also considered: hybridization buffer composition, temperature, reaction volume, and the incubation time. Among these factors, buffer composition and temperature were found to play an important role in specificity and sensitivity of the hybridization. We previously [13] demonstrated that the 600 mM salt concentration in the neutral pH buffer at 37 °C for the *L. pneumophila* RNA-DNA hybridization resulted in the highest specificity. As discussed in the Materials and methods section, all on-chip assays have thus been performed at a temperature of 37°C.

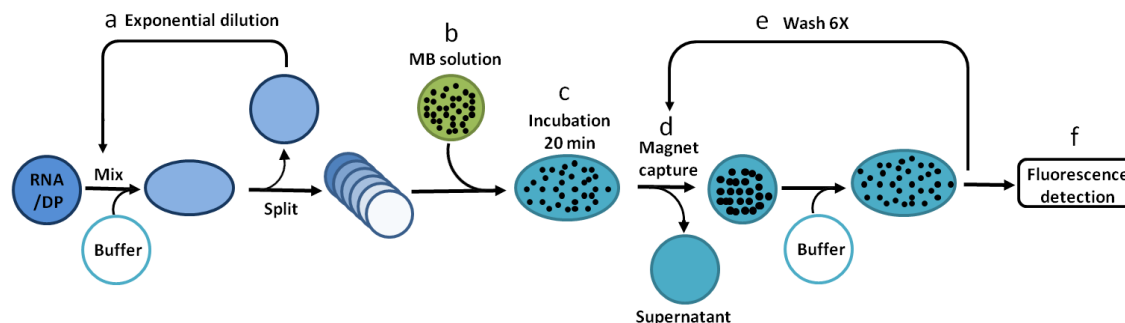


Figure 11-3 Schematics protocol showing the serial dilution and hybridization of 16s rRNA on the DMF devices. a) Creation of the exponential dilution of the RNA sample into six concentrations. b) Mixing of the diluted RNA droplets with the magnetic beads. c) Incubation of the magnetic beads with six concentrations of 16s rRNA. d) Capture of magnetic beads and separation of supernatant e) Six times washing of magnetic beads. f) Fluorescent measurement.

To validate the on-chip 16s rRNA hybridization protocol and optimize the speed of on-chip assays, we have first performed a series of simple on-chip measurements to assess the effect of incubation time on hybridization efficiency. For on-chip tests, *L. pneumophila* 16s rRNA and the detector probes were first mixed together off-chip. Then, for each incubation time reported in Figure 11-2b, one droplet of a 100 nM RNA solution was dispensed and mixed on-chip with one droplet containing magnetic beads coated with immobilized capture probes. As described more in details in Section 11-4, the mixed droplet was washed six times and fluorescent measurements were carried out immediately. As can be seen in Figure 11-2b, the intensity of fluorescence increased from one minute up to 20 minutes after which fluorescent signal is seen to saturate. Therefore, we chose 20 minutes as the optimal incubation time for further experiments.

The reaction volume of the RNA sample on which the detection experiment is performed is another key factor that can affect the results of the detection assay. In conventional laboratory experiments, the reaction volume is typically on the order of tens of μL or higher. On the other hand, by integrating the assay into DMF devices, we were able to reduce the reaction volume required for one hybridization assay to only 30 nL

(i.e., only two individual droplets). It is also noteworthy that, due to the small electrodes of our DMF devices (0.5×0.5 mm), this volume is also smaller by a factor of 10 to 100 times compared with other reported reaction volumes for bioanalytical assays performed in DMF [34, 264, 266]. The developed integrated assay thus offers the interesting prospect to significantly decrease both the reagent consumption and minimal sample volume. In particular, the reduced consumption of streptavidin coated magnetic beads to only 15 nL per hybridization assay (about 3600 particles) offers the potential to reduce the cost of each assay. On the other hand, the reduced sample volume can obviously impact the ultimate limit of detection of the assay. We show next how the limit of detection of the developed assay has been evaluated by performing serial dilutions on-chip.

11.2.3 On-chip serial dilution and hybridization

To evaluate the limit of detection of the assay in DMF devices, we have performed on-chip the protocol shown schematically in Figure 11-3. Figure 4 shows sequential images illustrating the various steps required to perform this protocol in DMF. The first steps, which are summarized in Figure 11-3a and Figure 11-4a, involve the generation of sample droplets containing a series of different concentrations. One droplet from the RNA reservoir is first dispensed and transported to the mixing area. Next, another droplet is dispensed from the buffer reservoir and transferred to the same mixing area. In the mixing area, the two droplets are mixed with rapid circular movements and split into two identical daughter droplets, one of which is moved either to the storage area for later use or to the waste reservoir (depending on the targeted concentration profile). The other daughter droplet is kept at the mixing area for another dilution step with a droplet from

the buffer reservoir. In this way, an exponential dilution series of the original droplet is obtained. For the developed assay, droplets having concentrations of about 500 nM, 125 nM, 8 nM, 1.0 nM, 0.5 nM and 0.12 nM were analyzed.

It is noteworthy that any variation in the volume of the dispensed droplets will introduce some errors on the RNA concentration in the dilution series compared with nominal values. In our DMF devices, we have found the dispensed droplets have an average volume of 15.3 nL with a standard deviation of about 0.4 nL (about 3%). This variability on the droplet volume accumulates through the dilution protocol and can thus give rise to significant uncertainties on the RNA concentration for the higher dilutions. By propagating the standard deviation of droplet volume on the 13 dilutions steps required to decrease the RNA concentration from 1 μ M to 0.12 nM, it is possible to show that the relative error (standard deviation) on the concentration reaches about 30% (see ESI for a detailed analysis). We believe that this error is small enough not to affect the outcome of the assay.

As shown in Figure 11-3b-c and Figure 4b, each droplet from the dilution series is then actively incubated with magnetic beads. To that end, one droplet from the reservoir containing the magnetic beads functionalized with *L. pneumophila* CP probe is first dispensed and transferred to the adjunct mixing area. In the next step, one of the droplets from the dilution series of *L. pneumophila*'s RNA is transferred from the storage area to the same mixing area. After mixing, the new larger mixed droplet is transferred to sample preparation area. Subsequently, all of the six *L. pneumophila*'s RNA concentrations are mixed with magnetic beads and transferred to the sample preparation area. The droplets are incubated for around 20 minutes during which they are slowly moved on the sample

preparation area to create fluid recirculation, minimize sedimentation and maximize the hybridization efficiency. Finally, as shown in Figure 11-3d-e and Figure 11-4c, the magnetic particles are captured and washed to remove the un-hybridized RNA. To capture the magnetic beads, two 2.5 mm diameter cylindrical neodymium rare-earth magnets are positioned on top of the DMF chip (each magnet is located in the center top of the three sample preparation electrodes - see Figure 11-4c).

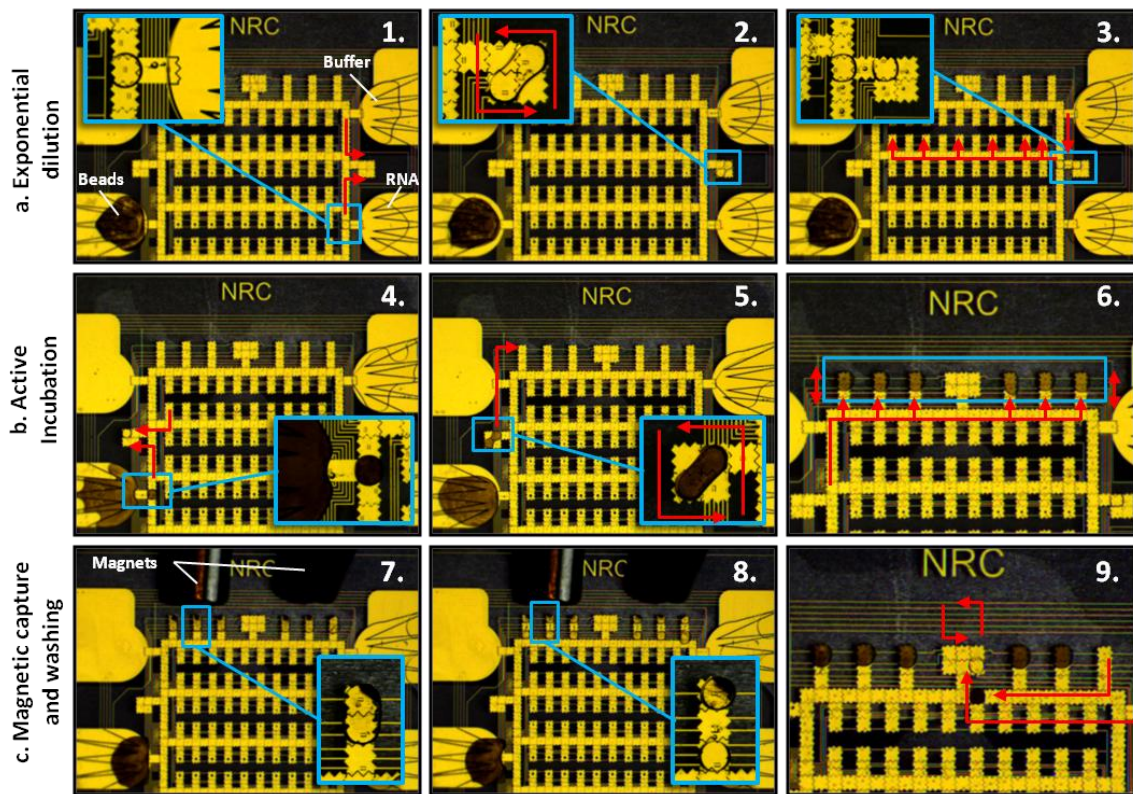


Figure 11-4 Top view image sequence showing the digital microfluidic protocol used for the RNA serial dilution and hybridization assay. a) Creation of the exponential dilution profile of the RNA sample into 6 droplets (1. to 3.). b) Mixing of the diluted RNA droplets with the magnetic beads and incubation (4. to 6.). c) Magnetic capture and washing of the incubated droplets (7. to 9.).

The magnets are positioned to attract and concentrate the magnetic beads on the top part of the droplet. After capture of the magnetic beads, all the six droplets are split simultaneously into the two daughter droplets and the droplets containing the supernatant

are transferred to the waste reservoir. The magnets are then removed temporarily and each droplet containing the magnetic beads are washed by (i) transferring them one at a time to the mixing area located on top of the chip and (ii) mixing them with one droplet from the buffer reservoir. The mixed droplet is then transferred back to its previous location in the sample preparation area. The capture and wash sequence of the magnetic beads is repeated for a total of six times.

In general, to capture and separate magnetic beads in a droplet, the magnetic force should be sufficient enough to capture the magnetic particles but not too strong as to cause irreversible particle aggregation [34, 268, 269]. As described, the two permanent magnets placed on top of the DMF allowed concentrating efficiently the magnetic beads on top of the droplets, removing supernatant and performing several washes. On the other hand, we observed that sedimentation of the magnetic particles on the bottom plate of the device could make capturing the magnetic beads difficult. In order to alleviate this issue, we implemented a new strategy to improve capture and separation of the magnetic beads. In this strategy, the droplet was spread on two electrodes on top of the sample preparation area by activating both electrodes in the presence of magnets (Figure 11-4-7). This was followed by switching on and off only the top electrode while the bottom electrode was kept activated. This switching was found to facilitate the re-capture of sedimented magnetic beads while ensuring that the pellet of captured magnetic beads remained intact. To achieve acceptable particle separation, a frequency around 7 Hz was used for the switching process. We hypothesize that the switching creates fluid recirculation inside the droplets, which causes the sedimented particles to be resuspended in solution and captured by magnet. Finally, it is noteworthy that the use of Pluronic F-127 in the buffer

solutions was also found to improve the re-suspension of the particles after magnetic capture.

The choice of the washing protocol should also be considered when separating the un-hybridized RNA and detector probes from the magnetic beads. In our experiments, we observed that a total of six washes with 1:1 ratio of buffer to sample were sufficient in removing the supernatant from magnetic particles before fluorescence measurement.

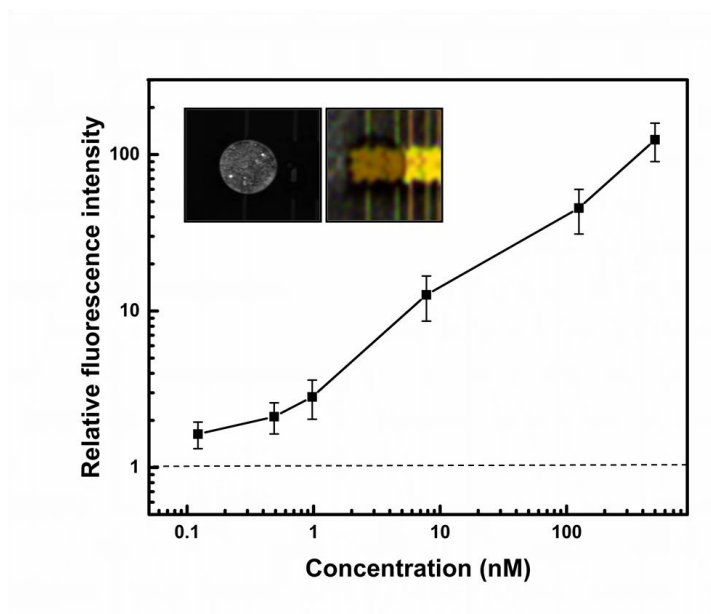


Figure 11-5 Measured relative fluorescent intensity versus *L. pneumophila*'s RNA concentration using superparamagnetic beads and Cy3 fluorescent tagged detector probe. (see ESI for the calculation of the error on the concentration). Inset: A bright-field and fluorescent images of a droplet containing captured RNA onto the magnetic beads.

This number of washes is also in accordance with a similar reported protocol [34]. In this method, the magnet was manually removed after the 'capture and separation' step and the droplet containing magnetic beads was re-suspended in wash buffer droplet in the mixing area (Figure 11-4-9). The removal of the magnet ensures that there won't be any entrapment of the unhybridized RNAs and detector probes in the pellet of the captured magnetic beads. We hypothesize that this is advantageous compared to other previously

reported methods where the magnet was at the same place throughout the whole washing process. For example, when the magnet position is kept constant, it has been reported that up to 18 washes are required [236] when the buffer to sample ratio is of 1:1 and 5 washes [268] for a buffer to sample ratio of 5:1.

11.2.4 Limit of detection for *L. pneumophila*'s RNA

As described earlier, six different concentrations of the *L. pneumophila*'s RNA ranging from 0.5 μM to 122 pM were made on the DMF chip and hybridized with functionalized magnetic beads for twenty minutes at 37°C. After six times washing with buffer, the fluorescent intensity for each droplet was measured directly on-chip and subtracted from the negative control. As can be seen in Figure 11-5, the developed system could successfully detect 16s rRNA at concentrations as low as 122 pM in less than 30 minutes. Considering the 15 nL volume of the RNA droplet, this amount is equivalent to 1.8 attomoles of 16s rRNA. Due to the very low dead volumes offered by the proposed system, the LOD in terms of absolute amount is thus around 250 to 10,000 times less than the LOD reported for 16s rRNA using amplification-free detection systems such as SPRi [13], and electrochemical [270] techniques respectively. Moreover, with a total analysis time of only 30 minutes, the system provides a measurement 6 times faster than the aforementioned methods. One of the limiting factors in our sensitivity was the auto-fluorescence of the DMF device, which interfered with the signal obtained from the droplet at low concentrations. We believe that, by alleviating this problem (for e.g., by choosing materials with lower auto-fluorescence), the signal-to-noise ratio and the LOD could even be increased further. Finally, it is also worthwhile noting that the developed

assay offers a rather large dynamic range, providing a regular signal increase for more than three orders of magnitude of RNA concentration (Figure 11-5).

11.2.5 Multiplex detection of pathogenic and non-pathogenic Legionella

As described in the introduction, the multiplex detection and ability to distinguish the pathogenic from non-pathogenic bacteria is a critical feature required for monitoring environmental water samples. Thus, in addition to *L. pneumophila*, we designed a series of capture and detector probes targeting the 16s rRNA from *L. israelensis* as a non-pathogenic *Legionella* species, since there is no report of human disease from this species.

In order to perform the multiplex detection of these two target RNAs, the detector probe specific to *L. israelensis* (*L.i*) was functionalized with Cy5 dye in contrast to the *L. pneumophila's* (*L.p*) detector probe which was tagged with Cy3 dye. Two sets of functionalized MB with a concentration of 2.4×10^8 particles/mL were also prepared, each with one of the two capture probes (*L.p* MB and *L.i* MB).

For the multiplex protocol, the on-chip incubation, magnetic separation, and washing steps were performed in a similar manner to the exponential dilution protocol discussed before (see Figure 11-4). However, in this case, RNA concentration was fixed at 100 nM and two additional reservoirs were used for the *L.i* MBs and for *L.i* RNAs. Also, instead of performing a dilution series, fluidic operations were such that the two different types of functionalized magnetic beads (i.e., *L.p* MB and *L.i* MB) were each hybridized with three different RNA samples prepared by mixing (i) a *L.p* droplet with a buffer droplet, (ii) a *L.i* droplet with a buffer droplet and (iii) a *L.p* with a *L.i* droplet. A total of six different hybridization measurements were thus performed to evaluate the specificity of

the developed assay.

Figure 11-6 shows the resulting measured fluorescence intensity for the six hybridization tests for both the Cy3 and Cy5 filters (corresponding respectively to the dyes of *L.p* and *L.i* detector probes). As expected, the reaction of *L.p* RNA with *L.p* MB resulted in a significant fluorescent signal only with Cy3 filter, indicating that only *L.p* detector probes hybridized significantly to the beads. The opposite trend was observed for the reaction of *L.i* RNA with *L.i* MB, which resulted in a strong signal only in Cy5 filter (i.e., only *L.i* detector probe was hybridized). On the other hand, much smaller signals were measured in both Cy3 and Cy5 filters when *L.p* RNA was incubated with *L.i* MB or when *L.i* RNA was incubated with *L.p* MB, indicating that neither the *L.p* detector probes nor the *L.i* detector probes were hybridized to the beads. Finally, for the mixed sample containing both *L.p* and *L.i* RNA, the normalized fluorescent intensities for Cy3 and Cy5 filters were in the same level as those obtained for *L.p* RNA with *L.p* MB and *L.i* RNA with *L.i* MB respectively. In summary, these results confirm that the developed assay based on two sets of independent capture and detector probes can achieve a specificity high enough to discriminate between RNA from two *Legionella* species.

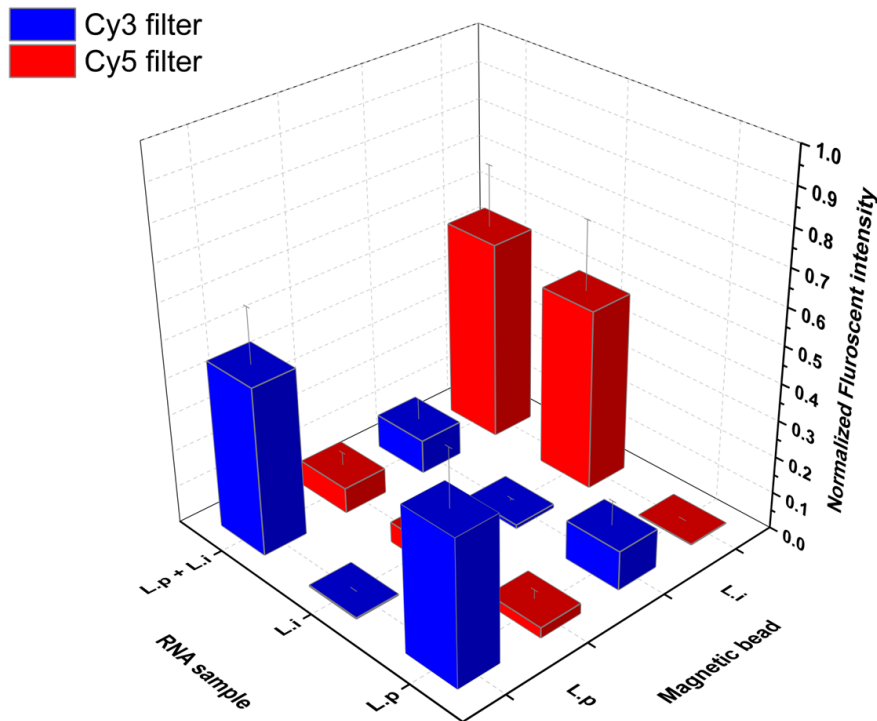


Figure 11-6 Multiplex detection of *Legionella* 16s rRNAs including pathogenic, *L. pneumophila* (*L.p*) and non-pathogenic *L. israelensis* (*L.i*). Detector probe specific to *L.p* RNA sample was tagged with Cy3 dye while the detector probe specific to *L.i* RNA sample was tagged with Cy5 dye. Three RNA samples including *L.p*, *L.i* and mixture of *L.p* and *L.i* were incubated with two types of magnetic beads functionalized with either *L.i* or *L.p* capture probes. The fluorescent measurements were carried out with Cy3 and Cy5 filters for each droplet.

11.3 Conclusion

We have shown the successful integration of a multiplex RNA assay in DMF for the specific detection of *Legionella* species using 16s rRNA targets. An advanced DMF platform was designed to integrate the developed assays, which offered the possibility to perform on-chip complex fluidic manipulations with multiple droplets. The various steps of the assays, including magnetic capture, hybridization duration, washing steps, and assay temperature were first optimized. The advanced fluidic capabilities of the platform were then used to perform exponential dilutions to evaluate, in the same assay and under

the identical condition, the signal from multiple RNA concentrations. We have shown that, by integrating the assay in DMF devices, we were able not only to reduce drastically reagent and magnetic beads consumption, but also to decrease the minimum amount of RNA required to achieve positive sample identification to about only 1.8 attomoles, which demonstrates the potential of the developed system to achieve amplification-free detection based on 16s RNA. Finally, we have shown that specific detection for pathogenic and non-pathogenic species of *Legionella* can be achieved by using capture and detector DNA probes for each 16s rRNA target. We have thus demonstrated a proof of concept for the automated multiplex detection of pathogenic and non-pathogenic *Legionella* in DMF.

The developed DMF devices also offer the interesting prospect to simplify the sample preparation steps required to extract and purify RNA from bacteria. Because of the high specificity of the detection system and the possibility to hybridize the magnetic beads and target rRNA directly within the crude cell lysate, we envisage that all the sample preparation and hybridization steps could be performed on-chip using thermal lysis. By integrating sample preparation, the proposed detection and fluid manipulation system could thus be used as a versatile tool for high-throughput and multiplex detection of several types of bacteria with minimum reagent consumption.

11.4 Materials and methods

11.4.1 Chemical and reagents

BioMag Streptavidin coated superparamagnetic beads were purchased from Bangs Laboratories (Fishers, IN, U.S.A). Pluronic F-127 was purchased from Sigma-Aldrich (St. Louis, MO, U.S.A.). Oligonucleotides were purchased from Integrated DNA

Technologies (Coralville, IA, U.S.A.). SSPE buffer (20X buffer is 3.0 M NaCl, 0.2 M NaH₂PO₄, and 0.02 M EDTA at pH 7.4.), was purchased from Invitrogen (Carlsbad, CA, U.S.A.). Silicone oil (viscosity of 2 cSt) was purchased from Clearco (Bensalem, PA U.S.A), SU8 photoresists from Gersteltec (Pully, Switzerland) and Teflon AF from Dupont (Mississauga, ON, Canada).

11.4.2 DMF device fabrication

The DMF devices were fabricated by first depositing and patterning, by standard lithography, layers of 10 nm thick Cr and 100 nm thick Au on a borosilicate glass wafer to form a network of contact pads and 200 μm wide connection lines. A first layer of about 5 μm thick SU8 dielectric was then deposited by spin-coating and UV exposed through a mask to open interconnection vias in specific locations. A second layer of Cr and Au was then patterned on top of the first dielectric layer to form the 500 \times 500 μm active electrodes and reservoirs of the devices. The electrodes were finally covered with a second layer of about 2.5 μm thick SU8 dielectric and a thin 30 nm layer of hydrophobic coating based on Teflon AF. The top plate of the devices was made by covering ITO-coated plate (Delta technologies, Stillwater, MN, USA) with the same hydrophobic coating. As a final step, the DMF devices were finally post-baked at 200°C for 2h.

11.4.3 Microfluidic platform and DMF device operation

The DMF devices were powered with a home-developed AC voltage source capable of amplifying the 5 V DC voltage from a USB connection to a 0.3 to 3 kHz square-wave of 0 to 150 V. The use of AC voltage minimizes the amount of charge trapping occurring

inside the dielectric of the devices compared to DC voltage, thus improving both the reliability of droplet displacement and DMF lifetime. A typical operation voltage of about 85V RMS at 1 kHz was used for droplet displacements, which was found to provide reliable droplet displacement at a speed of 10 electrodes per second. The 24 independent electrical inputs of the devices were contacted with a custom clip made from spring-loaded pogo-pins. A home-developed software providing advanced sequence programming capabilities has been developed to control the electrical inputs and automate the droplet displacements.

The devices were filled by dispensing droplets of about 1 μl on the bottom electrodes forming the reservoir of the DMF devices using a pipette. Before reservoir filling, a small amount (i.e., $< 0.1 \mu\text{l}$) of silicone oil was applied on the reservoir by touching the device with a the tip of a pipette As discussed elsewhere [271], the oil naturally forms a thin shell around the droplets, which has been shown to facilitate droplet displacements and improve device reliability. The top plate of the device is then electrically grounded and put in place along with a spacer providing a constant gap of about 70 μm . Individual droplets of about 15 nL are then dispensed from the reservoirs of the devices by applying a sequence of voltage on the electrode of the DMF devices. The temperature was controlled by mounting the DMF devices on a thermoelectric element connected to an H-bridge electrical circuit controlled by an Arduino microcontroller in communication with a computer. While performing the RNA assay, the temperature in the DMF devices was kept constant at 37°C to favor hybridization. To minimize the evaporation of the small 15 nL droplets, DI water was dispensed around the edge of the DMF devices. In this configuration, only marginal evaporation was observed for the duration of the assay

(about 30 min). No significant evaporation of the thin oil shell around the droplet was observed. Many reagents used in biological applications such as proteins are susceptible to non-specific adsorption to the hydrophobic layer of the DMF devices, increasing dragging forces and eventually preventing droplet displacement [272]. In our experiments, we have found that the droplets containing the streptavidin-coated paramagnetic beads could not be manipulated reliably despite the presence of an oil shell around the droplet. Reliable droplet displacement was obtained by adding 0.1% (v/v) Pluronic F127 to the solutions.

11.4.4 DNA probe design and hybridization condition

DNA capture probes (CP), complementary to *L. pneumophila* and *L. israelensis*'s 16S rRNA, were designed using bioinformatics software packages from Cardiff University, England. Particular features such as loops and hairpins, were checked for and avoided. The specificity of these probes was confirmed using the Check Probe program and Ribosomal Database Project (RDP). In terms of detection probes, a fluorescent-tagged DNA probe with zero base pair gap between the capture and detection probes (DP) for each target RNA sequence was designed. Cy3 (excitation at 550 nm, emission at 570 nm) and Cy5 (excitation at 649 nm, emission at 670 nm) dyes were used for *L. pneumophila* and *L. israelensis* detector probes respectively. The length of each detector probe was determined to ensure similar melting temperatures while avoiding cross-reactivity and hybridization to any capture probes. The cross reactivity of these detector probes was tested against the capture probe, revealing no significant interaction (data not shown). Two RNAs (60bp in length) from the *L. pneumophila* and *L. israelensis*'s 16S rRNA,

which contains complementary sequences for the designed capture and detector probes, were synthesized by Integrated DNA Technology (Table 11-1).

Table 11-1 Oligonucleotide sequences employed in the experiments

Name	Sequence 5'--3'
<i>L. pneumophila</i> CP	/Biotin/TTTTTTTTTTTCAGGTCGCCCTTCGCCGCC
<i>L. israelensis</i> CP	/Biotin/TTTTTTTTTTTGGCCAGGCCATAAGGTCCC
<i>L. pneumophila</i> DP	CTCTGTATCGGCCATTGTAGCTTTTTTTTTTT/Cy3/
<i>L. israelensis</i> DP	CAGCTTTACTCCAAAGAGCATATGCGGTTTTTTTTTTT/Cy5/
<i>L. pneumophila</i> 's RNA	UACACACGUGCUACAAUGGCCGAUACAGAGGGCGGCGAAGG GGCGACCUGGAGCAAUCC
<i>L. israelensis</i> RNA	CTAATACCGCATATGCTCTTTGGAGTAAAGCTGGGGACCTTAT GGCCTGGCGCTTTAAGA

11.4.5 Microparticle preparation and signal measurement

The hybridization buffer was chosen based on previously reported work.[13] Briefly all the reagents were diluted in 4X SSPE buffer containing 600 mM NaCl and hybridization experiments were carried out at 37°C inside the DMF chip.

Before the start of the assay, the streptavidin coated superparamagnetic particles (MB) were washed off-chip three times with 4X SSPE buffer containing 0.01% pluronic F-127 and were concentrated to the final concentration of 2.2 mg/mL (2.4×10^8 particles/mL). In order to immobilize the biotin capture probes on magnetic beads, an excess amount of DNA capture probe (4 μ L of 100 μ M) was incubated off-chip with 100 μ L of the magnetic bead solution for 15 min at room-temperature. This was followed by three times

washing with 4X SSPE buffer. The same protocol was used for the preparation of the MB used in the capture of *L. pneumophila* and *L. israelensis*. The functionalized beads were kept at 4°C before use.

An inverted fluorescence microscope (Nikon TE 2000-E) was used for measurement of the fluorescence intensity of the droplets inside the chip. All images were captured using a CCD camera and analyzed by ImageJ (National Institutes of Health, Bethesda, MD). The Fluorescent measurements were carried out on the chip by locking at the target droplet under the microscope. All measurements were subtracted by the intensity obtained from a negative control. The negative control droplet contained magnetic beads with the detector probe and was washed six times using the same protocol as the other droplets. For the multiplex detection of RNA, the fluorescent intensities for each sample were normalized for each filter independently by the positive control (the mixture of the magnetic bead, RNA and proper detector probe). The lower detection limit was defined as the smallest concentration of an analyte, calculated as the blank signal plus or minus three standard deviations. All data were expressed as the mean \pm standard deviation.

11.5 Acknowledgments

We acknowledge National Science and Engineering Research Council of Canada strategic Research program, National Research Council of Canada, Genome Canada/Genome Quebec, Nano-Quebec, Le Fonds Québécois de la Recherche sur la Nature et les Technologies and Centre for Biorecognition and Biosensors for their financial support. The authors would also like to thank Dr. X. Zhang for scientific discussion, and Dr. M. Mekhail and K. Jahan for their comments on the manuscript, M. Mounier, C. Miville-Godin and K. Côté for their technical assistance in the fabrication of

the DMF devices and F. Normandin for the development of the Lab-view control software.

11.6 Electronic Supplementary Information (ESI)

11.6.1 Evaluation of the error caused by droplet volume variability during an exponential dilution series in digital microfluidics

We evaluate here how the random variability in the droplet volume in digital microfluidics gives rise to an error in the reagent concentration during an exponential dilution series. To create this dilution series a buffer droplet is mixed with a reagent droplet. The resulting droplet is then split in two droplets and one of the resulting droplets is kept for the next dilution step. This process is repeated for n steps to create the exponential dilution series.

1. First dilution step

To create the first dilution step of the series, a droplet of volume V_0 and reagent concentration of C_0 is mixed with a buffer droplet of volume V_B and concentration $C = 0$. The concentration C_1 of the mixed droplet is thus given by:

$$C_1 = \frac{C_0 V_0}{V_0 + V_B}$$

The relative error $\Delta C_1 / C_1$ on C_1 is thus given by:

$$\left(\frac{\Delta C_1}{C_1}\right)^2 = \left(\frac{\Delta C_0}{C_0}\right)^2 + \left(\frac{\Delta V_0}{V_0}\right)^2 + \left(\frac{\Delta(V_0 + V_B)}{V_0 + V_B}\right)^2$$

where ΔC_0 is the standard deviation of the concentration from the bulk solution, and ΔV_0 and ΔV_B are respectively the standard deviation of the volume of the reagent and buffer droplets. As both the buffer and the reagent droplets were obtained from the same on-chip dispensing protocol, we can assume that $\Delta V_0 = \Delta V_B = \Delta V$, where ΔV is the standard deviation of droplet volume following dispensing from a reservoir. We thus have:

$$\Delta(V_0 + V_B) = \sqrt{(\Delta V_0)^2 + (\Delta V_B)^2} = \sqrt{2} \Delta V$$

As both droplets were obtained by the same dispensing process, we also neglect herein any systematic volume difference between V_0 and V_B such that $V_0 \cong V_B = V$. We thus have:

$$\left(\frac{\Delta C_1}{C_1}\right)^2 = \left(\frac{\Delta C_0}{C_0}\right)^2 + \left(\frac{\Delta V}{V}\right)^2 + \left(\frac{\sqrt{2} \Delta V}{2V}\right)^2$$

$$\left(\frac{\Delta C_1}{C_1}\right)^2 = \left(\frac{\Delta C_0}{C_0}\right)^2 + \frac{3}{2}\left(\frac{\Delta V}{V}\right)^2$$

Knowing the standard deviation of the droplet volume, this expression can be used to evaluate the error on the concentration of the first dilution level.

2. Second dilution step

For the second dilution step, we first have to split the mixed droplet into two individual droplets. Neglecting systematic error that might occur during this splitting process, the volume of the new split droplet is given by:

$$V_1 = \frac{V_0 + V_B}{2}$$

Thus the error on V_1 is:

$$\Delta V_1 = \sqrt{(\Delta V_0)^2 + (\Delta V_B)^2} = \sqrt{2} \Delta V$$

The concentration C_2 of the mixed droplet after the second dilution step is given by:

$$C_2 = \frac{C_1 V_1}{V_1 + V_B}$$

The error on the concentration after the second dilutions step can thus be found using the same process as for the first dilution step:

$$\left(\frac{\Delta C_2}{C_2}\right)^2 = \left(\frac{\Delta C_1}{C_1}\right)^2 + \left(\frac{\Delta V_1}{V_1}\right)^2 + \left(\frac{\Delta(V_1 + V_B)}{V_1 + V_B}\right)^2$$

$$\left(\frac{\Delta C_2}{C_2}\right)^2 = \left(\frac{\Delta C_1}{C_1}\right)^2 + 2\left(\frac{\Delta V}{V}\right)^2 + \left(\frac{\sqrt{3}\Delta V}{2V}\right)^2$$

$$\left(\frac{\Delta C_2}{C_2}\right)^2 = \left(\frac{\Delta C_1}{C_1}\right)^2 + \frac{11}{4}\left(\frac{\Delta V}{V}\right)^2$$

3. nth dilution step

In general, it is possible to show that, for the nth dilution step, the error on the concentration is given by (for n>0):

$$\left(\frac{\Delta C_n}{C_n}\right)^2 = \left(\frac{\Delta C_{n-1}}{C_{n-1}}\right)^2 + \frac{5n+1}{4} \left(\frac{\Delta V}{V}\right)^2$$

This formula can be used to find the error of the n^{th} dilution step knowing the error on the $(n-1)$ step.

Using arithmetic series, we can then show that the error of the n^{th} dilution step can be obtained directly from:

$$\left(\frac{\Delta C_n}{C_n}\right)^2 = \left(\frac{\Delta C_0}{C_0}\right)^2 + \frac{5n^2 + 7n}{8} \left(\frac{\Delta V}{V}\right)^2$$

Thus, if we consider that the initial concentration of the bulk solution at the beginning of the dilution series is known (i.e., $\Delta C_0 = 0$), the error on the concentration of the n^{th} step is function of only the error on the droplet volume:

$$\frac{\Delta C_n}{C_n} = \frac{\Delta V}{V} \sqrt{\frac{5n^2 + 7n}{8}}$$

The following table provides numerical analysis of the error as a function of the dilution step:

Dilution Step	$\Delta C_n/C_n$	C_n/C_0
0	0	1
1	1.22 $\Delta V/V$	$\frac{1}{2}$
2	2.06 $\Delta V/V$	$\frac{1}{4}$
3	2.87 $\Delta V/V$	$\frac{1}{8}$
4	3.67 $\Delta V/V$	$\frac{1}{16}$
5	4.47 $\Delta V/V$...
6	5.27 $\Delta V/V$	
7	6.06 $\Delta V/V$	
8	6.86 $\Delta V/V$	
9	7.65 $\Delta V/V$	

10	8.44 $\Delta V/V$	
11	9.23 $\Delta V/V$...
12	10.0 $\Delta V/V$	1/4096
13	10.8 $\Delta V/V$	1/8192

For example, assuming an initial standard deviation of $\Delta V/V = 3\%$, the standard deviation of the concentration after 13 dilutions step is of about 32%.

Note:

It is important to note that we considered only the random variability in droplet volume in our analysis. Systematic error would have to be taken into account separately. For example, if the buffer droplets are systematically larger than the reagent droplets or if the splitting process is systematically biased, the average concentration of the various steps of the dilution series has to be shifted accordingly

Chapter 12 General Discussion, Conclusion

12.1 Summary of Achievements

In this thesis, we have demonstrated that by integrating a DNA based hybridization assay targeting the 16s rRNA with versatile fluidic manipulation provided by DMF microfluidics, a sensitive and specific detection system with enhanced analytical capabilities for multiplex and rapid detection of *Legionella* can be realized. In the following sections, a summary of the accomplishments towards the three objectives set during this PhD project is presented.

Objective 1: Develop a simple detection system that ensures the detection of viable *Legionella* with high specificity and sensitivity

In order to detect only viable bacteria, 16s rRNA from *Legionella* was targeted through the design of a series of DNA probes. DNA probes were designed using special software and were screened against a database of ribosomal RNA of all bacteria to further ensure high specificity. Two DNA probes were selected for each of the targets in the 16s rRNA region. The first and second probes acted as a capture probe (immobilized on the sensor surface) and as a detector probe respectively for further enhancement of the signal while ensuring the specificity. In order to improve the detection sensitivity of the SPRi system, quantum dots were used for SPR signal amplification.

We showed that the distance between the capture and detector probes is very critical in obtaining high sensitivity. We accordingly designed these two probes to address this criterion and demonstrated that the zero pair base distance results in the highest signal. In addition, the buffer composition, temperature, and pre-treatment of the 16s rRNA factors

affecting the hybridization efficiency were optimized to ensure the desired specificity and sensitivity. The phosphate buffer with 0.6 M salt concentration at 37°C resulted in the best hybridization condition. To alleviate the hindrance effect of the secondary structure of 16s rRNA on accessibility of probes to the target region, the fragmentation RNA method was performed to achieve the high hybridization efficiency. The optimal hybridization conditions and parameters were implemented to detect the *in vitro* transcribed 16s rRNA at a concentration as low as 1 pM per 500 µL (0.5 femtomole) in less than three hours.

Objective 2: Implementation of the detection platform for the detection of *L. pneumophila* in complex environmental water samples

The specificity and sensitivity of the detection platform was validated using total RNA extracted from *L. pneumophila* in spiked water co-cultured with amoebae. We demonstrated that targeting 16s rRNA in *L. pneumophila* gives meaningful insight into the metabolic state of the bacteria by exposing it to a nutrition-deprived environment and monitoring the change in 16s rRNA expression with time. Our results showed that after only six hours of exposure of *L. pneumophila* to a nutrition-deprived environment, the 16s rRNA expression level decreased significantly. Interestingly, the presence of amoebae with *L. pneumophila*, in nutrition-deprived AC buffer enhanced the expression of 16s rRNA after one day. We demonstrated that the presence of amoebae with *L. pneumophila*, especially in nutrition-deprived samples, increased the amount of *L. pneumophila* 15-fold after one week. Using the developed detection method, we were also able to successfully detect *L. pneumophila* within three hours, both in the presence and absence of amoebae in complex environmental samples obtained from a cooling

water tower.

Objective 3: Integration of the developed detection system with a digital microfluidic chip towards on-site application

An advanced DMF platform was designed to integrate the developed assays with on-chip complex fluidic manipulations of multiple droplets for on-site applications. The use of DMF provides many advantages over the standard continuous-flow microfluidic device, since it did not require an external pump or microfabricated moving parts to manipulate and control individual droplets. The droplet paths were fully programmable, allowing for the complete automation of the assay. The advanced fluidic capabilities of the platform were first used to perform exponential dilutions and to evaluate simultaneously the signal from multiple RNA concentrations. After the optimization of magnetic capture, hybridization duration, washing steps, and temperature, within the DMF devices, we were able not only to drastically reduce the reagent and magnetic beads consumption, but also decrease the minimum detected amount of RNA to 1.8 attomoles. This level of RNA concentration is at least 250 times less than reported for 16s rRNA amplification-free detection systems for positive sample identification [13]. Finally, we have shown that the multiplex detection of a pathogenic and a non-pathogenic species of *Legionella* can be achieved in less than 30 minutes on the chip.

12.2 Original claims

The originality of this project lies in two major areas: (i) design and development of a unique DNA hybridization assay for detection of metabolic active *Legionella* in complex environment water samples, and (ii) development of a portable and low-cost biosensor

based on DMF for rapid and multiplexed detection of *Legionella*.

The differentiation between live and dead bacteria is crucial for risk assessment for any water system. Among different targets from *Legionella* (i.e. cell receptors, DNAs, RNAs, proteins and toxins) we chose to work with the 16s rRNA as target for detection of *Legionella*. This choice was based on the fact that 16s rRNA undergoes rapid degradation after bacterial death and could therefore be a good tool to estimate only the alive bacteria in the water samples. This differentiation is especially critical for evaluation of the water disinfectant efficiency, in which most other detection methods (targeting DNA or cell receptors) result in false-positive readout. We were the first to report on utilizing 16s rRNA for the detection of *L. pneumophila* with SPRI. We designed a new series of DNA probes specifically targeting the *L. pneumophila* 16s rRNA. We then demonstrated the effect of different factors such as hybridization conditions, DNA probe design and Quantum dots use for signal post amplification on sensitivity and specificity of developed detection system.

We further demonstrated that the expression level of 16s rRNA in *L. pneumophila* was extremely sensitive to its milieu and therefore can be used for assessing the metabolic state of the bacteria. Amoeba was shown to play an important role in survival and amplification of the *Legionella* in environmental systems [27]. Successful detection of *L. pneumophila* both in the presence and absence of amoebae in complex environmental samples obtained from a cooling water tower was accomplished.

We were the first to demonstrate the detection of 16s rRNA in a DMF setup with a LOD of 1.8 attomoles RNA within 30 minutes [13]. This level of sensitivity for 16s rRNA amplification-free detection systems has not reported so far in the literature. This

biosensor also demonstrated the capability to perform multiplex assays such as differentiating various species of *Legionella* on a DMF chip. Taken together, our results show that integrating DMF device with our detection platform will introduce a new means for fabricating low-cost, portable biosensor for rapid and multiplex detection of different *Legionella* species in environmental water samples to improve the risk assessment and likelihood of prediction of any possible outbreak.

12.3 Limitations and Future Perspectives

The successful implementation of the *Legionella* detection platform developed through this PhD thesis requires further improvement to be used for on-site detection of pathogenic bacteria in the environmental samples. The limitations of our approach and the future directions to overcome those limitations are discussed in the following sections.

12.3.1 16s rRNA expression

We showed in Chapter 10 that the expression level of 16s rRNA in *Legionella* is extremely dependent on the milieu. The signal from the detection system is proportional to the amount of 16s rRNA in the bacteria and to obtain more accurate information regarding the number of bacteria and their metabolic state, it is necessary to establish a correlation between the 16s rRNA expression level and the milieu. It is therefore suggested to establish a correlation between expression levels of 16s rRNA per bacteria in the specific water samples, based on residency time and temperature of the sample. Because of the variations in the 16s rRNA expression as a function of the metabolical activity, it is also desirable to target a reference DNA gene in addition to 16s rRNA as an internal reference to get a better idea of expression of 16s rRNA per bacteria. Obviously

the feasibility of targeting the single copy DNA gene is dependent on the very high sensitivity of the detection system.

12.3.2 Toward development of true on-site biosensor

Although we have successfully presented in Chapter 11 an integration of developed detection system with a DMF setup for multiplex detection of *Legionella*, some modifications and future work are needed in order to realize a true on-site biosensor.

12.3.2.1 Integration of sample preparation with the DMF chip

Although in our DMF detection device, an important part of dilution processes and assay protocols were carried out on-chip, the sample preparation including collecting the bacteria from water samples and extracting RNA were performed off-chip. A true on-site biosensor should be able to contain all the necessary steps (self-contained) including the sample preparation steps. Currently, RNA/DNA has been extracted on the microfluidic chips using heat, chemical, electrical or mechanical forces [273]. For our current DMF setup, the integration of a device enabling the thermal lyses of the bacteria would be very convenient for the following reasons: 1) The device has already an integrated temperature control, 2) there is no need for additional reagents or materials to the chip unlike chemical and mechanical lyses methods, 3) the heat will help the denaturation of the secondary structure of the 16s rRNA and will improve the hybridization process, and 4) hybridization of the DNA probes with the target 16s rRNA and thermal lysis can be performed in the same droplet.

12.3.2.2 Improving the limit of detection

Limit of detection of the developed biosensor is around 100 CFU in each droplet. This level of sensitivity is not enough for water risk assessment. Several modifications should

therefore be implemented individually or in combination, such as 1) reducing the background fluorescence, 2) decreasing the droplet volume, and 3) implementing digitized readout (compartmentalization).

High background fluorescent signal from DMF electrodes was one of the major limitations for obtaining low limit of detection. There are few options for reducing the background fluorescence. One possibility could be to use materials other than gold with lower auto-fluorescence. Another option could be to design special electrodes with a circular opening window for fluorescence measurement.

Since the bacteria are lysed within a single droplet, decreasing the volume of the droplet will result in higher concentration of the released RNA from a bacterium. Assuming 7000 copy of 16s rRNA per *Legionella*, lysing a single *Legionella* in a droplet of 15 nL (current droplet volume in DMF) will lead to a final concentration of 16s rRNA under 1 pM. Decreasing the droplet volume to a pico liter range will increase the concentration of 16s rRNA up to nM range from a single cell and therefore reduce the sensitivity to single bacteria in each droplet. Smaller droplets can be produced either by fabricating smaller electrodes or reducing the gap between the electrode layer and top plate in a new DMF device.

Digital readouts have proven to be advantageous and far more sensitive (single molecule level) than conventional assays [274]. The concentration is determined digitally instead of total analog signal. In addition, one way of compartmentalization of the output signal can be achieved using magnetic microparticles. In order to obtain the compartmentalization in the DMF chip, an array of microwells could be designed on the top plate where each well would contain only one magnetic bead. One of the challenges

of this setup is keeping the microparticles inside the microwells. This issue can be addressed either placing a magnet above the top plate to prevent the magnetic bead to wash away from the wells or by designing hydrophilic microwells in the hydrophobic surface (teflon coated top or bottom plates of DMF device) to localize also the aqueous solution within the microwells. To incorporate these features, a standard lift-off method can be used to pattern Teflon on the top plate to produce a dense array of microwells. For quantification, the hydrophilic wells containing a bead have to be identified by its fluorescent signal for the precise determination of the ratio of “on” and “off” wells. This method would open the door for highly sensitive at the level of single molecule and multiplex detection of the target analytes.

12.3.2.3 Mass production

Feasibility for mass production and cost reduction are two critical factors to be considered in the success of point-of-care and on-site biosensors. Paper and plastic are two potential substrate candidates for the production of disposable and low cost DMF devices. Producing DMF on paper has been previously demonstrated, but remains far away from mass production or even from providing the complexity that is needed for conventional bioassays [275]. The alternative substrate is plastic, which remains unexplored for DMF applications. The use of plastic substrate reduces the time and operational cost significantly. The selection of plastic substrate should meet the fast replication needs with respect to its thermal, optical and mechanical properties. The feasibility of using plastics in making DMF device was shown in a recent report where injected printed silver electrodes on a polyethylene terephthalate (PET) substrate was used to fabricate an electrowetting valve [276].

12.3.2.4 Transducer integration

The development of the portable and integrated transducer is necessary for point-of-care and on-site applications. There are some comprehensive reviews on the optical imaging systems for such applications [277-279]. In this PhD work, the DMF chip was used in combination with a conventional fluorescent microscope. This is rather encouraging, since there are reports on miniaturization of the fluorescent microscope and its integration with smart phones [280-282] as well as on compact and portable SPR biosensors [278, 279]. We have used SPRi during the development of our detection platform and the fluorescent microscope with DMF detection platform. Therefore, the integration of a more versatile transducer system should be considered in the future development of DMF device.

12.3.2.5 Molecular beacons for one-step detection

In any biosensor setup especially for on-site applications, minimizing the steps and their complexities are essential. In the developed detection system, the magnetic bead capturing-and-washing protocol is a tedious process. The washing step was needed to remove the excess detector probes (unhybridized probes). In order to simplify the hybridization process, the DNA molecular beacons can be used. These probes are designed with two functional tails in the native state; one is a fluorophore at one terminus and another a quencher molecule at the other end in the proximity of each other. The molecular beacon consists of stem and loop section. The stem is composed of the small parts of the each end of the probe that are complementary to each other while the loop section is complementary to the target sequences. When the target RNA is hybridized to the loop section of the probe, the formed duplex becomes more stable than the stem (because of more base pairs). This leads to the separation of the stem and therefore

separation of the fluorophore and quencher, which will result in fluorescent emission. As such, the fluorescent signal level is in direct correlation with the target RNA concentration, and the detection of the target RNA can be achieved only in one step. Molecular beacons can be present in the droplet containing the bacteria, while lysis and hybridization can occur simultaneously without a need for addition or removal of any reagent.

References

1. Swanson, M. and B. Hammer, *Legionella pneumophila* pathogenesis: a fateful journey from amoebae to macrophages. Annual Reviews in Microbiology, 2000. 54(1): p. 567-613.
2. CDC, [Increasing incidence of] Legionellosis in the United States, 2000-2009. . Centers for Disease Control and Prevention, 2011(60): p. 1083-1086.
3. Nygård, K., et al., An Outbreak of Legionnaires Disease Caused by Long-Distance Spread from an Industrial Air Scrubber in Sarpsborg, Norway. Clinical Infectious Diseases, 2008. 46(1): p. 61-69.
4. Von Baum, H., et al., Preliminary report: outbreak of Legionnaires' disease in the cities of Ulm and Neu-Ulm in Germany, December 2009–January 2010. Euro Surveill, 2010. 15(4): p. 19472.
5. Craun, G.F., et al., Causes of Outbreaks Associated with Drinking Water in the United States from 1971 to 2006. Clinical Microbiology Reviews, 2010. 23(3): p. 507-528.
6. Yang, G., et al., *Legionella nagasakiensis* sp. nov., isolated from water samples and from a patient with pneumonia. International Journal of Systematic and Evolutionary Microbiology, 2012. 62(2): p. 284-288.
7. Kusić, D., et al., Identification of water pathogens by Raman microspectroscopy. Water Research, 2014. 48(0): p. 179-189.
8. Wadowsky, R., et al., Multiplication of *Legionella* spp. in tap water containing *Hartmannella vermiformis*. Applied and environmental microbiology, 1991. 57(7): p. 1950-1955.
9. WHO. World health organization, *Emerging Issues in Water and Infectious Disease* 2003; pp. 1–24].
10. Lazcka, O., F.J.D. Campo, and F.X. Muñoz, *Pathogen detection: A perspective of traditional methods and biosensors*. Biosensors and Bioelectronics, 2007. 22(7): p. 1205-1217.
11. Foudeh, A.M., et al., *Microfluidic designs and techniques using lab-on-a-chip devices for pathogen detection for point-of-care diagnostics*. Lab on a Chip, 2012. 12(18): p. 3249-3266.
12. Deisingh, A.K. and M. Thompson, *Detection of infectious and toxigenic bacteria*. Analyst, 2002. 127(5): p. 567-581.
13. Foudeh, A.M., et al., *Sub-femtomole detection of 16S rRNA from Legionella pneumophila using surface plasmon resonance imaging*. Biosensors and Bioelectronics, 2014. 52(0): p. 129-135.
14. Skottrup, P.D., M. Nicolaisen, and A.F. Justesen, *Towards on-site pathogen detection using antibody-based sensors*. Biosensors and Bioelectronics, 2008. 24(3): p. 339-348.
15. McKillip, J.L., L.-A. Jaykus, and M. Drake, *rRNA Stability in Heat-Killed and UV-Irradiated Enterotoxigenic Staphylococcus aureus and Escherichia coli O157: H7*. Applied and environmental microbiology, 1998. 64(11): p. 4264-4268.
16. Clarridge, J.E., 3rd, *Impact of 16S rRNA gene sequence analysis for identification of bacteria on clinical microbiology and infectious diseases*. Clin Microbiol Rev, 2004. 17(4): p. 840-62, table of contents.
17. Coenye, T. and P. Vandamme, *Intragenomic heterogeneity between multiple 16S ribosomal RNA operons in sequenced bacterial genomes*. FEMS Microbiol Lett, 2003. 228(1): p. 45-9.

18. Bockisch, B., et al., *Immobilized stem-loop structured probes as conformational switches for enzymatic detection of microbial 16S rRNA*. *Nucleic acids research*, 2005. 33(11): p. e101.
19. Xie, H., C. Zhang, and Z. Gao, *Amperometric Detection of Nucleic Acid at Femtomolar Levels with a Nucleic Acid/Electrochemical Activator Bilayer on Gold Electrode*. *Analytical Chemistry*, 2004. 76(6): p. 1611-1617.
20. Elsholz, B., et al., *Automated detection and quantitation of bacterial RNA by using electrical microarrays*. *Anal Chem*, 2006. 78(14): p. 4794-802.
21. Gerasimova, Y.V. and D.M. Kolpashchikov, *Detection of bacterial 16S rRNA using a molecular beacon-based X sensor*. *Biosensors and Bioelectronics*, 2012(0).
22. Hwang, K.-Y., et al., *Rapid detection of bacterial cell from whole blood: Integration of DNA sample preparation into single micro-PCR chip*. *Sensors and Actuators B: Chemical*, 2011. 154(1): p. 46-51.
23. Riahi, R., et al., *Molecular Detection of Bacterial Pathogens using Particle Enhanced Double-Stranded DNA Probes*. *Analytical Chemistry*, 2011. 83(16): p. 6349-6354.
24. Stephen, K.E., et al., *Surface enhanced Raman spectroscopy (SERS) for the discrimination of Arthrobacter strains based on variations in cell surface composition*. *Analyst*, 2012. 137(18): p. 4280-4286.
25. Joung, H.-A., et al., *High sensitivity detection of 16s rRNA using peptide nucleic acid probes and a surface plasmon resonance biosensor*. *Analytica chimica acta*, 2008. 630(2): p. 168-173.
26. Small, J., et al., *Direct detection of 16S rRNA in soil extracts by using oligonucleotide microarrays*. *Applied and environmental microbiology*, 2001. 67(10): p. 4708-4716.
27. Borella, P., et al., *Water ecology of Legionella and protozoan: environmental and public health perspectives*, in *Biotechnology Annual Review*, M.R. El-Gewely, Editor 2005, Elsevier. p. 355-380.
28. Barbaree, J.M., et al., *Isolation of protozoa from water associated with a legionellosis outbreak and demonstration of intracellular multiplication of Legionella pneumophila*. *Applied and environmental microbiology*, 1986. 51(2): p. 422-424.
29. Dupuy, M., et al., *Efficiency of water disinfectants against Legionella pneumophila and Acanthamoeba*. *Water Research*, 2011. 45(3): p. 1087-1094.
30. Bouyer, S., et al., *Long-term survival of Legionella pneumophila associated with Acanthamoeba castellanii vesicles*. *Environmental Microbiology*, 2007. 9(5): p. 1341-1344.
31. Cirillo, J.D., S. Falkow, and L.S. Tompkins, *Growth of Legionella pneumophila in Acanthamoeba castellanii enhances invasion*. *Infection and Immunity*, 1994. 62(8): p. 3254-3261.
32. Moffat, J.F. and L.S. Tompkins, *A quantitative model of intracellular growth of Legionella pneumophila in Acanthamoeba castellanii*. *Infection and Immunity*, 1992. 60(1): p. 296-301.
33. Lau, H. and N. Ashbolt, *The role of biofilms and protozoa in Legionella pathogenesis: implications for drinking water*. *Journal of applied microbiology*, 2009. 107(2): p. 368-378.
34. Ng, A.H.C., et al., *Digital Microfluidic Magnetic Separation for Particle-Based Immunoassays*. *Analytical Chemistry*, 2012. 84(20): p. 8805-8812.
35. Miller, E.M., et al., *A digital microfluidic approach to heterogeneous immunoassays*. *Analytical and bioanalytical chemistry*, 2011: p. 1-9.

36. Barbulovic-Nad, I., S.H. Au, and A.R. Wheeler, *A microfluidic platform for complete mammalian cell culture*. *Lab on a Chip*, 2010. 10(12): p. 1536-1542.
37. Malic, L., M.G. Sandros, and M. Tabrizian, *Designed Biointerface Using Near Infra-Red Quantum Dots for Ultrasensitive Surface Plasmon Resonance Imaging Biosensors*. *Analytical Chemistry*, 2011. 83(13): p. 5222-5229.
38. Chang, Y.H., et al., *Integrated polymerase chain reaction chips utilizing digital microfluidics*. *Biomedical Microdevices*, 2006. 8(3): p. 215-225.
39. Malic, L., T. Veres, and M. Tabrizian, *Two-dimensional droplet-based surface plasmon resonance imaging using electrowetting-on-dielectric microfluidics*. *Lab on a Chip*, 2009. 9(3): p. 473-475.
40. Scheller, F.W., et al., *Biosensors: trends and commercialization*. *Biosensors*, 1985. 1(2): p. 135-160.
41. Morrison, D.W., et al., *Clinical applications of micro-and nanoscale biosensors 2008*: John Wiley and Sons, Inc., NJ, USA.
42. Wood, R., *On a remarkable case of uneven distribution of light in a diffraction grating spectrum*. *The London, Edinburgh, and Dublin Philosophical Magazine and Journal of Science*, 1902. 4(21): p. 396-402.
43. Raether, H., *Surface plasmons on smooth surfaces* 1988: Springer.
44. Willets, K.A. and R.P. Van Duyne, *Localized Surface Plasmon Resonance Spectroscopy and Sensing*. *Annual Review of Physical Chemistry*, 2007. 58(1): p. 267-297.
45. Homola, J., *Surface plasmon resonance sensors for detection of chemical and biological species*. *Chemical Reviews*, 2008. 108(2): p. 462-493.
46. Homola, J., S.S. Yee, and G. Gauglitz, *Surface plasmon resonance sensors: review*. *Sensors and Actuators B: Chemical*, 1999. 54(1-2): p. 3-15.
47. Rothenhäusler, B. and W. Knoll, *Surface plasmon microscopy*. 1988.
48. Nelson, B.P., et al., *Near-infrared surface plasmon resonance measurements of ultrathin films. 1. Angle shift and SPR imaging experiments*. *Analytical Chemistry*, 1999. 71(18): p. 3928-3934.
49. Zeng, S., et al., *Nanomaterials enhanced surface plasmon resonance for biological and chemical sensing applications*. *Chemical Society Reviews*, 2014. 43(10): p. 3426-3452.
50. Mayer, K.M. and J.H. Hafner, *Localized Surface Plasmon Resonance Sensors*. *Chemical Reviews*, 2011. 111(6): p. 3828-3857.
51. Hu, M., et al., *Gold nanostructures: engineering their plasmonic properties for biomedical applications*. *Chemical Society Reviews*, 2006. 35(11): p. 1084-1094.
52. Vance, S.A. and M.G. Sandros, *Zeptomole Detection of C-Reactive Protein in Serum by a Nanoparticle Amplified Surface Plasmon Resonance Imaging Aptasensor*. *Sci. Rep.*, 2014. 4.
53. Cao, S.-H., et al., *Surface Plasmon-Coupled Emission: What Can Directional Fluorescence Bring to the Analytical Sciences?* *Annual Review of Analytical Chemistry*, 2012. 5(1): p. 317-336.
54. Serrano, A., O.R. de la Fuente, and M. García, *Extended and localized surface plasmons in annealed Au films on glass substrates*. *Journal of Applied Physics*, 2010. 108(7): p. 074303.
55. Lee, K.S., et al., *Surface plasmon resonance biosensing based on target-responsive mobility switch of magnetic nanoparticles under magnetic fields*. *Journal of Materials Chemistry*, 2011. 21(13): p. 5156-5162.

56. Cao, L., et al., *Plasmon-assisted local temperature control to pattern individual semiconductor nanowires and carbon nanotubes*. Nano letters, 2007. 7(11): p. 3523-3527.
57. Wink, T., et al., *Liposome-Mediated Enhancement of the Sensitivity in Immunoassays of Proteins and Peptides in Surface Plasmon Resonance Spectrometry*. Analytical Chemistry, 1998. 70(5): p. 827-832.
58. Wu, L., et al., *Highly sensitive graphene biosensors based on surface plasmon resonance*. Optics Express, 2010. 18(14): p. 14395-14400.
59. Kabashin, A.V., et al., *Plasmonic nanorod metamaterials for biosensing*. Nat Mater, 2009. 8(11): p. 867-871.
60. Malic, L., et al., *Integration and detection of biochemical assays in digital microfluidic LOC devices*. Lab on a Chip, 2010. 10(4): p. 418-431.
61. Pollack, M.G., R.B. Fair, and A.D. Shenderov, *Electrowetting-based actuation of liquid droplets for microfluidic applications*. Applied physics letters, 2000. 77(11): p. 1725-1726.
62. Moon, H., et al., *Low voltage electrowetting-on-dielectric*. Journal of Applied Physics, 2002. 92(7): p. 4080-4087.
63. Jones, T.B., *On the Relationship of Dielectrophoresis and Electrowetting*. Langmuir, 2002. 18(11): p. 4437-4443.
64. Abdelgawad, M. and A.R. Wheeler, *The digital revolution: a new paradigm for microfluidics*. Advanced Materials, 2009. 21(8): p. 920-925.
65. Jones, T., *More about the electromechanics of electrowetting*. Mechanics Research Communications, 2009. 36(1): p. 2-9.
66. Kang, K.H., *How electrostatic fields change contact angle in electrowetting*. Langmuir, 2002. 18(26): p. 10318-10322.
67. Hsieh, T.-H. and S.-K. Fan. *Dielectric droplet manipulations by electropolarization forces*. in *Micro Electro Mechanical Systems, 2008. MEMS 2008. IEEE 21st International Conference on*. 2008. IEEE.
68. Chatterjee, D., et al., *Droplet-based microfluidics with nonaqueous solvents and solutions*. Lab on a Chip, 2006. 6(2): p. 199-206.
69. Katz, S. and J. Hammel, *The effect of drying, heat, and pH on the survival of Legionella pneumophila*. Annals of Clinical & Laboratory Science, 1987. 17(3): p. 150.
70. Ristroph, J.D., K.W. Hedlund, and R.G. Allen, *Liquid medium for growth of Legionella pneumophila*. Journal of Clinical Microbiology, 1980. 11(1): p. 19-21.
71. Diederer, B., *Legionella spp. and Legionnaires' disease*. Journal of Infection, 2008. 56(1): p. 1-12.
72. Fraser, D.W., et al., *Legionnaires' disease: description of an epidemic of pneumonia*. New England Journal of Medicine, 1977. 297(22): p. 1189-1197.
73. Gupta, S., T. Imperiale, and G. Sarosi, *Evaluation of the Winthrop-University Hospital criteria to identify Legionella pneumonia*. Chest, 2001. 120(4): p. 1064.
74. Fields, B.S., R.F. Benson, and R.E. Besser, *Legionella and Legionnaires' disease: 25 years of investigation*. Clin Microbiol Rev, 2002. 15(3): p. 506-26.
75. Bartram, J., *Legionella and the prevention of legionellosis* 2007: World Health Organization.
76. Stout, J.E., M.G. Best, and V.L. Yu, *Susceptibility of members of the family Legionellaceae to thermal stress: implications for heat eradication methods in water distribution systems*. Applied and environmental microbiology, 1986. 52(2): p. 396-399.

77. Antopol, S.C. and P.D. Ellner, *Susceptibility of Legionella pneumophila to ultraviolet radiation*. Applied and environmental microbiology, 1979. 38(2): p. 347.
78. Kim, B.R., et al., *Literature review—efficacy of various disinfectants against Legionella in water systems*. Water Research, 2002. 36(18): p. 4433-4444.
79. Landeen, L.K., M.T. Yahya, and C.P. Gerba, *Efficacy of copper and silver ions and reduced levels of free chlorine in inactivation of Legionella pneumophila*. Applied and environmental microbiology, 1989. 55(12): p. 3045-3050.
80. Stout, J.E., et al., *Controlling Legionella in hospital water systems: experience with the superheat-and-flush method and copper-silver ionization*. Infection control and hospital epidemiology, 1998: p. 911-914.
81. Pasculle, A., et al., *Pittsburgh pneumonia agent: direct isolation from human lung tissue*. The Journal of Infectious Diseases, 1980. 141(6): p. 727-732.
82. Edelstein, P. *The laboratory diagnosis of Legionnaires' disease*. 1987.
83. Maiwald, M., J. Helbig, and P. Lück, *Laboratory methods for the diagnosis of Legionella infections*. Journal of microbiological methods, 1998. 33(1): p. 59-79.
84. Joly, P., et al., *Quantitative real-time Legionella PCR for environmental water samples: data interpretation*. Applied and environmental microbiology, 2006. 72(4): p. 2801.
85. Yaradou, D., et al., *Integrated real-time PCR for detection and monitoring of Legionella pneumophila in water systems*. Applied and environmental microbiology, 2007. 73(5): p. 1452.
86. Wellinghausen, N., C. Frost, and R. Marre, *Detection of legionellae in hospital water samples by quantitative real-time LightCycler PCR*. Applied and environmental microbiology, 2001. 67(9): p. 3985.
87. Yanez, M., et al., *Quantitative detection of Legionella pneumophila in water samples by immunomagnetic purification and real-time PCR amplification of the dotA gene*. Applied and environmental microbiology, 2005. 71(7): p. 3433.
88. Yang, G., et al., *Dual detection of Legionella pneumophila and Legionella species by real-time PCR targeting the 23S-5S rRNA gene spacer region*. Clinical Microbiology and Infection, 2009. 16(3): p. 255-261.
89. Chang, B., et al., *Comparison of Ethidium Monoazide and Propidium Monoazide for the Selective Detection of Viable Legionella Cells*. Jpn. J. Infect. Dis, 2010. 63(2): p. 119-123.
90. Lee, J.V., et al., *An international trial of quantitative PCR for monitoring Legionella in artificial water systems*. Journal of applied microbiology, 2011. 110(4): p. 1032-1044.
91. Oh, B., et al., *Surface plasmon resonance immunosensor for detection of Legionella pneumophila*. Biotechnology and Bioprocess Engineering, 2003. 8(2): p. 112-116.
92. Oh, B.K., et al., *Immunosensor for detection of Legionella pneumophila using surface plasmon resonance*. Biosens Bioelectron, 2003. 18(5-6): p. 605-11.
93. Yacoub-George, E., et al., *Automated 10-channel capillary chip immunodetector for biological agents detection*. Biosensors and Bioelectronics, 2007. 22(7): p. 1368-1375.
94. Howe, E. and G. Harding, *A comparison of protocols for the optimisation of detection of bacteria using a surface acoustic wave (SAW) biosensor*. Biosensors and Bioelectronics, 2000. 15(11-12): p. 641-649.
95. Enrico, D.L., et al., *SPR based immunosensor for detection of Legionella pneumophila in water samples*. Optics Communications, 2013. 294(0): p. 420-426.
96. Li, N., et al., *Disposable Immunochips for the Detection of Legionella pneumophila Using Electrochemical Impedance Spectroscopy*. Analytical Chemistry, 2012. 84(8): p. 3485-3488.

97. Cooper, I., et al., *The rapid and specific real-time detection of Legionella pneumophila in water samples using Optical Waveguide Lightmode Spectroscopy*. Journal of microbiological methods, 2009. 78(1): p. 40-44.
98. Füchslin, H., et al., *Rapid and quantitative detection of Legionella pneumophila applying immunomagnetic separation and flow cytometry*. Cytometry Part A, 2010. 9999(9999).
99. Keserue, H.-A., et al., *Rapid detection of total and viable Legionella pneumophila in tap water by immunomagnetic separation, double fluorescent staining and flow cytometry*. Microbial Biotechnology, 2012. 5(6): p. 753-763.
100. Zhou, G., et al., *Development of a DNA microarray for detection and identification of Legionella pneumophila and ten other pathogens in drinking water*. International Journal of Food Microbiology, 2011. 145(1): p. 293-300.
101. Coenye, T. and P. Vandamme, *Intragenomic heterogeneity between multiple 16S ribosomal RNA operons in sequenced bacterial genomes*. FEMS Microbiology Letters, 2003. 228(1): p. 45-49.
102. Leskelä, T., et al., *Sensitive genus-specific detection of Legionella by a 16S rRNA based sandwich hybridization assay*. Journal of microbiological methods, 2005. 62(2): p. 167-179.
103. Nelson, B.P., et al., *Surface Plasmon Resonance Imaging Measurements of DNA and RNA Hybridization Adsorption onto DNA Microarrays*. Analytical Chemistry, 2000. 73(1): p. 1-7.
104. World Health Organization, *The World Health Report 2004* (World Health Organization, Genève, 2004)
105. Morens, D.M., G.K. Folkers, and A.S. Fauci, *The challenge of emerging and re-emerging infectious diseases*. Nature, 2004. 430(6996): p. 242-249.
106. Batt, C.A., *Materials science. Food pathogen detection*. Science (New York, NY), 2007. 316(5831): p. 1579.
107. CDC Estimates of Foodborne Illness in the United States, <http://www.cdc.gov/foodborneburden/2011-foodborne-estimates.html>, accessed February 01, 2012.
108. Yager, P., et al., *Microfluidic diagnostic technologies for global public health*. NATURE-LONDON-, 2006. 442(7101): p. 412.
109. Weigl, B., et al., *Towards non- and minimally instrumented, microfluidics-based diagnostic devices*. Lab on a Chip, 2008. 8(12): p. 1999-2014.
110. Talbot, E.A., et al., *Tuberculosis serodiagnosis in a predominantly HIV-infected population of hospitalized patients with cough, Botswana, 2002*. Clinical Infectious Diseases, 2004. 39(1): p. e1.
111. Engler, K., et al., *Immunochromatographic strip test for rapid detection of diphtheria toxin: description and multicenter evaluation in areas of low and high prevalence of diphtheria*. Journal of Clinical Microbiology, 2002. 40(1): p. 80-83.
112. Wong, R.C. and Y.T. Harley, *Lateral flow immunoassay 2008*: Humana Pr Inc.
113. Holliger, P. and P.J. Hudson, *Engineered antibody fragments and the rise of single domains*. Nature biotechnology, 2005. 23(9): p. 1126-1136.
114. Mulvaney, S., et al., *Rapid, femtomolar bioassays in complex matrices combining microfluidics and magnetoelectronics*. Biosensors and Bioelectronics, 2007. 23(2): p. 191-200.

115. James, C.D., et al., *High-efficiency magnetic particle focusing using dielectrophoresis and magnetophoresis in a microfluidic device*. Journal of Micromechanics and Microengineering, 2010. 20(4).
116. Bunyakul, N., et al., *Cholera toxin subunit B detection in microfluidic devices*. Analytical and bioanalytical chemistry, 2009. 393(1): p. 177-186.
117. Delehanty, J.B. and F.S. Ligler, *A microarray immunoassay for simultaneous detection of proteins and bacteria*. Analytical Chemistry, 2002. 74(21): p. 5681-5687.
118. Blicharz, T.M., et al., *Fiber-optic microsphere-based antibody array for the analysis of inflammatory cytokines in saliva*. Analytical Chemistry, 2009. 81(6): p. 2106-2114.
119. Taylor, A.D., et al., *Surface Plasmon Resonance (SPR) Sensors for the Detection of Bacterial Pathogens*

Principles of Bacterial Detection: Biosensors, Recognition Receptors and Microsystems, M.

- Zourob, S. Elwary, and A. Turner, Editors. 2008, Springer New York. p. 83-108.
120. Jung, J.H., et al., *A Graphene Oxide Based Immuno-biosensor for Pathogen Detection*. Angewandte Chemie International Edition, 2010. 49(33): p. 5708-5711.
121. Gómez, R., R. Bashir, and A.K. Bhunia, *Microscale electronic detection of bacterial metabolism*. Sensors and Actuators B: Chemical, 2002. 86(2-3): p. 198-208.
122. García-Aljaro, C., et al., *Conducting polymer nanowire-based chemiresistive biosensor for the detection of bacterial spores*. Biosensors and Bioelectronics, 2010. 25(10): p. 2309-2312.
123. Boehm, D.A., P.A. Gottlieb, and S.Z. Hua, *On-chip microfluidic biosensor for bacterial detection and identification*. Sensors and Actuators B: Chemical, 2007. 126(2): p. 508-514.
124. Reichmuth, D.S., et al., *Rapid microchip-based electrophoretic immunoassays for the detection of swine influenza virus*. Lab on a Chip, 2008. 8(8): p. 1319-1324.
125. Laczka, O., et al., *Improved bacteria detection by coupling magneto-immunocapture and amperometry at flow-channel microband electrodes*. Biosensors and Bioelectronics, 2011. 26(8): p. 3633-3640.
126. Guan, X.A., et al., *Rapid detection of pathogens using antibody-coated microbeads with bioluminescence in microfluidic chips*. Biomedical Microdevices, 2010. 12(4): p. 683-691.
127. Oh, B.K., et al., *Immunosensor for detection of Legionella pneumophila using surface plasmon resonance*. Biosensors and Bioelectronics, 2003. 18(5-6): p. 605-611.
128. Klostranec, J.M., et al., *Convergence of quantum dot barcodes with microfluidics and signal processing for multiplexed high-throughput infectious disease diagnostics*. Nano letters, 2007. 7(9): p. 2812-2818.
129. Tan, H.Y., et al., *A lab-on-a-chip for detection of nerve agent sarin in blood*. Lab on a Chip, 2008. 8(6): p. 885-891.
130. Birnbaumer, G.M., et al., *Detection of viruses with molecularly imprinted polymers integrated on a microfluidic biochip using contact-less dielectric microsensors*. Lab on a Chip, 2009. 9(24): p. 3549-3556.
131. Koo, O.K., et al., *Targeted Capture of Pathogenic Bacteria Using a Mammalian Cell Receptor Coupled with Dielectrophoresis on a Biochip*. Analytical Chemistry, 2009. 81(8): p. 3094-3101.
132. Kell, A.J., et al., *Vancomycin-modified nanoparticles for efficient targeting and preconcentration of Gram-positive and Gram-negative bacteria*. ACS Nano, 2008. 2(9): p. 1777-1788.

133. Lou, X., et al., *Micromagnetic selection of aptamers in microfluidic channels*. Proceedings of the National Academy of Sciences, 2009. 106(9): p. 2989.
134. Ahmad, K.M., et al., *Probing the Limits of Aptamer Affinity with a Microfluidic SELEX Platform*. PloS one, 2011. 6(11): p. e27051.
135. Torres-Chavolla, E. and E.C. Alocilja, *Aptasensors for detection of microbial and viral pathogens*. Biosensors and Bioelectronics, 2009. 24(11): p. 3175-3182.
136. Bunka, D.H.J. and P.G. Stockley, *Aptamers come of age—at last*. Nature Reviews Microbiology, 2006. 4(8): p. 588-596.
137. O'Sullivan, C.K., *Aptasensors—the future of biosensing?* Analytical and bioanalytical chemistry, 2002. 372(1): p. 44-48.
138. Mannoor, M.S., et al., *Electrical detection of pathogenic bacteria via immobilized antimicrobial peptides*. Proceedings of the National Academy of Sciences of the United States of America, 2010. 107(45): p. 19207-19212.
139. Le Nel, A., et al., *Controlled proteolysis of normal and pathological prion protein in a microfluidic chip*. Lab on a Chip, 2008. 8(2): p. 294-301.
140. Haupt, K. and K. Mosbach, *Molecularly Imprinted Polymers and Their Use in Biomimetic Sensors*. Chemical Reviews, 2000. 100(7): p. 2495-2504.
141. Bossi, A., et al., *Molecularly imprinted polymers for the recognition of proteins: the state of the art*. Biosensors and Bioelectronics, 2007. 22(6): p. 1131-1137.
142. Talasaz, A.A.H., et al., *Prediction of protein orientation upon immobilization on biological and nonbiological surfaces*. Proceedings of the National Academy of Sciences, 2006. 103(40): p. 14773.
143. Gold, L., et al., *Diversity of oligonucleotide functions*. Annual review of biochemistry, 1995. 64(1): p. 763-797.
144. Sen, A., T. Harvey, and J. Clausen, *A microsystem for extraction, capture and detection of E-Coli O157:H7*. Biomedical Microdevices, 2011. 13(4): p. 705-715.
145. Beyor, N., et al., *Immunomagnetic bead-based cell concentration microdevice for dilute pathogen detection*. Biomedical Microdevices, 2008. 10(6): p. 909-917.
146. Zhang, C.S., H.Y. Wang, and D. Xing, *Multichannel oscillatory-flow multiplex PCR microfluidics for high-throughput and fast detection of foodborne bacterial pathogens*. Biomedical Microdevices, 2011. 13(5): p. 885-897.
147. Kim, G.-Y. and A. Son, *Development and characterization of a magnetic bead-quantum dot nanoparticles based assay capable of Escherichia coli O157:H7 quantification*. Analytica chimica acta, 2010. 677(1): p. 90-96.
148. Leslie, D.C., et al., *Size-based separations as an important discriminator in development of proximity ligation assays for protein or organism detection*. Electrophoresis, 2010. 31(10): p. 1615-1622.
149. Zeng, Y., et al., *High-Performance Single Cell Genetic Analysis Using Microfluidic Emulsion Generator Arrays*. Analytical Chemistry, 2010. 82(8): p. 3183-3190.
150. Dharmasiri, U., et al., *Enrichment and Detection of Escherichia coli O157:H7 from Water Samples Using an Antibody Modified Microfluidic Chip*. Analytical Chemistry, 2010. 82(7): p. 2844-2849.
151. You, D.J., K.J. Geshell, and J.-Y. Yoon, *Direct and sensitive detection of foodborne pathogens within fresh produce samples using a field-deployable handheld device*. Biosensors & bioelectronics, 2011. 28(1): p. 399-406.
152. Lam, B., et al., *Polymerase Chain Reaction-Free, Sample-to-Answer Bacterial Detection in 30 Minutes with Integrated Cell Lysis*. Analytical Chemistry, 2011. 84(1): p. 21-25.

153. Dimov, I.K., et al., *Integrated microfluidic tmRNA purification and real-time NASBA device for molecular diagnostics*. Lab on a Chip, 2008. 8(12): p. 2071-2078.
154. Fernandez-Baldo, M.A., et al., *Microfluidic Immunosensor with Micromagnetic Beads Coupled to Carbon-Based Screen-Printed Electrodes (SPCEs) for Determination of Botrytis cinerea in Tissue of Fruits*. Journal of Agricultural and Food Chemistry, 2010. 58(21): p. 11201-11206.
155. Wang, L. and P.C.H. Li, *Gold nanoparticle-assisted single base-pair mismatch discrimination on a microfluidic microarray device*. Biomicrofluidics, 2010. 4(3).
156. Wang, L. and P.C.H. Li, *Optimization of a microfluidic microarray device for the fast discrimination of fungal pathogenic DNA*. Analytical Biochemistry, 2010. 400(2): p. 282-288.
157. Lutz, S., et al., *Microfluidic lab-on-a-foil for nucleic acid analysis based on isothermal recombinase polymerase amplification (RPA)*. Lab on a Chip, 2010. 10(7): p. 887-893.
158. Jung, J.H., G.-Y. Kim, and T.S. Seo, *An integrated passive micromixer-magnetic separation-capillary electrophoresis microdevice for rapid and multiplex pathogen detection at the single-cell level*. Lab on a Chip, 2011. 11(20): p. 3465-3470.
159. Sato, K., et al., *Microbead-based rolling circle amplification in a microchip for sensitive DNA detection*. Lab on a Chip, 2010. 10(10): p. 1262-1266.
160. Weng, X., et al., *An RNA-DNA hybridization assay chip with electrokinetically controlled oil droplet valves for sequential microfluidic operations*. Journal of Biotechnology, 2011. 155(3): p. 330-337.
161. Meltzer, R.H., et al., *A lab-on-chip for biothreat detection using single-molecule DNA mapping*. Lab on a Chip, 2011. 11(5): p. 863-873.
162. Qi, C., et al., *Phage M13KO7 detection with biosensor based on imaging ellipsometry and AFM microscopic confirmation*. Virus Research, 2009. 140(1-2): p. 79-84.
163. Li, Y.Y., C.S. Zhang, and D. Xing, *Integrated microfluidic reverse transcription-polymerase chain reaction for rapid detection of food- or waterborne pathogenic rotavirus*. Analytical Biochemistry, 2011. 415(2): p. 87-96.
164. Ferguson, B.S., et al., *Genetic Analysis of H1N1 Influenza Virus from Throat Swab Samples in a Microfluidic System for Point-of-Care Diagnostics*. Journal of the American Chemical Society, 2011. 133(23): p. 9129-9135.
165. Yamanaka, K., et al., *Rapid detection for primary screening of influenza A virus: microfluidic RT-PCR chip and electrochemical DNA sensor*. Analyst, 2011. 136(10): p. 2064-2068.
166. Thaitrong, N., et al., *Integrated Capillary Electrophoresis Microsystem for Multiplex Analysis of Human Respiratory Viruses*. Analytical Chemistry, 2010. 82(24): p. 10102-10109.
167. Liu, C., et al., *An isothermal amplification reactor with an integrated isolation membrane for point-of-care detection of infectious diseases*. Analyst, 2011. 136(10): p. 2069-2076.
168. Li, Y., C. Zhang, and D. Xing, *Fast identification of foodborne pathogenic viruses using continuous-flow reverse transcription-PCR with fluorescence detection*. Microfluidics and Nanofluidics, 2011. 10(2): p. 367-380.
169. Wang, C.-H., et al., *An integrated microfluidic loop-mediated-isothermal-amplification system for rapid sample pre-treatment and detection of viruses*. Biosensors and Bioelectronics, 2011. 26(5): p. 2045-2052.

170. Fang, X., et al., *Loop-Mediated Isothermal Amplification Integrated on Microfluidic Chips for Point-of-Care Quantitative Detection of Pathogens*. Analytical Chemistry, 2010. 82(7): p. 3002-3006.
171. Ramalingam, N., et al., *Microfluidic devices harboring unsealed reactors for real-time isothermal helicase-dependent amplification*. Microfluidics and Nanofluidics, 2009. 7(3): p. 325-336.
172. Deisingh, A.K. and M. Thompson, *Biosensors for the detection of bacteria*. Canadian journal of microbiology, 2004. 50(2): p. 69-77.
173. Weng, X., H. Jiang, and D. Li, *Microfluidic DNA hybridization assays*. Microfluidics and Nanofluidics, 2011. 11(4): p. 367-383.
174. Javanmard, M. and R. Davis, *A microfluidic platform for electrical detection of DNA hybridization*. Sensors and Actuators B: Chemical, 2011. 154(1): p. 22-27.
175. Berdat, D., et al., *Label-free detection of DNA with interdigitated micro-electrodes in a fluidic cell*. Lab on a Chip, 2008. 8(2): p. 302-308.
176. Schüller, T., et al., *A disposable and cost efficient microfluidic device for the rapid chip-based electrical detection of DNA*. Biosensors and Bioelectronics, 2009. 25(1): p. 15-21.
177. Chen, L., et al., *DNA hybridization detection in a microfluidic channel using two fluorescently labelled nucleic acid probes*. Biosensors and Bioelectronics, 2008. 23(12): p. 1878-1882.
178. Dutse, S.W. and N.A. Yusof, *Microfluidics-Based Lab-on-Chip Systems in DNA-Based Biosensing: An Overview*. Sensors, 2011. 11(6): p. 5754-5768.
179. Njoroge, S.K., et al., *Integrated microfluidic systems for DNA analysis*. Topics in current chemistry, 2011. 304: p. 203-60.
180. Rane, T.D., et al. *High-throughput single-cell pathogen detection on a droplet microfluidic platform*. 2011. IEEE.
181. Zanolli, L.M., et al., *Peptide nucleic acid molecular beacons for the detection of PCR amplicons in droplet-based microfluidic devices*. Analytical and bioanalytical chemistry, 2012: p. 1-10.
182. Zhang, C., et al., *PCR microfluidic devices for DNA amplification*. Biotechnology Advances, 2006. 24(3): p. 243-284.
183. Pan, X., et al., *A microfluidic device integrated with multichamber polymerase chain reaction and multichannel separation for genetic analysis*. Analytica chimica acta, 2010. 674(1): p. 110-115.
184. Wang, H.Y., C.S. Zhang, and D. Xing, *Simultaneous detection of Salmonella enterica, Escherichia coli O157:H7, and Listeria monocytogenes using oscillatory-flow multiplex PCR*. Microchimica Acta, 2011. 173(3-4): p. 503-512.
185. Asiello, P.J. and A.J. Baeumner, *Miniaturized isothermal nucleic acid amplification, a review*. Lab on a Chip, 2011. 11(8): p. 1420-1430.
186. Piepenburg, O., et al., *DNA Detection Using Recombination Proteins*. PLoS Biol, 2006. 4(7): p. e204.
187. John, R., et al., *Rolling-circle amplification of viral DNA genomes using phi29 polymerase*. Trends in microbiology, 2009. 17(5): p. 205-211.
188. Privorotskaya, N., et al., *Rapid thermal lysis of cells using silicon-diamond microcantilever heaters*. Lab on a Chip, 2010. 10(9): p. 1135-1141.
189. Grabski, A.C., *Advances in preparation of biological extracts for protein purification*. Methods in enzymology, 2009. 463: p. 285-303.
190. Huh, Y.S., et al., *Microfluidic cell disruption system employing a magnetically actuated diaphragm*. Electrophoresis, 2007. 28(24): p. 4748-4757.

191. Di Carlo, D., K.H. Jeong, and L.P. Lee, *Reagentless mechanical cell lysis by nanoscale barbs in microchannels for sample preparation*. *Lab on a Chip*, 2003. 3(4): p. 287-291.
192. Grahl, T. and H. Märkl, *Killing of microorganisms by pulsed electric fields*. *Applied Microbiology and Biotechnology*, 1996. 45(1): p. 148-157.
193. Cheong, K.H., et al., *Gold nanoparticles for one step DNA extraction and real-time PCR of pathogens in a single chamber*. *Lab on a Chip*, 2008. 8(5): p. 810-813.
194. Craw, P. and W. Balachandran, *Isothermal Nucleic Acid Amplification Technologies for Point-of-Care Diagnostics: A Critical Review*. *Lab on a Chip*, 2012.
195. Mori, Y. and T. Notomi, *Loop-mediated isothermal amplification (LAMP): a rapid, accurate, and cost-effective diagnostic method for infectious diseases*. *Journal of Infection and Chemotherapy*, 2009. 15(2): p. 62-69.
196. Fang, X. and J. Kong, *A Portable and Integrated Nucleic Acid Amplification Microfluidic Chip for Identifying Bacteria*. *Lab on a Chip*, 2012. 12(8): p. 1495-1499.
197. Chang, W.-H., et al., *Rapid isolation and detection of aquaculture pathogens in an integrated microfluidic system using loop-mediated isothermal amplification*. *Sensors and Actuators B: Chemical*, (0).
198. Zhang, Y., et al., *A surface topography assisted droplet manipulation platform for biomarker detection and pathogen identification*. *Lab on a Chip*, 2011. 11(3): p. 398-406.
199. Shen, F., et al., *Digital Isothermal Quantification of Nucleic Acids via Simultaneous Chemical Initiation of Recombinase Polymerase Amplification Reactions on SlipChip*. *Analytical Chemistry*, 2011. 83(9): p. 3533-3540.
200. Liu, C., et al., *A self-heating cartridge for molecular diagnostics*. *Lab on a Chip*, 2011. 11(16): p. 2686-2692.
201. Ahmad, F., et al., *A CCD-based fluorescence imaging system for real-time loop-mediated isothermal amplification-based rapid and sensitive detection of waterborne pathogens on microchips*. *Biomedical Microdevices*: p. 1-9.
202. Mahalanabis, M., et al., *An integrated disposable device for DNA extraction and helicase dependent amplification*. *Biomedical Microdevices*, 2010. 12(2): p. 353-359.
203. Compton, J., *Nucleic acid sequence-based amplification*. *Nature*, 1991. 350(6313): p. 91.
204. Lizardi, P.M., et al., *Mutation detection and single-molecule counting using isothermal rolling-circle amplification*. *Nature Genetics*, 1998. 19(3): p. 225-232.
205. Mahmoudian, L., et al., *Rolling Circle Amplification and Circle-to-circle Amplification of a Specific Gene Integrated with Electrophoretic Analysis on a Single Chip*. *Analytical Chemistry*, 2008. 80(7): p. 2483-2490.
206. Park, S., et al., *Continuous dielectrophoretic bacterial separation and concentration from physiological media of high conductivity*. *Lab on a Chip*, 2011. 11(17): p. 2893-2900.
207. Moncada-Hernandez, H. and B.H. Lapizco-Encinas, *Simultaneous concentration and separation of microorganisms: insulator-based dielectrophoretic approach*. *Analytical and bioanalytical chemistry*, 2010. 396(5): p. 1805-1816.
208. Cheng, I.F., et al., *A dielectrophoretic chip with a roughened metal surface for on-chip surface-enhanced Raman scattering analysis of bacteria*. *Biomicrofluidics*, 2010. 4(3).
209. Bhattacharyya, A. and C.A. Klapperich, *Microfluidics-based extraction of viral RNA from infected mammalian cells for disposable molecular diagnostics*. *Sensors and Actuators B-Chemical*, 2008. 129(2): p. 693-698.

210. Mujika, M., et al., *Magnetoresistive immunosensor for the detection of Escherichia coli O157: H7 including a microfluidic network*. *Biosensors and Bioelectronics*, 2009. 24(5): p. 1253-1258.
211. Didar, T.F. and M. Tabrizian, *Adhesion based detection, sorting and enrichment of cells in microfluidic Lab-on-Chip devices*. *Lab on a Chip*, 2010. 10(22): p. 3043-3053.
212. Edelstein, R., et al., *The BARC biosensor applied to the detection of biological warfare agents*. *Biosensors and Bioelectronics*, 2000. 14(10-11): p. 805-813.
213. Gijs, M.A.M., *Magnetic bead handling on-chip: new opportunities for analytical applications*. *Microfluidics and Nanofluidics*, 2004. 1(1): p. 22-40.
214. Lee, G.U., L.A. Chrisey, and R.J. Colton, *Direct measurement of the forces between complementary strands of DNA*. *Science*, 1994. 266(5186): p. 771.
215. Huang, S., et al., *Microvalve and micropump controlled shuttle flow microfluidic device for rapid DNA hybridization*. *Lab on a Chip*, 2010. 10(21): p. 2925-2931.
216. Zhang, J., et al., *Rapid detection of algal toxins by microfluidic immunoassay*. *Lab on a Chip*, 2011. 11(20): p. 3516-3522.
217. Kim, J. and B.K. Gale, *Quantitative and qualitative analysis of a microfluidic DNA extraction system using a nanoporous AlOx membrane*. *Lab on a Chip*, 2008. 8(9): p. 1516-1523.
218. Metz, S., et al., *Polyimide microfluidic devices with integrated nanoporous filtration areas manufactured by micromachining and ion track technology*. *Journal of Micromechanics and Microengineering*, 2004. 14: p. 324.
219. Cao, W., et al., *Chitosan as a Polymer for pH-Induced DNA Capture in a Totally Aqueous System*. *Analytical Chemistry*, 2006. 78(20): p. 7222-7228.
220. Witek, M.A., et al., *96-Well Polycarbonate-Based Microfluidic Titer Plate for High-Throughput Purification of DNA and RNA*. *Analytical Chemistry*, 2008. 80(9): p. 3483-3491.
221. Noeth, N., et al. *Micro-particle filter made in SU-8 for biomedical applications*. in *Solid-State Sensors, Actuators and Microsystems Conference, 2009. TRANSDUCERS 2009. International*. 2009.
222. Chen, X., et al., *Continuous flow microfluidic device for cell separation, cell lysis and DNA purification*. *Analytica chimica acta*, 2007. 584(2): p. 237-243.
223. Gao, Y.L., et al., *Multiplexed high-throughput electrokinetically-controlled immunoassay for the detection of specific bacterial antibodies in human serum*. *Analytica chimica acta*, 2008. 606(1): p. 98-107.
224. Didar, T.F., A.M. Foudeh, and M. Tabrizian, *Patterning Multiplex Protein Microarrays in a Single Microfluidic Channel*. *Analytical Chemistry*, 2011. 84(2): p. 1012-1018.
225. Lui, C., et al., *Low-power microfluidic electro-hydraulic pump (EHP)*. *Lab on a Chip*, 2010. 10(1): p. 74-79.
226. Brassard, D., et al. *Advanced EWOD-based digital microfluidic system for multiplexed analysis of biomolecular interactions*. in *IEEE 24th International Conference on Micro Electro Mechanical Systems (MEMS)*. 2011. IEEE.
227. Teh, S.Y., et al., *Droplet microfluidics*. *Lab on a Chip*, 2008. 8(2): p. 198-220.
228. Seemann, R., et al., *Droplet based microfluidics*. *Reports on Progress in Physics*, 2012. 75: p. 016601.
229. Beer, N.R., et al., *On-Chip Single-Copy Real-Time Reverse-Transcription PCR in Isolated Picoliter Droplets*. *Analytical Chemistry*, 2008. 80(6): p. 1854-1858.

230. Theberge, A.B., et al., *Microdroplets in microfluidics: An evolving platform for discoveries in chemistry and biology*. *Angewandte Chemie International Edition*, 2010. 49(34): p. 5846-5868.
231. Malic, L., T. Veres, and M. Tabrizian, *Biochip functionalization using electrowetting-on-dielectric digital microfluidics for surface plasmon resonance imaging detection of DNA hybridization*. *Biosensors and Bioelectronics*, 2009. 24(7): p. 2218-2224.
232. Choi, K., et al., *Integration of Field effect Transistor-Based Biosensors with Digital Microfluidic Device for a Lab-on-a-chip Application*. *Lab on a Chip*, 2012.
233. Moon, H., et al., *An integrated digital microfluidic chip for multiplexed proteomic sample preparation and analysis by MALDI-MS*. *Lab on a Chip*, 2006. 6(9): p. 1213-1219.
234. Nichols, K.P. and H.J.G.E. Gardeniers, *A digital microfluidic system for the investigation of pre-steady-state enzyme kinetics using rapid quenching with MALDI-TOF mass spectrometry*. *Analytical Chemistry*, 2007. 79(22): p. 8699-8704.
235. Srinivasan, V., V.K. Pamula, and R.B. Fair, *An integrated digital microfluidic lab-on-a-chip for clinical diagnostics on human physiological fluids*. *Lab on a Chip*, 2004. 4(4): p. 310-315.
236. Sista, R., et al., *Development of a digital microfluidic platform for point of care testing*. *Lab on a Chip*, 2008. 8(12).
237. Madou, M., et al., *Lab on a CD*. *Annu. Rev. Biomed. Eng.*, 2006. 8: p. 601-628.
238. Ramalingam, N., et al., *Real-time PCR-based microfluidic array chip for simultaneous detection of multiple waterborne pathogens*. *Sensors and Actuators B: Chemical*, 2010. 145(1): p. 543-552.
239. Martinez, A.W., et al., *Diagnostics for the developing world: microfluidic paper-based analytical devices*. *Analytical Chemistry*, 2009. 82(1): p. 3-10.
240. Pelton, R., *Bioactive paper provides a low-cost platform for diagnostics*. *Trac-Trends in Analytical Chemistry*, 2009. 28(8): p. 925-942.
241. Zhao, W. and A. van der Berg, *Lab on paper*. *Lab on a Chip*, 2008. 8(12): p. 1988.
242. Jokerst, J.C., et al., *Development of a Paper-Based Analytical Device for Colorimetric Detection of Select Foodborne Pathogens*. *Analytical Chemistry*, 2012. 84(6): p. 2900-2907.
243. Zhao, W.A., et al., *Paper-Based Bioassays Using Gold Nanoparticle Colorimetric Probes*. *Analytical Chemistry*, 2008. 80(22): p. 8431-8437.
244. Abe, K., et al., *Inkjet-printed paperfluidic immuno-chemical sensing device*. *Analytical and bioanalytical chemistry*, 2010. 398(2): p. 885-893.
245. Martinez, A.W., S.T. Phillips, and G.M. Whitesides, *Three-dimensional microfluidic devices fabricated in layered paper and tape*. *Proceedings of the National Academy of Sciences*, 2008. 105(50): p. 19606.
246. Liu, X.Y., et al. *A portable microfluidic paper-based device for ELISA*. in *Micro Electro Mechanical Systems (MEMS), 2011 IEEE 24th International Conference on*. 2011.
247. Ge, L., et al., *Three-dimensional paper-based electrochemiluminescence immunodevice for multiplexed measurement of biomarkers and point-of-care testing*. *Biomaterials*, 2011.
248. Liu, H. and R.M. Crooks, *Three-Dimensional Paper Microfluidic Devices Assembled Using the Principles of Origami*. *Journal of the American Chemical Society*, 2011. 133(44): p. 17564-17566.

249. Chen, D.F., et al., *An integrated, self-contained microfluidic cassette for isolation, amplification, and detection of nucleic acids*. Biomedical Microdevices, 2010. 12(4): p. 705-719.
250. Lafleur, L., et al., *Progress toward multiplexed sample-to-result detection in low resource settings using microfluidic immunoassay cards*. Lab on a Chip, 2012. 12(6).
251. Chin, C.D., et al., *Microfluidics-based diagnostics of infectious diseases in the developing world*. Nature Medicine, 2011. 17(8): p. 1015-1019.
252. Cannone, J.J., et al., *The comparative RNA web (CRW) site: an online database of comparative sequence and structure information for ribosomal, intron, and other RNAs*. BMC bioinformatics, 2002. 3(1): p. 2.
253. Stinear, T., et al., *Detection of a single viable Cryptosporidium parvum oocyst in environmental water concentrates by reverse transcription-PCR*. Applied and environmental microbiology, 1996. 62(9): p. 3385-90.
254. Molmeret, M., et al., *Amoebae as Training Grounds for Intracellular Bacterial Pathogens*. Applied and environmental microbiology, 2005. 71(1): p. 20-28.
255. Gourse, R.L., et al., *rRNA TRANSCRIPTION AND GROWTH RATE-DEPENDENT REGULATION OF RIBOSOME SYNTHESIS IN ESCHERICHIA COLI*. Annual Review of Microbiology, 1996. 50(1): p. 645-677.
256. Neumeister, B., et al., *Influence of Acanthamoeba castellanii on Intracellular Growth of Different Legionella Species in Human Monocytes*. Applied and environmental microbiology, 2000. 66(3): p. 914-919.
257. Ohno, A., et al., *Temperature-Dependent Parasitic Relationship between Legionella pneumophila and a Free-Living Amoeba (Acanthamoeba castellanii)*. Applied and environmental microbiology, 2008. 74(14): p. 4585-4588.
258. Declerck, P., et al., *Impact of Non-Legionella Bacteria on the Uptake and Intracellular Replication of Legionella pneumophila in Acanthamoeba castellanii and Naegleria lovaniensis*. Microbial Ecology, 2005. 50(4): p. 536-549.
259. World Health Organization, World Water Day Report 2000, World Health Organization, Genève, 2000.
260. Delgado-Viscogliosi, P., L. Solignac, and J.-M. Delattre, *Viability PCR, a Culture-Independent Method for Rapid and Selective Quantification of Viable Legionella pneumophila Cells in Environmental Water Samples*. Applied and environmental microbiology, 2009. 75(11): p. 3502-3512.
261. Fields, B.S., R.F. Benson, and R.E. Besser, *Legionella and Legionnaires' Disease: 25 Years of Investigation*. Clinical Microbiology Reviews, 2002. 15(3): p. 506-526.
262. Agresti, J.J., et al., *Ultrahigh-throughput screening in drop-based microfluidics for directed evolution*. Proceedings of the National Academy of Sciences, 2010. 107(9): p. 4004-4009.
263. Chai, S.C., et al., *Practical Considerations of Liquid Handling Devices in Drug Discovery*. Drug Discovery, ed. H. El-Shemy 2013.
264. Kuhnemund, M., et al., *Circle-to-circle amplification on a digital microfluidic chip for amplified single molecule detection*. Lab on a Chip, 2014. 14(16): p. 2983-2992.
265. Jebrail, M.J., et al., *World-to-Digital-Microfluidic Interface Enabling Extraction and Purification of RNA from Human Whole Blood*. Analytical Chemistry, 2014. 86(8): p. 3856-3862.
266. Rival, A., et al., *An EWOD-based microfluidic chip for single-cell isolation, mRNA purification and subsequent multiplex qPCR*. Lab on a Chip, 2014. 14(19): p. 3739-3749.

267. Zhao, Y. and C. K. *Pin-count-aware online testing of digital microfluidic biochips*. in *VLSI Test Symposium (VTS)*. 2010.
268. Sista, R.S., et al., *Heterogeneous immunoassays using magnetic beads on a digital microfluidic platform*. *Lab on a Chip*, 2008. 8(12): p. 2188-2196.
269. Yizhong, W., Z. Yuejun, and C. Sung Kwon, *Efficient in-droplet separation of magnetic particles for digital microfluidics*. *Journal of Micromechanics and Microengineering*, 2007. 17(10): p. 2148.
270. Gabig-Ciminska, M., et al., *Electric chips for rapid detection and quantification of nucleic acids*. *Biosensors and Bioelectronics*, 2004. 19(6): p. 537-546.
271. Brassard, D., et al., *Water-oil core-shell droplets for electrowetting-based digital microfluidic devices*. *Lab on a Chip*, 2008. 8(8): p. 1342-1349.
272. Luk, V.N., G.C.H. Mo, and A.R. Wheeler, *Pluronic Additives: A Solution to Sticky Problems in Digital Microfluidics*. *Langmuir*, 2008. 24(12): p. 6382-6389.
273. Kim, J., et al., *Microfluidic sample preparation: cell lysis and nucleic acid purification*. *Integrative Biology*, 2009. 1(10): p. 574-586.
274. Rissin, D.M., et al., *Single-molecule enzyme-linked immunosorbent assay detects serum proteins at subfemtomolar concentrations*. *Nat Biotech*, 2010. 28(6): p. 595-599.
275. Abadian, A. and S. Jafarabadi-Ashtiani, *Paper-based digital microfluidics*. *Microfluidics and Nanofluidics*, 2014. 16(5): p. 989-995.
276. He, F., et al., *A hybrid paper and microfluidic chip with electrowetting valves and colorimetric detection*. *Analyst*, 2014. 139(12): p. 3002-3008.
277. Zhu, H., et al., *Optical imaging techniques for point-of-care diagnostics*. *Lab on a Chip*, 2013. 13(1): p. 51-67.
278. Pierce, M., et al., *Optical Systems for Point-of-care Diagnostic Instrumentation: Analysis of Imaging Performance and Cost*. *Annals of Biomedical Engineering*, 2014. 42(1): p. 231-240.
279. Myers, F.B. and L.P. Lee, *Innovations in optical microfluidic technologies for point-of-care diagnostics*. *Lab on a Chip*, 2008. 8(12): p. 2015-2031.
280. Zhu, H., et al., *Optofluidic Fluorescent Imaging Cytometry on a Cell Phone*. *Analytical Chemistry*, 2011. 83(17): p. 6641-6647.
281. Breslauer, D.N., et al., *Mobile phone based clinical microscopy for global health applications*. *PLoS one*, 2009. 4(7): p. e6320.
282. Wei, Q., et al., *Fluorescent Imaging of Single Nanoparticles and Viruses on a Smart Phone*. *ACS Nano*, 2013. 7(10): p. 9147-9155.

Lab on a Chip

Cite this: *Lab Chip*, 2012, 12, 3249–3266

www.rsc.org/loc

CRITICAL REVIEW

Microfluidic designs and techniques using lab-on-a-chip devices for pathogen detection for point-of-care diagnostics

Amir M. Foudeh,^a Tohid Fatanat Didar,^a Teodor Veres^{ab} and Maryam Tabrizian^{*a}

Received 31st May 2012, Accepted 26th June 2012

DOI: 10.1039/c2lc40630f

Effective pathogen detection is an essential prerequisite for the prevention and treatment of infectious diseases. Despite recent advances in biosensors, infectious diseases remain a major cause of illnesses and mortality throughout the world. For instance in developing countries, infectious diseases account for over half of the mortality rate. Pathogen detection platforms provide a fundamental tool in different fields including clinical diagnostics, pathology, drug discovery, clinical research, disease outbreaks, and food safety. Microfluidic lab-on-a-chip (LOC) devices offer many advantages for pathogen detection such as miniaturization, small sample volume, portability, rapid detection time and point-of-care diagnosis. This review paper outlines recent microfluidic based devices and LOC design strategies for pathogen detection with the main focus on the integration of different techniques that led to the development of sample-to-result devices. Several examples of recently developed devices are presented along with respective advantages and limitations of each design. Progresses made in biomarkers, sample preparation, amplification and fluid handling techniques using microfluidic platforms are also covered and strategies for multiplexing and high-throughput analysis, as well as point-of-care diagnosis, are discussed.

1. Introduction

The World Health Organization (WHO) recently reported that infectious diseases are the second leading cause of mortality throughout the world after cardiovascular disease.¹ This

problem is particularly severe in developing countries and deprived areas of developed countries, that suffer from poor hygiene and limited access to centralized labs for diagnostics and treatments. Half of the mortality in poor countries is due to infectious disease.² As in developed countries, despite great progress in enhancing health conditions, there are still several issues that remain to be resolved in regards to food industries, pathogen outbreaks, and sexually transmitted diseases.³ It is worth mentioning that in the USA alone, food-borne pathogens were the main cause of more than 50 million illnesses reported in

^aBiomedical Engineering Department, McGill University, Montreal, QC, H3A 2B4, Canada. E-mail: Maryam.Tabrizian@mcgill.ca; Fax: +1-514-298-7461; Tel: +1-514-398-8129

^bNational Research Council of Canada, 75 Boul. de Mortagne, Québec, Boucherville, J4B 6Y4, Canada



Amir Foudeh

Amir M. Foudeh is a PhD student in the Department of Biomedical Engineering at McGill University. He received his bachelor's degree in Chemical Engineering from Isfahan University of Technology, Iran and obtained his master's degree in Biotechnology from Chalmers University of Technology, Goteborg, Sweden. His primary research is focused on developing microfluidic-based biosensors for the detection of pathogens.



Tohid Fatanat Didar

Tohid Fatanat Didar is a PhD student in the Department of Biomedical Engineering at McGill University. He received his bachelor's degree in mechanical engineering from Sharif University of Technology. During his master's studies, he worked on micro/nano fabrication of microfluidic platforms. His current research involves implementing micro and nanofabrication principles to produce micro-chips for biological applications. He designs microfluidic platforms with bio-functional interfaces to specifically detect, separate or investigate biological elements.

2011.⁴ Overall, pathogens are of great importance in many different fields, including diagnostics, pathology, drug discovery, clinical research, biological warfare, disease outbreaks, and food safety.

Conventional and standard methods of pathogen detection include cell culture, PCR, and enzyme immunoassay, which are often laborious and take from several hours to days to perform. Pathogen detection methods should be cost-effective, fast, sensitive, and accurate. For point of care (POC) applications, the detection platform should also be simple to use and interpret, stable under a wide range of operating conditions (such as temperature, humidity), preferably portable and disposable.⁵ Furthermore, they should provide the required sensitivity and specificity.⁶ The ability to perform multiplex tests is another important prerequisite for pathogen detection devices, especially in the case of diseases with several pathogen sources, such as lower respiratory infections.⁵ One of most successful non-microfluidic POC devices so far is the immunochromatographic strip (ICS), which is currently used in developing countries.⁷⁻⁹ Despite some issues with the test's sensitivity and specificity, ICS is considered an ideal model for the development of microfluidic-based devices for pathogen detection by taking advantage of low cost, sensitivity, specificity, portability, and the simplicity of microfluidic options. Microfluidics provides a higher surface to volume ratio, a faster rate of mass and heat transfer, and the ability to precisely handle very small volumes of reagents, ranging from nano to picoliters, in microchannels. Because of these characteristics, microfluidic devices provide better performance than conventional systems for providing a rapid detection time. The use of microfluidics in the context of Lab-On-a-Chip (LOC) devices has begun to play an important role in the analytical investigations of biological and chemical samples in a single miniaturized device. These devices inherently possess characteristics that make them suitable for POC applications.

Here, we review the present status of microfluidic-based devices for pathogen diagnostics, emphasizing innovative designs, strategies, and trends during the past three years.

2. Biomarkers

The specific identification of biological species or their strains is essential for pathogen detection. Pathogens are generally recognized based on two main properties: by genetic contents, using nucleic acid-based probes, or by specific epitopes on the pathogen membrane or their produced toxins, using antibodies or antibody alternatives. Usually, the latter approach provides a lower specificity compared to nucleic acid-based approach, because the epitopes present on the cell's surface are normally found throughout the species. Then, generally, genus-level detection is achieved,¹⁰ but this can provide results in a shorter time with less manipulation. List of different biomarkers used to detect pathogens summarized in Table 1.

2.1. Antibodies

Antibody-based detection is one of the main analytical techniques used for the detection of pathogens. Although labour-intensive, antibody-based detection has proven to be a crucial and important factor in the specific and high-affinity detection of pathogens. Engineering antibody fragments, recombinant antibody-fragments (rAbs), single chain variable fragments (scFv) and monovalent antibody fragments (Fabs) are recent approaches that have originated from antibody-based detection. The use of these fragments is more cost-effective while providing the same specificity limits as conventional antibody methods.¹¹ The detection of specific proteins and of the whole cell are the two most common applications of antibody-based probes.

2.1.1 Protein and toxin detection using antibodies. Recently, antibody-based probes were used for the detection of several toxins, including Ricin A chain (RCA), staphylococcal enterotoxin B (SEB) toxin surrogate,¹² ovalbumin,¹³ and cholera toxin subunit B (CTB).¹⁴ Microarray immunoassays have also been used extensively for the multiplex detection of proteins and toxins.^{15,16}



Teodor Veres

Teodor Veres is a Senior Research Officer and the group leader of the Functional Nanomaterials Group in the Life Sciences Division of the National Research Council of Canada. He is also adjunct professor in the Department of Biomedical Engineering at McGill University. In NRC, Dr Veres is leading the activities related to the design, fabrication and use of microfluidic components and systems for diagnostics applications as well as the synthesis and characterization of functional nanostructures for applications in drug delivery, bio-sensing isolation of molecular of biological targets in microfluidic systems.



Maryam Tabrizian

Maryam Tabrizian is full professor at the Department of Biomedical Engineering at McGill University. She is FRSQ-Chercheur National awardee and became the Guggenheim Fellow in Biomedical Sciences in 2010. M. Tabrizian's core competency is in the field of biointerface, biorecognition systems and microfluidics and their integration with biosensing devices for cell behaviour investigation in stimulated microenvironments. For more than 10 years, her laboratories have been working on the development of microfluidic platforms compatible with impedance spectroscopy and surface plasmon resonance spectroscopy for the detection and high throughput analysis of biomarkers, proteins, peptides, DNA, drugs and other biologically active substances.

Table 1 Detection of pathogens implemented in microfluidic devices

Pathogen	Probe	LOD	Sample	Time of analysis	Amplification	Ref
<i>E. coli</i> O157:H7	Antibody	10 ⁶ CFU mL ⁻¹	Soil sample			43
	Antibody, primer	200 CFU mL ⁻¹	Synthetic		PCR	44
	Primer	3.58 × 10 ³ copies μL ⁻¹	Synthetic	13 min	PCR	45
		10 ⁸ CFU mL ⁻¹	Hotdog, banana, milk			
		1 bacteria μL ⁻¹	Synthetic			34
	AMP (Antimicrobial peptide magainin I)					
	DNA probe	25 CFU mL ⁻¹	Synthetic			46
	Antibody	32 CFU μL ⁻¹	Synthetic	20 min		25
	Antibody/DNA probe	100 bacteria	Synthetic		PCR	47
	Primer	1 cell in 10 ³	Synthetic	4 h	PCR	48
<i>E. coli</i> K12 and O157:H7	Polyclonal antibody/primer	0.6 CFU L ⁻¹	Lake water	5 h	PCR	49
	Antibody					
<i>E. coli</i> K12	Antibody	10 CFU mL ⁻¹	Iceberg lettuce	6 min		50
<i>E. coli</i> BL21	Antibody	55 cells mL ⁻¹	PBS	1 h		24
<i>E. coli</i> DH5α, <i>S. saprophyticus</i>	Primer	100 cells mL ⁻¹	Milk			
<i>E. coli</i> (BL21(DE3))	Primer	10 ⁶ cells mL ⁻¹	Blood samples	1 h	PCR	51
<i>E. coli</i> XL-1	PNA probe	1 CFU μL ⁻¹	Synthetic	30 min		52
<i>E. coli</i> DH5R	DNA probe	100 CFU μL ⁻¹	Urine			
	Antibody	10 ⁴ CFU mL ⁻¹	Synthetic			22
	Primer	1000 Bacteria mL ⁻¹	Synthetic	30 min	NASBA	53
	DNA probe	10 ⁸ CFU mL ⁻¹	Clinical urine sample	40 min		54
<i>Botrytis cinerea</i>	Antibody	80 CFU mL ⁻¹	Synthetic			
	DNA probe	0.008 μg mL ⁻¹	Apple (Red Delicious)	40 min		55
<i>B. cinerea</i> , <i>D. bryoniae</i> , and <i>B. squamosa</i>	DNA probe	8 fmol	Synthetic	1 h		56
<i>Staphylococcus aureus</i>	Primer/probe	0.2 ng μL ⁻¹	Synthetic	3 min	PCR	57
<i>Salmonella enterica</i>	Primer	<10 copies	Synthetic	<20 min	RPA	58
<i>Salmonella bertea</i>	Antibody	1 CFU	Synthetic	30 min		59
<i>Bacillus globigii</i>	Primer, probe	8.8 ng mL ⁻¹	Synthetic		RCA	60
Surrogate biotoxin (ovalbumin)	DNA probe	10 ⁷ CFU mL ⁻¹	Synthetic	25 min		61
Cholera toxin subunit B (CTB)	Antibody	1 CFU mL ⁻¹	Synthetic	30 min		21
Botulinum toxoid	Antibody	50 ppb (18 ng mL ⁻¹)	Raw milk sample			13
Phage M13K07	DNA/antibody	1.0 ng mL ⁻¹	Synthetic	1 h		14
Rotaviruses	Anti-M13	25 pg	Synthetic			62
	Primer	10 ⁹ pfu mL ⁻¹	Synthetic			63
H1N1	Primer/probe	3.6 × 10 ⁴ RNA copies μL ⁻¹	Stool	1 h	RT-PCR	64
Swine influenza virus	Antibody	10 TCID ₅₀	Throat swab	3.5 h	RT-PCR	65
Influenza A virus (AH1pdm)	Primer	610 TCID ₅₀ mL ⁻¹	Synthetic	6 min		23
Influenza B, coronavirus OC43, influenza A, and human metapneumo virus	Primer	5.36 × 10 ² copies mL ⁻¹	Synthetic	15 min	RT-PCR	66
HIV-1	Primer	4.8, 6.3, 10, and 167 copies, respectively	Synthetic	2 h	RT-PCR	67
Noroviruses (NVs) and rotaviruses (RVs)	Primer	10 HIV particles	Spiked saliva sample		RT-LAMP	68
Nervous necrosis virus (NNV)	Primer	6.4 × 10 ⁴ copies μL ⁻¹	Synthetic	1 h	RT-PCR	69
Pseudorabies virus (PRV)	Primer	10 fg of cDNA	Groupers larvae	1 h	RT-LAMP	70
Severe acute respiratory syndrome (SARS) virus DNA	Primer	10 fg DNA μL ⁻¹	Synthetic	1 h	LAMP	71
	Primer	3 × 10 ⁷ copies μL ⁻¹	Synthetic		HDA	72

2.1.2 Whole cell detection. Antibody cell-based pathogen detection in microfluidic systems has been demonstrated using different biosensing tools, including Surface Plasmon Resonance (SPR),¹⁷ fluorescence,¹⁸ impedance,¹⁹ chemiluminescence,²⁰ conducting polymers,²¹ and impedance.²²

Applying a whole-cell detection approach, pathogens such as influenza,²³ *E. coli*,^{24,25} *L. pneumophila*,²⁶ hepatitis B, hepatitis C, and HIV²⁷ could be detected.

2.1.3 Alternatives to the antibody. Although antibodies are widely accessible and easy to use, they have several drawbacks, such as expensive cost, poor chemical and physical stability,

large size, use of animals for antibody production, limited antibody availability for all potential analytes, and quality-assured preparations. There are several emerging alternatives to antibodies, including enzyme-substrate reactions,²⁸ molecularly imprinted polymers,²⁹ protein-based,³⁰ small molecule probes,³¹ aptamers,^{32,33,36,37,40} and antimicrobial peptides (AMPs).³⁴

The main advantage of enzyme-substrate reactions in comparison to antibody-antigen is that they can be regenerated several times without loss of affinity or specificity. For instance, there are enzyme inhibition-based sensors for toxin detection, e.g., the detection of sarin (a highly toxic material) in blood by using immobilized cholinesterase on a microfluidic chip.²⁸ Enzymes

can also be used to target proteins. For instance, Le Nel *et al.*³⁵ developed a microfluidic chip for the detection of pathological prion protein (PrP) by proteinase K (PK)-mediated protein digestion.

Molecularly imprinted polymers (MIPs), which can be produced at a low cost in relatively high stability and reproducibility, are another alternative to antibodies.^{36,37} A microfluidic chip coupled to the MIP method was developed for the detection of the tobacco mosaic virus (TMV) and the human rhinovirus serotype 2 (HRV2) using impedance measurement.²⁹

Protein-based pathogen detection is another approach in which the crucial point is preserving the native state and orientation of the protein in order to provide high specificity and sensitivity.³⁸ For instance, heat shock protein 60 (Hsp60), which is a receptor for listeria adhesion protein (LAP) during *L. monocytogenes* infection, was utilized for the detection of the LAP. By using Hsp60, higher sensitivity and capture efficiency was achieved in comparison to the use of a monoclonal antibody. Another feature of this protein is that it can be produced in *E. coli* by the recombination of cDNA, making it a cost-effective choice.³⁰

Small molecule probes have also emerged as alternatives to antibody-based detection. For instance, Kell *et al.*³¹ developed a vancomycin-modified nanoparticle for the isolation of gram-positive and -negative bacteria. Although its selectivity is less than those of monoclonal antibodies, it is a useful tool for capturing a wide range of bacteria with single vancomycin-functionalized nanoparticles. It was shown that the architecture and orientation of the molecule are crucial to efficient target capture. Overall, by using small molecule probes, the long-term stability, reaction conditions, and temperature for surface modification are more flexible compared to those of an antibody-based approach.

Aptamers are fairly recent options to replace antibodies.³⁹ Aptamers are nucleic acid molecules developed by an *in vitro* process, which can bind to their molecular targets, such as small molecules, proteins, or cells,⁴⁰ with high affinity and specificity.⁴¹ Aptamers have several distinct advantages over antibodies, including enhanced affinity and specificity, resulting in better limit of detection (LOD) for biosensing applications. Typically, they are also smaller than antibodies, enabling them to bind to epitopes that are otherwise inaccessible to antibodies.⁴⁰ Aptamers are selected in conditions similar to those of a real matrix and can be modified during immobilization, without any adverse effect on their affinity. Finally, they can be subjected to several cycles of regeneration.⁴²

On the other hand, aptamers require a long selection time and several resources to target a specific epitope. Normally, the systematic evolution of ligands by exponential enrichment (SELEX) is used to isolate aptamers. Lou *et al.*⁵² developed a magnetic bead-assisted SELEX technique using microfluidics to reduce processing time. This design could isolate the target aptamers after a single round, as compared to conventional SELEX methods, which usually require 8–15 rounds of selection. A particular feature of this device is ferromagnetic patterns embedded in the microchannel, which are capable of producing highly localized magnetic field gradients that provide precise control over a small number of beads. This device also benefits from the laminar flow characteristics, which result in minimizing

the molecular diffusion to obtain higher purity. As a proof of concept, aptamers were selected for botulinum neurotoxin type A. In another effort to reduce aptamer discovery time, Ahmad *et al.*³³ developed a microfluidic SELEX platform in which they found new aptamer sequences for PDGF-BB in only three rounds.

Antimicrobial peptides (AMPs) are also used to benefit from their intrinsic stability, ease of synthesis, and long-term functionality compared to antibodies. AMPs can be found in nature, such as in the extracellular milieu of bacteria and on the skin of higher organisms.³⁴ Mannoor *et al.*³⁴ used AMP for the detection of *E. coli*, using impedance measurement as a label-free and portable biosensor platform. The semi-selective antimicrobial peptide magainin I, which occurs naturally on the skin of African clawed frogs, was immobilized on the arrays of gold electrodes for the detection of *E. coli*. The LOD of one bacterium per μL was obtained. Depending on the targeted application, AMPs provide advantages and disadvantages. If the goal is to detect a broad range of pathogens, they would be useful because AMPs are semi-selective toward their target. However for the identification of a very specific target in a pathogenic mixture, they might not be appropriate.

2.2. DNA/PNA

DNA hybridization assays provide unique advantages compared to conventional antibody-based approaches due to their capabilities for sensitive, specific, and rapid detection of target nucleic acids.⁷³ Recently, various microfluidic DNA-based probes were coupled to different measurement techniques, including SPRi,⁷⁴ conductance impedance,^{65,75–77} and (FRET) fluorescence.⁷⁸ For more information please refer to a review paper⁷⁹ on DNA microfluidic-based and an integrated microfluidic systems for DNA analysis.⁸⁰

Wang *et al.*⁵⁶ implemented two different methods to distinguish a single mismatch using gold nanoparticles (GNPs). In the first approach, a glass surface was coated with a monolayer of GNPs, which increased the hybridization efficiency due to nanoscale spacing between the probes. In the second approach, a DNA amplicon bound to GNPs was introduced to the probe-functionalized surface. Riahi *et al.*⁵⁴ used a double stranded DNA probe for the detection of bacterial 16 S rRNA. Double stranded DNA is composed of an actual complementary DNA to probe the target with a fluorescent dye at the 5' end. A shorter probe is then hybridized to the first probe, with a quencher at the 3' end, in which the 5' of the first probe is in the proximity of the 3' of the second probe. After introducing the target, the quencher probe is replaced by the target, resulting in a fluorescent signal. This setup was used to detect different pathogens in a clinical urine samples, and a total experimental time of less than 40 min was achieved.

Peptide nucleic acid (PNA) is a DNA analogue with a peptide backbone instead of a sugar phosphate backbone. PNAs normally exhibit chemical and thermal stability, resistance to enzymatic degradation, faster hybridization kinetics, and the ability to hybridize at lower salt concentrations. Lower salt concentrations help to denature the secondary structures of targets, such as RNA. PNA beacons were designed for the detection of 16 S rRNA from *E. coli* in a droplet-based

microfluidic device, without any pre-amplification steps. In this method, DNA beacons were labeled with fluorescent dyes and quenchers at both ends. Because of the loop shape of the beacons, they are both in proximity of each other in an unhybridized state. After hybridization, this loop broke down, and the quencher became ineffective, due to its distance from the dye, resulting in the fluorescence emission.⁸¹ In another approach, PNA molecular beacons were used for the detection of the PCR amplicons. The PNA beacon had a reporter and a quencher at each end in proximity of each other before hybridization. After hybridization with the target DNA, fluorescence emission from the reporter occurred upon excitation. This setup could discriminate a single base mutation at a 100 nM concentration.⁸² Conversely, a LOD of 1 CFU μL^{-1} in 30 min was obtained by Lam *et al.*⁵² when a PNA probe immobilized on the nanostructured microelectrodes (NMEs) is used for the detection of *S. saprophyticus* and *E. coli*. One of the drawbacks of the PNA probes is their relatively high cost compared to DNA probes.

3. Amplification methods

3.1. PCR and its design

Polymerase Chain Reaction (PCR) is a molecular technique for DNA amplification. It plays a key role in genetic analysis, biology, and biochemistry research, since it is able to replicate a specific fragment of a target nucleic acid by cycling through three temperature steps and creating several million DNA copies within a few hours. Integrating microfluidics with PCR not only could provide the previously mentioned advantages in implementing microfluidic systems, but also could yield lower thermal capacities and a higher heat transfer rates, and could significantly reduce the reaction time.⁸³ Pan *et al.*⁸⁴ developed a multichamber PCR microfluidic chip coupled to multichannel separation and temperature control units for parallel genetic analysis. The device did not require any additional fluidic control unit and was easy and simple to operate. PCR products were separated and detected in these channels utilizing electrophoresis. The hepatitis B virus (HBV), *Mycobacterium tuberculosis* (MTB), and the genotyping of human leucocyte antigen (HLA) were detected using this platform.

Preventing sample evaporation is one of the main challenges to overcome with using PCR in microfluidic systems. This issue is particularly problematic in open reaction channels. To address this challenge, Wang *et al.*⁸⁵ used non-miscible mineral oil to cover the liquid and prevent its evaporation during the experiment. *Salmonella enterica*, *Escherichia coli*, and *Listeria monocytogenes* could then be simultaneously detected using an oscillatory-flow multiplex PCR. This design achieved an evaporation loss of less than 5% while decreasing the detection time to less than 24 min.

In some cases when entire bacteria were introduced to the detection PCR platforms, captured bacteria inside the microfluidic device could be lysed by thermal,⁸⁶ chemical,⁸⁷ physical^{88,89} and electrical means.⁹⁰ For instance, Cheong *et al.*⁹¹ developed a one-step real-time PCR method for pathogen detection. In this design, Au nanorods were used to transform near-infrared energy into thermal energy and subsequently lyse the pathogens. Next, DNA was extracted and amplified in the

PCR chamber. This one-step lysis improved the overall efficiency of the device because there was no need to change or remove reagents.

PCR was integrated with different sample preparation and separation devices to obtain higher sensitivity and specificity. For instance, sample cleanup was used along with PCR to detect human respiratory viral pathogens. Capillary electrophoresis was implemented for post amplification sample cleanup and the separation step in conjunction with PCR, and results were obtained in less than two hours.⁶⁷ Target enrichment, capture, lysis, and real-time qPCR were used for the detection of *E. coli* in water samples in eight different samples independently and simultaneously. Before capturing the target cell, two filtration steps were performed to remove particles, followed by sample enrichment. Antibodies coated on the PMMA surface were used to capture the target cells in the next step. After washing to remove nonspecific attachment, cells were removed using a cell stripper solution and thermally lysed. Next, the genetic contents were used in real-time qPCR amplification, and a LOD of 6 CFU was achieved in less than 5 h.⁴⁹

3.2. Isothermal

The isothermal amplification^{92,95} of DNA/RNA have recently drawn interest since it does not require large thermal momentum and energy for temperature cycles as compared to PCR systems. Therefore, it is a simpler and more energy efficient approach, making it an excellent choice for POC applications. Methods for isothermal amplification, include loop-mediated isothermal amplification (LAMP),⁹⁶ helicase-dependent amplification (HDA),⁹⁹ nucleic acid sequence-based amplification (NASBA),⁵³ recombinase polymerase amplification (RPA)^{58,100} and rolling circle amplification (RCA).⁵⁴

One of the most common isothermal amplification methods is LAMP. Although this technique is primarily used for DNA amplification, by reverse transcriptase it can also be implemented for RNA samples. The obtained signal can be visualized either by fluorescent intensity measurements or by the naked eye for turbidity due to precipitation, which makes it suitable for locations with limited resources. Generally, four primers are used to recognize six distinct sequences of the target DNA with a working temperature of around 60–65 °C (Fig. 1-iii). Fang *et al.*⁷¹ used LAMP amplification for the detection of pseudorabies viral DNA. The design consisted of eight parallel microchannels, enabling simultaneous reactions for high-throughput analysis. The entire device is sealed with uncured PDMS, which prevents evaporation and bubble formation. The result can be visualized by a compact real-time absorbance device or even by the naked eye. Using this method, 10 fg of DNA per μL were detected within 1 h, which is faster and more sensitive than PCR, and consumes smaller sample volumes. The higher sensitivity, simplicity, and low cost of this design make it suitable for use in POC diagnostics. In another approach, the LAMP method was used in a disposable self-heating cartridge.¹⁰¹ The temperature control was provided by the exothermic reaction, using a Flameless Ration Heater (FRH) activated by water. A DNA sample collected from *E. coli* in urine samples was detected via the LOD of the 10 *E. coli* DNA within 1 h. LAMP was also integrated with a low-cost CCD-based

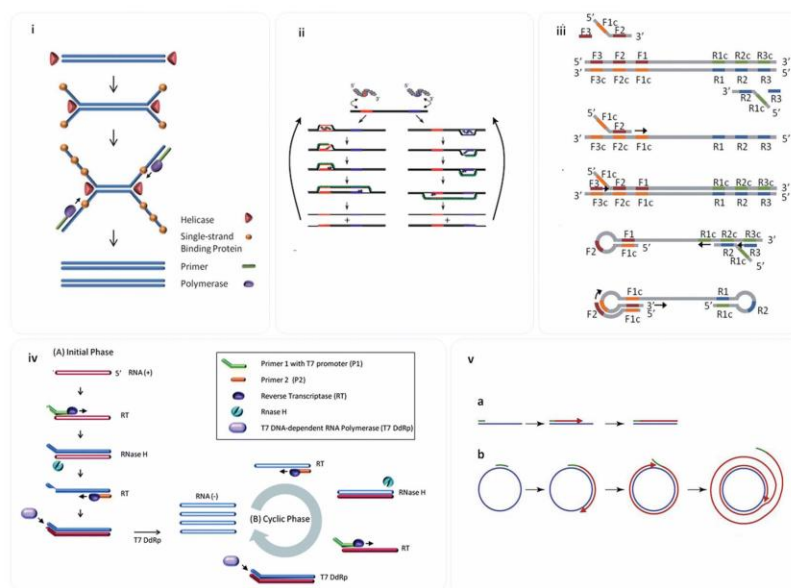


Fig. 1 Schematics of isothermal amplification methodologies: (i) HDA: dsDNA is unwound by the helicase enzyme then a single-strand binding protein stabilizes the strands. Finally a double-stranded copy is produced using primers and polymerase. (Reproduced from Ref. 92 with permission from Royal Society of Chemistry.) (ii) RPA: Primers bind to template DNA and a copy of the amplicon is produced by extension of the primers using a DNA polymerase. (Reproduced from Ref. 93 with permission from Public Library of Science.) (iii) LAMP: Template synthesis initiated by the primer sets resulting in stem-loop DNAs with several inverted repeats of the target sequence. In this schematic, only the process using forward primer set is shown. (Reproduced from Ref. 92 with permission from Royal Society of Chemistry.) (iv) NASBA: (A) The initial phase to synthesize complementary RNA to the target RNA and (B) in the cyclic phase, each newly synthesized RNA can be copied, leading to exponential amplification. (Reproduced from Ref. 92 with permission from Royal Society of Chemistry.) (v) RCA: (a) Linear template and single primer (b) circular template and single primer. Blue and green lines represent target DNA and oligonucleotide primers respectively. (Reproduced from Ref. 94 with permission from Elsevier.)

fluorescent imaging system.¹⁰² Various features of the imaging system, such as gain, offset, and exposure time, were optimized to achieve better sensitivity. The performance of this low-cost CCD imaging system was comparable to commercially available PCR systems. Six different waterborne pathogens were tested with this device, and it could detect single DNA copies in 2 μ L in less than 20 min. Using RNA as a target in the LAMP method requires a reverse transcription to convert the RNA into DNA. This method was implemented to detect HIV RNA⁶⁸ and the nervous necrosis virus (NNV) in grouper larvae.⁷⁰ For NNV detection, functionalized magnetic beads (MB) conjugated with a specific probe were used to capture the RNA from the grouper tissues. To generate a uniform temperature, an array-type micro-heater was utilized. As a result, more specific and faster extraction could be achieved. A LOD of 10 fg of DNA was found which was 100-fold more sensitive than RT-PCR.

For HDA method, the helicase enzyme opens the double-stranded DNA in order to let the primers hybridize, extend, and become two copies (Fig. 1-i). This mechanism operates in the same temperature range as LAMP, but it is simpler because it requires two enzymes and, similar to PCR, only two specific target oligos. However, compared to the LAMP method, it is

longer. The HDA method was successfully used to detect the ovarian cancer biomarker RSF-1,⁹⁹ severe acute respiratory syndrome (SARS) virus DNA,⁷² and *E. coli*.¹⁰³

HDA was also used in a fully integrated microfluidic system, which contained bacteria lysis, extraction, and HDA amplification of the DNA on a disposable cartridge. With this setup, 10 CFU of *E. coli* were detected in less than one hour.¹⁰³

In the transcription-based RNA amplification system or NASBA, initially developed by Compton *et al.*¹⁰⁴ (Fig. 1-iv), three enzymes are involved in the reaction, namely avian myeloblastosis virus reverse transcriptase, RNase H, and T7 RNA polymerase. Generally, NASBA produces more than 10⁹ copies in 90 min at a temperature around 40 °C and different types of nucleic acids, including tmRNA, rRNA, mRNA, ssDNA, and virus nucleic acid, can be analyzed. One of the drawbacks of this method is its inability to amplify the double strand of DNA since an initial temperature of 95 °C is required, adding more complications to the design. Dimov *et al.*⁵³ used a NASBA method for the detection of *E. coli*. The tmRNA (10 saRNA) was used as a target because of its high stability compared to mRNA, high copy number, and presence in most bacteria. This characteristic increased the sensitivity and

shortened the experimental time. Before the amplification step, silica beads were used for the purification and concentration of RNA from the sample. Applying real-time detection, a LOD of 100 cells in less than 30 min was achieved.

RPA was first introduced in 2006,⁹³ (Fig. 1-ii) for DNA amplification at low temperature (37 °C). RPA couples strand-displacement DNA synthesis with isothermal recombinase-driven primer targeting of the sample, resulting in an exponential amplification. The sensitivity of the RPA is similar to that of conventional PCR. For instance, the *mecA* gene from *Staphylococcus aureus* was detected with an LOD of 10 copies in less than 20 min.⁵⁸

RCA is another alternative method to RPA, which is also performed at a low temperature (37 °C). RCA (Fig. 1-v) is useful for circular DNAs, such as viruses, plasmids, and bacteriophage genomes. This method can be used to amplify circular probes, which are designed to circularize upon binding to a target and seal by ligation.¹⁰⁶ For instance, it has been shown that circular viral DNA could be amplified by RCA using bacteriophage phi29 DNA polymerase without the use of primers.⁹⁴ *V. cholerae* DNA was also detected with a LOD of 25 ng DNA in around 1 h using an electrophoretic microchip setup.¹⁰⁷ In another attempt, Sato *et al.*⁶⁰ developed a fully integrated microchip by using padlock probes and RCA in which solid phase capture in the microchannel was used to employ RCA on the bead for single molecule detection. Thirty amol genetic DNA from *Salmonella* was detected by this system.

4. Sample preparation

Placing an initial sample in contact with a biomarker without sample preparation will hinder sensitivity and specificity. Therefore, sample preparation steps are of high importance in achieving high sensitivity and specificity in any detection platform. The enrichment of the target analyte and/or the removal of inhibitors are two main strategies in this regard. This is especially important in the case of complex matrices, such as blood, saliva, interstitial fluid, and environmental samples composed of many different entities. Dielectrophoresis (DEP), micro/nano particles, and filters are three simple and straightforward approaches for sample preparation.

4.1. DEP

In the presence of electric fields, particles express dielectrophoretic activity. When subjected to a non-uniform electric field, polarised particles will move towards regions of high or low electric fields. A particle's polarisability in its surrounding medium induces dielectrophoretic motion towards (positive DEP) or away from (negative DEP) the electrode surface. The strength of this force depends on several factors, including the particle's electrical properties, shape and size, and the frequency of the electric field. Therefore, to manipulate a group of desired particles, a particular frequency should be applied. However, positive DEP cannot be used to enrich bacteria in physiological media, which has a high conductivity, since it only works in the media with low conductivity.

To overcome said limitation, Park *et al.*¹⁰⁵ used a combination of positive and negative DEP to continuously separate and concentrate bacteria from physiological samples, such as

cerebrospinal fluid and blood. This microfluidic platform was used to concentrate the bacteria up to 104-fold by taking millilitre volumes of the target samples. The separation efficiency in the buffer was 87.2% for *E. coli* in human cerebrospinal fluid and blood, as shown in Fig. 2.

In another effort,¹⁰⁸ a DC insulator DEP was developed in which arrays of cylindrical insulators were implemented inside a microchannel. By using negative DEP, *E. coli* and *Saccharomyces cerevisiae* were enriched and separated in less than 2 min. Applying different configurations of electrodes are effective in terms of the decay of the field and control over targets. For example, three-dimensional DEP was developed by positioning the electrodes on the top and bottom of a microchannel. In this research, different bacteria, such as *Staphylococcus aureus* and *Pseudomonas aeruginosa*, were continuously sorted and concentrated with a higher efficiency than that of 2D electrode configuration.¹⁰⁹

4.2. Particles and beads

Magnetic, metallic, polymeric, and liposome-based micro/nano particles have proven to be effective in obtaining higher sensitivity and selectivity for pathogen detection. Micro-beads, due to their high surface-to-volume ratios and low diffusion times, can increase the chance of biorecognition.¹²

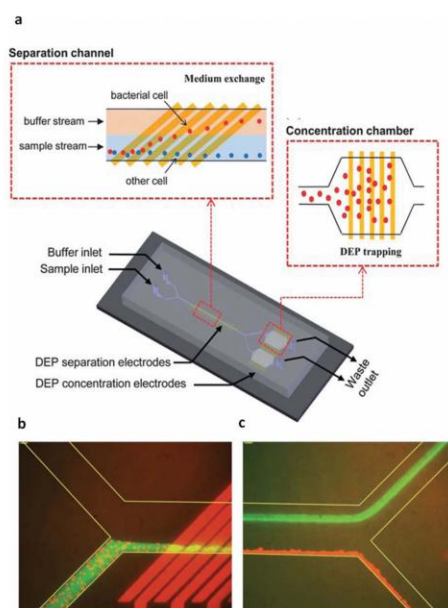


Fig. 2 (a) Schematic of DEP integrated in a microfluidic device for continuous cell separation and concentration. (b) Fluorescence microscopy image of separation channel inflow (c) fluorescent image of separation channel outflow. (Reproduced from Ref. 105 with permission from Royal Society of Chemistry.)

4.2.1 Micro/nano particles. Micro/nano particles have been extensively used for nucleic acid extraction and enrichment^{48,53,70,110} or for whole cell enrichment.^{24,25,44,48,59,111,112} Silica beads were employed to extract RNA from biological samples in a microfluidic system,^{53,110} reducing the chance of contamination and RNA degradation. Bhattacharyya *et al.*¹¹⁰ used a solid-phase extraction system, which was formed by trapping silica particles in a porous polymer monolith. RNA of the influenza A (H1N1) virus could attach to silica particles, be isolated from the infected mammalian cells and detached later for further manipulation. In another approach, silica beads were immobilized on a bed to purify and concentrate RNA from a mammalian cell sample infected with influenza. Immobilized beads increased the capture efficacy by passing the solution back and forth on the bed to increase the RNA capture efficiency by 10^2 - to 10^3 -fold as compared to that of non-immobilized beads.⁵³ For whole-cell detection, antibody-immobilised glass beads were applied inside a microchannel to capture *E. coli* with up to 96% efficiency.²⁵

4.2.2 Magnetic beads. Although microparticles provide a high surface-to-volume ratio and fast diffusion time, their manipulation is uniquely dependent on the applied flow conditions. To add another degree of freedom for particle manipulation, magnetic beads can be used and controlled by magnetic fields. This would increase the selectivity through enhanced discrimination between specific and non-specific targets.^{113,114}

A popular strategy for magnetic bead-based detection relies on enhancing the mixing and capturing of the probe-functionalized beads with the sample, followed by applying a magnetic field to capture the beads and surface rinsing. For instance, Wang *et al.*⁷⁰ used a specific probe conjugated to magnetic beads to capture the target RNA from the entire tissue lysate. After target hybridization, the beads are immobilized on the surface using a permanent magnet, and the lysate is washed out in the channel. This is followed by isothermal amplification of the captured RNA (Fig. 3-i). Applying this strategy, magnetic beads were also used to capture and enrich target cells from the sample. To obtain an even distribution of beads in the channels, after each split the beads were situated in a bifurcated channel. In this way, a bed of beads is formed by a magnetic field. The sample flowed through this bed, and after washing, off-chip PCR and CE were performed to enhance the capture efficiency of *E. coli* O157 in a background of *E. coli* K12.⁴⁴ Using the same approach, magnetic beads could be functionalized with enzyme-labeled antibodies for the electrochemical detection of pathogens, such as *E. coli*.²⁴ Since non-specific binding is at least an order of magnitude weaker than specific ligand-receptor binding,¹¹⁵ the Fluidic Force Discrimination (FFD) method could be used to control target attachment and nonspecific detachment under flow conditions in microfluidic channels, as well as target capture selectivity.¹² Mulvaney *et al.*¹² employed FFD by applying sufficient force using the speed of laminar flow to selectively remove the nonspecific binding materials and to distinguish between specific and non-specific binding. Magnetic beads were used for the detection of the target in complex matrices, such as whole blood. After capturing the analyte by magnetic beads on the surface, the controlled flow passed over the analyte to remove non-specific bindings due to the fact that non-specific

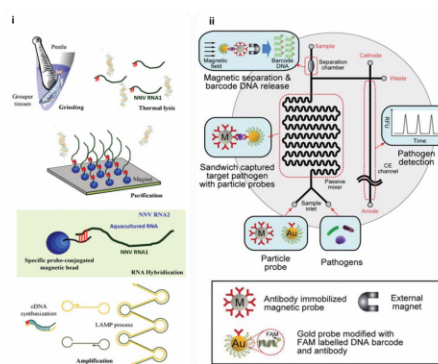


Fig. 3 (i) Schematic diagram of integrated microfluidic LAMP system for RNA purification and NNV detection. (Reproduced from Ref. 70 with permission from Elsevier.) (ii) Schematic illustrations of an integrated PMMS-CE microdevice for multiplex pathogen detection. The microdevice consists of a passive mixer, a magnetic separator and a capillary electrophoretic microchannel to identify target pathogens. (Reproduced from Ref. 59 with permission from Royal Society of Chemistry.)

bindings are at least an order of magnitude weaker than the specific ligand-receptor bindings.¹¹⁵ The number of the beads was counted either by optical microscopy or a magnetoelectronic sensor to obtain the density of the beads. As such, ricin A chain (RCA) and staphylococcal enterotoxin B (SEB) were detected with an LOD of around 300 fM.

Mujika *et al.*¹¹¹ developed a magnetoresistive immunosensor for the detection of *E. coli*. The device could detect small variations in the magnetic field caused by the conjugation of magnetic beads to previously immobilized antigens on the surface (antibody-antigen-antibody-magnetic bead). The results showed a very high specificity for *E. coli*, with the 105 CFU mL⁻¹ *E. coli* being compared to *Salmonella* spp. as a negative control.

Passive mixing and detection using magnetic beads is another strategy in which mixing and target capture occur in flow conditions. Microfluidic design and flow control are important factors in this approach. Antibody-conjugated magnetic beads as capture probes and gold nanoparticles conjugated to the same antibody and fluorescently labelled DNA barcodes as complementary probes were used to detect bacteria that were sandwiched between the functionalized magnetic particles and gold nanoparticles.⁵⁹ Passive mixing was obtained through the design of the micromixer, which was used to attain the maximum cell capture efficiency. This design included an intestine-shaped serpentine channel around 18 cm in length, which could hold around 4 μ L (Fig. 3-ii). Increasing the retention time in this setup caused higher mixing, and as a result, a high cell capture efficiency up to 75% capture was achieved with 20 min retention time. This was followed by separation of the MB-*E. coli*-GNP complex through applying a magnetic field and then purification of the non-conjugated particles by rinsing. DNA barcodes were then detached from the GNPs by heating (up to 90 °C) and were

detected using fluorescence microscopy. A high number of the obtained DNA barcodes per GNP resulted in the single-cell detection of three different pathogens (*Staphylococcus aureus*, *E. coli* O157 : H7, and *Salmonella typhimurium*) in less than 30 min.

4.3. Filter

Filters are a cost-effective and straightforward alternative for the rapid preparation and enrichment of samples. Physical filtration systems can be made of aluminum oxide,¹¹⁸ polyimide,¹¹⁹ chitosan,¹²⁰ poly carbonate,¹²¹ SU-8¹²² and silica.¹²³ Using multistep polycarbonate-based membranes (10 μ m and 0.1 μ m), *E. coli* cells could be enriched up to 2×10^2 -fold in a microfluidic system.⁴⁹ Nano-sized membranes can also be used to separate small biological elements, such as antibodies and viruses. For example, Reichmuth *et al.*²³ used nanoporous polyacrylamide membranes (10 nm) to detect the influenza virus. The size-exclusion characteristics of the *in situ* polymerized membrane led to the simultaneous concentration of viral particles and the separation of virus-fluorescent antibody complexes, while unbound antibodies passed through the membrane. Compared to electrophoretic immunoassay solely, applying the membrane resulted in a faster detection time and higher sensitivity.²³

Filters can be chemically functionalized to be even more specific to selectively capture the target. For instance, Liu *et al.*⁶⁸ used Flinders Technology Associates (Whatman FTA) membranes as a filter for the isolation, concentration, and purification of nucleic acids. This filter specifically captures nucleic acids and also enhances the removal of inhibitors, which drastically increases the sensitivity of the detection platform.

3D microstructures in microfluidic platforms can be applied to physically filter biological elements. In this regard, microfabrication is required to produce structures such as micro-pillars. The patterned micropillars can later be chemically functionalized using microfluidics. Hwang *et al.*⁵¹ implemented microfabricated micropillars with an affinity for bacterial cells inside a PCR chip to detect *E. coli* in blood samples. Bacteria were first captured on the micropillars, and the rest of the sample, containing PCR inhibitors, was washed away.

5. Design strategies for pathogen detection

Many efforts have been made towards the development of novel designs based on microfluidic principles for rapid, automated, and high-throughput analysis of pathogen detection in order to obtain robust and detailed information from complex samples containing different pathogens.

5.1. Strategies to develop high-throughput multiplex devices

Rapid, multiplex and high-throughput detection of multiple pathogens requires the implementation of parallel microchannels, embedding micro-pumps, micro-valves, and/or discretizing the flow into controllable droplets. These features could be only obtained through appropriate design of automated microfluidic LOC platforms that can assure the operation of the device, especially for non-technical operators.^{27,48,116,124,125}

An automated shutter flow device embedded with micro-valves and a micro-pump was implemented for the high-throughput hybridization of dengue virus DNA (Fig. 4-ii).¹¹⁶ This device was composed of 48 hybridization units, which could run assays in high-throughput mode. An LOD of 100 pM was achieved in only 90 s using 1 μ l of sample.

Combining an embedded micro-pump with droplet-based microfluidics could enhance automation and high-throughput analysis. For instance, Zeng *et al.*⁴⁸ developed a droplet-based microfluidic system for single-cell genetic analysis (Fig. 4-i). In this setup, multiplex PCR amplification integrated with a microfluidic emulsion generator (up to 3.4×10^6 droplets per hour) was performed for large-scale quantitative genotypic studies of biological samples. The design included glass-PDMS-glass hybrid substrates that were integrated with a three-valve diaphragm micropump, which helped transport and encapsulate cells inside the droplets. The entire process, including PCR amplification, lasted around 4 h, and led to single-cell-level sensitivity.

Designing parallel detection chambers is a simple approach to performing high-throughput sample analysis (Fig. 4-iii). Zhang *et al.*¹¹⁷ developed a chip composed of two layers: a patterned, fluidic layer at the top and a pneumatic control layer at the bottom. This chip consisted of seven immune-reaction columns with micromechanical valves, and concentrations of target toxins were read out by measuring the color intensity of the micro-columns. Detection of the toxins, such as microcystin, were achieved in less than 25 min with an LOD of 0.02 ng mL⁻¹.

Microfluidic quantum dot (QD)-based barcodes for multiplex high-throughput detection of the hepatitis B virus, hepatitis C virus, and HIV were developed. Three QDs with different emission wavelengths were selected and conjugated to a specific antibody for each target. Using an electrokinetically driven, microfluidic system, real-time readout of the barcodes with a picomolar LOD was achieved in less than one hour.²⁷ Despite efforts to develop multiplex high-throughput devices, they still cannot be used in POC or on field detection systems.

5.2. Strategies to develop POC devices

Recently, efforts have been made to develop detection platforms suitable for POC diagnostics. Low cost, portability, ease of use, fast detection time, and minimal side accessories are the main characteristics of microchips for POC diagnostics. Several factors should be considered in developing microchips with the aforementioned specifications. Transducers and pumping systems normally occupy larger spaces, consume more power, and are costly. Indeed, most research in this field is being directed towards eliminating or minimizing the need for external accessories and power.

For instance, a low-power and low-cost pump system so-called Electro-Hydraulic Pump (EHP) was developed by Lui *et al.*¹²⁶ This system consists of two separate sections: an electrolyte chamber and a reagent chamber. On top of these two chambers, there is a hydraulic fluid separated by a flexible membrane. First, gold electrodes are used for electrolysis. As a result, bubbles are formed and expand the flexible membrane. This pressure forces the fluid to move out of the reagent chamber. Since this system is mainly made of PDMS and polystyrene, it is suitable for mass

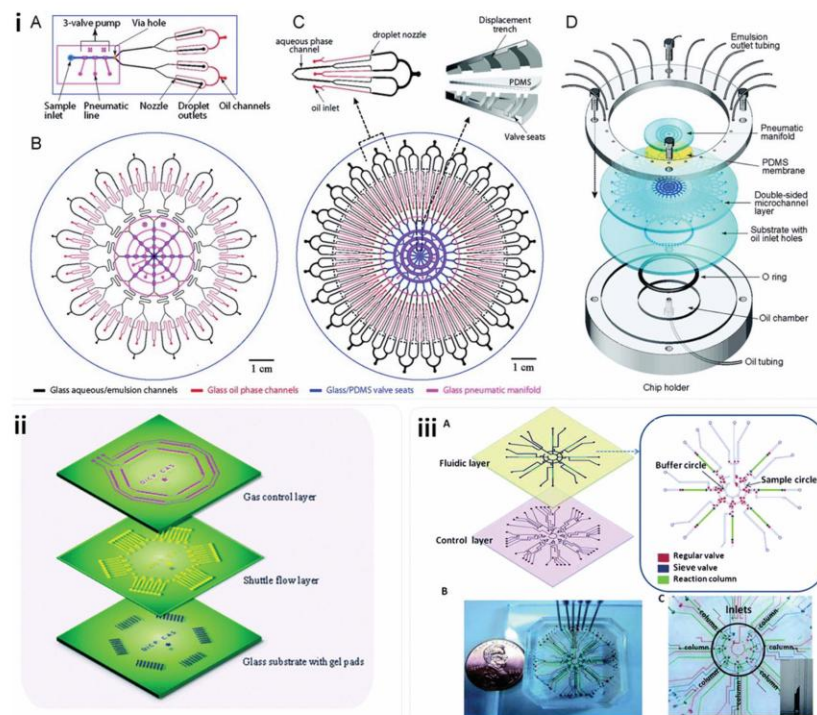


Fig. 4 (i) Schematic of microfluidic emulsion generator (MEGA) array device. (A) Design of a glass-PDMS-glass hybrid four-channel MEGA device and (B) layout of a 32-channel MEGA device. (C) Layout of a 96-channel MEGA device. (D) Illustration of complete four layer 96-channel MEGA device and the plexiglass assembly module. (Reproduced from Ref. 48 with permission from American Chemical Society.) (ii) Exploded view of the microfluidic chip containing shuttle flow channels, micropumps and microvalves. (Reproduced from Ref. 116 with permission from Royal Society of Chemistry.) (iii) (A) Schematic representation of an immunoreaction chip used for detection of algal toxins. Red and blue color represent the regular valves and sieve valves respectively. (B) and (C) Pictures of the microfluidic chip and central area of the chip. (Reproduced from Ref. 117 with permission from Royal Society of Chemistry.)

production. A broad range of flow rates generated by EHP (from 1.25 to 30 $\mu\text{L min}^{-1}$), and its simple fabrication method makes it a suitable option for many lab-on-a-chip applications (Fig. 5).¹²⁶

Since handling liquids in microfluidic devices, without pumps or valves, would be a tremendous step towards developing portable POC devices, Weng *et al.*⁶¹ developed a microfluidic chip that does not require syringe pumps, valves, and tubing for liquid handling. The device operates by gravity-based pressure-driven flow, and electrokinetically controlled oil-droplet sequence valves (ECODSVs) were implemented inside this microfluidic chip. Electroosmotic flow was used to control the ECODSVs and hence the sequential fluidic operation of the chip. Using this setup, an RNA-DNA hybridization assay was carried out in less than 25 min.

5.2.1 Droplet-based and digital microfluidics. Another approach that eliminates the need for pumping and valve systems can be achieved by droplet-based microfluidics. The overall configuration and process is straightforward, which

makes the setup practical for POC applications. Droplet-based microfluidics^{128,129} is based on the generation and manipulation of individual droplets. Therefore, each droplet can potentially be a bioreactor, which is an important advantage compared to continuous flow microfluidic devices. Droplets are typically generated by the flow of at least two liquids, and controlled either by volume or pressure. Unlike continuous flow microfluidics, scaling up does not increase device size or complexity, making it a good candidate for high-throughput screening and analysis. Different biological assays, such as PCR¹³⁰ and DNA hybridization,^{81,131} were carried out with droplet-based microfluidics. For instance, a droplet-based platform was used for the high-throughput detection of *E. coli*.⁸¹ PNA probes were designed to specifically target 16 S rRNA from *E. coli*. To do so, the cell sample and detection probes were mixed, and after droplet production, cell lyses and hybridization was carried out in each droplet. Finally, using confocal fluorescence spectroscopy, a detection signal was obtained.

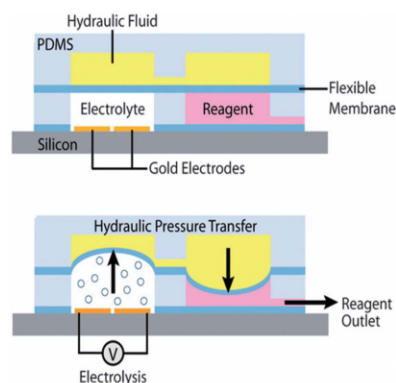


Fig. 5 Activation mechanism of the electro-hydraulic pump. Bubbles are formed by electrolysis of the pumping fluid applying electrical current. The produced pressure is transferred through a flexible membrane to a hydraulic fluid chamber, which then pushes fluid out of the reagent chamber. (Reproduced from Ref. 126 with permission from Royal Society of Chemistry.)

In a new design for transporting reagents between droplets, micro-elevation was implemented to form slits that facilitate the splitting of the super paramagnetic particles from droplets (Fig. 6-i). Material transfer between each droplet was carried out by silica superparamagnetic particles, which acted as carriers. The embedded slits were either V-shaped or pairs of micropillars. Genetic analysis, steps of cell lysis, DNA binding, washing, elution, amplification, and detection are performed within each individual droplet. This platform was also equipped with a thermal cycler for PCR amplification. Using this chip, PCR and HDA (Helicase dependent amplification) were performed for the detection of ovarian cancer biomarker Rsf-1 and *E. coli*. Although this material transfer method is a simple solution to reduce complexity, it is still dependent on magnetic forces, which makes its applications in POC diagnostics challenging.⁹⁹

In droplet-based microfluidics, droplets are moved in series in one direction, restricted to microchannel geometries. Unlike the droplet-based microfluidic setup, digital microfluidic analysis (DMF) is able to address each droplet discreetly in an array of electrodes which can then be moved based on the electrowetting on dielectric (EWOD) principle on a 2D plane. This ability makes the DMF an excellent choice for multiplex high-throughput assays. So far, DMF has been used for many applications, including cell culturing,¹³² DNA hybridization,^{74,133} PCR,¹³⁴ and immunoassays.¹³⁵ Different transducers have also been integrated with DMF, such as SPR imaging,¹³⁶ field effect transistors (FET),¹³⁷ matrix-assisted laser desorption/ionization mass spectrometry (MALDI-MS),^{138,139} and UV/Vis spectroscopy.¹⁴⁰ For instance, a DMF platform made of 500 electrodes in the bottom substrate and a disposable plastic top substrate with 100 detection spots was developed. In this setup, many detection tests could be carried out by replacing the top plastic substrate with a 5 DC USB connection (Fig. 6-ii). Overall, having the capability of high-throughput analysis with an

exchangeable disposable plastic detection layer and running on a very low power supply, makes DMF a platform suitable for locations with few resources.¹²⁷ A portable DMF cartridge was designed, which benefited from magnetic bead-based immunoassay and PCR, which was primarily targeted for POC applications because of its low cost of fabrication and versatility.¹⁴¹

5.2.2 Lab on a disk devices. Centrifugal pumping, also called “lab-on-a-CD” is another approach to eliminate the need for tubing and external pumping systems because it only requires a simple electric motor for fluid handling.^{58,142} Compared to conventional (vacuum suction) systems, this method provides less signal variations between replicate samples. Wang *et al.*⁵⁷ developed a sophisticated microfluidic microarray in which centrifugal pumping was the driving force (Fig. 7). This device was composed of radial and spiral microchannels for parallel DNA detection at the level of single-base-pair discrimination. The hybridization occurred in the intersection of the radial probe line and spiral channels, which deliver the target. Sensitivity was further enhanced by controlling the flow rate and channel depth. By lowering the flow rate, the residence time will increase, resulting in better hybridization. At the same time, mass transport was enhanced by decreasing the channel depth, resulting in a better signal to noise ratio because the shallower channel has better mass transport as compared to the deeper channel. Using this device, over 100 samples were analyzed in parallel in 3 min.

A variety of phenomena in nature operate based on capillary forces. Mimicking this concept and implementing it into microfluidic devices is an ideal alternative for accessory-free liquid handling. For instance, a capillary-based microfluidic platform was implemented to simultaneously detect four different waterborne pathogens using real-time PCR.¹⁴³

5.2.3 Paper-based devices. Compared to other capillary-based microfluidic devices developed for pathogen detection, paper-based microchips^{144,145} provide an innovative approach to produce disposable, biodegradable, cost-effective, portable and simple chips. These devices are generally made from abundant materials such as cellulose fiber, have low volume and are easy to fabricate.¹⁴⁶

Various detection strategies have been implemented in paper-based microfluidic devices to recognize pathogen presence, most of which are based on the colorimetric method.^{147,148} Lateral flow immunochromatographic is one such common test method where the result can be observed by the naked eye. Abe *et al.*¹⁴⁹ used immunochromatography to detect IgG antibodies and a LOD of $10 \mu\text{g L}^{-1}$ was achieved within 20 min. It is noteworthy that conventional single-layer paper-based platforms are not comparable with conventional LOC devices in terms of sensitivity, accuracy, and multiplex analysis capabilities. As a result, there have been many efforts to design multiplex paper-based devices with higher sensitivities. Specifically, paper-based three-dimensional microfluidic devices have emerged to enable more complicated analysis. In addition to movement along each layer, reagents can also move up and down between the top and bottom layers. Martinez *et al.*¹⁵⁰ developed such a microfluidic platform (Fig. 8-i) by stacking layers of patterned paper in which each layer can have a different pattern of biomarkers and

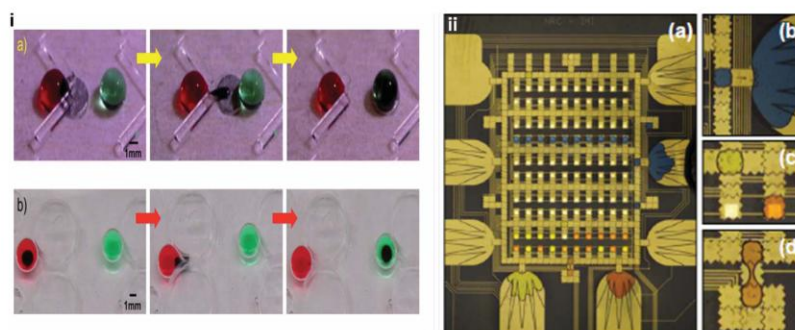


Fig. 6 (i) Droplet based microfluidic chip implementing magnetic actuation. Demonstration of droplet manipulation in (c) air and (d) oil mediums. (Reproduced from Ref. 99 with permission from Royal Society of Chemistry.) (ii) (a) Top view of an EWOD-based digital microfluidic device, (b) a reservoir, (c) analysis spots, and (d) region for mixing, storing and splitting droplets. (Reproduced from Ref. 127 with permission from IEEE.)

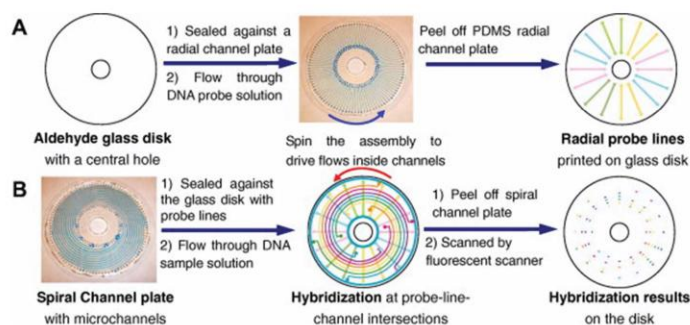


Fig. 7 Schematic diagram of the microfluidic microarray. Procedure for (A) probe printing and (B) hybridization. (Reproduced from Ref. 57 with permission from Elsevier.)

reagents. Despite the sophisticated technology involved in the fabrication of this device, its final cost is very low, making it a promising candidate for POC diagnostics in resource-limited settings.

Enzyme-Linked Immunosorbent Assays (ELISA)¹⁵¹ and Electrochemiluminescence (ECL) have also been performed using 3D paper-based microfluidics.¹⁵² Liu *et al.*¹⁵¹ reported a 3D paper-based device using ELISA in which all necessary reagents were stored within the device in dry state. Using this setup, only 2 μ L of sample was required to perform the analysis (Fig. 8-ii). The colorimetric results can be captured by cell phone or scanner and sent to an off-site location for further analysis. Using this setup, the IgG antibody was detected in 43 min with an LOD of 330 pM.¹⁵¹

ECL immunoassay was also integrated on a 3D paper-based microfluidic device.¹⁵² In this setup, eight working carbon electrodes were screen-printed on the first paper substrate and on the second paper substrate all patterns included both the same Ag/AgCl reference and carbon counter electrodes. In addition to the advantages provided by 3D design, the device could also benefit from the higher sensitivity and specificity provided by the ECL method.¹⁵²

Although the emergence of such devices is an important step towards producing real diagnostic devices for POC applications, there is still a need to reduce fabrication complexity while benefiting from the advantages of 3D design. The origami concept can be used in this regard to simplify fabrication complexity. Origami is a traditional Japanese paper folding technique, which is used to construct 3D geometries from a single paper sheet. Liu *et al.*¹⁵³ fabricated an entire paper-based device from a single sheet using one-step photolithography based on origami demonstrating that complex patterns can be produced without additional fabrication overhead. Another advantage of this system is that it is performed using an automated printing technique and assembled without tools (Fig. 8-iii).¹⁵³

5.2.4 Integration towards sample-to-result POC devices. A multitude of design and detection methods were introduced in the previous sections, each providing specific advantages regarding pathogen detection. The proper integration of these techniques into a single chip would address most of the drawbacks seen when each one is used individually. This would bring the end goal of developing POC devices into reality by

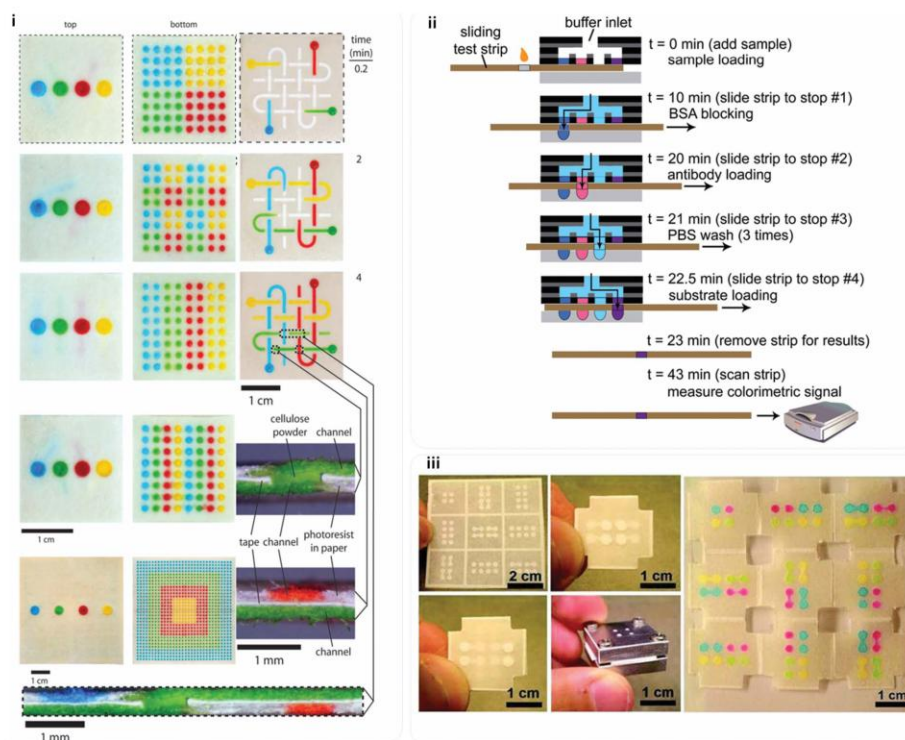


Fig. 8 Three-dimensional paper-based microfluidic platform. (i) Demonstration of the fabrication, design and patterning of a three-dimensional paper-based microfluidic platform. (Reproduced from Ref. 150 with permission from Proceedings of the National Academy of Sciences.) (ii) Schematic of operating procedures of ELISA in a three-dimensional paper-based microfluidic device. (Reproduced from Ref. 151 with permission from IEEE.) (iii) A three-dimensional paper-based microfluidic device using origami principle. (Reproduced from Ref. 153 with permission from American Chemical Society.)

performing sample-to-result diagnostic tests with low LODs in a reasonable time.

A fully integrated, disposable, and portable device was developed to detect the H1N1 virus from a throat swab sample, based on microfluidics⁶⁵ where the immunomagnetic target capture, pre-concentration and purification, PCR amplification, and sequence specific electrochemical detection steps were performed on a single monolithic chip (Fig. 9-i). A DNA probe complementary to the H1N1 virus was immobilized on a gold electrode. The amplified ssDNA was introduced for 30 min and target hybridization induced a conformational change in the probe that led to a decrease in the electrical current. The LOD of this device for the H1N1 influenza virus was 10 TCID₅₀, four orders of magnitude below those of clinically relevant viral titers with total analysis time of 3.5 h. This device could have a great potential in POC applications because of its high sensitivity in testing real samples. Further improvement, such as finding alternatives for the syringe pumps and heaters would make these devices an excellent option for POC applications.

Another fully integrated device was developed by Lam *et al.*⁵² (Fig. 9-ii). This platform enabled the detection of pathogenic bacteria in urine samples in less than 30 min. Generally, cells were first lysed in a chamber by applying an electrical field resulting in the release of their genetic content. Then, nanostructured microelectrodes were implemented for the electrochemical detection of the genetic content. *E. coli* and *S. saprophyticus* were successfully tested in urine samples with 100 CFU μL^{-1} (clinical relevant concentration) using this platform. The device does not require sample preparation or amplification steps while providing the necessary sensitivity in a faster time and more straightforward approach.

Lutz *et al.*⁵⁸ developed a self-sufficient lab on a foil system, based on a centrifugal lab on a CD principle for automatic nucleic acid amplification, capable of performing 30 reactions simultaneously. The structure was micromilled on a cyclic olefin copolymer, and foil formation was achieved by hot embossing. The reagents for signal amplification were stored inside a glass capsule, which increased the shelf life of the device. The liquid

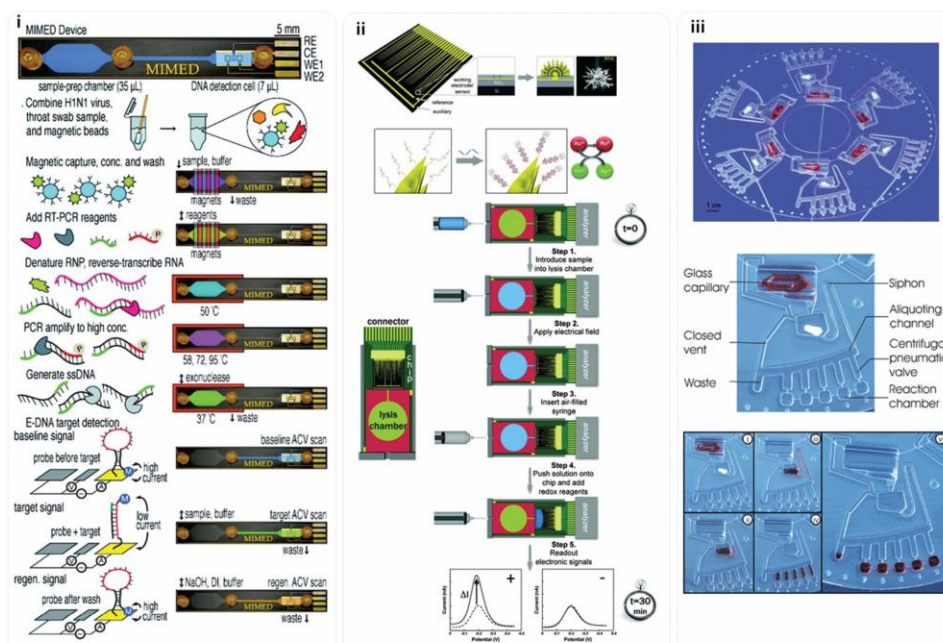


Fig. 9 (i) Schematic illustration of the microfluidic chip for sample-to-answer genetic analysis of H1N1 virus. (Reproduced from Ref. 65 with permission from American Chemical Society.) (ii) Schematic diagram of the chip consisting of a lysis chamber and nanostructured microelectrodes integrated to the sensing system for detection of bacterial pathogens. (Reproduced from Ref. 52 with permission from American Chemical Society.) (iii) Picture of a foil based lab on a disc with liquid reagent containers and its operating procedure. (Reproduced from Ref. 58 with permission from Royal Society of Chemistry.)

was then released by crushing the glass capsule container, and centrifugal forces was applied to control the fluid flow between chambers. Isothermal amplification at a low temperature (37 °C) was performed to minimize energy consumption (Fig. 9-iii). The total detection time was less than 20 min.

A microfluidic device based on a nucleic acid was developed to detect different pathogens. This device was mainly made of low cost and disposable materials (polycarbonate). The operation was automatically controlled by an analyzer that provided pouch and valve actuation *via* electrical motors. The presence of bacterial *B. Cereus*, viral armored RNA HIV, and the HIV I virus in saliva samples was tested.¹⁵⁴

Lafleur *et al.*¹⁵⁵ developed a disposable multiplexed sample-to-result microfluidic device based on immunoassay (Fig. 10-ii). This device was able to detect disease-specific antigens or IGM antibodies from blood. For instance, the detection of the malaria antigen and IgM to *Salmonella* Typhi LPS was carried out. This microfluidic chip was based on flow through the membrane immunoassay on porous nitrocellulose. After introducing the blood to the system, blood cells were removed by passing the sample onto the plasma extraction membrane. The separated plasma was divided into two samples, one for antigen detection and another for IgM detection. For IgM detection, the IgG antibodies present inside the sample were removed using protein-

G beads. After capturing the target, signal enhancement was achieved using gold nanoparticles conjugated with detection antibodies. An LOD of 10–20 ng mL⁻¹ was achieved in 30 min, which is comparable to benchtop ELISA tests. Bubble formation caused by the pneumatic fluid handling system in this device is one of the challenges that will need to be addressed. In addition, finding an alternative to the fluidic handling system (preferably accessory free) would help to reduce the size, cost, and complexity of device operation.

An interesting example of accessory-free POC devices was developed by Liu *et al.*¹⁰¹ In this disposable self-heating cartridge-based device, after performing isothermal amplification, the outcome could be visualized by the naked eye using a low-cost LED signal (Fig. 10-i). Heat was provided by an exothermic reaction of the Mg–Fe alloy and water, and the flow rate was controlled by utilizing a porous filter paper inside the device. Temperature control was achieved using paraffin as a phase change material. If necessary, paraffin could absorb the extra heat during melting. Using this device, as few as 10 *E. coli* DNA copies were detected.¹⁰¹

Recently, another promising POC microchip for the simultaneous detection of HIV and syphilis was developed, which was also tested in field studies in three developing countries (Fig. 10-iii). This cost-effective handheld microchip uses only 1 µL of

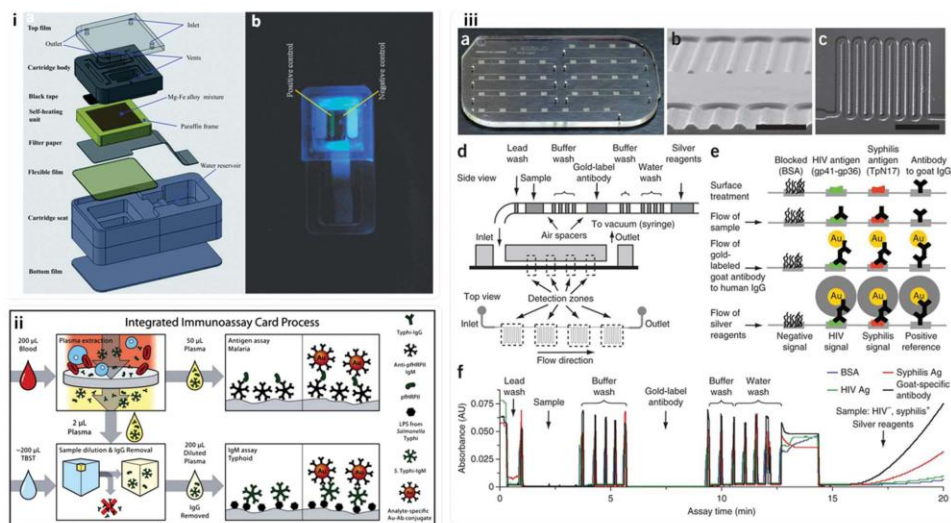


Fig. 10 (i) Schematic presentation and images of self-heating cartridge based device for isothermal amplification (a) exploded view, (b) green fluorescence emission from a test amplification chamber. (Reproduced from Ref. 101 with permission from Royal Society of Chemistry.) (ii) Schematic diagram of the DxBox integrated immunoassay cards for detection of the malaria antigen and *S. Typhi*-IgM from blood sample. (Reproduced from Ref. 155 with permission from Royal Society of Chemistry.) (iii) Schematic diagram and pictures of a POC microfluidic device based on an ELISA-like assay. (a) Picture of the microfluidic chip. (b) Scanning electron microscope image of a cross-section of the microchannels. (c) Transmitted light micrograph of channels. (d) Illustration of the passive delivery mechanism for multiple reagents. (e) Diagram of biochemical reactions in detection zones at different steps of immunoassay. (f) Absorbance traces of a complete HIV-syphilis duplex test as reagent plugs pass through detection zones. (Reproduced from Ref. 156 with permission from Nature publishing group.)

unprocessed blood sample, without a need for any moving parts, electricity, or external instrumentation. Implementing injection molding technology was the key to mass producing the device, resulting in a very low final cost. The passive reagent delivery method was utilized to manipulate the reagents and samples in which blocks of reagents were introduced sequentially into a tube and separated by air spacers. For capturing HIV and treponema-specific antibodies from blood, the envelope antigen and the outer membrane antigen (Tpn17) were immobilized on the chip surface, respectively. In the next step, a gold-labeled antibody to human IgG was introduced, and signal amplification was achieved through the reduction of silver ions onto gold nanoparticles. The optical density of the silver film could be measured through low-cost and robust optics, such as light-emitting diodes and photodetectors. This device could provide sensitivity and specificity comparable to bench-top ELISA and other conventional detection methods within 20 min on the site.¹⁵⁶ The very promising field study results obtained using the device open new avenues in the implementation of microfluidic-based devices for POC applications all over the world, especially in developing countries with poor healthcare resources.

6. Outlook and future trends

During the past decade, engineering tools have been implemented to study different aspects of pathogen detection

platforms, including design, micro/nanofabrication, sample preparation and amplification, miniaturization, automation, multiplexing, and high-throughput analysis. Despite recent technological advances, the development of a cost effective, accessory-free single device capable of simultaneously achieving high-throughput and multiplex analysis with high specificity and sensitivity remains elusive. Biomarkers with higher specificity along with miniaturized, cost-effective designs with minimum side accessories and high sensitivity are required to achieve this goal.

Biomarker selection is a critical factor in obtaining the required specificity. Antibodies are the most common biomarkers, although they cannot deliver the desired specificity, nor are they available to diagnose all pathogens. However, in terms of the detection of epidemic and life-threatening diseases, such as HIV and tuberculosis, especially in developing countries, they can play a critical role in controlling the rate of disease propagation. Among new alternatives to antibodies, aptamers are promising candidates. However, the time and cost required to discover and design aptamers should be reduced. For cases requiring very high specificity, molecular-based diagnostics can be implemented. This could be achieved by designing DNA probes for target hybridization, followed by specific primers for the amplification of the target gene. In the applications where high stability is required, PNA probes could provide better stability and hybridization than DNA probes.

Molecular amplification of the target genes is an essential component of bench-top diagnostic techniques in order to attain higher sensitivity. Among these techniques, PCR has been widely used through its integration into microfluidic chips. However, the requirement for precise temperature control for thermocycling at the micro scale makes the chip design more complicated as compared to macro-scale experiments. To address this issue, isothermal amplification techniques have emerged as an alternative to PCR in microfluidic chips. Among isothermal methods, low-temperature isothermal amplification could be useful because it operates at 37 °C. However, the LAMP technique which requires a higher performance temperature (60 °C), is currently at the center of attention for POC applications as test results can be visualized with the naked eye.

Sample preparation is key to achieving high sensitivity and specificity. Among the diverse techniques for sample preparation, the use of magnetic beads is one of the most promising approaches, as it is not only sensitive and cost-effective, but also provides better control over captured reagents' motions inside the chip.

In designing microchips, the desired biosensor chip should be able to deliver the same LOD as bench-top methods (around 10–1000 CFU mL⁻¹). Automation, the potential for mass production, and portability are also important specifications to be considered in the design of microchips for POC applications. The LOD and assay time for detection of different pathogens summarized in Table 1.

In terms of automation and high-throughput analysis, digital microfluidics has proven to be one of the most interesting technologies since thousands of individual droplets can be discretely manipulated and analyzed. Though there is still a need for modification to produce a portable and accessory-free system, selecting proper materials in the fabrication of LOC devices can play an important role in producing cost effective devices. Paper-based microfluidic devices are very promising platforms to provide a disposable, portable, biodegradable, and easy-to-fabricate detection microchip. Despite the efforts made in developing paper-based devices, such as the production of 3D paper-based platforms and the integration of different detection methods, these devices do not provide the desired sensitivity. In this regard, the proper functionalization and immobilization of biomolecules on paper-based substrates will enhance device sensitivity.

This review pointed out the design and modification of various components for the development of a universal sample-to-result LOC device which should be performed with view to producing a totally integrated self-contained, accessory-free microchip that also provide the required sensitivity and specificity. The future will belong to simple LOC microfluidic devices that possess the desired sensitivity and specificity while providing complex diagnostics in remote areas, without a need for centralized laboratories.

Acknowledgements

The authors acknowledge the financial support from Genome Quebec and NanoQuebec. A.M. Foudh would like to thank the NSERC-CREATE integrated sensor systems program for its financial support. T.F. Didar would like to thank the faculty of

medicine at McGill and Fonds de Recherche du Québec - Nature et Technologies (FQRNT) for their financial support. The authors would also like to thank Dr J. Daoud and K. Bowey for their comments on the manuscript.

References

- World Health Organization, The World Health Report 2004, World Health Organization, Genève, 2004.
- D. M. Morens, G. K. Folkers and A. S. Fauci, *Nature*, 2004, **430**, 242–249.
- C. A. Batt, *Science*, 2007, **316**, 1579.
- CDC Estimates of Foodborne Illness in the United States, <http://www.cdc.gov/foodborneburden/2011-foodborne-estimates.html>, accessed February 01, 2012.
- P. Yager, T. Edwards, E. Fu, K. Helton, K. Nelson, M. R. Tam and B. H. Weigl, *Nature*, 2006, **442**, 412.
- B. Weigl, G. Domingo, P. LaBarre and J. Gerlach, *Lab Chip*, 2008, **8**, 1999–2014.
- E. A. Talbot, D. C. H. Burgess, N. M. Hone, M. F. Iademarco, M. J. Mwasekaga, H. J. Moffat, T. L. Moeti, R. A. Mwansa, P. Letsatsi and N. T. Gokhale, *Clin. Infect. Dis.*, 2004, **39**, e1.
- K. Engler, A. Efstratiou, D. Norn, R. Kozlov, I. Selga, T. Glushkevich, M. Tam, V. Melnikov, I. Mazurova and V. Kim, *J. Clin. Microbiol.*, 2002, **40**, 80–83.
- R. C. Wong and Y. T. Harley, *Lateral Flow Immunoassay*, Humana Pr Inc, 2008.
- P. D. Skottrup, M. Nicolaisen and A. F. Justesen, *Biosens. Bioelectron.*, 2008, **24**, 339–348.
- P. Holliger and P. J. Hudson, *Nat. Biotechnol.*, 2005, **23**, 1126–1136.
- S. Mulvaney, C. Cole, M. Kniller, M. Malito, C. Tamanaha, J. Rife, M. Stanton and L. Whitman, *Biosens. Bioelectron.*, 2007, **23**, 191–200.
- C. D. James, J. McClain, K. R. Pohl, N. Reuel, K. E. Achyuthan, C. J. Bourdon, K. Rahimian, P. C. Galambos, G. Ludwig and M. S. Derzon, *J. Micromech. Microeng.*, 2010, **20**.
- N. Bunyakul, K. A. Edwards, C. Promptmas and A. J. Baumner, *Anal. Bioanal. Chem.*, 2009, **393**, 177–186.
- J. B. Delehanty and F. S. Ligler, *Anal. Chem.*, 2002, **74**, 5681–5687.
- T. M. Blicharz, W. L. Siqueira, E. J. Helmerhorst, F. G. Oppenheim, P. J. Wexler, F. F. Little and D. R. Walt, *Anal. Chem.*, 2009, **81**, 2106–2114.
- A. D. Taylor, J. Ladd, J. Homola, S. Jiang, ed. M. Zourob, S. Elwary and A. Turner, Springer, New York, 2008, pp. 83–108.
- J. H. Jung, D. S. Cheon, F. Liu, K. B. Lee and T. S. Seo, *Angew. Chem., Int. Ed.*, 2010, **49**, 5708–5711.
- R. Gómez, R. Bashir and A. K. Bhunia, *Sens. Actuators, B*, 2002, **86**, 198–208.
- E. Yacoub-George, W. Hell, L. Meixner, F. Wenninger, K. Bock, P. Lindner, H. Wolf, T. Kloth and K. A. Feller, *Biosens. Bioelectron.*, 2007, **22**, 1368–1375.
- C. García-Aljaro, M. A. Bangar, E. Baldrich, F. J. Muñoz and A. Mulchandani, *Biosens. Bioelectron.*, 2010, **25**, 2309–2312.
- D. A. Boehm, P. A. Gottlieb and S. Z. Hua, *Sens. Actuators, B*, 2007, **126**, 508–514.
- D. S. Reichmuth, S. K. Wang, L. M. Barrett, D. J. Throckmorton, W. Einfeld and A. K. Singh, *Lab Chip*, 2008, **8**, 1319–1324.
- O. Laczka, J.-M. Maesa, N. Godino, J. del Campo, M. Fougthansen, J. P. Kutter, D. Snakenborg, F.-X. Muñoz-Pascual and E. Baldrich, *Biosens. Bioelectron.*, 2011, **26**, 3633–3640.
- X. A. Guan, H. J. Zhang, Y. N. Bi, L. Zhang and D. L. Hao, *Biomed. Microdevices*, 2010, **12**, 683–691.
- B. K. Oh, Y. K. Kim, W. Lee, Y. M. Bae, W. H. Lee and J. W. Choi, *Biosens. Bioelectron.*, 2003, **18**, 605–611.
- J. M. Klostranec, Q. Xiang, G. A. Farcas, J. A. Lee, A. Rhee, E. I. Lafferty, S. D. Perrault, K. C. Kain and W. C. W. Chan, *Nano Lett.*, 2007, **7**, 2812–2818.
- H. Y. Tan, W. K. Loke, Y. T. Tan and N. T. Nguyen, *Lab Chip*, 2008, **8**, 885–891.
- G. M. Birnbaumer, P. A. Lieberzeit, L. Richter, R. Schirhagl, M. Milnera, F. L. Dickert, A. Bailey and P. Ertl, *Lab Chip*, 2009, **9**, 3549–3556.
- O. K. Koo, Y. S. Liu, S. Shuaib, S. Bhattacharya, M. R. Ladisch, R. Bashir and A. K. Bhunia, *Anal. Chem.*, 2009, **81**, 3094–3101.

- 31 A. J. Kell, G. Stewart, S. Ryan, R. Peytavi, M. Boissinot, A. Huletsky, M. G. Bergeron and B. Simard, *ACS Nano*, 2008, **2**, 1777–1788.
- 32 X. Lou, J. Qian, Y. Xiao, L. Viel, A. E. Gerdon, E. T. Lagally, P. Atzberger, T. M. Tarasow, A. J. Heeger and H. T. Soh, *Proc. Natl. Acad. Sci. U. S. A.*, 2009, **106**, 2989.
- 33 K. M. Ahmad, S. S. Oh, S. Kim, F. M. McClellan, Y. Xiao and H. T. Soh, *PLoS One*, 2011, **6**, e27051.
- 34 M. S. Mannoor, S. Y. Zhang, A. J. Link and M. C. McAlpine, *Proc. Natl. Acad. Sci. U. S. A.*, 2010, **107**, 19207–19212.
- 35 A. Le Nel, N. Minc, C. Smadja, M. Slovakova, Z. Bilkova, J. M. Peyrin, J. L. Viovy and M. Taverna, *Lab Chip*, 2008, **8**, 294–301.
- 36 K. Haupt and K. Mosbach, *Chem. Rev.*, 2000, **100**, 2495–2504.
- 37 A. Bossi, F. Bonini, A. Turner and S. Piletsky, *Biosens. Bioelectron.*, 2007, **22**, 1131–1137.
- 38 A. A. H. Talasaz, M. Nemat-Gorgani, Y. Liu, P. Stahl, R. W. Dutton, M. Ronaghi and R. W. Davis, *Proc. Natl. Acad. Sci. U. S. A.*, 2006, **103**, 14773.
- 39 E. Torres-Chavolla and E. C. Alocilja, *Biosens. Bioelectron.*, 2009, **24**, 3175–3182.
- 40 D. H. J. Bunka and P. G. Stockley, *Nat. Rev. Microbiol.*, 2006, **4**, 588–596.
- 41 L. Gold, B. Polisky, O. Uhlenbeck and M. Yarus, *Annu. Rev. Biochem.*, 1995, **64**, 763–797.
- 42 A. K. Deisingh and M. Thompson, *Can. J. Microbiol.*, 2004, **50**, 69–77.
- 43 A. Sen, T. Harvey and J. Clausen, *Biomed. Microdevices*, 2011, **13**, 705–715.
- 44 N. Beyor, T. S. Seo, P. Liu and R. A. Mathies, *Biomed. Microdevices*, 2008, **10**, 909–917.
- 45 C. S. Zhang, H. Y. Wang and D. Xing, *Biomed. Microdevices*, 2011, **13**, 885–897.
- 46 G.-Y. Kim and A. Son, *Anal. Chim. Acta*, 2010, **677**, 90–96.
- 47 D. C. Leslie, A. Sohrabi, P. Ikonomi, M. L. McKee and J. P. Landers, *Electrophoresis*, 2010, **31**, 1615–1622.
- 48 Y. Zeng, R. Novak, J. Shuga, M. T. Smith and R. A. Mathies, *Anal. Chem.*, 2010, **82**, 3183–3190.
- 49 U. Dharmasiri, M. A. Witek, A. A. Adams, J. K. Osiri, M. L. Hupert, T. S. Bianchi, D. L. Roelke and S. A. Soper, *Anal. Chem.*, 2010, **82**, 2844–2849.
- 50 D. J. You, K. J. Geshell and J.-Y. Yoon, *Biosens. Bioelectron.*, 2011, **28**, 399–406.
- 51 K.-Y. Hwang, S.-Y. Jeong, Y.-R. Kim, K. Namkoong, H.-K. Lim, W.-S. Chung, J.-H. Kim and N. Huh, *Sens. Actuators B*, 2011, **154**, 46–51.
- 52 B. Lam, Z. Fang, E. H. Sargent and S. O. Kelley, *Anal. Chem.*, 2011, **84**, 21–25.
- 53 I. K. Dimov, J. L. Garcia-Cordero, J. O'Grady, C. R. Poulsen, C. Viguier, L. Kent, P. Daly, B. Lincoln, M. Maher, R. O'Kennedy, T. J. Smith, A. J. Riccio and L. P. Lee, *Lab Chip*, 2008, **8**, 2071–2078.
- 54 R. Riahi, K. E. Mach, R. Mohan, J. C. Liao and P. K. Wong, *Anal. Chem.*, 2011, **83**, 6349–6354.
- 55 M. A. Fernandez-Baldo, G. A. Messina, M. I. Sanz and J. Raba, *J. Agric. Food Chem.*, 2010, **58**, 11201–11206.
- 56 L. Wang and P. C. H. Li, *Biomicrofluidics*, 2012, **4**.
- 57 L. Wang and P. C. H. Li, *Anal. Biochem.*, 2010, **400**, 282–288.
- 58 S. Lutz, P. Weber, M. Focke, B. Faltin, J. Hoffmann, C. Muller, D. Mark, G. Roth, P. Munday, N. Armes, O. Piepenburg, R. Zengerle and F. von Stetten, *Lab Chip*, 2010, **10**, 887–893.
- 59 J. H. Jung, G.-Y. Kim and T. S. Seo, *Lab Chip*, 2011, **11**, 3465–3470.
- 60 K. Sato, A. Tachihara, B. Renberg, K. Mawatari, K. Sato, Y. Tanaka, J. Jarvius, M. Nilsson and T. Kitamori, *Lab Chip*, 2010, **10**, 1262–1266.
- 61 X. Weng, H. Jiang, C. H. Chon, S. Chen, H. H. Cao and D. Q. Li, *J. Biotechnol.*, 2011, **155**, 330–337.
- 62 R. H. Meltzer, J. R. Krogmeier, L. W. Kwok, R. Allen, B. Crane, J. W. Griffiths, L. Knaian, N. Kojanian, G. Malkin, M. K. Nahas, V. Papkov, S. Shaikh, K. Vyavahare, Q. Zhong, Y. Zhou, J. W. Larson and R. Gilmanshin, *Lab Chip*, 2011, **11**, 863–873.
- 63 C. Qi, Y. Lin, J. Feng, Z.-H. Wang, C.-F. Zhu, Y.-H. Meng, X.-Y. Yan, L.-J. Wan and G. Jin, *Virus Res.*, 2009, **140**, 79–84.
- 64 Y. Y. Li, C. S. Zhang and D. Xing, *Anal. Biochem.*, 2011, **415**, 87–96.
- 65 B. S. Ferguson, S. F. Buchsbaum, T. T. Wu, K. Hsieh, Y. Xiao, R. Sun and H. T. Soh, *J. Am. Chem. Soc.*, 2011, **133**, 9129–9135.
- 66 K. Yamanaka, M. Saito, K. Kondoh, M. M. Hossain, R. Koketsu, T. Sasaki, N. Nagatani, K. Ikuta and E. Tamiya, *Analyst*, 2011, **136**, 2064–2068.
- 67 N. Thaitrong, P. Liu, T. Briese, W. I. Lipkin, T. N. Chiesl, Y. Higa and R. A. Mathies, *Anal. Chem.*, 2010, **82**, 10102–10109.
- 68 C. Liu, E. Geva, M. Mauk, X. Qiu, W. R. Abrams, D. Malamud, K. Curtis, S. M. Owen and H. H. Bau, *Analyst*, 2011, **136**, 2069–2076.
- 69 Y. Li, C. Zhang and D. Xing, *Microfluid. Nanofluid.*, 2011, **10**, 367–380.
- 70 C.-H. Wang, K.-Y. Lien, T.-Y. Wang, T.-Y. Chen and G.-B. Lee, *Biosens. Bioelectron.*, 2011, **26**, 2045–2052.
- 71 X. Fang, Y. Liu, J. Kong and X. Jiang, *Anal. Chem.*, 2010, **82**, 3002–3006.
- 72 N. Ramalingam, T. C. San, T. J. Kai, M. Y. M. Mak and H. Q. Gong, *Microfluid. Nanofluid.*, 2009, **7**, 325–336.
- 73 X. Weng, H. Jiang and D. Li, *Microfluid. Nanofluid.*, 2011, **11**, 367–383.
- 74 L. Malic, M. G. Sandros and M. Tabrizian, *Anal. Chem.*, 2011, **83**, 5222–5229.
- 75 M. Javanmard and R. Davis, *Sens. Actuators B*, 2011, **154**, 22–27.
- 76 D. Berdat, A. C. M. Rodriguez, F. Herrera and M. A. M. Gijis, *Lab Chip*, 2008, **8**, 302–308.
- 77 T. Schuler, R. Kretschmer, S. Jessing, M. Urban, W. Fritzsche, R. Moller and J. Popp, *Biosens. Bioelectron.*, 2009, **25**, 15–21.
- 78 L. Chen, S. Lee, M. Lee, C. Lim, J. Choo, J. Y. Park, S. W. Joo, K. H. Lee and Y. W. Choi, *Biosens. Bioelectron.*, 2008, **23**, 1878–1882.
- 79 S. W. Dutse and N. A. Yusof, *Sensors*, 2011, **11**, 5754–5768.
- 80 S. K. Njoroge, H.-W. Chen, M. A. Witek and S. A. Soper, *Top. Curr. Chem.*, 2011, **304**, 203–260.
- 81 T. D. Rane, H. Zec, C. Puleo, A. Lee, T. H. Wang, 2011.
- 82 T. D. Rane, H. Zec, C. Puleo, A. P. Lee and W. Tza-Huei, *Electro Mechanical Systems (MEMS)*, 2011 IEEE 24th International Conference on, 2011.
- 83 C. Zhang, J. Xu, W. Ma and W. Zheng, *Biotechnol. Adv.*, 2006, **24**, 243–284.
- 84 X. Pan, L. Jiang, K. Liu, B. Lin and J. Qin, *Anal. Chim. Acta*, 2010, **674**, 110–115.
- 85 H. Y. Wang, C. S. Zhang and D. Xing, *Microchim. Acta*, 2011, **173**, 503–512.
- 86 N. Privorotskaya, Y.-S. Liu, J. Lee, H. Zeng, J. A. Carlisle, A. Radadia, L. Millet, R. Bashir and W. P. King, *Lab Chip*, 2010, **10**, 1135–1141.
- 87 A. C. Grabski, *Methods Enzymol.*, 2009, **463**, 285–303.
- 88 Y. S. Huh, J. H. Choi, T. J. Park, Y. K. Hong, W. H. Hong and S. Y. Lee, *Electrophoresis*, 2007, **28**, 4748–4757.
- 89 D. Di Carlo, K. H. Jeong and L. P. Lee, *Lab Chip*, 2003, **3**, 287–291.
- 90 T. Grahl and H. Markl, *Appl. Microbiol. Biotechnol.*, 1996, **45**, 148–157.
- 91 K. H. Cheong, D. K. Yi, J.-G. Lee, J.-M. Park, M. J. Kim, J. B. Edel and C. Ko, *Lab Chip*, 2008, **8**, 810–813.
- 92 P. J. Asiello and A. J. Baemner, *Lab Chip*, 2011, **11**, 1420–1430.
- 93 O. Piepenburg, C. H. Williams, D. L. Stemple and N. A. Armes, *PLoS Biol.*, 2006, **4**, e204.
- 94 R. John, H. Muller, A. Rector, M. Van Ranst and H. Stevens, *Trends Microbiol.*, 2009, **17**, 205–211.
- 95 P. Craw and W. Balachandran, *Lab Chip*, 2012, **12**, 2469.
- 96 Y. Mori and T. Notomi, *J. Infect. Chemother.*, 2009, **15**, 62–69.
- 97 X. Fang and J. Kong, *Lab Chip*, 2012, **12**, 1495–1499.
- 98 W.-H. Chang, S.-Y. Yang, C.-H. Wang, M.-A. Tsai, P.-C. Wang, T.-Y. Chen, S.-C. Chen and G.-B. Lee, *Sens. Actuators B*.
- 99 Y. Zhang, S. Park, K. Liu, J. Tsuan, S. Yang and T.-H. Wang, *Lab Chip*, 2011, **11**, 398–406.
- 100 F. Shen, E. K. Davydova, W. Du, J. E. Kreutz, O. Piepenburg and R. F. Ismagilov, *Anal. Chem.*, 2011, **83**, 3533–3540.
- 101 C. Liu, M. G. Mauk, R. Hart, X. Qiu and H. H. Bau, *Lab Chip*, 2011, **11**, 2686–2692.
- 102 F. Ahmad, G. Seyrig, D. Tourlousse, R. Stedfeld, J. Tiedje and S. Hashsham, *Biomed. Microdevices*, 2011, **13**, 929–937.
- 103 M. Mahalanabis, J. Do, H. ALMuayad, J. Y. Zhang and C. M. Klapperich, *Biomed. Microdevices*, 2010, **12**, 353–359.
- 104 J. Compton, *Nature*, 1991, **350**, 91.
- 105 S. Park, Y. Zhang, T.-H. Wang and S. Yang, *Lab Chip*, 2011, **11**, 2893–2900.
- 106 P. M. Lizardi, X. Huang, Z. Zhu, P. Bray-Ward, D. C. Thomas and D. C. Ward, *Nat. Genet.*, 1998, **19**, 225–232.

- 107 L. Mahmoudian, N. Kaji, M. Tokeshi, M. Nilsson and Y. Baba, *Anal. Chem.*, 2008, **80**, 2483–2490.
- 108 H. Moncada-Hernandez and B. H. Lapizco-Encinas, *Anal. Bioanal. Chem.*, 2010, **396**, 1805–1816.
- 109 I. F. Cheng, C. C. Lin, D. Y. Lin and H. Chang, *Biomicrofluidics*, 2010, **4**.
- 110 A. Bhattacharyya and C. A. Klapperich, *Sens. Actuators, B*, 2008, **129**, 693–698.
- 111 M. Mujika, S. Arana, E. Castano, M. Tijero, R. Vilares, J. Ruano-Lopez, A. Cruz, L. Sainz and J. Berganza, *Biosens. Bioelectron.*, 2009, **24**, 1253–1258.
- 112 T. F. Didar and M. Tabrizian, *Lab Chip*, 2010, **10**, 3043–3053.
- 113 R. Edelstein, C. Tamanaha, P. Sheehan, M. Miller, D. Baselt, L. Whitman and R. Colton, *Biosens. Bioelectron.*, 2000, **14**, 805–813.
- 114 M. A. M. Gijs, *Microfluid. Nanofluid.*, 2004, **1**, 22–40.
- 115 G. U. Lee, L. A. Chrisey and R. J. Colton, *Science*, 1994, **266**, 771.
- 116 S. Huang, C. Li, B. Lin and J. Qin, *Lab Chip*, 2010, **10**, 2925–2931.
- 117 J. Zhang, S. Liu, P. Yang and G. Sui, *Lab Chip*, 2011, **11**, 3516–3522.
- 118 J. Kim and B. K. Gale, *Lab Chip*, 2008, **8**, 1516–1523.
- 119 S. Metz, C. Trautmann, A. Bertsch and P. Renaud, *J. Micromech. Microeng.*, 2004, **14**, 324.
- 120 W. Cao, C. J. Easley, J. P. Ferrance and J. P. Landers, *Anal. Chem.*, 2006, **78**, 7222–7228.
- 121 M. A. Witek, M. L. Hupert, D. S. W. Park, K. Fears, M. C. Murphy and S. A. Soper, *Anal. Chem.*, 2008, **80**, 3483–3491.
- 122 N. Noeth, S. Keller, S. Fetz, O. Geschke, A. Boisen, *Solid-State Sensors, Actuators and Microsystems Conference (TRANSDUCERS)*, 2009.
- 123 X. Chen, D. Cui, C. Liu, H. Li and J. Chen, *Anal. Chim. Acta*, 2007, **584**, 237–243.
- 124 Y. L. Gao, P. M. Shermanb, Y. Sun and D. Li, *Anal. Chim. Acta*, 2008, **606**, 98–107.
- 125 T. F. Didar, A. M. Foudeh and M. Tabrizian, *Anal. Chem.*, 2011, **84**, 1012–1018.
- 126 C. Lui, S. Stelick, N. Cady and C. Batt, *Lab Chip*, 2010, **10**, 74–79.
- 127 D. Brassard, L. Malic, C. Miville-Godin, F. Normandin, T. Veres, *Micro Electro Mechanical Systems (MEMS)*, IEEE 24th International Conference, 2011.
- 128 S. Y. Teh, R. Lin, L. H. Hung and A. P. Lee, *Lab Chip*, 2008, **8**, 198–220.
- 129 R. Seemann, M. Brinkmann, T. Pfohl and S. Herminghaus, *Rep. Prog. Phys.*, 2012, **75**, 016601.
- 130 N. R. Beer, E. K. Wheeler, L. Lee-Houghton, N. Watkins, S. Nasarabadi, N. Hebert, P. Leung, D. W. Arnold, C. G. Bailey and B. W. Colston, *Anal. Chem.*, 2008, **80**, 1854–1858.
- 131 A. B. Theberge, F. Courtois, Y. Schaeferli, M. Fischlechner, C. Abell, F. Hollfelder and W. T. S. Huck, *Angew. Chem., Int. Ed.*, 2010, **49**, 5846–5868.
- 132 I. Barbulovic-Nad, S. H. Au and A. R. Wheeler, *Lab Chip*, 2010, **10**, 1536–1542.
- 133 L. Malic, T. Veres and M. Tabrizian, *Biosens. Bioelectron.*, 2009, **24**, 2218–2224.
- 134 Y. H. Chang, G. B. Lee, F. C. Huang, Y. Y. Chen and J. L. Lin, *Biomed. Microdevices*, 2006, **8**, 215–225.
- 135 E. M. Miller, A. H. C. Ng, U. Uddayasankar and A. R. Wheeler, *Anal. Bioanal. Chem.*, 2011, **1**–9.
- 136 L. Malic, T. Veres and M. Tabrizian, *Lab Chip*, 2009, **9**, 473–475.
- 137 K. Choi, J.-Y. Kim, J.-H. Ahn, J.-M. Choi, M. Im and Y.-K. Choi, *Lab Chip*, 2012, **12**, 1533.
- 138 H. Moon, A. R. Wheeler, R. L. Garrell and J. A. Loo, *Lab Chip*, 2006, **6**, 1213–1219.
- 139 K. P. Nichols and H. J. G. E. Gardeniers, *Anal. Chem.*, 2007, **79**, 8699–8704.
- 140 V. Srinivasan, V. K. Pamula and R. B. Fair, *Lab Chip*, 2004, **4**, 310–315.
- 141 R. Sista, Z. Hua, P. Thwar, A. Sudarsan, V. Srinivasan, A. Eckhardt, M. Pollack and V. Pamula, *Lab Chip*, 2008, **8**, 2188.
- 142 M. Madou, J. Zoval, G. Jia, H. Kido, J. Kim and N. Kim, *Annu. Rev. Biomed. Eng.*, 2006, **8**, 601–628.
- 143 N. Ramalingam, Z. Rui, H.-B. Liu, C.-C. Dai, R. Kaushik, B. Ratnahratika and H.-Q. Gong, *Sens. Actuators, B*, 2010, **145**, 543–552.
- 144 A. W. Martinez, S. T. Phillips, G. M. Whitesides and E. Carrilho, *Anal. Chem.*, 2009, **82**, 3–10.
- 145 R. Pelton, *TrAC, Trends Anal. Chem.*, 2009, **28**, 925–942.
- 146 W. Zhao and A. van der Berg, *Lab Chip*, 2008, **8**, 1988.
- 147 J. C. Jokerst, J. A. Adkins, B. Bisha, M. M. Mentele, L. D. Goodridge and C. S. Henry, *Anal. Chem.*, 2012, **84**, 2900–2907.
- 148 W. A. Zhao, M. M. Ali, S. D. Aguirre, M. A. Brook and Y. F. Li, *Anal. Chem.*, 2008, **80**, 8431–8437.
- 149 K. Abe, K. Kotera, K. Suzuki and D. Citterio, *Anal. Bioanal. Chem.*, 2010, **398**, 885–893.
- 150 A. W. Martinez, S. T. Phillips and G. M. Whitesides, *Proc. Natl. Acad. Sci. U. S. A.*, 2008, **105**, 19606.
- 151 X. Y. Liu, C. M. Cheng, A. W. Martinez, K. A. Mirica, X. J. Li, S. T. Phillips, M. Mascareñas, G. M. Whitesides, *Micro Electro Mechanical Systems (MEMS)*, IEEE 24th International Conference on, 2011.
- 152 L. Ge, J. Yan, X. Song, M. Yan, S. Ge and J. Yu, *Biomaterials*, 2011, **33**, 1024–1031.
- 153 H. Liu and R. M. Crooks, *J. Am. Chem. Soc.*, 2011, **133**, 17564–17566.
- 154 D. F. Chen, M. Mauk, X. B. Qiu, C. C. Liu, J. T. Kim, S. Ramprasad, S. Ongagna, W. R. Abrams, D. Malamud, P. Corstjens and H. H. Bau, *Biomed. Microdevices*, 2010, **12**, 705–719.
- 155 L. Lafleur, D. Stevens, K. McKenzie, S. Ramachandran, P. Spicarni, M. Singh, A. Arjyal, J. Osborn, P. Kauffman, P. Yager and B. Lutz, *Lab Chip*, 2012, **12**, 1119.
- 156 C. D. Chin, T. Laksanasopin, Y. K. Cheung, D. Steinmiller, V. Linder, H. Parsa, J. Wang, H. Moore, R. Rouse and G. Umvilighozo, *Nat. Med.*, 2011, **17**, 1015–1019.



Contents lists available at ScienceDirect

Biosensors and Bioelectronics

journal homepage: www.elsevier.com/locate/bios

Sub-femtomole detection of 16s rRNA from *Legionella pneumophila* using surface plasmon resonance imaging



Amir M. Foudeh^{a,1}, Jamal T. Daoud^{a,1}, Sebastien P. Faucher^{c,2}, Teodor Veres^{a,d,3},
Maryam Tabrizian^{a,b,*}

^a Department of Biomedical Engineering, Faculty of Medicine, McGill University, Montreal, Canada

^b Faculty of Dentistry, McGill University, Strathcona Anatomy & Dentistry Building 3640 University Street Montreal, Quebec, Canada

^c Department of Natural Resource Sciences, McGill University, Quebec, Canada

^d National Research Council of Canada, Quebec, Boucherville, Canada

ARTICLE INFO

Article history:

Received 9 July 2013

Received in revised form

16 August 2013

Accepted 19 August 2013

Available online 28 August 2013

Keywords:

Legionella pneumophila

Surface plasmon resonance imaging

Pathogen detection

16s rRNA

Quantum dot

Hybridization

ABSTRACT

Legionellosis has been and continues to be a life-threatening disease worldwide, even in developed countries. Given the severity and unpredictability of Legionellosis outbreaks, developing a rapid, highly specific, and sensitive detection method is thus of great pertinence. In this paper, we demonstrate that sub-femtomole levels of 16s rRNA from pathogenic *Legionella pneumophila* can be timely and effectively detected using an appropriate designed capture, detector probes, and a QD SPRI signal amplification strategy. To achieve specific and sensitive detection, optimal hybridization conditions and parameters were implemented. Among these parameters, fragmentation of the 16s rRNA and further signal amplification by QDs were found to be the main parameters contributing to signal enhancement. The appropriate design of the detector probes also increased the sensitivity of the detection system, mainly due to secondary structure of 16s rRNA. The use of 16s rRNA from *L. pneumophila* allowed for the detection of metabolically active pathogens with high sensitivity. Detection of 16s rRNA in solutions as diluted as 1 pM at 450 μL (0.45 femtomole) was achieved in less than 3 h, making our approach suitable for the direct, timely, and effective detection of *L. pneumophila* within man-made water systems.

© 2013 Elsevier B.V. All rights reserved.

1. Introduction

Legionellosis is an acute form of pneumonia and Pontiac fever, a milder form of the disease with flu-like symptoms (Swanson and Hammer, 2000) that has been and continues to be devastating worldwide, even in developed countries. This is mainly attributed to unpredictable outbreaks, such as recent incidents reported in Canada, the U.S.A., Norway, and Germany (CDC, 2011; Nygård

et al., 2008; Von Baum et al., 2010). *Legionella pneumophila* is the causative agent of Legionellosis. The fatality rate of Legionellosis ranges between 10% and 40% and approaches 50% within hospital and industrial outbreak settings, particularly affecting individuals with compromised health status (Swanson and Hammer, 2000). *L. pneumophila* is found in most natural and engineered water systems, where it contaminates and multiplies inside amoeba (Wadowsky et al., 1991). The literature indicates that modern water systems, such as air-conditioning units, showers, and industrial refrigeration towers provide optimal growth conditions for *L. pneumophila* and propagate its transmission through aerosol (WHO, 2003). Transmission to the human host thus occurs through the inhalation of contaminated water droplets. Once in the lungs, *L. pneumophila* infects and replicates inside alveolar macrophages and causes widespread tissue damage (Swanson and Hammer, 2000).

Current conventional detection methods include identification via laboratory culture and polymerase chain reaction (PCR) (Foudeh et al., 2012; Lazcka et al., 2007). Laboratory culture is the gold standard method employed to detect *L. pneumophila*. However, laboratory culture suffers from low sensitivity, especially if the samples under study contain microorganisms that inhibit *Legionella*'s growth. Another drawback is its inability to detect

* Corresponding author at: Department of Biomedical Engineering, Faculty of Medicine, McGill University, Montreal, Canada. Tel.: +1 514 398 8129; fax: +1 514 398 7461.

E-mail addresses: amir.foudeh@mail.mcgill.ca (A.M. Foudeh), jamal.daoud@mail.mcgill.ca (J.T. Daoud), sebastien.faucher2@mcgill.ca (S.P. Faucher), Teodor.Veres@nrc-nrc.gc.ca (T. Veres), maryam.tabrizian@mcgill.ca (M. Tabrizian).

¹ 3775 University Street, Department of Biomedical Engineering, Faculty of Medicine, McGill University, Montreal (QC), Canada H3A 2B4. Tel.: +1 514 398 3469; fax: +1 514 398 7469.

² Department of Natural Resource Sciences, Macdonald Campus, 12 McGill University, 21,111 Lakeshore, Ste-Anne-de-Bellevue, Quebec, H9X 3V9. Tel.: +1 514 398 13 7886; fax: +1 514 398 7990.

³ National Research Council Canada, 75 Boul. de Mortagne Boucherville, QC, Canada J4B 6Y4. Tel.: +1 450 641 5232; fax: +1 450 641 5105.

viable but non-culturable *Legionella* even though they might potentially be pathogenic. While laboratory culture entails long procedures requiring several days, PCR is a faster detection methodology and highly specific. However, it is laborious and normally requires centralized laboratory facilities. PCR is especially unreliable when analyzing environmental samples due to the presence of PCR inhibitors.

Other methods, namely antibody-based detection, have also been investigated (Oh et al., 2003). This method is fairly rapid, but cross-reactivity between species is an important shortcoming that limits the specificity of the technique. DNA/PNA microarray-based detection targeting DNA in bacteria is another alternative that provides the desired specificity by targeting species-specific sequences in DNA (Zhou et al., 2011).

The main drawback of all the aforementioned methods is their inability to differentiate between live and dead bacterial cells, which is critical for achieving accurate and reliable results.

To overcome the limitations of using DNA and antigen targeting-based techniques, detection of the bacterial RNA is a viable alternative approach. The presence of RNA in bacteria is directly correlated with microbial activity since, following bacterial death, the associated RNA degrades relatively rapidly (McKillip et al., 1998), further enhancing the associated accuracy and reliability of bacterial detection. Among RNA types, 16s rRNA is highly conserved between different species of bacteria and has been utilized for microbial identification (Clarridge, 2004; Coenye and Vandamme, 2003). The presence of high copy numbers of 16s rRNA in each bacterium is another motivation to identify bacteria through the direct detection of 16s rRNA. However, instability and the presence of a secondary structure are significant drawbacks of using ribosomal RNA. The secondary structure renders access to the target sequence difficult. This is why methods such as using multiple adjunct probes, heat denaturation, and fragmentation have been used to circumvent this issue (Hwang et al., 2011; Small et al., 2001).

Focusing on the detection of 16s rRNA, various sensing techniques, including electrochemical sensors (Bockisch et al., 2005; Xie et al., 2004), impedance (Elsholz et al., 2006), fluorescent microscopy (Gerashimova and Kolpashchikov, 2012; Hwang et al., 2011; Riahi et al., 2011), surface-enhanced Raman spectroscopy (SERS) (Stephen et al., 2012), and surface plasmon resonance (SPR) (Joung et al., 2008; Small et al., 2001) were used for bacterial species-specific detection. Among these methods, SPR imaging (SPRI) has proven to be a versatile tool for the real-time study of genomic and proteomic interactions and kinetics. In contrast to classical wavelength or scanning angle SPR systems, SPRI provides visualization of the multiple interactions simultaneously in real time thanks to the integration of a charge-coupled device (CCD) camera with the associated sensogram. In contrast to other endpoint measurement systems, the use of SPRI allows detailed kinetic analysis, monitored in real time, to elucidate analyte binding behavior further, as well as to differentiate better between specific and non-specific adsorptions. To date, few reports on detecting 16s rRNA within a SPR setup are available in the literature. Nelson et al. detected 16s rRNA from *E. coli* with a limit of detection (LOD) of 2 nM through the use of DNA probes (Nelson et al., 2000). Joung et al. used PNA probes and electrostatic interaction between positively charged gold nanoparticles and negatively charged RNA as a signal post amplification method, achieving an LOD of around 100 pM (Joung et al., 2008), which is far from the desired sensitivity in the context of the detection of pathogenic *L. pneumophila* in a water sample.

This work presents the first report on utilizing 16s rRNA for the detection of *L. pneumophila* with SPRI. To overcome the lack of desired SPRI sensitivity for the detection of this species, near-infrared quantum dots (QDs) are employed as a post-amplification strategy. We previously demonstrated that QDs with an emission

of 800 nm induce the strongest SPR signal enhancement among QDs with differing wavelengths (Malic et al., 2011). As such, our aim was to address the main challenges associated with the detection of *L. pneumophila* through the use of 16s rRNA from *L. pneumophila*, allowing for the detection of only metabolically active pathogens with high sensitivity. With the design of two probes, one to capture the RNA on the substrate and the other to increase the detection sensitivity, for each target region, the high specificity of the detection system is further ensured (Scheme 1). The effect of experimental parameters, including temperature, buffer composition, length of the spacer between the detector probe and the biotin, and the pre-treatment of 16s rRNA were investigated and optimized to reach a sensitivity detection of *L. pneumophila* in the femtomole range.

2. Materials and methods

2.1. Chemical and reagents

6-Mercapto-1-hexanol (MCH), potassium phosphate dibasic solution, 1 M, pH 8.9 (1 M K_2HPO_4), sodium chloride (NaCl), sodium hydroxide (NaOH), sulfuric acid (H_2SO_4), hydrogen peroxide (H_2O_2), and ethanol were purchased from Sigma-Aldrich (St. Louis, MO, U.S.A.). A fragmentation kit was obtained from Ambion. Oligonucleotides (ODN) were purchased from Integrated DNA Technologies (Coralville, IA, U.S.A.). Streptavidin-coated quantum dots, Qdot 800 STVD, SSPE buffer (20 × buffer is 3.0 M NaCl, 0.2 M NaH_2PO_4 , and 0.02 M EDTA at pH 7.4), and Denhardt's solution [50 × solution is 1% Ficoll (type 400), 1% polyvinylpyrrolidone, and 1% bovine serum albumin] were purchased from Invitrogen (Carlsbad, CA, U.S.A.).

2.2. DNA probe design

Two specific DNA capture probes (CP), referring to leg1 CP and leg2 CP, complementary to *L. pneumophila*'s 16s rRNA, were designed using bioinformatics software packages from Cardiff University, England. Particular features in the sequence, such as loops and hairpin curves, were checked and avoided. The specificity of these probes was confirmed by submitting the sequence to the Check Probe program of the Ribosomal Database Project (RDP). In terms of detection probes, two different biotinylated probes with gap of 0 bp and 7 bp (Leg1 DP 0/7 bp and Leg2 DP 0/7 bp) between the capture and detection probes for each target RNA sequence were designed. Finally, a DNA probe and a universal probe (EU capture probe) were used as negative and positive controls, respectively. The length of each detector probe was determined to ensure similar melting temperatures while avoiding cross-reactivity and hybridization to any capture probes. This was verified by including a detector-only control for each hybridization experiment conducted (data not shown). The secondary structure model of *L. pneumophila* was obtained from <http://www.rna.cccb.utexas.edu> (Cannone et al., 2002).

2.3. RNA preparation

Synthetic 60 bp RNA from the *L. pneumophila*'s 16s rRNA, which contains complementary sequences for Leg1 capture and detector probes, was synthesized by Integrated DNA Technology Table S1. Moreover, 16s rRNA of *L. pneumophila* was produced using T7 RNA polymerase-driven in vitro synthesis methodology. Briefly, the 16s rRNA gene of *L. pneumophila* was amplified by PCR from DNA extracted from *L. pneumophila* using specific primers (5'-AGACAAC-TGTGTGGGCACCTTGG-3' and 5'-TGGGCACCTTGATTCCTCTGTGC-3'). The PCR fragment was then inserted into the pGEM-T (Promega)

vector downstream of the T7 promoter. The plasmid was then transformed and propagated in JM109 high-efficiency competent cells. The PCR fragments could become inserted in the sense or antisense orientation. Plasmids carrying fragments in the sense orientation were identified and utilized for further experiments. The identification of colonies carrying plasmids containing fragments in each orientation were identified by PCR, and the correct sequence of the fragment was validated by sequencing. The plasmids carrying the correct sequences were isolated and used as a template for T7 RNA polymerase (New England Biolabs) to produce 16s rRNA. The resulting RNA product was further purified by acid-phenol and stored in -80°C for further use.

2.4. Surface chemistry on SPRi chip

Gold-coated slides (Horiba, France) were cleaned with UV/ozone for 10 min, rinsed thoroughly with MQ water, and treated with piranha solution for another 5 min. After rinsing with MQ water, the slides were dried under a stream of nitrogen. DNA immobilization was performed using $1\ \mu\text{M}$ thiol-modified oligonucleotide probes comprising a 10T spacer in $1\ \text{M}\ \text{KH}_2\text{PO}_4$ for 180 min. Following the immobilization, substrates were treated with $1\ \text{mM}$ MCH for 90 min to improve the orientation of the probes and attenuate non-specific adsorption. The slides were further passivated with 2.5X Denhardt solution for 10 min and stored at 4°C before further use.

2.5. RNA pre-treatment

Denaturation of the 16s rRNA was carried out by the incubation of samples for 65°C for 5 min. Fragmentation of the 16s rRNA was performed according to the protocol provided by the manufacturer (Ambion) except that different concentrations of the fragmentation buffer (zinc solution) were used in these experiments. Frag1 and Frag2 represent the use of 1 and $2\ \mu\text{L}$ of the fragmentation buffer, respectively. Then the solution was mixed with $1.28\ \mu\text{g}$ of 16s rRNA in $20\ \mu\text{L}$ of total reaction volume. The solution was kept at 75°C for 15 min, followed by the addition of blocking solution (EDTA). The samples were kept on ice until further use.

2.6. SPRi measurements

SPRi detection of biomolecular binding to the chip surface was performed using a scanning-angle SPRi instrument (model SPRi-Lab+, GenOptics, France). The SPRi apparatus, equipped with an 800 nm LED source, a CCD camera, and a microfluidic cell, was placed in an incubator (Memmert Peltier, Rose Scientific, Canada). The SPRi measurements for each spot were taken as described previously (Malic et al., 2011). The entire biochip surface was imaged during the angular scan. At least five spots were selected for each experiment to monitor the binding events with both the probes and the controls, and each experiment was repeated at least three times.

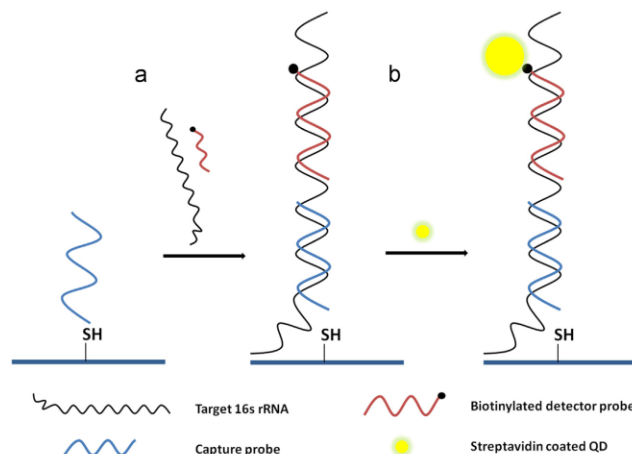
RNA hybridization experiments were carried at 37°C with an injection volume of $450\ \mu\text{L}$. A baseline signal was first obtained for the hybridization buffer, followed by the hybridization signal for the targets. Detector probes were pre-mixed with the RNA samples before injection. Following the hybridization of the target RNA with the capture probe and the detection probe, streptavidin-conjugated Qdots (SA-QDs), $1\ \text{nM}$ in concentration in hybridization buffer, were injected and allowed to bind to the biotinylated detector probes for 10 min. At each step, the substrate was washed with buffer, and the difference in the reflected intensity ($\Delta\%R$) was computed by taking the difference between the initial and final buffer signals. Successive hybridizations were followed by surface regeneration using $50\ \text{mM}$ NaOH, without significant binding efficiency loss.

2.7. Statistics

The lower detection limit was defined as the smallest concentration of an analyte, calculated as the blank signal plus or minus three standard deviations. All data were expressed as the mean \pm SD. Statistical comparisons between two groups were done using Student's paired *t*-test, while multiple comparisons were done using one-way ANOVA, followed by the post hoc Tukey test.

3. Results and discussion

Two different regions of the *L.pneumophila*'s 16s rRNA sequence were targeted to investigate the regional effects on hybridization



Scheme 1. Schematic illustration of the RNA hybridization using capture and detector probes, before and after addition of SA-QDs. (a) Mixture of target RNA and biotinylated detector probe pass through the detection surface. (b) Addition of streptavidin-QDs after hybridization of target RNA to capture probe and detector probe.

efficiency and specificity, as well as the proximity of the detector and capture probes. One specific capture probe was designed for each region. In addition to these two specific capture probes for *L. pneumophila*, one universal probe and one control probe were selected as positive and negative controls, respectively. A summary of the oligonucleotide sequences for probes are given in Table S1.

Since significant non-specific hybridization to the control probes was observed at room temperature (data not shown) the hybridization temperature was set at 37 °C. Then, to detect *L. pneumophila* with high specificity and in very low concentrations, the effect of experimental parameters, namely the buffer composition, the length of the spacer between detector probe and biotin, and the pre-treatment of 16s rRNA were investigated.

3.1. Effect of buffer composition and detector probe spacer on hybridization efficiency

In addition to the hybridization temperature, the buffer composition and the proximity between the detection probe and its respective biotin functional group also play an important role in the stringency and efficiency of the hybridization (Bockisch et al., 2005; Small et al., 2001).

A 60 bp synthetic RNA sequence was selected from *L. pneumophila*'s 16s rRNA sequences complementary to the Leg1 CP. Therefore, 60 bp synthetic RNA (Table S1) was utilized to investigate the effect of the buffer composition and the detector probe spacer.

The effect of buffer compositions on the SPRI differential reflectivity ($\Delta\%R$) of synthetic RNA hybridization for an incubation time of 18 min is illustrated in Fig. 1. To better compare the different buffer compositions, the signals obtained from the control probes were subtracted from the Leg1 CP hybridization signals at each buffer composition (Fig. 1 inset). Increasing the salt concentrations by four-fold (from 150 mM to 600 mM) resulted in higher hybridization efficiency. A further increase of the salt concentration to 900 mM showed a slight increase in hybridization efficiency but caused an increase in non-specific adsorption to the control probe. Thus, 600 mM SSPE was set as the optimal hybridization buffer. As for the optimal biotinylated spacer, different spacers, such as dT and TEG (containing a 15C spacer), were investigated, whereas TEG yielded the highest signal (data not shown). These optimized hybridization parameters were then set for the detection of 16s rRNA in further investigations.

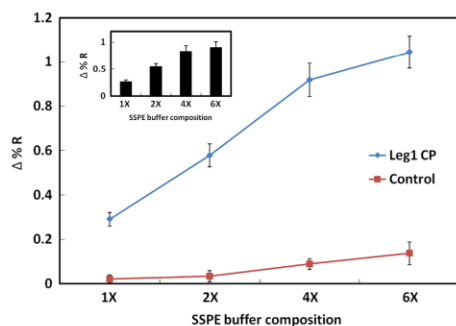


Fig. 1. Effect of buffer composition on hybridization efficiency. Hybridization of 10 nM synthetic RNA for 18 min on the biochip expressed as $\Delta\%R$ as a function of buffer composition ($1 \times -6 \times$ SSPE). The inset represents the difference between the hybridization signal of the Leg1 CP and that of the control probes. All data is expressed as mean \pm standard deviation ($n=5$).

3.2. *L. pneumophila* 16s rRNA pre-treatment

Conversely, to address the steric hindrance resulting from the secondary structure of 16s rRNA, the effect of different pre-treatment methods was investigated. Fig. 2a shows the changes in SPRI differential reflectivity signals representing 18-minute hybridization for pre-treated, as well as intact, 16s rRNA to the Leg1, Leg2 and EU CPs.

In general, Leg1 CP produced stronger hybridization signals compared to the Leg2 and EU capture probes. This may be attributed to several factors, including: (i) the higher melting temperature of Leg1 CP compared to the Leg2 and EU CPs, (ii) the position of the Leg1 CP complementary sequence, located on the more exposed region of the 16s rRNA secondary structure, and (iii) the weaker secondary structure of 16s rRNA to be disrupted by the Leg1 CP compared to the Leg2 and EU capture probes (Fig. 3a and b). To arrive at the optimized fragmentation protocol, two methods with varying fragmentation solution concentrations were used to obtain the 16s rRNA fragments, referred to as Frag1 and Frag2. As shown in Fig. 2a, denaturation through heating of the 16s rRNA resulted only in a significant increase of $\Delta\%R$ for hybridization to EU CP, but not Leg1 and Leg2 CPs. The same trend was also observed for Frag1. In addition, Frag2 resulted in the highest improvement in hybridization efficiency among the three capture probes relative to intact 16s rRNA. This is due to the higher concentration of cations in Frag2 compared to those in Frag1, which results in smaller fragments and, in turn,

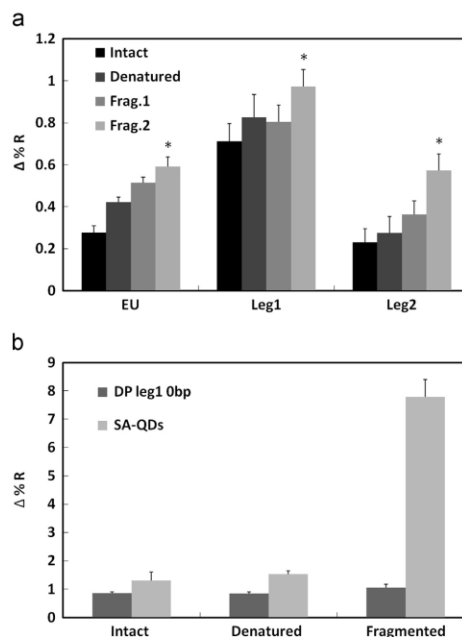


Fig. 2. Effect of fragmentation and denaturation pre-treatment methods on 16s rRNA on hybridization efficiency. (a) Hybridization of 10 nM 16s rRNA after 18 min incubation with EU, Leg1 and Leg2 capture probes. (b) Effect of 16s rRNA pre-treatment on QDs post amplification. 100 nM Leg1 DP 0 bp with 10 nM 16s rRNA were used and hybridization efficiency with Leg1 CP followed by addition of the 1 nM SA-QDs was investigated. All data is expressed as mean \pm standard deviation ($n=5$, $P < 0.05$ versus intact, denatured and Frag1).

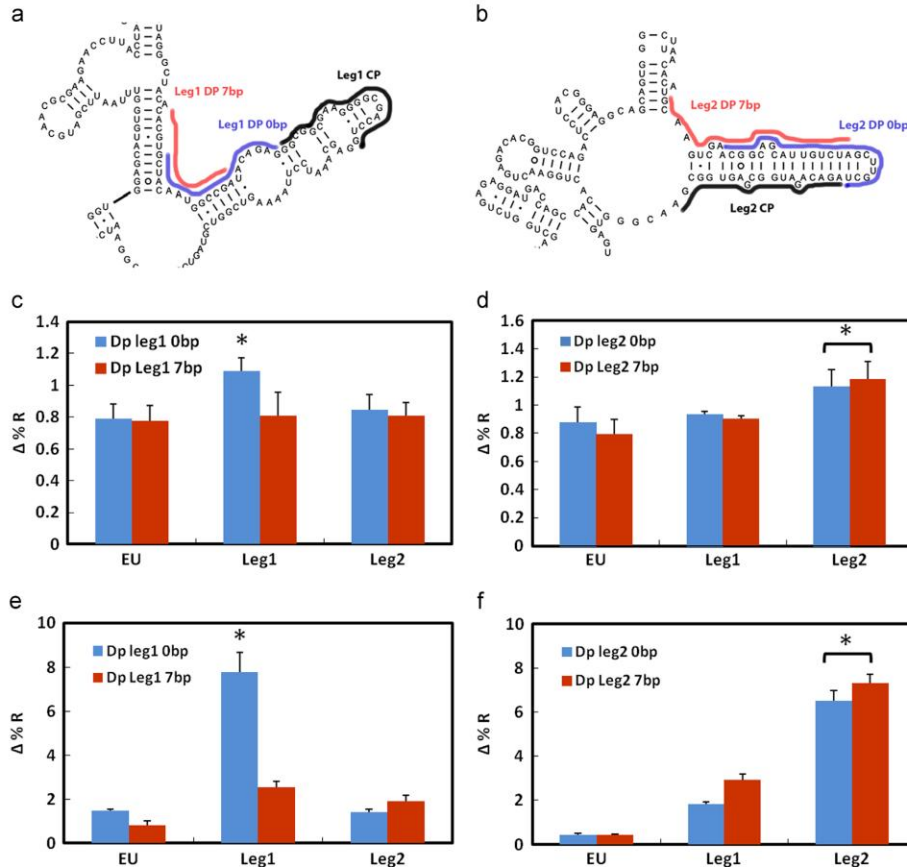


Fig. 3. Effect of different detector probes on hybridization efficiency. x-axis represents capture probes. (a,b) Secondary structure diagrams for *Legionella pneumophila* based on *L. pneumophila* model (accession number M34113) (Cannone et al., 2002) for area complementary to Leg1 CP and Leg2 CP respectively. Lines next to the diagrams indicate the position of capture and detector probes. (c,d) Change in reflectivity was measured after 18 min for three different capture probes (EU, Leg1 and Leg2 CPs) for 10 nM fragmented 16s rRNA corresponding to a and b respectively. (e,f) Addition of 1 nM SA-QDs for 10 min corresponding to c and d respectively. All data is expressed as mean \pm standard deviation ($n=5$, $P < 0.05$ versus other capture probes).

higher accessibility of the capture probes. For simplicity's sake, fragmentation will henceforth refer to Frag2.

To further investigate the effect of pre-treatment of the 16s rRNA, biotinylated detector probes located 0 bp away from the Leg1 CP were investigated for hybridization efficiency and subsequent signal amplification through the addition of SA-QDs. Leg1 DP 0 bp was pre-mixed with fragmented, denatured, and intact 16s rRNA samples before injection into the SPRI system. Fig. 2b shows the $\Delta\%R$ for hybridization, using Leg1 CP, of 16s rRNA pre-mixed with Leg1 DP 0 bp for 18 min, followed by the addition of SA-QDs and a 10 min reaction time, as a function of the pre-treatment methodology. Addition of the detector probe resulted in a slight increase in the signal, with the highest for fragmented 16s rRNA. SA-QDs addition also resulted in a drastic change in $\Delta\%R$ for fragmented 16s rRNA versus slight signal enhancement for intact and denatured RNAs. The enhanced hybridization efficiency could be explained by a higher number of hybridized detector probes for

fragmented RNA due to the easy access of smaller RNA as well as the ease of access of SA-QDs to the small 16s rRNA fragments compared to the whole 16s rRNA.

3.3. Determination of the SPRI limit of detection for 16s rRNA from *L. pneumophila*

The optimal experimental parameters, the pre-treatment fragmentation, and the SA-QD post amplification strategy were used to investigate two more critical factors, the distance between the capture and the detector probe and the hybridization time, affecting the specificity and efficiency of the target sequence hybridization extracted from *L. pneumophila* and to determine the SPRI limit of detection (LOD) (Small et al., 2001).

To investigate the effect of the detector probe's proximity to the capture probe on the specificity and sensitivity of the detection system, two detector probes for the Leg1 and Leg2 capture probes

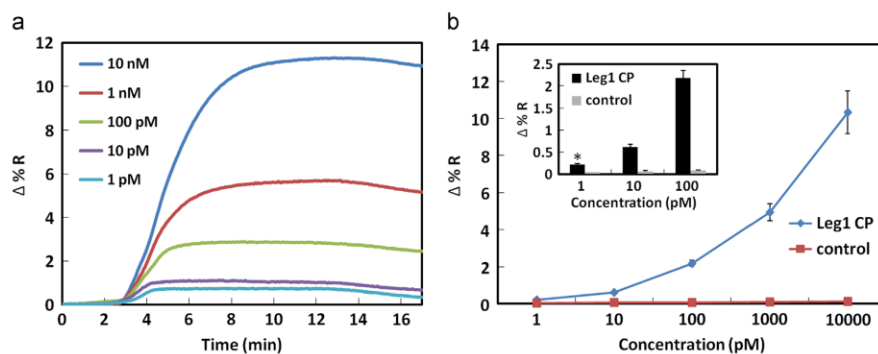


Fig. 4. Fragmented 16S rRNA hybridization with Leg1 CP with series of ultralow RNA concentrations: 10 nM, 1 nM, 100 pM, 10 pM, 1 pM. (a) Normalized real-time SPRi kinetic curve for detection of ultralow concentration of 16S rRNA. (b) The reflectivity change was plotted versus concentration after 150 min. The inset figure shows the differential reflectivity change ($\Delta\%R$) for 1 pM, 10 pM and 100 pM. All data expressed as mean \pm standard deviation ($n=5$, $P < 0.05$ versus control probe).

were designed to hybridize to the 16S rRNA sequence 0 and 7 bp away from the respective capture probes (Fig. 3a and b). Fig. 3c–f shows the hybridization of four detector probes with fragmented 16S rRNA along with the use of SA-QD signal amplification for incubation times of 18 and 10 min, respectively. The results indicated that Leg2 CP possessed a higher signal when Leg2 DPs (Leg2 DPs at 0 and 7 bp) were used compared to Leg1 DPs (Leg1 DPs at 0 and 7 bp) (Fig. 3c and d). This was further accentuated after the addition of SA-QDs. Both Leg2 DPs produced significantly higher signals compared to Leg1 DPs (Fig. 3e and f). This could be due to the position of these probes on the secondary structure of 16S rRNA. As shown in Fig. 3b, Leg2 CP and Leg2 DPs target the same stem-loop in the 16S rRNA secondary structure. The presence of Leg2 DPs, therefore, causes disruption of this stem-loop and further facilitates the reaction with Leg2 CP.

The same hybridization trend was therefore expected for Leg1 CP with both Leg1 DPs. However, only Leg1 DP 0 bp showed a markedly enhanced signal either with 16S rRNA hybridization or the following SA-QD post amplification. Further examination of the secondary structure of *L. pneumophila* revealed that the position of Leg1 DP 0 bp and Leg1 DP 7 bp contributes significantly to this difference. As shown in Fig. 3a, Leg1 DP 0 bp contains two internal loops compared to Leg1 DP 7 bp, which possesses only one internal loop. Upon further examination of the secondary structure, it was apparent that, for Leg1 DP 7 bp hybridize to 16S rRNA, it needs to overcome a stronger secondary structure compared to Leg1 DP 0 bp (14 bonds compared to 9). Since the Leg1 DP 0 bp produced the most pronounced SPRi signal, it was selected for further experiments.

Finally, to determine the effect of hybridization time, fixed volumes of fragmented 16S rRNA were used with incubation times ranging from 4.5 min to 150 min, obtained by varying the flow rate to the SPRi system. The range of incubation was purposely selected to maintain the time of analysis comparable to that of PCR. Fig. S1 presents the effect of hybridization time on $\Delta\%R$ for Leg1 CP. As expected, increased incubation time was directly related to enhanced hybridization efficiency.

An incubation time of 150 min was then chosen, along with optimal hybridization conditions, to investigate the SPRi sensitivity and its LOD for the detection of 16S rRNA from *L. pneumophila*. 16S rRNA hybridization with multiple samples containing fragmented 16S rRNA varying in concentration from 1 pM to 10 nM, with 100 nM Leg1 DP 0 bp in $4 \times$ SSPE buffer were taken, and the hybridization adsorption kinetics were monitored in real time

with SPRi measurements employing the SA-QD signal amplification strategy. The normalized SPRi kinetic curves for SA-QD adsorption for various 16S rRNA concentrations ranging from 1 pM to 10 nM are given in Fig. 4a. Fig. 4b shows the plot of the $\Delta\%R$ for Leg1 and control capture probes for the aforementioned concentrations. The inset in Fig. 4b shows the $\Delta\%R$ for low concentrations of 16S rRNA (1, 10, and 100 pM). A significant difference in the SPR signal was observed between Leg1 CP and the control probe even at 1 pM 16S rRNA, which clearly established a limit of detection on the order of 1 pM *L. pneumophila* 16S rRNA. This value could be translated to the equivalent of 88.5 CFU μL^{-1} with the assumption of 6800 ribosomes per bacteria (Leskelä et al., 2005). This limit of detection is far lower than the previously reported value for RNA detection using an SPR biosensing system (Joung et al., 2008; Nelson et al., 2000).

4. Conclusions

Developing a detection system that distinguishes metabolic active pathogens with the desired specificity, sensitivity, and time of detection is of great importance and relevance for the rapid detection of pathogens in environmental samples. In this paper, we conclusively demonstrated that a sub-femtomole level of 16S rRNA from pathogenic *L. pneumophila* can be specifically detected using an optimized experimental protocol, adequate design of capture and detector probes, and employing a QD signal amplification strategy with a SPRi biosensor. The proposed approach offers several distinct advantages compared to other conventional detection systems, including high specificity through the design of two probes (capture and detector) for the target, high sensitivity through using QD signal post amplification, and rapid and reliable quantification using *L. pneumophila*'s 16S rRNA, which is a good representation of metabolically active bacteria.

To achieve specific and sensitive detection, optimal hybridization conditions and parameters were implemented. We showed that the SPRi detection of 16S rRNA in solutions as diluted as 1 pM at 500 μL (0.5 femtomole) can be achieved in less than three hours, making the SPRi detection system suitable for the direct detection of *L. pneumophila*, in man-made water systems. Through the integration of a microfluidic system with SPRi and further automation, it would be possible to reduce further the detection volume to less than 1 μL and improve the LOD significantly.

Acknowledgments

We acknowledge National Science and Engineering Research Council of Canada-Collaborative Research program and Discovery program, Genome Canada/Genome Quebec, Nano-Quebec and Le Fonds Québécois de la Recherche sur la Nature et les Technologies-Centre for Biorecognition and Biosensors for their financial support. The authors would also like to thank Dr J.-J. Drieux and Dr P. Hiernaux from Magnus for their technical support and advice, S. Shapka and S. Filion-Côté for scientific discussions regarding SPRi and Dr T. Fatanat Didar for his comments on the manuscript. Work in SPF laboratory is supported by NSERC Discovery Grant 418289-2012.

Appendix A. Supporting information

Supplementary data associated with this article can be found in the online version at <http://dx.doi.org/10.1016/j.bios.2013.08.032>.

References

- Bockisch, B., Grunwald, T., Spillner, E., Bredehorst, R., 2005. *Nucleic Acids Research* 33 (11), e101.
- Cannone, J.J., Subramanian, S., Schnare, M.N., Collett, J.R., D'Souza, L.M., Du, Y., Feng, B., Lin, N., Madabasi, L.V., Müller, K.M., 2002. *BMC Bioinformatics* 3 (1), 2.
- CDC, 2011. *MMWR*, 1083–1086.
- Clarridge 3rd, J.E., 2004. *Clinical Microbiology Reviews* 17 (4), 840–862. (table of contents).
- Coenye, T., Vandamme, P., 2003. *FEMS Microbiology Letters* 228 (1), 45–49.
- Elsholz, B., Worl, R., Blohm, L., Albers, J., Feucht, H., Grunwald, T., Jurgen, B., Schweder, T., Hintsche, R., 2006. *Analytical Chemistry* 78 (14), 4794–4802.
- Foudeh, A.M., Fatanat Didar, T., Veres, T., Tabrizian, M., 2012. *Lab on a Chip* 12 (18), 3249–3266.
- Gerasimova, Y.V., Kolpashchikov, D.M., 2012. *Biosensors and Bioelectronics*, 0).
- Hwang, K.-Y., Jeong, S.-Y., Kim, Y.-R., Namkoong, K., Lim, H.-K., Chung, W.-S., Kim, J.-H., Huh, N., 2011. *Sensors and Actuators B: Chemical* 154 (1), 46–51.
- Joung, H.-A., Lee, N.-R., Lee, S.K., Ahn, J., Shin, Y.B., Choi, H.-S., Lee, C.-S., Kim, S., Kim, M.-G., 2008. *Analytica Chimica Acta* 630 (2), 168–173.
- Lazcka, O., Campo, F.J.D., Muñoz, F.X., 2007. *Biosensors and Bioelectronics* 22 (7), 1205–1217.
- Leskelä, T., Tilsala-Timisjärvi, A., Kusnetsov, J., Neubauer, P., Breitenstein, A., 2005. *Journal of Microbiological Methods* 62 (2), 167–179.
- Malic, L., Sandros, M.G., Tabrizian, M., 2011. *Analytical Chemistry* 83 (13), 5222–5229.
- McKilip, J.L., Jaykus, L.-A., Drake, M., 1998. *Applied and Environmental Microbiology* 64 (11), 4264–4268.
- Nelson, B.P., Grimsrud, T.E., Liles, M.R., Goodman, R.M., Corn, R.M., 2000. *Analytical Chemistry* 73 (1), 1–7.
- Nygård, K., Werner-Johansen, Ø., Rønsen, S., Caugant, D.A., Simonsen, Ø., Kanestrøm, A., Ask, E., Ringstad, J., Ødegård, R., Jensen, T., Krogh, T., Høiby, E.A., Raghildstveit, E., Aberg, I.S., Aavitsland, P., 2008. *Clinical Infectious Diseases* 46 (1), 61–69.
- Oh, B.K., Kim, Y.K., Lee, W., Bae, Y.M., Lee, W.H., Choi, J.W., 2003. *Biosensors and Bioelectronics* 18 (5–6), 605–611.
- Riahi, R., Mach, K.E., Mohan, R., Liao, J.C., Wong, P.K., 2011. *Analytical Chemistry* 83 (16), 6349–6354.
- Small, J., Call, D.R., Brockman, F.J., Straub, T.M., Chandler, D.P., 2001. *Applied and Environmental Microbiology* 67 (10), 4708–4716.
- Stephen, K.E., Homrighausen, D., DePalma, G., Nakatsu, C.H., Irudayaraj, J., 2012. *Analyst* 137 (18), 4280–4286.
- Swanson, M., Hammer, B., 2000. *Annual Reviews in Microbiology* 54 (1), 567–613.
- Von Baum, H., Härter, G., Essig, A., Lück, C., Gonser, T., Embacher, A., Brockmann, S., 2010. *Eurosurveillance* 15 (4), 19472.
- Wadowsky, R., Wilson, T., Kapp, N., West, A., Kuchta, J., Dowling, J., Yee, R., 1991. *Applied and Environmental Microbiology* 57 (7), 1950–1955.
- WHO, 2003. pp. 1–24.
- Xie, H., Zhang, C., Gao, Z., 2004. *Analytical Chemistry* 76 (6), 1611–1617.
- Zhou, G., Wen, S., Liu, Y., Li, R., Zhong, X., Feng, L., Wang, L., Cao, B., 2011. *International Journal of Food Microbiology* 145 (1), 293–300.

Sub-femtomole Detection of 16s rRNA from *Legionella Pneumophila*

Using Surface Plasmon Resonance Imaging

*Amir M. Foudeh¹, Jamal S. Daoud¹, Sebastien P. Faucher³, Teodor Veres^{1,4} and
Maryam Tabrizian^{1,2*}*

¹Biomedical Engineering Department, ²Faculty of Dentistry, ³ Department of
Natural Resource Sciences, McGill University, Quebec, Canada, ⁴ National
Research Council of Canada, 75 Boul. de Mortagne, Quebec, Boucherville, Canada

Supplementary Information:

Table S1. Oligonucleotide sequences employed as capture and detector probes.

Name	Sequence 5'--3'
EUB342	ACTGCTGCCTCCCGTAG
Control	TCAATGAGCAAAGGTAT
<i>Legionella pneumophila</i> 1	CAGGTCGCCCCCTTCGCCGCC
<i>Legionella pneumophila</i> 2	TCGCCACTCGCCATCTGTCT
Detector probe Leg1 0bp	CTCTGTATCGGCCATTGTAGC
Detector probe Leg1 7bp	TCGGCCATTGTAGCACGTGTG
Detector probe Leg2 0bp	AGCAAGCTAGACAATGCTGCCGT
Detector probe Leg2 0bp	TAGACAATGCTGCCGTTCGACTTGC
Synthetic <i>Legionella pneumophila</i> 's RNA	UACACACGUGCUACAAUGGCCGAUACAGAGGGCGG CGAAGGGGCGACCUGGAGCAAUCC

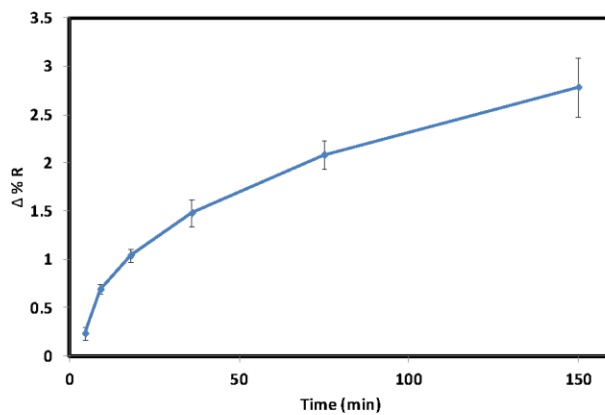


Figure S1. Effect of hybridization time of 10 nM fragmented 16S rRNA with Leg1 Cp on hybridization efficiency. All data is expressed as mean \pm standard deviation (n = 5).

Lab on a Chip



PAPER

View Article Online
View Journal | View Issue



Rapid and multiplex detection of *Legionella's* RNA using digital microfluidics†

Cite this: *Lab Chip*, 2015, 15, 1609

Amir M. Foudeh,^{‡a} Daniel Brassard,^{‡b} Maryam Tabrizian^a and Teodor Veres^{*ab}

Despite recent advances in the miniaturization and automation of biosensors, technologies for on-site monitoring of environmental water are still at an early stage of development. Prevention of outbreaks caused by pathogens such as *Legionella pneumophila* would be facilitated by the development of sensitive and specific bioanalytical assays that can be easily integrated in miniaturized fluidic handling systems. In this work, we report on the integration of an amplification-free assay in digital microfluidics (DMF) for the detection of *Legionella* bacteria based on targeting 16s rRNA. We first review the design of the developed DMF devices, which provide the capability to store up to one hundred nL-size droplets simultaneously, and discuss the challenges involved with on-chip integration of the RNA-based assay. By optimizing the various steps of the assay, including magnetic capture, hybridization duration, washing steps, and assay temperature, a limit of detection as low as 1.8 attomoles of synthetic 16s rRNA was obtained, which compares advantageously to other amplification-free detection systems. Finally, we demonstrate the specificity of the developed assay by performing multiplex detection of 16s rRNAs from a pathogenic and a non-pathogenic species of *Legionella*. We believe the developed DMF devices combined with the proposed detection system offers new prospects for the deployment of rapid and cost-effective technologies for on-site monitoring of pathogenic bacteria.

Received 15th December 2014,
Accepted 23rd January 2015

DOI: 10.1039/c4lc01468e

www.rsc.org/loc

1. Introduction

Water-related diseases are responsible for more than 3.4 million deaths annually.¹ Among these diseases, legionellosis, an acute form of pneumonia, is a major concern for outbreaks, as shown by recent incidents reported in Canada, USA, Norway, and Germany.^{2–4} *Legionella*, the causative agent of this disease, was responsible for more than 30% of water borne disease outbreaks in the USA between 2001–2006.⁵ Legionellosis outbreaks are associated with high mortality rates (15 to 20%),⁶ which can reach up to 50% for individuals with a compromised health condition.⁷ *Legionella* is found in most natural and man-made water systems⁸ such as cooling towers, air conditioners and showerheads. These systems not only provide optimal growth conditions, but can also propagate *Legionella* through aerosol.⁹ Presently, more than 50 *Legionella* species have been identified with approximately half of these species being associated with human

disease.^{10,11} To have an accurate and reliable evaluation of the risk involved with various water systems, it is thus crucial to design detection systems that can distinguish between pathogenic and non-pathogenic *Legionella*. A biosensor for detection of *Legionella* should thus be specific and sensitive with capability of multiplex detection of different bacteria's species. Also, development of on-site systems that are portable, automated, cost-effective and rapid is required to monitor the water systems routinely and better predict any potential outbreaks. Today, detection of *Legionella* continues to rely to a large extent on the conventional culturing method, which is very time-consuming and expensive.

Molecular methods such as polymerase chain reaction (PCR), DNA microarray and immunology have also been used for the detection of *Legionella* in laboratory settings. Automatic robotic liquid handling systems using standard well plates can be used to perform the numerous liquid handling steps required by these methods. These robotic systems can perform at rate of tens of assays per minute. However, they require sample volumes of μL or more. Below this level, evaporation and capillary forces are major issues.¹² In addition the robotic liquid handling systems are very sensitive to the viscosity and nature of the sample solutions. For instance handling solution containing nucleic acid and proteins with high concentrations would be challenging.¹³ Large size, instrumentation complexity and cost are among other major

^a 3775 University Street, Department of Biomedical Engineering, Faculty of Medicine, McGill University H3A 2B4, Montreal, (QC), Canada

^b National Research Council Canada, 75 de Mortagne Blvd., J4B 6Y4 Boucherville, QC, Canada. E-mail: Teodor.Veres@nrc-nrc.gc.ca; Tel: +1 450 641 5232

† Electronic supplementary information (ESI) available. See DOI: 10.1039/c4lc01468e

‡ These two authors made equal contributions.

drawbacks of these robotic systems that make them less practical for field applications such as on-site monitoring. Also, field applications do not necessarily require high speeds and massive parallelisation, but rather precise control over complex protocols with instrumentation that have small footprint and low-cost.

Therefore, miniaturization of pathogen detection methods and their integration in microfluidic devices has been gaining much attention as it can not only lead to the reduction of reagent consumption and analysis time but can also facilitate on-site deployment of chemical and biological assays.¹⁴ Digital microfluidics (DMF) has recently arisen as a promising and versatile platform for chemical and biological applications. In DMF, as opposed to continuous flow microfluidics, individual droplets (of pL to μ L) are manipulated independently by applying electric potential to an array of electrodes. Multiple droplets containing different reagents can be manipulated simultaneously and the operation scheme can be reprogrammed without the need to change the device design. Each droplet can thus act as microreactor from which independent tests can be performed concurrently in a confined environment, therefore making DMF a promising candidate for applications involving complex and multistep assays.¹⁵ Also, compared to conventional continuous flow microfluidic devices using fixed channel arrangements, the very high reconfigurability of DMF can help improving assay optimization and decrease development costs. On the other hand, until recently, most DMF devices were primarily designed and utilized for simple assays requiring only a few steps and limited number of droplets. The developed devices thus typically lacked the complexity required to perform multiplexed bioassays in which numerous tests must be performed concurrently.

While different bioassays have been performed using DMF, including immunoassays,¹⁶ cell culture,¹⁷ DNA hybridization,¹⁸ PCR¹⁹ and isothermal amplification,²⁰ most pathogen detection assays were based on either immunoassay or DNA hybridization and PCR amplification. Even if PCR and other amplification techniques provide rapid results with high sensitivity, they are susceptible to inhibitors, which is a key issue for samples coming from environmental water systems. Another major drawback for the DNA-based and immunoassay techniques is their inability to distinguish between live and dead bacteria. This is a major concern in environmental water settings because of the false-positive results that can occur after water treatments. In contrast, targeting ribosomal RNA (rRNA) is a viable alternative that overcomes the aforementioned shortcomings. Indeed, since RNA expression level is directly correlated to the microbial activity, it provides a more reliable and accurate target for detection of live *Legionella*.²¹

There have been only few attempts to develop detection assays in DMF based on RNA. For example, Jebrail *et al.*²² demonstrated the feasibility of RNA extraction from blood using magnetic beads within a DMF device. In another recent work, Rival *et al.*²³ performed single cell analysis using micro

RNA from human HaCaT cells followed by mRNA capture on magnetic beads, mRNA conversion to DNA and Reverse Transcriptase PCR (RT-PCR) amplification. The use of RT-PCR, even if it provides high sensitivity, can require elaborate sample preparation steps, expensive enzymes and reagents, and precise control of the temperature, making this method less desirable for on-site applications.

In this work, we report the multiplex and amplification-free detection of synthetic 16S rRNA from *Legionella* bacteria using DMF devices capable of handling complex assays. We present the design and conception of the DMF devices, demonstrate simultaneous manipulation of multiple droplets on-chip and investigate the optimal hybridization conditions and limit of detection for *L. pneumophila* 16S rRNA. We additionally demonstrate that the developed assay, which is based on two sets of DNA as capture and detector probes, can achieve a high degree of selectivity by showing the multiplex detection of rRNA from two different species of *Legionella*, one pathogenic (*L. pneumophila*) and one non-pathogenic (*L. israelensis*). We believe the DMF device combined with the proposed detection system have great potential for rapid, high-throughput, multiplex, and inexpensive detection of pathogens with minimal sample and reagent volume.

2. Results and discussion

2.1 Design of the DMF devices

The integration of multiplex protocols in DMF requires the development of devices that can manipulate and store multiple droplets simultaneously to perform the dilution, mixing and analysis steps required by the assay. Unfortunately, it is challenging to design and fabricate DMF devices containing enough active electrodes to handle complex protocols while simultaneously keeping fabrication cost and process complexity low enough for typical biomedical applications. To simplify the fabrication of the devices, we have developed a process where negative SU-8 photoresists is used directly as the dielectric for the fabrication of advanced DMF requiring multiple levels of metallization (see Materials and methods section for more details).²⁴ We have indeed found that SU-8 not only offers good electrical properties (dielectric breakdown ~ 4 MV cm^{-1} and relative dielectric constant of about 4), but also ease of deposition and patterning, long term resistance to humid environment and saline buffers, resistance to scratches and pinhole formation, and good temperature stability.

The design of the developed DMF devices is shown in Fig. 1a. The device contains 560 active electrodes, 7 reservoirs and multiple regions for mixing and sample preparation. The device also includes enough storage regions to hold up to 100 individual droplets, as we have found that the maximum assay complexity that can be integrated in DMF is often limited by the maximum number of droplets that can be stored simultaneously on-chip. It is noteworthy that the DMF device shown in Fig. 1 is capable of handling assays even more complex than those demonstrated in this paper. This was done on

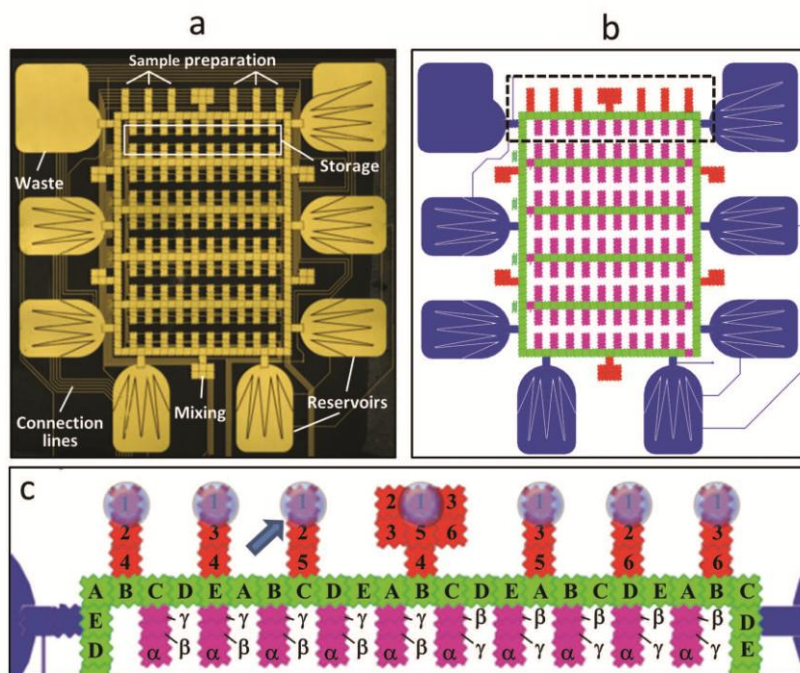


Fig. 1 a) Top view of the developed digital microfluidic device. b) Schematic of electrical input pin to electrowetting electrode assignment. Each color represents a partition to which specific input pins are assigned. The partitions were defined according to the functions of the electrowetting electrodes: dispensing (blue), transportation (green), preparation (red), and storage (purple). c) Example of pin assignment in top section of the chip, each number/letter representing a specific electrical input.

purpose to so as to take full advantage of the very high reconfigurability of DMF, where only one chip can be easily designed to handle the needs of various different assays by simply changing the droplet programming sequence.

To limit the complexity of the electronic circuits and facilitate electrical connection to the device, we have limited the number of independent electrical inputs to only 24. Thus, each electrical input is connected simultaneously to multiple active electrodes by using connection lines placed on a different metallization level. The assignment of the electrical inputs to each active electrode has to be cleverly designed to avoid as much interferences as possible when multiple droplets are on the DMF devices simultaneously. To minimize unwanted interactions between the fluidic operations, the input-to-electrode assignment has been divided into partitions²⁵ according to the function of the electrodes (see Fig. 1b): 8 electrical input pins were assigned for dispensing (blue), 5 pins for transportation (green), 6 pins for preparation (red), 4 pins for storage (purple), and 1 pin is connected to top plate (not shown). As shown in Fig. 1c, the pin assignment within each partition has also been optimized to maximize interdependence of fluidic operations when multiple droplets are

located in the same partition. For example, to move only the droplet marked with an arrow from the sample preparation to the transportation partition, the electrical input pins would be actuated as follow: 2 - 5 - 1 - C. The input pins are also assigned in a similar manner in the storage region, except that smaller active electrodes (labelled γ and β) are used to minimize the real estate of the device. Finally, the distribution of the 8 independent electrical pins within the reservoir partition (blue color in Fig. 1b), ensures that a droplet can be dispensed independently from each reservoir.

2.2 Assay design and optimization

Due to presence of many species of *Legionella*, it is critical to design assays with a high selectivity capable of differentiating pathogenic from non-pathogenic species. As shown schematically in Fig. 2a, we have developed an assay based on the hybridization of *Legionella*'s 16s rRNA on magnetic beads. In order to achieve high specificity, two DNA probes were designed for each target. One probe served as a capture probe and was immobilized on magnetic beads while the second probe, in addition to ensuring the high specificity, is used as

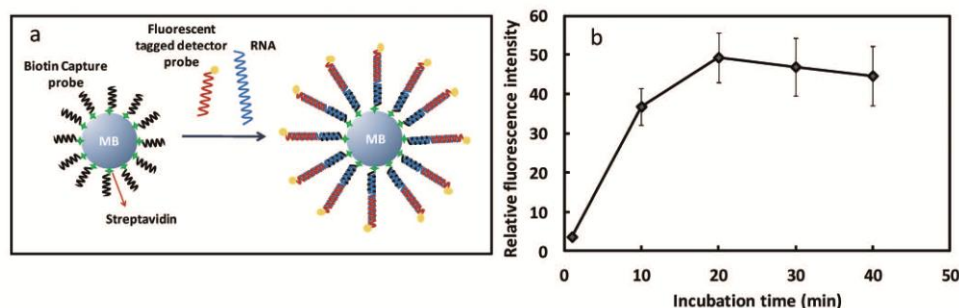


Fig. 2 a) Schematic showing the hybridization of target RNA on the magnetic beads using designed capture and detector probes. b) Effect of the incubation time on the detected fluorescence intensity for on-chip hybridization assays performed at a concentration of 100 nM target RNA.

a detector probe functionalized with a fluorescent dye (Fig. 2a).

Before integrating the assay in the DMF devices, different critical parameters were evaluated to obtain the highest hybridization efficiency with minimum analyte consumption, and the shortest assay time. The following factors were also considered: hybridization buffer composition, temperature, reaction volume, and the incubation time. Among these factors, buffer composition and temperature were found to play an important role in specificity and sensitivity of the hybridization. We previously²¹ demonstrated that the 600 mM salt concentration in the neutral pH buffer at 37 °C for the *L. pneumophila* RNA-DNA hybridization resulted in the highest specificity. As discussed in the Materials and methods section, all on-chip assays have thus been performed at a temperature of 37 °C.

To validate the on-chip 16s rRNA hybridization protocol and optimize the speed of on-chip assays, we have first performed a series of simple on-chip measurements to assess the effect of incubation time on hybridization efficiency. For on-chip tests, *L. pneumophila* 16s rRNA and the detector probes were first mixed together off-chip. Then, for each incubation time reported in Fig. 2b, one droplet of a 100 nM RNA solution was dispensed and mixed on-chip with one droplet containing magnetic beads coated with immobilized capture probes. As described more in details in section 2.3, the mixed droplet was washed six times and fluorescent measurements were carried out immediately. As can be seen in Fig. 2b, the intensity of fluorescence increased from one minute up to 20 minutes after which fluorescent signal is seen to saturate. Therefore, we chose 20 minutes as the optimal incubation time for further experiments.

The reaction volume of the RNA sample on which the detection experiment is performed is another key factor that can affect the results of the detection assay. In conventional laboratory experiments, the reaction volume is typically on the order of tens of μL or higher. On the other hand, by integrating the assay into DMF devices, we were able to reduce the reaction volume required for one hybridization assay to

only 30 nL (*i.e.*, only two individual droplets). It is also noteworthy that, due to the small electrodes of our DMF devices (0.5×0.5 mm), this volume is also smaller by a factor of 10 to 100 times compared with other reported reaction volumes for bioanalytical assays performed in DMF.^{15,20,23} The developed integrated assay thus offers the interesting prospect to significantly decrease both the reagent consumption and minimal sample volume. In particular, the reduced consumption of streptavidin coated magnetic beads to only 15 nL per hybridization assay (about 3600 particles) offers the potential to reduce the cost of each assay. On the other hand, the reduced sample volume can obviously impact the ultimate limit of detection of the assay. We show next how the limit of detection of the developed assay has been evaluated by performing serial dilutions on-chip.

2.3 On-chip serial dilution and hybridization

To evaluate the limit of detection of the assay in DMF devices, we have performed on-chip the protocol shown schematically in Fig. 3. Fig. 4 shows sequential images illustrating the various steps required to perform this protocol in DMF. The first steps, which are summarized in Fig. 3a and 4a, involve the generation of sample droplets containing a series of different concentrations. One droplet from the RNA reservoir is first dispensed and transported to the mixing area. Next, another droplet is dispensed from the buffer reservoir and transferred to the same mixing area. In the mixing area, the two droplets are mixed with rapid circular movements and split into two identical daughter droplets, one of which is moved either to the storage area for later use or to the waste reservoir (depending on the targeted concentration profile). The other daughter droplet is kept at the mixing area for another dilution step with a droplet from the buffer reservoir. In this way, an exponential dilution series of the original droplet is obtained. For the developed assay, droplets having nominal concentrations of 500 nM, 125 nM, 8 nM, 1.0 nM, 0.5 nM and 0.12 nM were analyzed.

It is noteworthy that any variation in the volume of the dispensed droplets will introduce some errors on the RNA

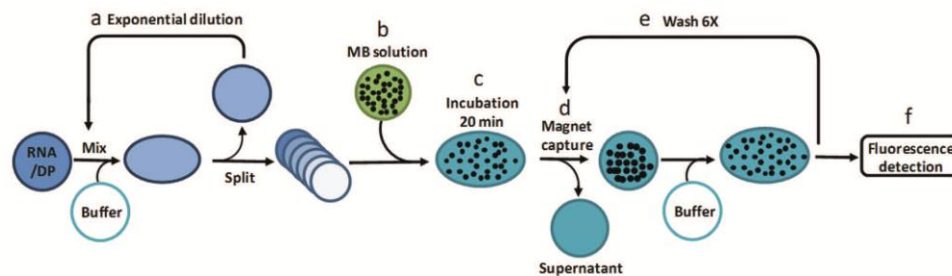


Fig. 3 Schematics protocol showing the serial dilution and hybridization of 16s rRNA on the DMF devices. a) Creation of the exponential dilution of the RNA sample into six concentrations. b) Mixing of the diluted RNA droplets with the magnetic beads. c) Incubation of the magnetic beads with six concentrations of 16s rRNA. d) Capture of magnetic beads and separation of supernatant e) Six times washing of magnetic beads. f) Fluorescent measurement.

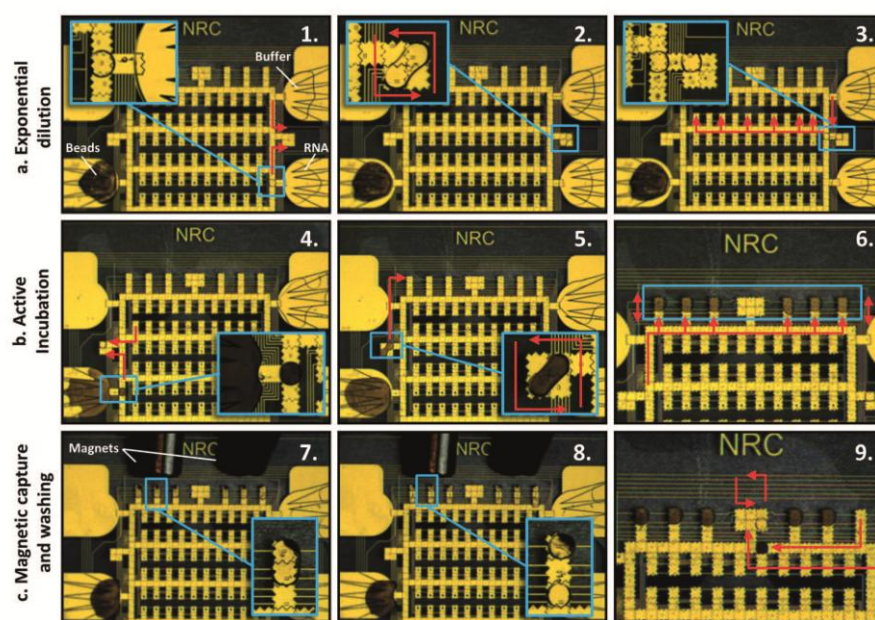


Fig. 4 Top view image sequence showing the digital microfluidic protocol used for the RNA serial dilution and hybridization assay. a) Creation of the exponential dilution profile of the RNA sample into 6 droplets (1. to 3.). b) Mixing of the diluted RNA droplets with the magnetic beads and incubation (4. to 6.). c) Magnetic capture and washing of the incubated droplets (7. to 9.).

concentration in the dilution series compared with nominal values. In our DMF devices, we have found the dispensed droplets have an average volume of 15.3 nL with a standard deviation of about 0.4 nL (about 3%). This variability on the droplet volume accumulates through the dilution protocol and can thus give rise to significant uncertainties on the RNA concentration for the higher dilutions. By

propagating the standard deviation of droplet volume on the 13 dilutions steps required to decrease the RNA concentration from 1 μM to 0.12 nM, it is possible to show that the relative error (standard deviation) on the concentration reaches about 30% (see ESI† for a detailed analysis). We believe that this error is small enough not to affect the outcome of the assay.

As shown in Fig. 3b–c and 4b, each droplet from the dilution series is then actively incubated with magnetic beads. To that end, one droplet from the reservoir containing the magnetic beads functionalized with *L. pneumophila* CP probe is first dispensed and transferred to the adjunct mixing area. In the next step, one of the droplets from the dilution series of *L. pneumophila*'s RNA is transferred from the storage area to the same mixing area.

After mixing, the new larger mixed droplet is transferred to sample preparation area. Subsequently, all of the six *L. pneumophila*'s RNA concentrations are mixed with magnetic beads and transferred to the sample preparation area. The droplets are incubated for around 20 minutes during which they are slowly moved on the sample preparation area to create fluid recirculation, minimize sedimentation and maximize the hybridization efficiency.

Finally, as shown in Fig. 3d–e and 4c, the magnetic particles are captured and washed to remove the un-hybridized RNA. To capture the magnetic beads, two 2.5 mm diameter cylindrical neodymium rare-earth magnets are positioned on top of the DMF chip (each magnet is located in the center top of the three sample preparation electrodes – see Fig. 4c). The magnets are positioned to attract and concentrate the magnetic beads on the top part of the droplet. After capture of the magnetic beads, all the six droplets are split simultaneously into the two daughter droplets and the droplets containing the supernatant are transferred to the waste reservoir. The magnets are then removed temporarily and each droplet containing the magnetic beads are washed by (i) transferring them one at a time to the mixing area located on top of the chip and (ii) mixing them with one droplet from the buffer reservoir. The mixed droplet is then transferred back to its previous location in the sample preparation area. The capture and wash sequence of the magnetic beads is repeated for a total of six times.

In general, to capture and separate magnetic beads in a droplet, the magnetic force should be sufficient enough to capture the magnetic particles but not too strong as to cause irreversible particle aggregation.^{15,26,27} As described, the two permanent magnets placed on top of the DMF allowed concentrating efficiently the magnetic beads on top of the droplets, removing supernatant and performing several washes. On the other hand, we observed that sedimentation of the magnetic particles on the bottom plate of the device could make capturing the magnetic beads difficult. In order to alleviate this issue, we implemented a new strategy to improve capture and separation of the magnetic beads. In this strategy, the droplet was spread on two electrodes on top of the sample preparation area by activating both electrodes in the presence of magnets (Fig. 4-7). This was followed by switching on and off only the top electrode while the bottom electrode was kept activated. This switching was found to facilitate the re-capture of sedimented magnetic beads while ensuring that the pellet of captured magnetic beads remained intact. To achieve acceptable particle separation, a frequency around 7 Hz was used for the switching process.

We hypothesize that the switching creates fluid recirculation inside the droplets, which causes the sedimented particles to be resuspended in solution and captured by magnet. Finally, it is noteworthy that the use of Pluronic F-127 in the buffer solutions was also found to improve the re-suspension of the particles after magnetic capture.

The choice of the washing protocol should also be considered when separating the un-hybridized RNA and detector probes from the magnetic beads. In our experiments, we observed that a total of six washes with 1 : 1 ratio of buffer to sample were sufficient in removing the supernatant from magnetic particles before fluorescence measurement. This number of washes is also in accordance with a similar reported protocol.¹⁵ In this method, the magnet was manually removed after the 'capture and separation' step and the droplet containing magnetic beads was re-suspended in wash buffer droplet in the mixing area (Fig. 4-9). The removal of the magnet ensures that there won't be any entrapment of the unhybridized RNAs and detector probes in the pellet of the captured magnetic beads. We hypothesize that this is advantageous compared to other previously reported methods where the magnet was at the same place throughout the whole washing process. For example, when the magnet position is kept constant, it has been reported that up to 18 washes are required³⁸ when the buffer to sample ratio is of 1 : 1 and 5 washes²⁶ for a buffer to sample ratio of 5 : 1.

2.4 Limit of detection for *L. pneumophila*'s RNA

As described earlier, six different concentrations of the *L. pneumophila*'s RNA ranging from 0.5 μ M to 122 pM were made on the DMF chip and hybridized with functionalized magnetic beads for twenty minutes at 37 °C. After six times washing with buffer, the fluorescent intensity for each droplet was measured directly on-chip and subtracted from the negative control. As can be seen in Fig. 5, the developed

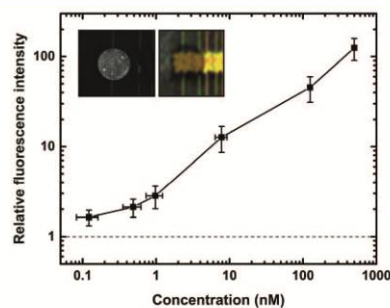


Fig. 5 Measured relative fluorescent intensity versus *L. pneumophila*'s RNA concentration using superparamagnetic beads and Cy3 fluorescent tagged detector probe (see ESI† for the calculation of the error on the concentration). Inset: a bright-field and fluorescent images of a droplet containing captured RNA onto the magnetic beads.

system could successfully detect 16s rRNA at concentrations as low as 122 pM in less than 30 minutes. Considering the 15 nL volume of the RNA droplet, this amount is equivalent to 1.8 attomoles of 16s rRNA. Due to the very low dead volumes offered by the proposed system, the LOD in terms of absolute amount is thus around 250 to 10 000 times less than the LOD reported for 16s rRNA using amplification-free detection systems such as SPRI,²¹ and electrochemical²⁹ techniques respectively. Moreover, with a total analysis time of only 30 minutes, the system provides a measurement 6 times faster than the aforementioned methods. One of the limiting factors in our sensitivity was the auto-fluorescence of the DMF device, which interfered with the signal obtained from the droplet at low concentrations. We believe that, by alleviating this problem (for *e.g.*, by choosing materials with lower auto-fluorescence), the signal-to-noise ratio and the LOD could even be increased further. Finally, it is also worthwhile noting that the developed assay offers a rather large dynamic range, providing a regular signal increase for more than three orders of magnitude of RNA concentration (Fig. 5).

2.5 Multiplex detection of pathogenic and non-pathogenic *Legionella*

As described in the introduction, the multiplex detection and ability to distinguish the pathogenic from non-pathogenic bacteria is a critical feature required for monitoring environmental water samples. Thus, in addition to *L. pneumophila*, we designed a series of capture and detector probes targeting the 16s rRNA from *L. israelensis* as a non-pathogenic *Legionella* species, since there is no report of human disease from this species.

In order to perform the multiplex detection of these two target RNAs, the detector probe specific to *L. israelensis* (*Li*) was functionalized with Cy5 dye in contrast to the *L. pneumophila*'s (*Lp*) detector probe which was tagged with Cy3 dye. Two sets of functionalized MB with a concentration of 2.4×10^8 particles mL⁻¹ were also prepared, each with one of the two capture probes (*Lp* MB and *Li* MB).

For the multiplex protocol, the on-chip incubation, magnetic separation, and washing steps were performed in a similar manner to the exponential dilution protocol discussed before (see Fig. 4). However, in this case, RNA concentration was fixed at 100 nM and two additional reservoirs were used for the *Li* MBs and for *Li* RNAs. Also, instead of performing a dilution series, fluidic operations were such that the two different types of functionalized magnetic beads (*i.e.*, *Lp* MB and *Li* MB) were each hybridized with three different RNA samples prepared by mixing (i) a *Lp* droplet with a buffer droplet, (ii) a *Li* droplet with a buffer droplet and (iii) a *Lp* with a *Li* droplet. A total of six different hybridization measurements were thus performed to evaluate the specificity of the developed assay.

Fig. 6 shows the resulting measured fluorescence intensity for the six hybridization tests for both the Cy3 and Cy5 filters (corresponding respectively to the dyes of *Lp* and *Li* detector

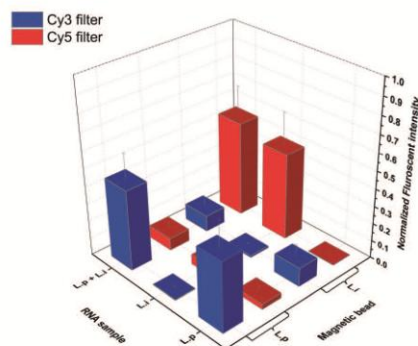


Fig. 6 Multiplex detection of *Legionella* 16s rRNAs including pathogenic, *L. pneumophila* (*Lp*) and non-pathogenic *L. israelensis* (*Li*). Detector probe specific to *Lp* RNA sample was tagged with Cy3 dye while the detector probe specific to *Li* RNA sample was tagged with Cy5 dye. Three RNA samples including *Lp*, *Li* and mixture of *Lp* and *Li* were incubated with two types of magnetic beads functionalized with either *Li* or *Lp* capture probes. The fluorescent measurements were carried out with Cy3 and Cy5 filters for each droplet.

probes). As expected, the reaction of *Lp* RNA with *Lp* MB resulted in a significant fluorescent signal only with Cy3 filter, indicating that only *Lp* detector probes hybridized significantly to the beads. The opposite trend was observed for the reaction of *Li* RNA with *Li* MB, which resulted in a strong signal only in Cy5 filter (*i.e.*, only *Li* detector probe was hybridized). On the other hand, much smaller signals were measured in both Cy3 and Cy5 filters when *Lp* RNA was incubated with *Li* MB or when *Li* RNA was incubated with *Lp* MB, indicating that neither the *Lp* detector probes nor the *Li* detector probes were hybridized to the beads. Finally, for the mixed sample containing both *Lp* and *Li* RNA, the normalized fluorescent intensities for Cy3 and Cy5 filters were in the same level as those obtained for *Lp* RNA with *Lp* MB and *Li* RNA with *Li* MB respectively. In summary, these results confirm that the developed assay based on two sets of independent capture and detector probes can achieve a specificity high enough to discriminate between RNA from two *Legionella* species.

3. Conclusion

We have shown the successful integration of a multiplex RNA assay in DMF for the specific detection of *Legionella* species using 16s rRNA targets. An advanced DMF platform was designed to integrate the developed assays, which offered the possibility to perform on-chip complex fluidic manipulations with multiple droplets. The various steps of the assays, including magnetic capture, hybridization duration, washing steps, and assay temperature were first optimized. The advanced fluidic capabilities of the platform were then used to perform exponential dilutions to evaluate, in the same

Table 1 Oligonucleotide sequences employed in the experiments

Name	Sequence 5'–3'
<i>L. pneumophila</i> CP	/Biotin/TTTTTTTTTCAGGTCGCCCTTCGCCGCC
<i>L. israelensis</i> CP	/Biotin/TTTTTTTTTGGCCAGGCCATAAGGTCCC
<i>L. pneumophila</i> DP	CTCTGTATCGGCCATTGTAGCTTTTTTTTT/Cy3/
<i>L. israelensis</i> DP	CAGCTTACTCCAAGAGCATATGCGGTTTTTTTT/Cy5/
<i>L. pneumophila</i> 's RNA	UACACACGUGCUACA AUGGCCGAUACAGAGGGCGCGAAGGGGCGACCUAGGAGCAAUCC
<i>L. israelensis</i> RNA	CTAATACCGCATATGCTCTTTGGAGTAAAGCTGGGGACCTTATGGCTGGCGCTTAAAGA

assay and under the identical condition, the signal from multiple RNA concentrations. We have shown that, by integrating the assay in DMF devices, we were able not only to reduce drastically reagent and magnetic beads consumption, but also to decrease the minimum amount of RNA required to achieve positive sample identification to about only 1.8 attomoles, which demonstrates the potential of the developed system to achieve amplification-free detection based on 16S RNA. Finally, we have shown that specific detection for pathogenic and non-pathogenic species of *Legionella* can be achieved by using capture and detector DNA probes for each 16S rRNA target. We have thus demonstrated a proof of concept for the automated multiplex detection of pathogenic and non-pathogenic *Legionella* in DMF.

The developed DMF devices also offer the interesting prospect to simplify the sample preparation steps required to extract and purify RNA from bacteria. Because of the high specificity of the detection system and the possibility to hybridize the magnetic beads and target rRNA directly within the crude cell lysate, we envisage that all the sample preparation and hybridization steps could be performed on-chip using thermal lysis. By integrating sample preparation, the proposed detection and fluid manipulation system could thus be used as a versatile tool for high-throughput and multiplex detection of several types of bacteria with minimum reagent consumption.

4. Materials and methods

4.1 Chemical and reagent

BioMag Streptavidin coated superparamagnetic beads were purchased from Bangs Laboratories (Fishers, IN, U.S.A.). Pluronic F-127 was purchased from Sigma-Aldrich (St. Louis, MO, U.S.A.). Oligonucleotides were purchased from Integrated DNA Technologies (Coralville, IA, U.S.A.). SSPE buffer (20× buffer is 3.0 M NaCl, 0.2 M NaH₂PO₄, and 0.02 M EDTA at pH 7.4), was purchased from Invitrogen (Carlsbad, CA, U.S.A.). Silicone oil (viscosity of 2 cSt) was purchased from Clearco (Bensalem, PA U.S.A.), SU8 photoresists from Gersteltec (Pully, Switzerland) and Teflon AF from Dupont (Mississauga, ON, Canada).

4.2 DMF device fabrication

The DMF devices were fabricated by first depositing and patterning, by standard lithography, layers of 10 nm thick Cr and 100 nm thick Au on a borosilicate glass wafer to form a

network of contact pads and 200 μm wide connection lines. A first layer of about 5 μm thick SU8 dielectric was then deposited by spin-coating and UV exposed through a mask to open interconnection vias in specific locations. A second layer of Cr and Au was then patterned on top of the first dielectric layer to form the 500 × 500 μm active electrodes and reservoirs of the devices. The electrodes were finally covered with a second layer of about 2.5 μm thick SU8 dielectric and a thin 30 nm layer of hydrophobic coating based on Teflon AF. The top plate of the devices was made by covering ITO-coated plate (Delta technologies, Stillwater, MN, USA) with the same hydrophobic coating. As a final step, the DMF devices were finally post-baked at 200 °C for 2 h.

4.3 Microfluidic platform and DMF device operation

The DMF devices were powered with a home-developed AC voltage source capable of amplifying the 5 V DC voltage from a USB connection to a 0.3 to 3 kHz square-wave of 0 to 150 V. The use of AC voltage minimizes the amount of charge trapping occurring inside the dielectric of the devices compared to DC voltage, thus improving both the reliability of droplet displacement and DMF lifetime. A typical operation voltage of about 85 V RMS at 1 kHz was used for droplet displacements, which was found to provide reliable droplet displacement at a speed of 10 electrodes per second. The 24 independent electrical inputs of the devices were contacted with a custom clip made from spring-loaded pogo-pins. A home-developed software providing advanced sequence programming capabilities have been developed to control the electrical inputs and automate the droplet displacements.

The devices were filled by dispensing droplets of about 1 μl on the bottom electrodes forming the reservoir of the DMF devices using a pipette. Before reservoir filling, a small amount (*i.e.*, <0.1 μl) of silicone oil was applied on the reservoir by touching the device with a tip of a pipette as discussed elsewhere,³⁰ the oil naturally forms a thin shell around the droplets, which has been shown to facilitate droplet displacements and improve device reliability. The top plate of the device is then electrically grounded and put in place along with a spacer providing a constant gap of about 70 μm. Individual droplets of about 15 nL are then dispensed from the reservoirs of the devices by applying a sequence of voltage on the electrode of the DMF devices. The temperature was controlled by mounting the DMF devices on a thermoelectric element connected to an H-bridge electrical circuit

controlled by an Arduino microcontroller in communication with a computer. While performing the RNA assay, the temperature in the DMF devices was kept constant at 37 °C to favor hybridization. To minimize the evaporation of the small 15 nL droplets, DI water was dispensed around the edge of the DMF devices. In this configuration, only marginal evaporation was observed for the duration of the assay (about 30 min). No significant evaporation of the thin oil shell around the droplets was observed.

Many reagents used in biological applications such as proteins are susceptible to non-specific adsorption to the hydrophobic layer of the DMF devices, increasing dragging forces and eventually preventing droplet displacement.³¹ In our experiments, we have found that the droplets containing the streptavidin-coated paramagnetic beads could not be manipulated reliably despite the presence of an oil shell around the droplet. Reliable droplet displacement was obtained by adding Plutonic F127 to the solutions with final concentration of 0.01% (v/v).

4.4 DNA probe design and hybridization condition

DNA capture probes (CP), complementary to *L. pneumophila* and *L. israelensis*'s 16S rRNA, were designed using bioinformatics software packages from Cardiff University, England. Particular features such as loops and hairpins, were checked for and avoided. The specificity of these probes was confirmed using the Check Probe program and Ribosomal Database Project (RDP). In terms of detection probes, a fluorescent tagged DNA probe with zero base pair gap between the capture and detection probes (DP) for each target RNA sequence was designed. Cy3 (excitation at 550 nm, emission at 570 nm) and Cy5 (excitation at 649 nm, emission at 670 nm) dyes were used for *L. pneumophila* and *L. israelensis* detector probes respectively. The length of each detector probe was determined to ensure similar melting temperatures while avoiding cross-reactivity and hybridization to any capture probes. The cross reactivity of these detector probes was tested against the capture probe, revealing no significant interaction (data not shown). Two RNAs (60 bp in length) from the *L. pneumophila* and *L. israelensis*'s 16S rRNA, which contains complementary sequences for the designed capture and detector probes, were synthesized by Integrated DNA Technology (Table 1).

4.5 Microparticle preparation and signal measurement

The hybridization buffer was chosen based on previously reported work.²¹ Briefly all the reagents were diluted in 4× SSPE buffer containing 600 mM NaCl and hybridization experiments were carried out at 37 °C inside the DMF chip.

Before the start of the assay, the streptavidin coated superparamagnetic particles (MB) were washed off-chip three times with 4× SSPE buffer containing 0.01% pluronic F-127 and were concentrated to the final concentration of 2.2 mg mL⁻¹ (2.4 × 10⁸ particles mL⁻¹). In order to immobilize the biotin capture probes on magnetic beads, an excess amount of DNA capture probe (4 μL of 100 μM) was incubated off-chip with

100 μL of the magnetic bead solution for 15 min at room-temperature. This was followed by three times washing with 4× SSPE buffer. The same protocol was used for the preparation of the MB used in the capture of *L. pneumophila* and *L. israelensis*. The functionalized beads were kept at 4 °C before use.

An inverted fluorescence microscope (Nikon TE 2000-E) was used for measurement of the fluorescence intensity of the droplets inside the chip. All images were captured using a CCD camera and analyzed by ImageJ (National Institutes of Health, Bethesda, MD). The fluorescent measurements were carried out on the chip by locking at the target droplet under the microscope. All measurements were subtracted by the intensity obtained from a negative control. The negative control droplet contained magnetic beads with the detector probe and was washed six times using the same protocol as the other droplets. For the multiplex detection of RNA, the fluorescent intensities for each sample were normalized for each filter independently by the positive control (the mixture of the magnetic bead, RNA and proper detector probe). The lower detection limit was defined as the smallest concentration of an analyte, calculated as the blank signal plus or minus three standard deviations. All data were expressed as the mean ± standard deviation.

Acknowledgements

We acknowledge National Science and Engineering Research Council of Canada strategic Research program, National Research Council of Canada, Genome Canada/Genome Quebec, Nano-Quebec, Le Fonds Québécois de la Recherche sur la Nature et les Technologies, Centre for Biorecognition and Biosensors and Magnus company for their financial support. The authors would also like to thank Dr. X. Zhang for scientific discussion, and Dr. M. Mekhail and K. Jahan for their comments on the manuscript, M. Mounier, C. Miville-Godin and K. Côté for their technical assistance in the fabrication of the DMF devices and F. Normandin for the development of the Lab-view control software.

References

- 1 World Health Organization, *World Water Day Report 2000*, World Health Organization, Genève, 2000.
- 2 CDC, *Centers for Disease Control and Prevention*, 2011, pp. 1083–1086.
- 3 K. Nygård, Ø. Werner-Johansen, S. Rønsen, D. A. Caugant, Ø. Simonsen, A. Kanestrøm, E. Ask, J. Ringstad, R. Ødegård, T. Jensen, T. Krogh, E. A. Høiby, E. Ragnhildstveit, I. S. Aaberge and P. Aavitsland, *Clin. Infect. Dis.*, 2008, **46**, 61–69.
- 4 H. Von Baum, G. Härter, A. Essig, C. Lück, T. Gonser, A. Embacher and S. Brockmann, *Euro Surveill.*, 2010, **15**, 19472.
- 5 G. F. Craun, J. M. Brunkard, J. S. Yoder, V. A. Roberts, J. Carpenter, T. Wade, R. L. Calderon, J. M. Roberts, M. J. Beach and S. L. Roy, *Clin. Microbiol. Rev.*, 2010, **23**, 507–528.
- 6 P. Delgado-Viscogliosi, L. Solignac and J.-M. Delattre, *Appl. Environ. Microbiol.*, 2009, **75**, 3502–3512.

- 7 M. Swanson and B. Hammer, *Annu. Rev. Microbiol.*, 2000, **54**, 567–613.
- 8 R. Wadowsky, T. Wilson, N. Kapp, A. West, J. Kuchta, J. Dowling and R. Yee, *Appl. Environ. Microbiol.*, 1991, **57**, 1950–1955.
- 9 B. S. Fields, R. F. Benson and R. E. Besser, *Clin. Microbiol. Rev.*, 2002, **15**, 506–526.
- 10 G. Yang, R. F. Benson, R. M. Ratcliff, E. W. Brown, A. G. Steigerwalt, W. L. Thacker, M. I. Daneshvar, R. E. Morey, A. Saito and B. S. Fields, *Int. J. Syst. Evol. Microbiol.*, 2012, **62**, 284–288.
- 11 D. Kusić, B. Kampe, P. Rösch and J. Popp, *Water Res.*, 2014, **48**, 179–189.
- 12 J. J. Agresti, E. Antipov, A. R. Abate, K. Ahn, A. C. Rowat, J.-C. Baret, M. Marquez, A. M. Klibanov, A. D. Griffiths and D. A. Weitz, *Proc. Natl. Acad. Sci. U. S. A.*, 2010, **107**, 4004–4009.
- 13 S. C. Chai, A. N. Goktug, J. Cui, J. Low and T. Chen, *Practical Considerations of Liquid Handling Devices in Drug Discovery*, 2013.
- 14 A. M. Foudeh, T. Fatanat Didar, T. Veres and M. Tabrizian, *Lab Chip*, 2012, **12**, 3249–3266.
- 15 A. H. C. Ng, K. Choi, R. P. Luoma, J. M. Robinson and A. R. Wheeler, *Anal. Chem.*, 2012, **84**, 8805–8812.
- 16 E. M. Miller, A. H. C. Ng, U. Uddayasankar and A. R. Wheeler, *Anal. Bioanal. Chem.*, 2011, **1**–9.
- 17 I. Barbulovic-Nad, S. H. Au and A. R. Wheeler, *Lab Chip*, 2010, **10**, 1536–1542.
- 18 L. Malic, M. G. Sandros and M. Tabrizian, *Anal. Chem.*, 2011, **83**, 5222–5229.
- 19 Y. H. Chang, G. B. Lee, F. C. Huang, Y. Y. Chen and J. L. Lin, *Biomed. Microdevices*, 2006, **8**, 215–225.
- 20 M. Kuhnemund, D. Witters, M. Nilsson and J. Lammertyn, *Lab Chip*, 2014, **14**, 2983–2992.
- 21 A. M. Foudeh, J. T. Daoud, S. P. Faucher, T. Veres and M. Tabrizian, *Biosens. Bioelectron.*, 2014, **52**, 129–135.
- 22 M. J. Jebrail, A. Sinha, S. Vellucci, R. F. Renzi, C. Ambriz, C. Gondhalekar, J. S. Schoeniger, K. D. Patel and S. S. Branda, *Anal. Chem.*, 2014, **86**, 3856–3862.
- 23 A. Rival, D. Jary, C. Delattre, Y. Fouillet, G. Castellan, A. Bellemin-Comte and X. Gidrol, *Lab Chip*, 2014, **14**, 3739–3749.
- 24 D. Brassard, L. Malic, C. Miville-Godin, F. Normandin and T. Veres, *IEEE 24th International Conference on Micro Electro Mechanical Systems (MEMS)*, 2011, pp. 153–156.
- 25 Y. Zhao and K. Chakrabarty, Pin-Count-Aware Online Testing of Digital Microfluidic Biochips, in *Proceedings of the IEEE VLSI Test Symposium*, 2010, pp. 111–116.
- 26 R. S. Sista, A. E. Eckhardt, V. Srinivasan, M. G. Pollack, S. Palanki and V. K. Pamula, *Lab Chip*, 2008, **8**, 2188–2196.
- 27 W. Yizhong, Z. Yuejun and C. Sung Kwon, *J. Micromech. Microeng.*, 2007, **17**, 2148.
- 28 R. Sista, Z. Hua, P. Thwar, A. Sudarsan, V. Srinivasan, A. Eckhardt, M. Pollack and V. Pamula, *Lab Chip*, 2008, **8**.
- 29 M. Gabig-Ciminska, A. Holmgren, H. Andresen, K. Bundvig Barken, M. Wümpelmann, J. Albers, R. Hintsche, A. Breitenstein, P. Neubauer, M. Los, A. Czyz, G. Wegrzyn, G. Silfversparre, B. Jürgen, T. Schweder and S. O. Enfors, *Biosens. Bioelectron.*, 2004, **19**, 537–546.
- 30 D. Brassard, L. Malic, F. Normandin, M. Tabrizian and T. Veres, *Lab Chip*, 2008, **8**, 1342–1349.
- 31 V. N. Luk, G. C. H. Mo and A. R. Wheeler, *Langmuir*, 2008, **24**, 6382–6389.

Evaluation of the error caused by droplet volume variability during an exponential dilution series in digital microfluidics

We evaluate here how the random variability in the droplet volume in digital microfluidics gives rise to an error in the reagent concentration during an exponential dilution series. To create this dilution series a buffer droplet is mixed with a reagent droplet. The resulting droplet is then split in two droplets and one of the resulting droplets is kept for the next dilution step. This process is repeated for n steps to create the exponential dilution series.

1. First dilution step

To create the first dilution step of the series, a droplet of volume V_0 and reagent concentration of C_0 is mixed with a buffer droplet of volume V_B and concentration $C = 0$. The concentration C_1 of the mixed droplet is thus given by:

$$C_1 = \frac{C_0 V_0}{V_0 + V_B}$$

The relative error $\Delta C_1 / C_1$ on C_1 is thus given by:

$$\left(\frac{\Delta C_1}{C_1}\right)^2 = \left(\frac{\Delta C_0}{C_0}\right)^2 + \left(\frac{\Delta V_0}{V_0}\right)^2 + \left(\frac{\Delta(V_0 + V_B)}{V_0 + V_B}\right)^2$$

where ΔC_0 is the standard deviation of the concentration from the bulk solution, and ΔV_0 and ΔV_B are respectively the standard deviation of the volume of the reagent and buffer droplets. As both the reagent and the buffer droplets were obtained from the same on-chip dispensing protocol, we can assume that $\Delta V_0 = \Delta V_B = \Delta V$, where ΔV is the standard deviation of droplet volume following dispensing from a reservoir. We thus have:

$$\Delta(V_0 + V_B) = \sqrt{(\Delta V_0)^2 + (\Delta V_B)^2} = \sqrt{2} \Delta V$$

As both droplets were obtained by the same dispensing process, we also neglect herein any systematic volume difference between V_0 and V_B such that $V_0 \cong V_B = V$. We thus have:

$$\left(\frac{\Delta C_1}{C_1}\right)^2 = \left(\frac{\Delta C_0}{C_0}\right)^2 + \left(\frac{\Delta V}{V}\right)^2 + \left(\frac{\sqrt{2} \Delta V}{2V}\right)^2$$

$$\left(\frac{\Delta C_1}{C_1}\right)^2 = \left(\frac{\Delta C_0}{C_0}\right)^2 + \frac{3}{2} \left(\frac{\Delta V}{V}\right)^2$$

Knowing the standard deviation of the droplet volume, this expression can be used to evaluate the error on the concentration of the first dilution level.

2. Second dilution step

For the second dilution step, we first have to split the mixed droplet into two individual droplets. Neglecting systematic error that might occur during this splitting process, the volume of the new split droplet is given by:

$$V_1 = \frac{V_0 + V_B}{2}$$

Thus the error on V_1 is:

$$\Delta V_1 = \sqrt{(\Delta V_0)^2 + (\Delta V_B)^2} = \sqrt{2} \Delta V$$

The concentration C_2 of the mixed droplet after the second dilution step is given by:

$$C_2 = \frac{C_1 V_1}{V_1 + V_B}$$

The error on the concentration after the second dilutions step can thus be found using the same process as for the first dilution step:

$$\left(\frac{\Delta C_2}{C_2}\right)^2 = \left(\frac{\Delta C_1}{C_1}\right)^2 + \left(\frac{\Delta V_1}{V_1}\right)^2 + \left(\frac{\Delta(V_1 + V_B)}{V_1 + V_B}\right)^2$$

$$\left(\frac{\Delta C_2}{C_2}\right)^2 = \left(\frac{\Delta C_1}{C_1}\right)^2 + 2\left(\frac{\Delta V}{V}\right)^2 + \left(\frac{\sqrt{3}\Delta V}{2V}\right)^2$$

$$\left(\frac{\Delta C_2}{C_2}\right)^2 = \left(\frac{\Delta C_1}{C_1}\right)^2 + \frac{11}{4}\left(\frac{\Delta V}{V}\right)^2$$

3. nth dilution step

In general, it is possible to show that, for the nth dilution step, the error on the concentration is given by (for n>0):

$$\left(\frac{\Delta C_n}{C_n}\right)^2 = \left(\frac{\Delta C_{n-1}}{C_{n-1}}\right)^2 + \frac{5n+1}{4}\left(\frac{\Delta V}{V}\right)^2$$

This formula can be used to find the error of the nth dilution step knowing the error on the (n-1) step.

Using arithmetic series, we can then show that the error of the nth dilution step can be obtained directly from:

$$\left(\frac{\Delta C_n}{C_n}\right)^2 = \left(\frac{\Delta C_0}{C_0}\right)^2 + \frac{5n^2 + 7n}{8}\left(\frac{\Delta V}{V}\right)^2$$

Thus, if we consider that the initial concentration of the bulk solution at the beginning of the dilution series is known (i.e., $\Delta C_0 = 0$), the error on the concentration of the n^{th} step is function of only the error on the droplet volume:

$$\frac{\Delta C_n}{C_n} = \frac{\Delta V}{V} \sqrt{\frac{5n^2 + 7n}{8}}$$

The following table provides numerical analysis of the error as a function of the dilution step:

Dilution Step	$\Delta C_n/C_n$	C_n/C_0
0	0	1
1	1.22 $\Delta V/V$	1/2
2	2.06 $\Delta V/V$	1/4
3	2.87 $\Delta V/V$	1/8
4	3.67 $\Delta V/V$	1/16
5	4.47 $\Delta V/V$...
6	5.27 $\Delta V/V$	
7	6.06 $\Delta V/V$	
8	6.86 $\Delta V/V$	
9	7.65 $\Delta V/V$	
10	8.44 $\Delta V/V$	
11	9.23 $\Delta V/V$...
12	10.0 $\Delta V/V$	1/4096
13	10.8 $\Delta V/V$	1/8192

For example, assuming an initial standard deviation of $\Delta V/V = 3\%$, the standard deviation of the concentration after 13 dilutions step is of about 32%.

Note:

It is important to note that we considered only the random variability in droplet volume in our analysis. Systematic error would have to be taken into account separately. For example, if the buffer droplets are systematically larger than the reagent droplets or if the splitting process is systematically biased, the average concentration of the various steps of the dilution series has to be shifted accordingly

Appendix B: Curriculum Vitae

Amir M. Foudeh

amir.foudeh@mail.mcgill.ca

Tel:5146607714

Education:

- 2010- **PhD in Biomedical Engineering, McGill University, Montreal, Canada.**
- Thesis: Development of a novel biosensor for rapid and specific detection of viable *Legionella* bacteria for on-site applications. Supervisor: Prof. Tabrizian, Co-supervisor: Dr. Veres.
- 2007-2009 **Master of Science in Biotechnology, Tissue engineering and Biomaterial track. Chalmers University of Technology. Sweden.**
- Thesis: “*High-throughput screening of cell-hydrogel interaction on engineered material array*”. Supervisor: Prof. Ali Khademhosseini. Harvard-MIT division of Health Sciences and Technology (HST), Center for Biomedical Engineering, Department of Medicine, Brigham and Women’s Hospital, Harvard Medical School.
- 2006 **Graduate level courses in a master program in chemical engineering with specialization in Biotechnology. University College of Boras. Sweden.**
- 2000-2005 **Bachelor of Science in Chemical Engineering, Isfahan University of Technology. Isfahan, Iran.**
- Thesis: “*Optimization of Lactic acid and Ethanol production from Apple Juice with help of R. Oryzae*”. Supervisor: Prof. M. Taherzadeh

Publications:

Amir M. Foudeh*, Daniel Brossard*, Maryam Tabrizian, Teodor Veres. Rapid and Multiplex detection of Legionella’s RNA using digital microfluidics. Lab on a Chip, 2015 15(6): p.1609-1618.

Amir M. Foudeh, Hana Trigui, Nilmini Mendis, Sebastian Faucher, Teodor Veres, Maryam Tabrizian. Sensitive and Specific SPRi Detection of *L. pneumophila* in Complex Environmental Water Samples (Submitted to Analytical and Bioanalytical Chemistry).

Sandrine Filion-Côté, Philip Roche, **Amir M. Foudeh**, Maryam Tabrizian, Andrew G. Kirk. Design and Analysis of a Spectro-Angular Surface Plasmon Resonance Biosensor Operating in the Visible Spectrum. Review of Scientific Instruments, 2014. 85, 093107.

Amir M. Foudeh, Jamal Daoud, Sebastian Faucher, Teodor Veres, Maryam Tabrizian. Sub-femtomole detection of 16s rRNA from *Legionella pneumophila* using surface plasmon resonance imaging. *Biosensors and Bioelectronics*, 2014. 52(0): p. 129-135.

Amir M. Foudeh, Tohid Fatanat Didar, Teodor Veres, Maryam Tabrizian. Microfluidic designs and techniques using lab-on-a-chip devices for pathogen detection for point-of-care diagnostics. *Lab on a Chip*, 2012. 12(18): p. 3249-3266.

Tohid Fatanat Didar, **Amir M. Foudeh**, Maryam Tabrizian. Patterning Multiplex Protein Microarrays in a Single Microfluidic Channel. *Analytical Chemistry*, 2011. 84(2): p. 1012-1018.

Chang Mo Hwang, Woo Y. Sim, Seung H. Lee, **Amir M Foudeh**, Hojae Bae, Sang-Hoon Lee and Ali Khademhosseini. Benchtop fabrication of PDMS microstructures by an unconventional photolithographic method. *Biofabrication*, 2010. 2(4): p. 045001.

Conferences:

Amir M. Foudeh. Developing a biosensor for detection of *Legionella pneumophila*. Bioengineering symposium, McGill University, September 2014, Canada, (invited talk).

Khalil Heileman, **Amir M. Foudeh**, Jamal Daoud, Francisco Rafael Castiello and Maryam Tabrizian. Detection of 16s RNA from *Legionella pneumophila* using impedance spectroscopy on microfluidic devices. 3rd International Conference and Exhibition on Biosensors & Bioelectronics. August 2014, San Antonio USA.

Amir M. Foudeh, Hana Trigui, Nilmini Mendis, Sebastian Faucher, Teodor Veres, Maryam Tabrizian. Rapid and sensitive detection of legionelle pneumophila in presence of amoeba in environmental water samples using surface plasmon resonance imaging. Biosensors World Congress, May 2014, Australia.

Amir Foudeh, Jamal Daoud, Sebastian Faucher, Teodor Veres, Maryam Tabrizian. Time Sensitive Detection of 16S rRNA from *Legionella pneumophila* using SPRi. Biomedical Engineering Symposium, September 12, 2013, Montreal, Canada.

Amir Foudeh, Sebastian Faucher, Teodor Veres, Maryam Tabrizian. A Post Amplification Strategy for Time Effective Detection of 16S rRNA from *Legionella pneumophila* in Water Sample Using SPRi. International Workshop on Recent Advances in Micro/Nano Sensors for Mono- and Multi-Target Assays. May 21, 2013, Kyiv, Ukraine (Oral presentation).

Amir Foudeh, Sebastian Faucher, Teodor Veres, Maryam Tabrizian. Detection of ribosomal RNA from legionella pneumophila through designed DNA probes. Integrated sensor system summer school, June 4, 2013, Montreal, Canada (Oral presentation).

Amir Foudeh, Sebastian Faucher, Teodor Veres, Maryam Tabrizian. Post amplification

strategy for time effective detection of 16S rRNA from Legionella pneumophila in water sample using SPRi. 245th American Chemical Society National Meeting and Exposition. April 7-11, 2013, New Orleans, Louisiana (Oral presentation).

Amir M. Foudeh, Jamal Daoud, Hubert Gagnon, Teodor Veres, Maryam Tabrizian. A post amplification strategy for time effective detection of Legionella pneumophila genetic content. Biosensors World Congress, May 2012, Mexico.

Fatanat Didar T, **Amir M. Foudeh** and M. Tabrizian, Multiplex immunoassay through combinatorial surface patterning in a single microfluidic channel for high throughput biological applications, World Biomaterial Conference June 2012, Chengdu, China. (Oral presentation).

Amir M. Foudeh, Teodor Veres, Maryam Tabrizian. A post amplification methodology for time effective detection of pathogenic bacteria. Integrated sensor system summer school, May 4, 2012, Montreal, Canada (Oral presentation).

Amir M. Foudeh, Teodor Veres, Maryam Tabrizian, Detection of Bacterial RNA using Surface Plasmon Resonance imaging, Biomedical Engineering Symposium, McGill university, September 2011, Montreal, Canada.

Amir M. Foudeh, Teodor Veres, Maryam Tabrizian. Designing DNA based probes to detect pathogenic bacteria using surface Plasmon resonance imaging (SPRi). Advances in biodetection and Biosensors, Hamburg, Germany. July 2011.

C. Hwang, O. Emiroglu, N. Kachouie, **A. Foudeh**, A. Khademhosseini, Engineered microchannels within multi-layered cell laden hyaluronic acid-collagen hydrogels. NEBEC2009 (Proceeding of the IEEE 35th annual northeast bioengineering conference, Boston, USA April 2009).

N.N. Kachouie, K. Ghosh, B.G. Chung, **A. Foudeh**, D. Ingber, A. Khademhosseini. Micro-engineered islets by microwell templated co-culture of β -cells and endothelial cells. Syscode conference (System-based Consortium for Organ Design and engineering), Boston, USA April 2009.

Ian Wheeldon, **Amir Foudeh**, Alex Bick, Nezam Kachouie, Ali Khademhosseini. Development of high throughput screens of biomaterials-cell interaction, Wyss Institute for Biologically Inspired Engineering, Harvard University, Cambridge, USA November 2009.

Book Chapter:

Hojae Bae, Jason W. Nichol, **Amir Foudeh**, Behnam Zamanian, Cheong hoon Kwon, and Ali Khademhosseini, Microengineering approach for directing embryonic stem cell differentiation, In "Biomaterials as Stem Cell Niche", edited by K. Roy. Springer-Verlag. p. 121-31 (2010).

Honors and Awards:

- 2014 GREAT travel award, Biomedical Engineering Department, McGill.
- 2014 Biomedical Engineering Excellence award, Faculty of Medicine, McGill.
- 2013 Biomedical Engineering Excellence award, Faculty of Medicine, McGill.
- 2011 NSERC-CREATE Integrated Sensor Systems Fellowship.
- 2011 International Graduate Travel Award, Faculty of Medicine, McGill, Canada.
- 2010 NSERC-CREATE integrated sensor systems (ISS) travel award.
- 2010 Graduate Enrolment & Recruitment Award, McGill, Canada.
- 2000 Member of Special Talents Committee in Isfahan University of Technology, Iran.

Experience:

- Jan 2010- **Research assistant**, Biomedical engineering department, McGill University, Canada. Prof. Tabrizian.
- Developed a biosensing method for specific and sensitive detection of RNA using SPRi
 - In collaboration with Department of Natural Resource Sciences in McGill university, be able to detect pathogenic *Legionella* bacteria in environmental water samples.
- May 2011- **Visiting researcher**, National Research Council Canada, Boucherville, Quebec, Dr. Veres.
- Developed an integrated digital microfluidic platform for multiplex detection of RNA from pathogenic bacteria.
- Fall 2012,13 **Teaching Assistant** for Biomaterials course, Biomedical Engineering Department, McGill University, Canada. Prof. Tabrizian
- Jan 2011-Oct 2012 **Chair** of the ISS Graduate student program committee (GSPC) NSERC CREATE training program in Integrated Sensor Systems (ISS).
- Organized the first two ISS NSERC-CREATE summer schools, June 2011 and May 2012.

- Sat on the ISS Program Committee and provided feed back to the program

Dec 2008- Dec 2009 **Visiting Researcher**, Harvard-MIT division of Health Sciences and Technology, Center for Biomedical Engineering, Department of Medicine, Brigham and Women's Hospital, Harvard Medical School. Prof. Khademhosseini.

- Developed a high-throughput screening platform for investigating the cell-hydrogel interaction on engineered material array.
- Microengineered islets by co-culture of β -cells and endothelial cells. in microwell template.
- Developed a hydrogel based soft lithography.

June-Nov 2008 **Research Assistant**, Department of Applied Physics, Biological Physics group. Prof. Gold.

- Investigated the effects of charge-doping materials in supported lipid bilayers on AHP cell.

Fall 2008 **Teaching Assistant** for Biomaterials course, Chalmers University of Technology, Sweden. Prof. Gold.

Fall 2008 **Teaching Assistant** for Materials in Medicine course, Chalmers University of Technology, Sweden. Prof. Gold.

Feb-May 2008 **Research project:** Department of Chemical and Biological Engineering, Chalmers University of Technology, Prof. Gatenholm.

- Developed a tissue engineered blood vessels using Bacterial cellulose as scaffold with help of pulsatile flow.

Leadership positions:

- **Jan 2011-Jan 2012** **VP Social** in Biomedical Engineering student's society, McGill.
- **Jan 2011-Oct 2012** **Chair** of the ISS Graduate student program committee (GSPC) NSERC CREATE training program in Integrated Sensor Systems